Nailing down the Arabidopsis root response to beneficial rhizobacteria

Eline Hendrike Verbon

Eline H. Verbon

Nailing down the Arabidopsis root response to beneficial rhizobacteria

PhD thesis, September 2019

Utrecht University | Plant-Microbe Interactions

ISBN 978-90-393-7159-6

Printed by: Proefschrift All in One

Photography: Hans van Pelt

Nailing down the Arabidopsis root response to beneficial rhizobacteria

De reactie van de Arabidopsis plantenwortel op goedaardige bodembacteriën

(met een samenvatting in het Nederlands)

Proefschrift

ter verkrijging van de graad van doctor van de Universiteit Utrecht op gezag van de rector magnificus, prof.dr. H.R.B.M. Kummeling, ingevolge het besluit van het college voor promoties in het openbaar te verdedigen op woensdag 18 september 2019 des ochtends te 10.30 uur

door

Eline Hendrike Verbon

geboren op 29 maart 1991

te Tilburg

Promotor: Prof. dr. ir. C.M.J. Pieterse
Copromotor: Dr. R. de Jonge

Dit proefschrift werd mogelijk gemaakt door financiële steun van de Nederlandse organisatie voor Wetenschappelijk Onderzoek (NWO EPS talent project nr. 831.14.001).

Contents

Chapter 1

General introduction

Eline H. Verbon

Adapted from:
Verbon, E.H., Liberman, L.M. (2016) Beneficial microbes affect endogenous mechanisms controlling root development. Trends in Plant Science, 21: 218-229.
Verbon, E.H., Trapet, P.L., Stringlis, I.A., Kruijs, S., Bakker, P.A.H.M., Pieterse, C.M.J. (2017) Iron and Immunity. Annual Review of Phytopathology, 55: 355-375.

Beneficial rhizobacteria in and around plant roots

Soil harbors the greatest bacterial diversity on earth, with 10^{10} prokaryotes per cm^3 (Torsvik *et al.*, 2002). In the early 1900s, Hiltner observed that microbial communities close to plant roots are more numerous and less diverse than communities in soil farther away from roots. He assumed that the increased number of micro-organisms was due to nutrient secretion by the plant and termed it 'the rhizosphere effect' (Hiltner, 1904). Since then, the rhizosphere has been defined as the soil around plant roots influenced by the root and its exudates, whereas the rest of the soil is referred to as bulk soil (Figure 1) (Prashar *et al.*, 2013). Both soil type (Fierer and Jackson, 2006; Bulgarelli *et al.*, 2012; Lundberg *et al.*, 2012; Schlaeppi *et al.*, 2014) and root exudates have been shown to affect the community composition of the rhizosphere microbiome (for examples see (Haichar *et al.*, 2008; Badri *et al.*, 2009; Micallef *et al.*, 2009b; a)).

Root exudates include sugars, amino acids, organic acids, fatty acids, phenolics, enzymes, and flavonoids (Chaparro *et al.*, 2013). The bacteria in the rhizosphere, the rhizobacteria, depend on their ability to move towards these plant-derived carbon sources to thrive (for more on chemo-

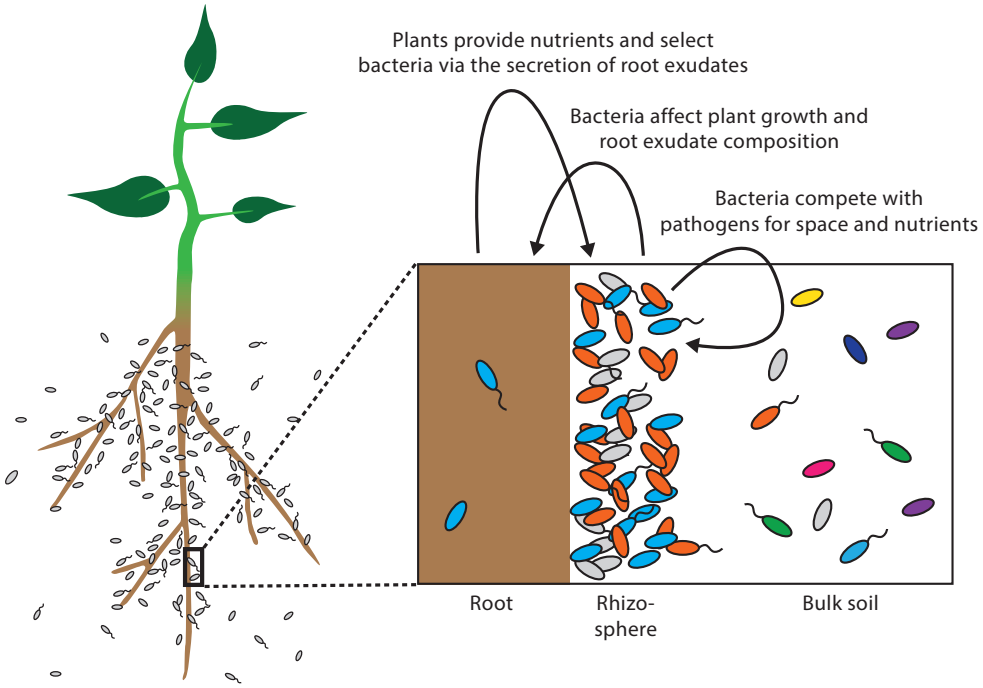

Figure 1 A plant and the bacteria in its rhizosphere influence each other. The rhizosphere, the thin layer of soil around plant roots that is affected by root exudates, harbors a more numerous and less diverse microbial community than bulk soil. Plants influence the composition of this rhizosphere microbiome via their root exudates, although the strength of this effect varies between studies. In return, bacteria affect plant growth and root exudate composition. In addition, they compete with pathogens for both space and nutrients. An even more select group of bacteria is found within the root. The selection of these so-called endophytes is probably mediated by the plant immune system.

taxis see (Vande Broek *et al.*, 1998; Weert *et al.*, 2002)) and to use them and other root-derived rhizodeposits, such as sloughed-off root cells or lysates, as energy sources (Jones *et al.*, 2004; Singh *et al.*, 2004; Dennis *et al.*, 2010). In turn, several microbes within the rhizosphere have been shown to modify root exudate composition (Heulin *et al.*, 1987; Phillips *et al.*, 2004; Matilla *et al.*, 2009; Dardanelli *et al.*, 2010). The endophytic bacterial community, the group of bacteria within a plant's root system, is even less diverse than the rhizosphere community (Micallef *et al.*, 2009a; Bulgarelli *et al.*, 2012; Lundberg *et al.*, 2012). The decreased bacterial diversity within the root is likely mediated by the plant immune system (Jones and Dangl, 2006), as mutant plants defective in multiple phytohormone signaling pathways have distinct endophytic microbial communities compared to wild-type plants (Lebeis *et al.*, 2015).

Interestingly, certain beneficial rhizobacteria enhance shoot growth (Ryu *et al.*, 2003; Carvalhais *et al.*, 2013), for example by increasing nutrient availability (Ferguson and Mathesius, 2014; Soyano *et al.*, 2014), or by increasing the root exploratory capacity by modifying root system architecture (Sukumar *et al.*, 2013; Vacheron *et al.*, 2013; Zamioudis *et al.*, 2013). Some beneficial rhizobacteria positively affect plant fitness by competing with pathogens (Lugtenberg and Kamilova, 2009; Pérez-Montaño *et al.*, 2014) or inducing systemic resistance (ISR) to pathogen attack (reviewed in (Pieterse *et al.*, 2014)) (Figure 1).

The Arabidopsis root

The effect of root colonization by beneficial microbes on plant fitness has been studied intensively in the model plant *Arabidopsis thaliana* (Arabidopsis). The Arabidopsis root consists of a primary root with lateral roots. The outermost cell layer is called the epidermis, followed by the cortex, the endodermis and the vasculature (Figure 2A). The root tip is protected by a group of gravity-sensing cells called the root cap (Figure 2A-B), which deposits mucilage, cell debris and whole cells into the rhizosphere as the root grows (Kumpf and Nowack, 2015).

Root cells are created in the stem cell niche in the meristematic zone of the root, which is established during embryogenesis (Scheres *et al.*, 1994). The stem cell niche within this zone contains the progenitor cells that give rise to the root cell types (Verbelen *et al.*, 2006). A quiescent center located at the center of the niche consists of four rarely-dividing cells (Dolan *et al.*, 1993) that repress differentiation of the surrounding initials, or stem cells (van den Berg *et al.*, 1997). There are initials for each cell type: columella, lateral root cap/epidermis, cortex/endodermis, and stele or vasculature initials (Dolan *et al.*, 1993; Van den Berg *et al.*, 1995). Upon exiting the meristematic zone, cells elongate up to 300% within three hours in the elongation zone (Figure 2B) (Verbelen *et al.*, 2006). Finally, they acquire their mature characteristics in the differentiation zone. The differentiation zone can be distinguished by the emergence of root hairs from trichoblasts; specialized epidermal cells overlying two cortical cells. Epidermal cells overlying one cortical cell, the atrichoblasts, do not form root hairs (Dolan *et al.*, 1994; Galway *et al.*, 1994). Another defining feature of the differentiation zone is the formation of the Casparian strip: a waxy cell wall thickening around endodermal cells that forms a protective barrier (Caspary, 1865; Geldner, 2013).

Lateral roots develop from differentiated parts of the primary root in a process that has been elegantly studied by several groups (Dubrovsky *et al.*, 2006; Péret *et al.*, 2009; Benková and Bielach, 2010; Van Norman *et al.*, 2013). Lateral root development starts in the pericycle, the

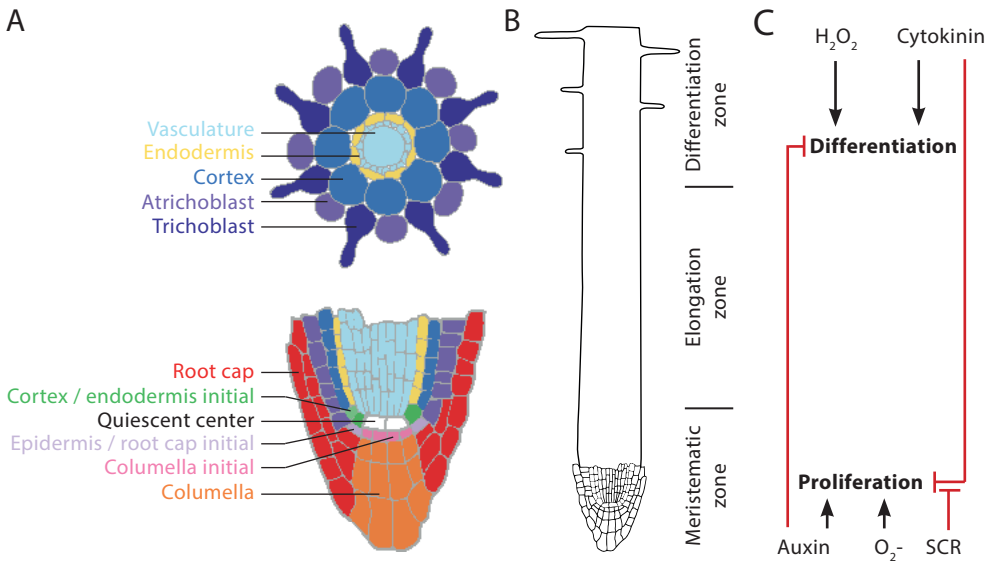

Figure 2 Arabidopsis root development. A) Above: a transverse section of a mature part of an Arabidopsis root showing the vasculature (light blue), surrounded by the endodermis (yellow), the cortex (blue), and the two cell types in the epidermis: the trichoblasts (dark purple) and the atrichoblasts (light purple). Below: a longitudinal section of the root meristem, where new cells are generated. The quiescent center (white) is surrounded by stem cells: the cortex/endodermal initial (green), the epidermal/lateral root cap initial (violet), the columella initials (pink) and the vasculature initials. The root cap (red) and columella (orange) form the outer layer of the root tip. B) The Arabidopsis root consists of three developmental zones: the meristematic zone, where the stem cell niche and rapidly dividing cells are located; the elongation zone, where cells increase in length; and the differentiation zone, where cell types acquire their unique features. C) The transition from proliferation to differentiation over the length of the root is controlled by several mechanisms. In the root tip, the high concentration of auxin induces division and inhibits differentiation. SCARECROW (SCR) inhibits differentiation within the quiescent center specifically by inhibiting the cytokinin response. More shootward, the decreasing concentration of auxin ultimately results in a balance between auxin and cytokinin that favors differentiation.The antagonistic action of hydrogen peroxide (H_2O_2) and superoxide (O_2-) is involved in determining the transition point between division and differentiation independent of auxin and cytokinin.

cell layer in the vasculature neighboring the endodermis. Pairs of cells in the pericycle, called lateral root founder cells, must first become competent to form a lateral root. These lateral root founder cells are activated, divide multiple times and differentiate to form the lateral root primordia (Malamy and Benfey, 1997). As the cells within the lateral root primordia continue to divide, the endodermal cells overlying the lateral root primordia separate, change shape and form small holes in the Casparian strip to accommodate the emerging lateral root (Laskowski *et al.*, 2006; Vermeer *et al.*, 2014). Further divisions and differentiation of the lateral root cells after emergence from the primary root ultimately results in a lateral root anatomy that is identical to the anatomy of the primary root, including a meristematic zone that controls the lateral root's growth rate (Malamy and Benfey, 1997).

Control of root development

The transition from cell division to differentiation along the longitudinal axis of the Arabidopsis root is controlled by the plant hormones auxin and cytokinin and by reactive oxygen species (ROS) (Figure 2C). The plant hormone auxin forms a gradient along the root with a maximum within the stem cell niche. This maximum is required for positioning and maintenance of the niche (Aida *et al.*, 2004; Galinha *et al.*, 2007; Grieneisen *et al.*, 2007). The transcription factors SHORTROOT (SHR) and SCARECROW (SCR) are also required to maintain stem cell niche identity (Benfey *et al.*, 1993; Scheres *et al.*, 1995; Aida *et al.*, 2004). SHR activates *SCR* expression (Nakajima *et al.*, 2001). SCR inhibits differentiation and maintains the identity of the surrounding stem cells in the quiescent center (Sabatini *et al.*, 2003) by suppressing cytokinin perception (Moubayidin *et al.*, 2013). More shootward in the root, the suppression of cytokinin perception is relieved. Cytokinin then reduces the expression of auxin efflux transport proteins, which leads to auxin redistribution and induces differentiation (Dello Ioio *et al.*, 2008).

ROS regulate the transition from proliferation to differentiation independent of auxin and cytokinin (Schmidt and Schippers, 2015). Two transcription factors, UPBEAT1 and MYB36, have been found to regulate reactive oxygen homeostasis (Tsukagoshi *et al.*, 2010; Liberman *et al.*, 2015). Repression of certain peroxidases shootward from the elongation zone increases hydrogen peroxide (H_2O_2) levels and decreases superoxide (O_2-) levels, resulting in differentiation. ROS potentially enhance differentiation by stopping the cell cycle and modifying cell walls to allow for cell expansion (Tsukagoshi *et al.*, 2010).

Cytokinin and auxin also function antagonistically during lateral root development. An auxin response is activated in the pericycle founder cells before the first division (Benková *et al.*, 2003). Downstream targets of auxin prevent clustering of lateral root competence sites and are essential for subsequent lateral root emergence (Hofhuis *et al.*, 2013). Cytokinin, on the other hand, inhibits lateral root formation (Li *et al.*, 2006; Laplaze *et al.*, 2007; Bielach *et al.*, 2012). Until recently, it was thought that an auxin maximum in the lateral root founder cells dictates lateral root formation (Péret *et al.*, 2009). Recently, it was shown that competence to form a lateral root is induced by periodic gene oscillations that appear to be induced by periodic programmed cell death in the root cap (Moreno-Risueno *et al.*, 2010; Xuan *et al.*, 2015, 2016).

Effects of rhizobacteria on root structure

Beneficial microbes generally change Arabidopsis root system architecture by inhibiting primary root growth and increasing the formation of lateral roots and root hairs (Figure 3) (Persello-Cartieaux *et al.*, 2001; Ryu *et al.*, 2005), although an increase in primary root growth has also been observed (Liu *et al.*, 2012; Schenk *et al.*, 2012).

The beneficial rhizobacteria *Pseudomonas simiae* WCS417 (WCS417) and *Bacillus megaterium* UMCV1 decrease primary root length by reducing cell elongation in the elongation zone (López-Bucio *et al.*, 2007; Zamioudis *et al.*, 2013). Possibly as a result of early differentiation, root hairs emerge closer to the root tip in roots colonized by rhizobacteria (López-Bucio *et al.*, 2007). In addition, WCS417 increases root hair density and length. The density is increased because of a greater number of cortical cells around the radial axis in WCS417-treated roots, resulting in an increased number of trichoblast. (Zamioudis *et al.*, 2013). WCS417 and *B. megaterium* UMCV1 increase the number of both lateral root primordia and lateral roots (López-Bucio *et al.*, 2007;

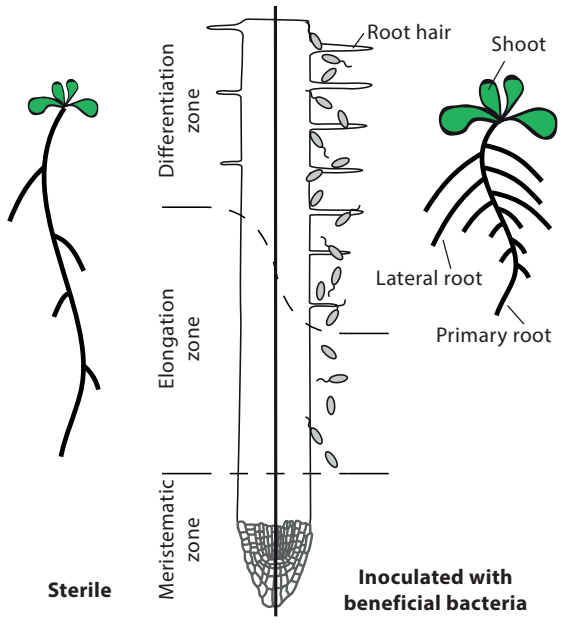

Figure 3 Rhizobacteria influence plant root development. Typically, beneficial bacteria enhance lateral root formation and and inhibit primary root growth. Differentiation is generally induced closer to the root tip and root hair density and length are increased. The establishment of these effects often requires functional auxin, cytokinin or ethylene signaling within the plant. These hormones are not produced by the bacteria. Rather, compounds required for bacterial processes like quorum sensing or biofilm production affect plant hormone levels or function as plant hormone mimics.

Zamioudis *et al.*, 2013). The induction of lateral root formation and shoot growth can take place without primary root growth inhibition: volatile organic compounds produced by WCS417 stimulate lateral root formation, but do not inhibit primary root growth (Zamioudis *et al.*, 2013).

The question remains how rhizobacteria induce the changes in root growth. The root system architecture changes induced by several rhizobacterial species and isolates have been shown to correlate with the amount of auxin produced by the rhizobacteria (Asghar *et al.*, 2002; Khalid *et al.*, 2004; Remans *et al.*, 2007; Lim and Kim, 2009; Spaepen *et al.*, 2014). In case of WCS417, the induction of lateral root outgrowth after exposure to WCS417 is accompanied by an increase in auxin-response maxima along the root and is dependent on auxin perception and transport in the plant (Zamioudis *et al.*, 2013). The response to *B. megaterium* is accompanied by a decreased auxin response in the primary root tip as measured with the auxin-responsive marker construct *DR5:uidA* (López-Bucio *et al.*, 2007).

Although a functional auxin response within the plant is essential for several of the effects of WCS417 on root development, WCS417 does not synthesize auxin (Zamioudis *et al.*, 2013). Instead, it might produce an auxin mimic, as has been shown for the pathogenic bacterium *P. aeruginosa* (Ortiz-Castro *et al.*, 2011). Alternatively, bacterial quorum sensing molecules may be involved. Quorum sensing is the process by which bacteria assess the population density to coordinate behavior like virulence or biofilm formation. Diketopiperazines (DKPs) are compounds produced by many bacterial species that are involved in quorum sensing. DKPs have a planar structure containing a heterocyclic system also found in auxin. Possibly because of this structural similarity, DKPs activate auxin-inducible gene expression, potentially by binding to the auxin receptor itself (Ortiz-Castro *et al.*, 2011). The auxin-responsive genes activated by DKPs induce lateral root growth but do not inhibit primary root growth (Ortiz-Castro *et al.*, 2011). Indole, a compound used by bacteria for a wide range of functions, such as biofilm formation

and virulence, enhances lateral root primordium development. Polar auxin transport is required for this effect but is not influenced by indole application. Moreover, although indole can be converted into auxin it does not significantly change auxin levels within the plant and impedes the ability of plants to respond to exogenous auxin. This suggests that indole is converted into an auxin antagonist within the plant (Bailly *et al.*, 2014).

N-acyl-homoserine lactones (AHLs) are a group of quorum sensing molecules that influence root development independent of auxin. AHLs possibly induce lateral root growth and inhibit primary root growth by modifying the cytokinin response instead of the auxin response (Ortíz-Castro *et al.*, 2008). The virulence factor pyocyanin (PCN), whose synthesis by *P. aeruginosa* is regulated by quorum sensing, induces root phenotypic changes independent of either auxin or cytokinin. This molecule may affect root development by manipulating ethylene levels, subsequently resulting in enhanced reactive oxygen species levels (Ortiz-Castro *et al.*, 2014). *B. megaterium* affects root system architecture independent of either auxin or ethylene by an unknown mechanism (López-Bucio *et al.*, 2007).

In summary, rhizobacteria generally decrease primary root growth and increase the number of lateral roots. These changes are often accompanied by changes in auxin and cytokinin transport or levels within the plant, but effects on ethylene levels have also been observed. While several beneficial rhizobacteria have been shown to produce these hormones themselves, molecules involved in essential bacterial processes, such as quorum sensing, can also function as phytohormone mimics or indirectly influence plant phytohormone homeostasis.

Rhizobacteria-induced plant resistance to disease

Apart from affecting root growth, some beneficial microbes in the rhizosphere induce resistance against pathogen attack. The molecular basis of ISR has been extensively studied in the Arabidopsis root colonized by WCS417 (Van der Ent *et al.*, 2008; Zamioudis *et al.*, 2014, 2015; Stringlis *et al.*, 2018b). The plant hormones jasmonic acid and ethylene are required for the WCS417-induced resistance phenotype, but their synthesis is not directly increased in response to WCS417 root colonization. Instead, the plants are primed for a faster and stronger expression of cellular defense responses after pathogen attack (Pieterse *et al.*, 2014).

MYB72 is among the genes that are induced in Arabidopsis roots colonized by WCS417 and is one of the genes known to be required for WCS417-mediated ISR (Verhagen *et al.*, 2004; Van der Ent *et al.*, 2008). Interestingly, other resistance-inducing beneficial microbes, such as *Pseudomonas capeferrum* WCS358, *Trichoderma harzianum* T-78, and *Trichoderma asperellum* T-34, also trigger *MYB72* expression in Arabidopsis (Zamioudis *et al.*, 2015; Martínez-Medina *et al.*, 2017). *MYB72* is also a known player in the response of Arabidopsis to iron (Fe) deficiency (Palmer *et al.*, 2013). In fact, not only *MYB72*, but 20% of the genes activated in Arabidopsis roots upon colonization by WCS417 is also induced under low Fe conditions (Zamioudis *et al.*, 2015).

The plant Fe deficiency response

Fe is an essential element for most organisms because it functions as the catalytic component of enzymes that mediate redox reactions in key cellular processes, such as DNA replication. Fe can fulfill this role because it can exist in both its ferric (Fe^{3+}) and its ferrous (Fe^{2+}) form. While Fe is abundantly present in the Earth's crust, its bioavailability is limited because Fe is mainly

present as ferric oxide, which is poorly soluble at neutral and high pH (Balk and Schaedler, 2014; Connorton *et al.*, 2017). In addition to Fe starvation, Fe excess is also not desirable, as it leads to the formation of hydroxyl radicals via the so-called Fenton reaction (Fenton, 1894; Haber and Weiss, 1934), which can cause damage to proteins, DNA and lipids (Luo *et al.*, 1994). Therefore, most organisms, including plants, have evolved sophisticated mechanisms that tightly regulate Fe uptake, efflux, and storage.

In low Fe conditions, plant roots initiate several root surface-enlarging morphological changes, such as increased root branching and root hair formation (Schmidt, 1999; Jin *et al.*, 2008). The shoot induces the activation of the Fe deficiency response in the root when it requires more Fe (Vert *et al.*, 2003). In Arabidopsis, a member of the oligopeptide (OPT) family of peptide transporters, OPT3, is required for the shoot-to-root signaling of Fe status, possibly because it can load Fe into leaf phloem (Stacey *et al.*, 2008; Mendoza-Cózatl *et al.*, 2014; Zhai *et al.*, 2014; Khan *et al.*, 2018). In addition, the expression of the IRON MAN family of peptides in plant shoots is believed to be required for the activation of the Fe deficiency response in the root (Grillet *et al.*, 2018).

The Fe deficiency responses of non-grass and grass plant species are distinct and are known as Strategy I and Strategy II, respectively (Figure 4) (Römheld, 1987). The molecular mechanisms underlying both responses have been thoroughly described in a number of excellent reviews (Guerinot and Ying, 1994; Walker and Connolly, 2008; Palmer and Guerinot, 2009; Ivanov *et al.*, 2012; Kobayashi and Nishizawa, 2012; Darbani *et al.*, 2013), so we only highlight the main characteristics here. Non-grass plants, including Arabidopsis, increase solubility of Fe^{3+} in the soil by lowering rhizosphere pH via the secretion of protons by the H^+-ATPase AHA2 (Santi and Schmidt, 2009). Solubilized Fe^{3+} is subsequently reduced to Fe^{2+} by the plasma membrane protein FERRIC REDUCTION OXIDASE2 (FRO2). Fe^{2+} is transported into the root epidermis via the high-affinity IRON-REGULATED TRANSPORTER1 (IRT1) (Eide *et al.*, 1996; Robinson *et al.*, 1999).

Grass plants, such as maize and wheat, use an Fe chelation-based strategy to mobilize and acquire Fe under Fe-limiting conditions. These so-called Strategy II plants convert methionine via nicotianamine (NA) into phytosiderophores (Ohata *et al.*, 1993; Bashir and Nishizawa, 2006). Phytosiderophores are released into the rhizosphere by the TRANSPORTER OF MUGINEIC ACID1 (TOM1) (Nozoye *et al.*, 2011). After binding Fe in the rhizosphere, the phytosiderophores are taken up by the plant via specific transporters, such as YELLOW STRIPE1 (YS1) or the YS1-like (YSL) (Curie *et al.*, 2001; Inoue *et al.*, 2009; Kobayashi and Nishizawa, 2012).

Molecular regulation of Fe homeostasis in Arabidopsis

The molecular regulation of Strategy I has been elucidated in Arabidopsis in detail (Figure 4). The basic helix-loop-helix (bHLH) transcription factor FER-LIKE IRON DEFICIENCY INDUCED TRANSCRIPTION FACTOR (FIT) emerged as the central regulator of the response (Colangelo and Guerinot, 2004; Jakoby *et al.*, 2004; Yuan *et al.*, 2005). Upon Fe deprivation, FIT is activated at the transcriptional and post-translational level, after which it interacts with other members of the bHLH transcription factor family (bHLH38/39/100/101) (Yuan *et al.*, 2008; Sivitz *et al.*, 2012; Wang *et al.*, 2013) to activate downstream Fe uptake genes, such as *FRO2* and *IRT1* (Colangelo and Guerinot, 2004; Ivanov *et al.*, 2012). Independent of FIT, another bHLH transcription factor called POPEYE (PYE) is upregulated upon Fe deficiency. Like FIT, PYE interacts with other bHLH

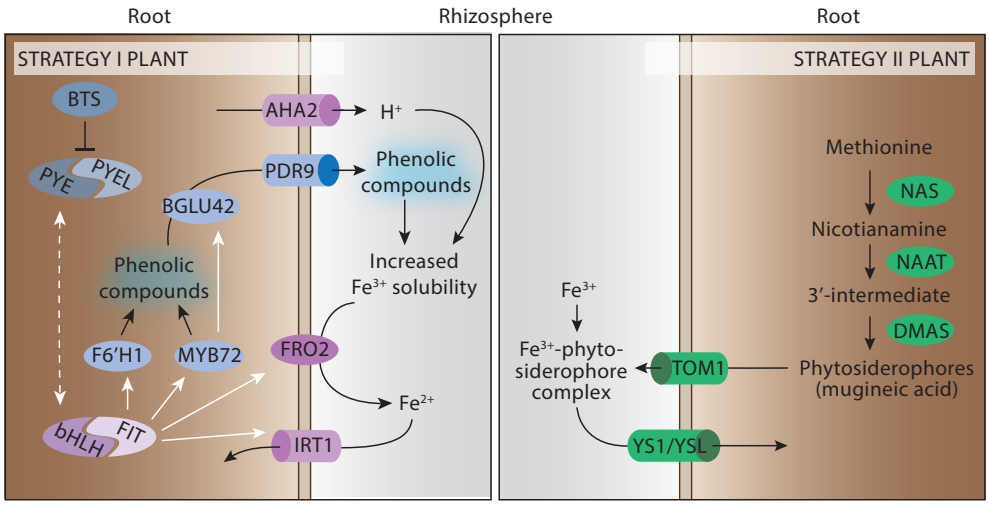

Figure 4 Fe uptake strategies by non-grass plants (Strategy I) and grass plants (Strategy II). Under Fe-limiting conditions, Strategy I plants (left) upregulate transcription of the basic helix-loop-helix (bHLH) transcription factor gene *FER-LIKE IRON DEFICIENCY INDUCED TRANSCRIPTION FACTOR (FIT)*. FIT interacts with other bHLH proteins to enhance the expression of *FERRIC REDUCTION OXIDASE 2 (FRO2)*, *IRON-REGULATED TRANSPORTER 1 (IRT1)* and *MYB72*. FRO2 and IRT1 localize to the plasma membrane. FRO2 reduces Fe^{3+} to Fe^{2+}, which is transported into the root epidermis by IRT1. The bHLH transcription factor gene *POPEYE (PYE)* is also upregulated upon Fe deficiency. PYE interacts with PYE-LIKE (PYEL) bHLHs, aiding Fe homeostasis through an as yet unknown mechanism. PYE and PYEL are negatively regulated by BRUTUS (BTS). Fe availability is enhanced by secretion of protons via the Arabidopsis H^+-ATPase 2 (AHA2) and the release of Fe-mobilizing phenolic compounds. This latter process is mediated by the transcription factor MYB72, the coumarin biosynthesis protein FERULOYL-COA 6'HYDROXYLASE 1 (F6'H1), the glucose hydroxylase β-GLUCOSIDASE 42 (BGLU42), and the ABC transporter PLEIOTROPIC DRUG RESISTANCE 9 (PDR9). In Strategy II plants, Fe deficiency induces the biosynthesis of the iron scavenger nicotianamine (NA) from its precursor methionine after which Fe-chelating phytosiderophores are produced by NA AMINOTRANSFERASE (NAAT) and DEOXYMUGENEIC ACID SYNTHASE (DMAS). Phytosiderophores are released into the rhizosphere by the TRANSPORTER OF MUGINEIC ACID 1 (TOM1). After binding Fe^{3+} in the rhizosphere, the complexes are transported back into the root by specific transporters, including YELLOW STRIPE 1 (YS1) and YS-like (YSL). Solid lines indicate established interactions; dashed lines indicate hypothetical interactions. White arrows indicate transcriptional activation.

transcription factors, such as PYE-like (PYEL), to function in the regulation of Fe homeostasis (Long *et al.*, 2010). PYE and PYEL are negatively regulated by the E3 ubiquitin-protein ligase BRUTUS (BTS) (Selote *et al.*, 2015). Both *pye* and *fit* mutants of Arabidopsis become chlorotic under Fe-limiting conditions (Colangelo and Guerinot, 2004; Long *et al.*, 2010), suggesting that both networks are necessary alongside each other to fine-tune Fe uptake in Strategy I plants.

In addition to *FRO2* and *IRT1*, FIT upregulates the transcription factor-encoding genes *MYB72* and *MYB10* (Palmer *et al.*, 2013). Together, MYB72 and MYB10 induce the production of the Fe scavenger NA by upregulating the NA synthase gene *NAS4* (Palmer *et al.*, 2013). NA is important for plant survival in alkaline soil where Fe availability is greatly restricted. Possibly, NA plays a role in the distribution of Fe within the plant via the transporter YELLOW STRIPE-LIKE2 (YSL2) (DiDonato *et al.*, 2004; Koen *et al.*, 2013). In addition to its role in NA synthesis, MYB72 controls a

gene module that regulates the biosynthesis and secretion of a specific subclass of fluorescent phenylpropanoids that belongs to the coumarin family (Zamioudis *et al.*, 2014). This is fitting for a MYB transcription factor, as MYB transcription factors are known to be central regulators in the biosynthesis of Fe-mobilizing phenylpropanoid-derived phenolic compounds (Dubos *et al.*, 2010; Liu *et al.*, 2015). Coumarins are essential for Fe uptake by Arabidopsis (Schmidt *et al.*, 2014) and are synthesized via FERULOYL-COA 6′-HYDROXYLASE1 (F6′H1) in the phenylpropanoid pathway (Rodriguez-Celma *et al.*, 2013; Schmid *et al.*, 2014). Downstream of *MYB72* the glucose hydrolase activity of β-GLUCOSIDASE42 (BGLU42) is involved in processing the fluorescent phenolic compounds to enable their secretion into the rhizosphere (Zamioudis *et al.*, 2014). This function corroborates the general role of β-glucosidases in chemical destabilization and release of stress-induced secondary metabolites (Morant *et al.*, 2008). Finally, coumarins are secreted into the rhizosphere by the Fe deficiency-regulated ABC transporter PLEIOTROPIC DRUG RESISTANCE9 (PDR9) (Rodriguez-Celma *et al.*, 2013; Fourcroy *et al.*, 2014). Upon release in the rhizosphere, coumarins can chelate and mobilize Fe^{3+} and make it available for reduction and uptake by the roots (Schmid *et al.*, 2014; Fourcroy *et al.*, 2016).

Once Fe is taken up, its transport and storage is regulated by Fe transporters called NATURAL RESISTANCE-ASSOCIATED MACROPHAGE PROTEINS (NRAMPs) (Curie *et al.*, 2000) and Fe storage proteins called FERRITINS (Theil, 1987; Briat *et al.*, 2010). NRAMPs coordinate Fe distribution across the cell (Curie *et al.*, 2000) and organize Fe transport out of vacuoles (Lanquar *et al.*, 2005). FERRITINS play an important role in averting oxidative stress by storing it away from other molecules with which it can react. Moreover, prior to storage, FERRITINS convert Fe to its non-reactive ferric form, which ensures that the phytotoxic Fenton reaction with oxygen will not occur (Laulhere and Briat, 1993; Deák *et al.*, 1999). Fe-bound FERRITINS are mostly located in chloroplasts and mitochondria (Nouet *et al.*, 2011).

Hormonal regulation of the Arabidopsis Fe deficiency response

The plant hormones auxin, ethylene, cytokinin and gibberellic acid are important regulators of the Fe deficiency response (Hindt and Guerinot, 2012; Shen *et al.*, 2016; Wild *et al.*, 2016). Ethylene and gibberellic acid increase *FRO2* and *IRT1* expression in the root epidermis (Romera *et al.*, 1999; García *et al.*, 2010; Wild *et al.*, 2016). Furthermore, ethylene and auxin stimulate the accumulation of nitric oxide in Fe-deficient roots. Both ethylene and the accumulated nitric oxide result in stabilization of FIT and enhanced Fe uptake (Meiser *et al.*, 2011; Romera *et al.*, 2011). In addition to stimulating the accumulation of nitric oxide, auxin stimulates formation and elongation of lateral roots, enabling the plant to take up more Fe (Giehl *et al.*, 2012). Cytokinin, in contrast, decreases root growth and suppresses genes involved in the Fe deficiency response (Séguéla *et al.*, 2008).

The major plant defense hormones salicylic acid and jasmonic acid also influence Fe acquisition. Salicylic acid affects auxin and ethylene signaling, thereby positively affecting the expression of the Fe uptake genes *FRO2* and *IRT1* (Shen *et al.*, 2016). Jasmonic acid negatively affects Fe acquisition by downregulating *FRO2* and *IRT1* in a FIT-independent manner (Maurer *et al.*, 2011). Considering that salicylic acid, jasmonic acid, ethylene and auxin play key roles in the regulation of the plant immune signaling network (Pieterse *et al.*, 2012), the fact that these hormones also affect Fe uptake responses in plant roots pinpoints a potentially important link between Fe homeostasis and immunity.

Activation of the Fe deficiency response is essential for triggering ISR and affects the composition of the rhizosphere microbiome

WCS417 colonization of the root induces activation of several genes involved in Fe homeostasis (Figure 5) (Zamioudis *et al.*, 2015). The activation of a subset of these genes is essential for WCS417-induced systemic resistance: knockout mutants of either *MYB72* or *BGLU42* do not become resistant upon root colonization by WCS417 or *T. asperellum* T-34 (Van der Ent *et al.*, 2008; Segarra *et al.*, 2009; Zamioudis *et al.*, 2014). Moreover, overexpression of *BGLU42* confers a broad-spectrum resistance to *P. syringae* pv. *tomato, B. cinerea,* and *Hyaloperonospora arabidopsidis* (Zamioudis *et al.*, 2014). Thus, the expression of *BGLU42* is essential for Fe deficiency-induced secretion of phenolic compounds and sufficient for the induction of systemic resistance. It is therefore tempting to speculate that the fluorescent phenolic compounds produced in

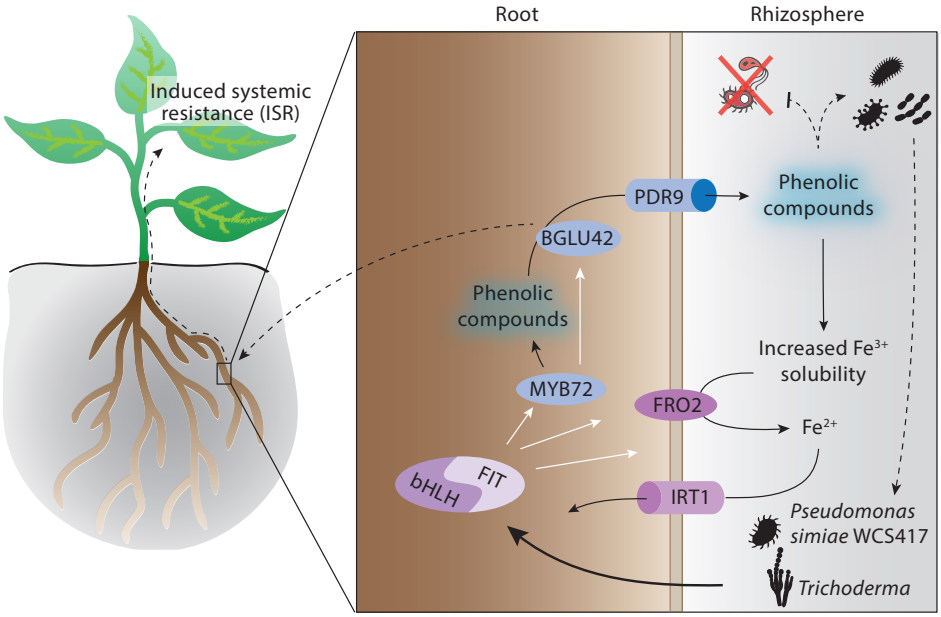

Figure 5 The induction of the Fe deficiency response by Arabidopsis in response to WCS417 might aid WCS417 by exerting antimicrobial effects on other micro-organisms. Schematic representation of root-specific molecular changes triggered by WCS417 and *Trichoderma*. Colonization of the root by these microbes activates the transcription factor gene *MYB72* and the Fe-uptake genes *FRO2* and *IRT1* in a *FIT*-dependent manner. MYB72 regulates the biosynthesis of fluorescent phenolic compounds, which are prepared for secretion into the rhizosphere by the glucose hydrolase BGLU42 and are secreted into the rhizosphere by the ABC transporter PDR9. The antimicrobial activity of some phenolic compounds may play a role in shaping the rhizosphere microbial community. *BGLU42* is required for WCS417-induced systemic resistance. When overexpressed, it confers resistance against a broad spectrum of plant pathogens. Hence, MYB72-dependent *BGLU42* activity in roots is speculated to play a role in the generation of a signal that is transported throughout the plant to induce resistance. In the rhizosphere, the fluorescent phenolic compounds chelate and mobilize Fe^{3+} and make it available for reduction and uptake by the root. Solid lines indicate established processes; dashed lines represent predicted processes. Black arrows indicate a positive effect; white arrows indicate transcriptional activation. Black objects represent beneficial soil microbes, red objects represent pathogenic microbes.

a MYB72-dependent manner and metabolized by the glucose hydrolase activity of BGLU42, function as long-distance signals inducing systemic resistance. Interestingly, similar phenolic compounds are produced in response to root colonization by the plant growth-promoting rhizobacteria *P. fluorescens* SS101 and *Paenibacillus polymyxa* BFKC01 (van de Mortel *et al.*, 2012; Zhou *et al.*, 2016). Activation of the Fe deficiency response in combination with inducing systemic resistance is not specific to WCS417, as *Bacillus subtilis* GB03 and *Trichoderma* spp. also induce systemic resistance and activate the expression of *FIT, IRT1*, and *FRO2* (Ryu *et al.*, 2004; Zhang *et al.*, 2009; Zamioudis *et al.*, 2015; Martínez-Medina *et al.*, 2017).

Several of the phenylpropanoid-derived metabolites secreted in response to both WCS417 and Fe starvation have antimicrobial properties (Shimizu *et al.*, 2000; Dixon, 2001; Kai *et al.*, 2006; El Oirdi *et al.*, 2010; Vogt, 2010; Sun *et al.*, 2014). The coumarin phytoalexin scopoletin is the major *MYB72*- and *BGLU42*-dependent root metabolite (Stringlis *et al.*, 2018a). Scopoletin has antimicrobial effects on the soil-borne fungal pathogens *Fusarium oxysporum* and *Verticillium dahliae*, but has little effect on WCS417 (Stringlis *et al.*, 2018a). Thus, the secretion of this compound seems to select those bacteria that induce growth and systemic resistance.

The selection of specific beneficial rhizobacteria is also observed in the rhizosphere of Fe-stressed red clover plants, which is enriched for siderophore-producing microbes that might help the plant take up Fe (Jin *et al.*, 2010). Microbial siderophores are Fe-chelating low molecular weight organic compounds (500-1500 KDa) that are produced and secreted under Fe-limiting conditions (Miethke and Marahiel, 2007). After chelating Fe in the soil, the Fe-siderophore complexes are recognized and taken up by specific receptors on the microbes and their associated siderophore transporters (Loper and Buyer, 1991; Miethke and Marahiel, 2007; Haas *et al.*, 2008; Berendsen *et al.*, 2015). The presence of siderophore-producing microbes could benefit the plant because Fe bound to microbe-secreted siderophores can in some cases be utilized by plants (Duijff *et al.*, 1994; Chen *et al.*, 1998; Yehuda *et al.*, 2000; Vansuyt *et al.*, 2007; Radzki *et al.*, 2013). Altogether, a picture emerges in which plants create favorable conditions for beneficial microbes in their rhizosphere.

Fe availability affects pathogen virulence

Apart from supplying plants with Fe, the production of high-affinity siderophores by beneficial rhizobacteria can outcompete soil-borne pathogens by depriving them of Fe in the rhizosphere (Figure 6A) (Lemanceau *et al.*, 2009). Low plant iron status can similarly decrease pathogen virulence: the bacterial pathogen *D. dadantii* and the necrotrophic fungus *Botrytis cinerea* are less virulent on Fe-starved Arabidopsis plants due to Fe deprivation (Figure 6B) (Kieu *et al.*, 2012). This dependency on Fe explains why the virulence of several plant pathogens depends on their capacity to secrete siderophores or to take up Fe via other systems (Dellagi *et al.*, 2005; Franza *et al.*, 2005; Oide *et al.*, 2006; Mei *et al.*, 1993; Eichhorn *et al.*, 2006).

In some cases, low plant Fe levels correlate with higher susceptibility to pathogens. For example, the soil-borne fungal pathogen *V. dahliae* and the maize pathogen *Colletotrichum graminicola* cause more disease symptoms in Fe-starved than Fe-sufficient plants (Krikun and Frank, 1975; Barash *et al.*, 1988; Macur *et al.*, 1991; Ye *et al.*, 2014). This effect might be due to Fe-deprived plants mounting a weaker oxidative burst at the site of pathogen infection (Figure 6B) (Ye *et al.*, 2014). In addition, Fe-deficient plants may be more susceptible to pathogen

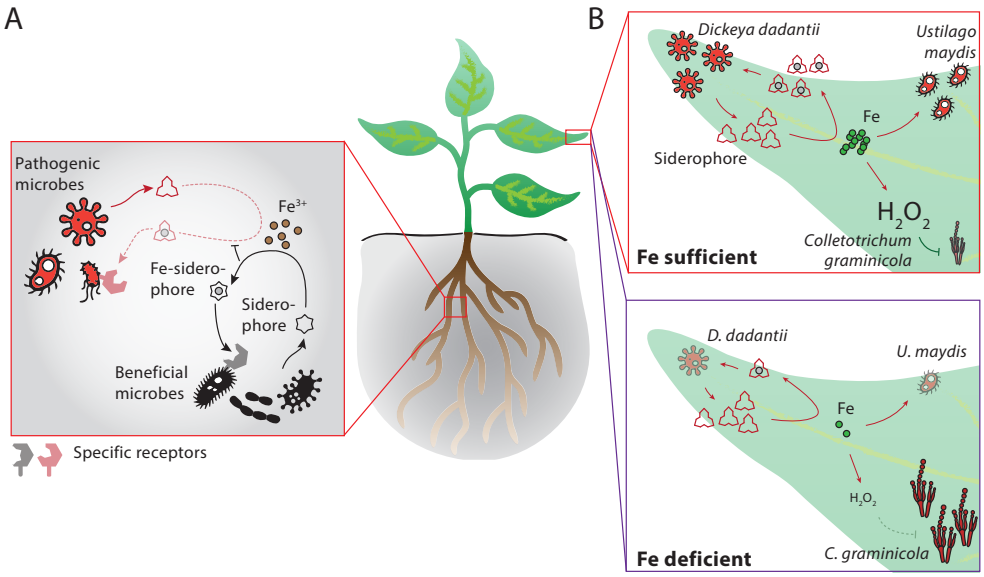

Figure 6 Effects of Fe availability on the virulence of pathogenic microbes. A) In soil, bacteria and fungi compete for available Fe (gray circles) by secreting Fe-chelating siderophores. Once the siderophores have bound Fe (Fe-siderophore), they can be taken up upon recognition by specific receptors. By producing siderophores with high Fe affinity, beneficial microbes can outcompete pathogenic microbes that produce siderophores with a lower Fe affinity. B) Fe availability influences the interaction between plants and foliar pathogens. The plant pathogens *Dickeya dadantii* and *Ustilago maydis* cause more disease on plants grown under Fe-sufficient conditions (top panel) than on plants grown under Fe-deficient conditions (bottom panel), because their virulence requires sufficient Fe uptake. In contrast, high Fe availability in the host can favor the development of an oxidative burst (symbolized by the size of 'H_2O_2'), thereby increasing defense against pathogens such as *Colletotrichum graminicola*. Solid lines and arrows indicate stronger activity of the indicated process than do dotted lines and arrows. Black, red, and green objects and arrows indicate beneficial microbes, pathogens, or plants and their processes, respectively.

attack because Fe-starvation induces pathogens to produce more toxic compounds. For example, the production of the virulence factor exotoxin by the opportunistic human pathogen *Pseudomonas aeruginosa* is dependent on the secretion of the Fe-starvation regulated siderophore pyoverdine (Lamont *et al.*, 2002). Similarly, pyoverdine produced by the tobacco plant pathogen *Pseudomonas syringae* pv. *tabaci* 6605 in response to Fe starvation controls the production of tabtoxin, a toxin that induces chlorosis in the leaves of its host (Taguchi *et al.*, 2010).

Redistribution of Fe within the plant in response to pathogen attack

Arabidopsis induces the expression of the Fe storage gene *FERRITIN1* (*FER1*) upon perception of the bacterial siderophores of *D. dadantii* (Dellagi *et al.*, 2005). Mutant *fer1* plants are more susceptible to *D. dadantii* (Dellagi *et al.*, 2005), suggesting that Fe sequestration by FERRITINS is part of an Fe-withholding defense strategy that is induced in response to pathogen invasion. In the same pathosystem, the pathogen's siderophores and its toxin chrysobactin stimulate the production of the defense hormone salicylic acid in the host, resulting in several defense

responses, including the induction of the *PATHOGENESIS-RELATED* defense marker gene *PR-1,* callose deposition along the leaf veins, and accumulation of hydrogen peroxide, resulting in an oxidative burst (Dellagi *et al.*, 2005, 2009; Aznar *et al.*, 2014). Interestingly, application of this leaf pathogen or its siderophores on shoots induces the expression of *FRO2* and *IRT1* in the roots, suggesting that microbe-induced changes in Fe homeostasis mechanisms can be systemic (Dellagi *et al.*, 2009; Segond *et al.*, 2009; Aznar *et al.*, 2014). Redistribution of plant Fe upon pathogen attack is also observed in other plant species. Attack of wheat leaves by the powdery mildew fungus *Blumeria graminis* f. sp. *tritici* leads to redistribution of Fe^{3+} to the apoplast of epidermal leaf cells, where it induces a defensive oxidative burst. The ensuing Fe deficiency in the cytosol of the epidermal cells induces the expression of *PR-1* (Liu *et al.*, 2007).

Concluding remarks

Plant roots are surrounded by billions of rhizobacteria, including beneficial rhizobacteria that increase plant growth and resistance (Lugtenberg and Kamilova, 2009; Pieterse *et al.*, 2014). Multiple beneficial rhizobacteria are known to affect plant root system architecture (Vacheron *et al.*, 2013; Verbon and Liberman, 2016). As root system architecture is a significant determinant of crop yield (Uga et al., 2013; Ning et al., 2014; Ogawa et al., 2014; Koevoets et al., 2016), further study of these changes might uncover signaling modules that positively affect plant growth.

In addition, some rhizobacteria mediate ISR (Pieterse *et al.*, 2014). Recently, it became clear that the induction of increased resistance by several beneficial rhizobacteria requires bacteria-mediated induction of the Fe deficiency response (Segarra *et al.*, 2009; Zamioudis *et al.*, 2015; Martínez-Medina *et al.*, 2017). Fe availability was already a recurrent theme in the research field of plant-microbe interactions over the past decades. An effect of Fe on plant-microbe interactions was first observed in disease suppressive soils, where siderophore-mediated competition for Fe between beneficial micro-organisms and soil-borne pathogens was identified as an important mechanism by which plant disease was suppressed (Kloepper *et al.*, 1980; Lemanceau *et al.*, 1988). In addition, Fe availability has been shown to influence plant resistance to pathogen attack (Aznar *et al.*, 2015b; Verbon *et al.*, 2017). As Fe seems to be a central player in the complex interplay between beneficial rhizobacteria, plants and pathogens, research into this interplay will enhance our understanding of plant immunity, root development and plant growth.

Thesis outline

In this thesis, we aimed to increase our understanding of the Arabidopsis root response to the beneficial rhizobacterium WCS417. In response to WCS417, Arabidopsis increases the number of lateral roots and root hairs (Zamioudis *et al.*, 2013). As root system architecture is recognized to be of crucial importance for plant fitness (Rogers and Benfey, 2015; Koevoets *et al.*, 2016), these changes might be essential for the establishment of the WCS417-mediated enhanced plant growth. To understand how the root architecture changes are established, we studied cell type-specific transcriptional changes in the Arabidopsis root in response to WCS417 in Chapter 2. We show that cell wall biosynthesis is decreased in specifically the endodermis and the cortex. Cell volume loss in the endodermis and cortex is required for lateral root initiation and emergence (Vermeer *et al.*, 2014). Possibly, the decrease in cell wall biosynthesis results in such cell volume loss, and thus allows for lateral root formation. In addition, we find increased

expression of genes required for suberin biosynthesis in the endodermis. Future research will need to determine whether suberin biosynthesis is indeed increased and how this affects the outcome of this plant-rhizobacterium interaction.

WCS417 is known to induce the Fe deficiency response (Zamioudis *et al.*, 2014, 2015; Stringlis *et al.*, 2018a). In Chapter 3 we study the effect of WCS417 on Arabidopsis Fe homeostasis. We show that increased Fe uptake upon root colonization by WCS417 is essential to prevent severe chlorosis as a result of WCS417-mediated plant growth promotion. Activation of the Fe deficiency response upon Fe limitation is known to be mediated by shoot-to-root signaling pathways (Stacey *et al.*, 2008; Grillet *et al.*, 2018). We show that the shoot is also required for WCS417-mediated induction of the Fe deficiency response, but our results indicate that the induction is not due to an increased Fe demand from the shoot. We hypothesize that plants activate the Fe deficiency response upon perception of a growth-promoting signal to prevent an Fe shortage.

Previously, activation of the Fe deficiency response genes *MYB72* and *BGLU42* was shown to be required for WCS417-mediated ISR. Fe deficiency in itself is also known to decrease plant disease, although the mechanism is unknown (Kieu *et al.*, 2012). In Chapter 4 we studied Fe deficiency-induced resistance. Our results are the first proof for an active role of the plant defense response in the decreased virulence of some pathogens on Fe deficient plants. The results suggest that Fe deficiency primes the plant defense response for a stronger or faster response to pathogen attack. This mechanism is similar to the mechanism of WCS-mediated ISR. We therefore studied whether these resistances are activated by the same molecular pathways in the root. We show that Fe deficiency-induced resistance does not require *MYB72* and *BGLU42*, indicating that Fe deficiency-induced resistance and WCS417-mediated ISR are not activated by the same root signaling pathways.

Finally, in Chapter 5 we describe how we set up translating ribosome affinity purification (TRAP) (Zanetti *et al.*, 2005) to study the Arabidopsis root response to Fe deficiency and root colonization by micro-organisms. Using this method, we studied the difference between the transcriptional and the translational response to Fe deficiency. Preliminary data analyses suggest that translational control selectively recruits a subset of up-regulated mRNA molecules, thereby adding an additional level of regulation to the Fe deficiency response. In addition, we show preliminary TRAP data of plant roots exposed to beneficial rhizobacteria, opening up exciting new avenues for future research.

In Chapter 6 we discuss our results in light of the current knowledge on plant-microbe interactions, plant immunity and Fe homeostasis.

Chapter 2

Cell type-specific gene expression changes orchestrate root system architecture modifications in response to beneficial rhizobacteria

Eline H. Verbon[1*], Louisa M. Liberman[2,3*], Cara Winter[2,3], Corné M.J. Pieterse[1], Philip N. Benfey[2,3], Ronnie de Jonge[1]

[*]These authors contributed equally to this work

[1]Plant-Microbe Interactions, Utrecht University, Department of Biology, The Netherlands
[2]Howard Hughes Medical Institute, Duke University, Durham, NC 27708, USA
[3]Department of Biology and HHMI, Duke University, Durham, NC 27708, USA

Abstract

Growth-promoting rhizobacteria hold great promise in agriculture for improving plant growth and health while reducing the use of synthetic fertilizers and pesticides. *Pseudomonas simiae* WCS417 is a well-studied growth- and resistance-promoting rhizobacterium that promotes growth and induces resistance in the model plant *Arabidopsis thaliana* (Arabidopsis). In response to root colonization by WCS417, Arabidopsis changes its root system architecture, among other things by increasing the number of lateral roots. To understand how root changes are established, we studied cell type-specific transcriptional changes within the Arabidopsis root in response to WCS417. We used fluorescence-activated cell sorting (FACS) and subsequent RNA sequencing to profile gene expression of five Arabidopsis root cell types two days after whole-root colonization by WCS417. We identify gene signatures indicating reduced cell wall biosynthesis and increased cell wall disassembly in the cortex and endodermis. A resulting reduction in cell wall deposition might allow cells in these cell layers to lose volume, a morphological change required for lateral root emergence and initiation. In addition, transcriptomic changes in the endodermis suggest increased suberin biosynthesis in this cell type. Increased suberin deposition could change root exudate patterns or restrict microbial entry into the root. Both lateral root number and suberization are known to be induced by changes in nutrient availability. Therefore, these changes might be induced in response to WCS417-mediated changes in nutrient availability or plant nutrient requirements. Finally, a detailed analysis of the different responses of the two cell types in the epidermis to WCS417 provides transcriptomic proof for the functional specialization of the two epidermal cell types. The untreated trichoblast gene expression signature revolves around growth and nutrient uptake, whereas that of atrichoblasts revolves around defense. Possibly, Arabidopsis physically separates the two main functions of the epidermis, defense and nutrient uptake, to ensure that they do not interfere with each other.

Introduction

Plants are sessile organisms that cannot move in response to changes in environmental conditions. Instead, they adapt to such changes by modifying their morphology. Modifications in the spatial configuration of roots, the root system architecture, are especially important as they allow plants to optimize water and nutrient uptake (Rogers and Benfey, 2015; Koevoets *et al.*, 2016; Li *et al.*, 2016; Shahzad and Amtmann, 2017). The root system of the model plant *Arabidopsis thaliana* (Arabidopsis) consists of a primary root with branching lateral roots (Petricka *et al.*, 2012; Motte *et al.*, 2019). Different environments have distinct effects on Arabidopsis root growth: in dry soils primary root growth increases to reach deeper-lying water sources, in phosphorus-limited soils the number of lateral roots and root hairs increases to expand the root system's exploratory capacity, and in response to iron (Fe), zinc or manganese deficiency the root partly breaks down protective barriers to increase nutrient uptake (Gilroy and Jones, 2000; Müller and Schmidt, 2004; Vishwanath *et al.*, 2015; Barberon *et al.*, 2016; Salazar-Henao *et al.*, 2016; Barberon, 2017).

Interestingly, plants also adapt their root system architecture in response to beneficial soil micro-organisms (Vacheron *et al.*, 2013; Li *et al.*, 2016; Verbon and Liberman, 2016), with Arabidopsis increasing either or both the number and length of lateral roots and root hairs in response to a diverse set of rhizobacteria and fungi (López-Bucio *et al.*, 2007; Contreras-Cornejo *et al.*, 2009; Felten *et al.*, 2009; Splivallo *et al.*, 2009; Zamioudis *et al.*, 2013; Khan *et al.*, 2016; Asari *et al.*, 2017; Huang *et al.*, 2017; Vacheron *et al.*, 2018). Notably, an increase in lateral root number is often accompanied by a decrease in primary root growth (López-Bucio *et al.*, 2007; Splivallo *et al.*, 2009; Vacheron *et al.*, 2013; Zamioudis *et al.*, 2013). A well-studied example of a beneficial rhizobacterium is *Pseudomonas simiae* WCS417 (Zamioudis *et al.*, 2013; Berendsen *et al.*, 2015). WCS417 stimulates Arabidopsis growth (Zamioudis *et al.*, 2013) and induces systemic resistance against a broad range of pathogens in both Arabidopsis and several crop species (Van Peer *et al.*, 1991; Leeman *et al.*, 1995; Pieterse *et al.*, 1996; Duijff *et al.*, 1998). In response to WCS417, Arabidopsis decreasies primary root growth and increases the number of lateral roots and root hairs (Zamioudis *et al.*, 2013). Since a root system with a greater surface area can mine more soil for nutrients, the induction of lateral root and root hair growth has been hypothesized to contribute to the plant growth-promoting properties of plant growth-promoting rhizobacteria (PGPR). In addition, the resulting expansion of root surface enlarges the area that can be colonized by the PGPR. Root system architecture changes might therefore contribute to the evolutionary advantage of the mutualistic interaction for both the plants and the PGPR involved.

The increased number of lateral roots in response to WCS417 is due to an increase in lateral root initiation events, observed as an increased number of lateral root primordia and increased outgrowth of these primordia (Zamioudis *et al.*, 2013). In Arabidopsis, lateral roots originate from the pericycle cells, a cell layer that surrounds the innermost tissues of the root, the vasculature (Malamy and Benfey, 1997; Du and Scheres, 2018). Select pericycle cells are primed for lateral root initiation in the root tip (Möller *et al.*, 2017; Ötvös and Benková, 2017). A subset of the primed pericycle cells is subsequently specified as lateral root founder cells, which can undergo several rounds of anticlinal and periclinal cell divisions to form the lateral root primordium: a dome-shaped structure that protrudes towards the outside of the root. Further cell divisions and growth ultimately result in a lateral root that passes through the three neighboring cell

files, the endodermis, the cortex, and finally the epidermis, to emerge from the primary root (Malamy and Benfey, 1997; Möller *et al.*, 2017; Ötvös and Benková, 2017; Du and Scheres, 2018). The plant hormone auxin is important for all phases of lateral root development (Du and Scheres, 2018), which might explain why the increase in lateral root number in response to WCS417 is dependent on functional auxin signaling (Zamioudis *et al.*, 2013).

Like the WCS417-mediated increase in lateral root number, the WCS417-mediated increase in root hair number is dependent on functional auxin signaling (Zamioudis *et al.*, 2013). In Arabidopsis, root hairs are formed by specialized cells in the epidermis, the trichoblasts. Together with cells of the other cell type in the epidermis, the atrichoblasts, they form the outermost cell layer of the Arabidopsis root (Gilroy and Jones, 2000; Schiefelbein, 2000; Ryan *et al.*, 2001). Trichoblasts and atrichoblasts are descendants from the same stem cells in the Arabidopsis root tip (Petricka *et al.*, 2012; Motte *et al.*, 2019). Cell fate specification into trichoblasts or atrichoblasts is controlled by the activity of several transcription factors, including TRANSPARENT TESTA GLABRA (TTG), GLABRA3 (GL3), ENHANCER OF GLABRA 3 (EGL3) and WEREWOLF (WER), and is dependent on the spatial localization of the cells, with cells located over two cortical cells (H position) becoming trichoblasts (Salazar-Henao *et al.*, 2016; Wei and Li, 2018). In response to WCS417, the increased number of root hairs is due to an increased number of cortical cells and therefore an increased number of cells becoming trichoblasts (Zamioudis *et al.*, 2013).

As is clear from the formation of root hairs and lateral roots, the structure of the Arabidopsis root system is defined by the distinct biological functions of each of the Arabidopsis root cell types. Therefore, studying cell type-specific transcriptome changes has the potential to greatly increase our understanding of the effects of WCS417 on the Arabidopsis root. We used an array of fluorescent marker lines to isolate trichoblast, atrichoblast, cortical, endodermal and vasculature cells with fluorescence-activated cell sorting (FACS) (Birnbaum *et al.*, 2003, 2005; Brady *et al.*, 2007a). Transcriptome analysis of the RNA obtained from the cell type-enriched samples allowed us to trace the transcriptomic changes upon PGPR colonization in a unique, spatially-oriented manner. Our data suggest that morphological changes in the cortex and endodermis in response to WCS417 promote lateral root formation. Interestingly, the endodermis increases suberin biosynthesis in response to WCS417. Further research will need to show whether suberin biosynthesis is indeed enhanced and if so, whether it is enhanced as a defense response, or in response to WCS417-mediated changes in nutrient availability or uptake. Finally, our transcriptomic data corroborate the functional specialization of the trichoblasts for nutrient uptake and suggest that untreated atrichoblasts may specialize in defense.

Materials and methods

Plant material and growth conditions. Arabidopsis accession Columbia-0 (Col-0) and transgenic Col-0 with the *COBRA-LIKE9*$_{pro}$*:GFP* (Brady *et al.*, 2007a; b), *WEREWOLF*$_{pro}$*:GFP* (Lee and Schiefelbein, 1999), *315*$_{pro}$*:GFP* (Lee *et al.*, 2006), *SCARECROW*$_{pro}$*:GFP* (Wysocka-Diller *et al.*, 2000), or *WOODENLEG*$_{truncated\_pro}$*:GFP* construct (Mähönen *et al.*, 2000) were grown as described previously (Dinneny *et al.*, 2008). Briefly, seeds were liquid sterilized in 50% bleach and stratified by incubation at 4°C for 2 days. Sterilized seeds were plated in two dense lines of three seeds thick each on nylon mesh (Nitex Cat 03-100/44, Sefar) on sterile 1x Murashige and Skoog medium (MS; (Murashige and Skoog, 1962)) 1% sucrose plates. Plates were sealed with Parafilm and placed vertically in long-day conditions (8-h night, 16-h day; 22^{0}C).

WCS417 treatment. Seedlings were inoculated with bacteria using a slightly adapted version of a previously published protocol (Zamioudis *et al.*, 2015) five days after seeds were plated. Briefly, rifampicin-resistant WCS417 was streaked from a frozen glycerol stock onto solid King's medium B (KB) (King *et al.*, 1954) containing 50 µg/ml rifampicin and grown at 30°C overnight. A day before plant treatment, a single colony from the plate was put in liquid KB with rifampicin and grown in a shaking incubator at 30°C overnight. The following morning, the bacterial suspension was diluted in fresh KB with rifampicin and grown in a shaker until the suspension reached an OD_{600} value between 0.6 and 1.0, after which the bacteria were washed twice with 10 mM $MgCl_2$.

To decide which bacterial concentration to add to the plants, the washed bacteria were resuspended in 10 mM $MgCl_2$ to a final density ranging from 10^1 to 10^8 / µl. Two horizontal lines of either 10 µl of 10 mM $MgCl_2$ or 10 µl of one of the bacterial dilutions were applied per 1x MS 1% sucrose plate. Five-day-old Col-0 seedlings were transferred on their mesh onto these plates. Seedlings were transferred such that the roots of the seedlings were on top of the bacteria. Finally, all plates were resealed with Parafilm and left to grow in long-day conditions. At 2 and 7 days after treatment, ten plants from each treatment were randomly picked and removed from the plate. The total number of emerged lateral roots was counted under a stereo microscope. ImageJ was used to determine primary root length per plant from images made with a scanner.

Based on the results of this trial, we chose a density of 10^6 bacteria / µl, amounting to 10^7 bacteria per row of plants, for the sorting experiment (see below). Wild-type Col-0 plants and plants of each of the five transgenic lines were exposed to this bacterial density after 5 days of plant growth as described above and left in long-day growth conditions for a further 2 days.

Fluorescence-activated cell sorting. After a total of 7 days of growth, roots were cut from the shoot with a carbon steel surgical blade. Whole roots of Col-0 destined for the unsorted control were immediately frozen in liquid N_2 in one Eppendorf tube per plate. For the other samples, all to be put through a cell sorter, roots were cut twice more and the root pieces from 4 - 6 plates were collected and protoplasted as described previously (Birnbaum *et al.*, 2003, 2005). Briefly, they were placed in a 70-µm cell strainer submerged in enzyme solution (50 ml 600 mM mannitol, 2 mM $MgCl_2$, 0.1% BSA, 2 mM $CaCl_2$, 2 mM MES, 10 mM KCl, pH 5.5 with 0.75 g cellulysin and 0.05 g pectolyase per 50 ml). Roots were mixed in the strainer at room temperature (RT) on an orbital shaker to dissociate protoplasts. After one hour, the suspension surrounding the strainer, containing the protoplasts, plus a few roots to pull the protoplasts down, were pipetted into a 15-ml conical tube and spun at 200 rcf for 6 min at RT. The top of the supernatant was pipetted off and the remaining solution resuspended in 700 µl of the protoplasting solution without enzymes (50 ml 600 mM mannitol, 2 mM $MgCl_2$, 0.1% BSA, 2 mM $CaCl_2$, 2 mM MES, 10 mM KCl, pH 5.5). This suspension was filtered through a 70-µm cell strainer and a 40-µm strainer. The filtrate was collected in a cell sorting tube and taken to the cell sorter (Astrios, Beckman Coulter) at RT.

Protoplasts sorted by the cell sorter were collected into RLT buffer (Qiagen) with β-mercaptoethanol. The samples were immediately placed on dry ice to inhibit RNA degradation. Samples were stored at -80°C until RNA isolation.

RNA isolation and sequencing. Whole root tissue for the unsorted control was lysed by grinding with a liquid-nitrogen-cooled mortar and pestle. RNA was isolated with the RNeasy Plant Mini Kit (Qiagen) for the six unsorted whole root samples and for six out of eight mock-sorted whole root samples. RNA from the remaining two sorted whole root samples and all cell type-enriched samples were isolated with the Micro Kit (Qiagen). RNA concentration was checked with a Qubit Fluorometer (Thermo Scientific) and total RNA integrity was assessed with a Bioanalyzer (Agilent Technologies). Subsequently, RNA libraries were made from samples with RNA integrity number (RIN) values above six. All libraries were made with the NEBNext Ultra RNA Library Prep Kit for Illumina (NEB). 100 ng of total RNA was poly-A selected using Dynal Oligo-dT beads for the six unsorted whole root samples and the first six mock-sorted whole root samples. The remaining libraries were generated from total RNA selected using NEBNext Oligo-dT beads. Because of limited RNA yields from some of the sorted-cell populations, 50 ng of total RNA was used as starting material for all sorted library preparations. Libraries were sequenced on an Illumina HiSeq 2500 using 50 base pair Single-Read (Duke University Sequencing Core). Three biological replicates were performed for each sample type and condition, except for the sorted control, for which we performed four biological replicates (Table S1).

Data analysis. The reads generated by Illumina sequencing were pseudoaligned to the TAIR10 cDNA database (Lamesch *et al.*, 2012) using Kallisto (v0.43.0) with 100 bootstraps and default settings (Bray *et al.*, 2016). The percentage of aligned reads was lower for the twelve samples that were poly-A selected using Dynal Oligo-dT beads because of a high number of rRNA sequences. This is probably due to differences in the bead-selection procedure and greater amount of RNA used as starting material. We do not expect this to interfere with our analyses, as the number of expressed genes in these samples is in the same range as previously published data in this species. The resulting transcript counts were summarized to the gene level with tximport (v1.2.0) (Soneson *et al.*, 2015). One bacteria-exposed sample enriched for trichoblasts was excluded from further analyses because of low coverage. Only genes with a count per million (cpm) greater than two in at least three samples were kept for analysis. The counts per gene of the remaining samples and genes were used to generate a digital gene expression list (DGE list) in EdgeR (v3.16.5) (Robinson *et al.*, 2010). A generalized linear model (glm) was fit using a negative binomial model and quasi-likelihood (QL) dispersion estimated from the deviance with the glmQLFit function in EdgeR. Differentially expressed genes were then determined by comparing the bacteria-exposed and the non-exposed samples with the glmQLFTest (FDR < 0.1; $-2 < \log_2 FC > 2$). GO term analysis was performed in R based on the genome wide annotation for Arabidopsis within org.At.tair.db (Carlson M, 2018) with the program GOstats (Falcon and Gentleman, 2007).

Fluorescence microscopy. Approximately 20 sterilized and vernalized seeds of the *COBL9pro:GFP*, *WERpro:GFP*, *315pro:GFP*, *SCRpro:GFP*, and *WOLtruncated_pro:GFP* transgenic lines were sown on a 1x MS 1% sucrose plate and placed in long-day conditions. After five days either 10^5 WCS417 cells in 10 µl $MgCl_2$ or sterile 10 µl $MgCl_2$ were inoculated onto each root tip. GFP localization was observed once per day in 5, 6 and 7-day-old seedlings with a 510 upright confocal microscope (Zeiss).

GLYCEROL-3-PHOSPHATE ACETYLTRANSFERASE 5pro:citrine (*$GPAT5_{pro}$:citrine*) plants (Barberon *et*

al., 2016) were grown on 1x MS plates in long-day conditions. After 5 days, WCS417 bacteria were washed in $MgCl_2$ and 10^5 bacteria were inoculated onto each root tip. Fluorescence was checked with a 510 upright confocal microscope (Zeiss) at 2 days after inoculation.

Data accessibility. Analysis scripts and the supplementary tables are part of the Online Supplementary Material and can be found here: https://cp.sync.com/dl/60fe897a0#fqt4xv25-em3ineic-y792dq3h-qrydpq97.

Results

Pseudomonas simiae WCS417 induces root developmental changes

PGPR are known to affect plant root system architecture (Vacheron *et al.*, 2013; Li *et al.*, 2016; Verbon and Liberman, 2016). Indeed, WCS417 decreased primary root length and increased the total number of lateral roots after seven days of co-inoculation (Figure 1). Interestingly, the effect on root system architecture is dose-dependent: two days after co-inoculation we only see increased formation of lateral roots when 10^7 or more bacteria were applied per row of plants (Figure 1). This is in line with previous results showing a dose-dependency of PGPR-

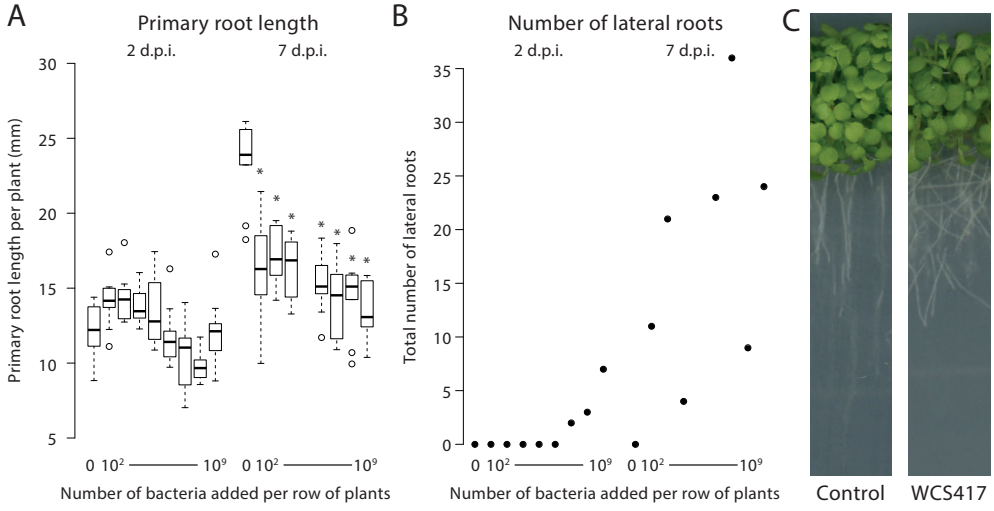

Figure 1 The effect of root colonization by WCS417 on Arabidopsis root system architecture. A) Quantification of primary root length at two and seven days post inoculation (d.p.i) with increasing concentrations of WCS417. Asterisks represent a significant difference compared to the control at the same time point (ANOVA, post hoc Tukey $P < 0.05$). B) The total number of lateral roots of ten seedlings two and seven days after inoculation with increasing concentrations of WCS417. C) Pictures of plants in the densely-sown set-up six days after application of a mock solution or a solution containing 10^7 bacteria per row of plants. Col-0 Arabidopsis plants were grown on 1x MS 1% sucrose for five days. After five days, seedlings were transferred to plates inoculated with 10 µl 10 mM $MgCl_2$ containing no, 10^2, 10^3, 10^4, 10^5, 10^6, 10^7, 10^8 or 10^9 WCS417. Ten plants were randomly removed from each plate at two and seven days after application. The total number of lateral roots of the ten seedlings was counted under a stereo dissecting microscope. Next, the plants were photographed with a scanner. Primary root length of the seedlings was measured in ImageJ from these pictures.

mediated increases in plant growth and resistance to disease (Raaijmakers *et al.*, 1995; Ryu *et al.*, 2003; Farag *et al.*, 2013; Asari *et al.*, 2017).

Cell type-specific transcriptional profiling of the Arabidopsis root

To create a spatial map of the Arabidopsis root transcriptional changes in response to whole root colonization by WCS417, we analyzed the transcriptomes of select root cell types using FACS. First, we confirmed that WCS417 does not affect the expression pattern of *GREEN FLUORESCENT PROTEIN* (*GFP*) when driven by the cell type-specific *WEREWOLF* promotor (*WER*; atrichoblast), *COBRA-LIKE9* promotor *(COBL9*; trichoblast), *315* promotor (cortex), *SCARECROW* promotor (*SCR*; endodermis), or truncated *WOODENLEG* promotor (*WOL*; vasculature) (Figure 2A). Subsequently, we grew the transgenic lines carrying these promotor-GFP fusions at a high density and exposed them to WCS417. Two days after inoculation with WCS417, we harvested the roots, performed FACS and isolated RNA (Figure 2B).

To determine whether the sorting procedure was succesful, we checked the expression of the marker genes *WER*, *COBL9*, *315*, *SCR* and *WOL* in our transcriptomic dataset (Figure 3A). In case of a succesful sorting procedure, the expression of each of these markers should be highest in the FACS samples obtained from the transgenic plant lines in which the corresponding promotor was used to drive *GFP* expression. Indeed, the expression of *WER*, *COBL9*, *315* and *SCR* is highest in the samples obtained from the WER_{pro}:*GFP*, $COBL9_{pro}$:*GFP*, 315_{pro}:*GFP* and SCR_{pro}:*GFP* lines, respectively (Figure 3B). The expression of *WOL*, in contrast, is not higher in the samples isolated from the $pWOL_{truncated\_pro}$:*GFP* line. However, the expression of other well-established vasculature marker genes, namely *INCURVATA4* and *SHORTROOT (SHR)*, is correctly enriched in these samples (Figure 3C). This suggests that only the truncated *WOL* promotor, and not the full promotor, is cell type-specific.

To study the global similarities and dissimilarities among samples and treatments, we performed multidimensional scaling on gene expression levels. The transcriptional profiles cluster by sample type ($P_{sample\ type} = 0.001$; Figure 3D). The cortical and endodermal cells cluster close together, as do the two epidermal cell types. This is in line with the known development of the Arabidopsis root, in which the cortex and endodermis develop from a shared stem cell population, as do the trichoblasts and atrichoblasts (Dolan *et al.*, 1993; Van den Berg *et al.*, 1995). In addition to the sample-type effect, we find an effect of bacterial treatment on gene expression ($P_{treatment} = 0.005$; Figure 3D). When comparing gene expression patterns of samples within sample types, each cell type except the vasculature clusters primarily based on bacterial treatment (Figure 3E).

Next, we determined which genes are differentially expressed (DEGs) in response to WCS417 in each of the cell types (Table S2). The number of DEGs upon WCS417 colonization differs greatly between the cell types, ranging from 30 DEGs in the vasculature to 1,109 DEGs in the cortex (Figure 4A). Apart from a quantitative difference, the response is also qualitatively different between cell types: of the 1,862 DEGs across all five cell types, 72% are affected in only one cell type and only six genes are affected in all cell types (Figure 4B). Notably, the majority of genes affected in a single cell type is not identified as differentially expressed in the whole root, while most genes affected in four or five cell types are identified as up-regulated in whole roots (Table 1). The same trend is observed for down-regulated genes (Table S3). Vice versa, the majority of the genes found to be up- or down-regulated in the sorted or unsorted control were

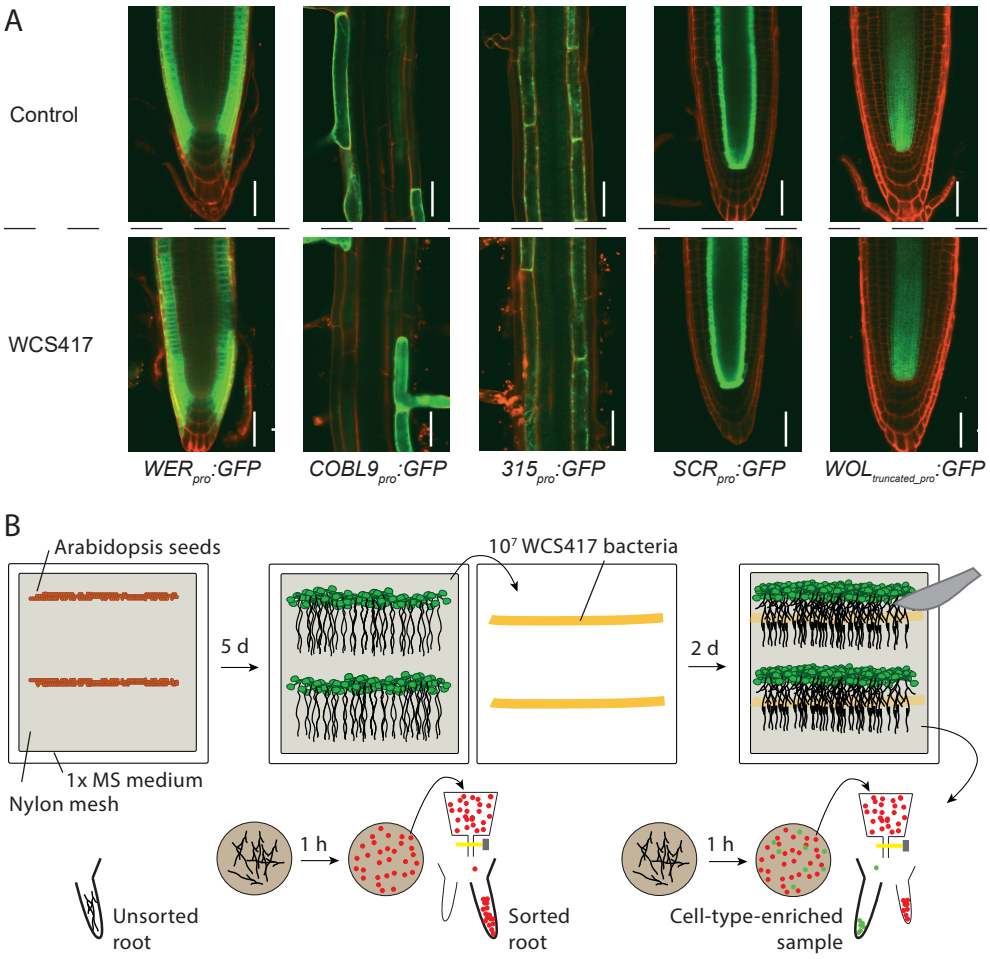

Figure 2 Exposure of five transgenic plant lines to WCS417 to obtain cell type-specific samples with fluorescence-activated cell sorting (FACS). A) Sterile and WCS417-exposed plants from the transgenic plant lines *WEREWOLFpro:GFP* (*WER*: immature epidermis and atrichoblast), *COBRA-LIKE9pro:GFP* (*COBL9*: trichoblast), *315pro:GFP* (*315*: cortex), *SCARECROWpro:GFP* (*SCR*: endodermis), and *WOODENLEGtruncated_pro:GFP* (*WOL*: vasculature). Seeds were sown non-densely on 1x MS 1% sucrose plates. After five days of growth,10 µl of a bacterial suspension with an OD_{600} value of 0.01 (10^7 colony forming units (cfu) / ml) or a mock solution of $MgCl_2$ was added to each root. Pictures of the seedlings were taken all along the root with a 510 upright confocal microscope (Zeiss) from day five (day of bacterial inoculation) to day seven. GFP settings were kept the same between bacteria-exposed and sterile-grown plants. Representative images are shown. Scale bars respresent 50 µm. B) Experimental design used to obtain control and WCS417-treated whole root samples and samples enriched for specific cell types. Sterilized and vernalized Col-0 Arabidopsis seeds were sown on 1x MS 1% sucrose plates. Five days later, half of the plants was transferred on their mesh onto MS plates with 10^7 cfu WCS417 per row of plants. Plants were left to grow for a further two days of growth before root harvest. Wild-type roots were either directly flash-frozen (unsorted control) or protoplasted and put through the cell sorter while collecting non-fluorescent cells (sorted control). Transgenic lines with cell type-specifc *GFP* expression were similarly protoplasted and put through the cell sorter to obtain cell type-enriched samples with fluoresence-activated cell sorting (FACS).

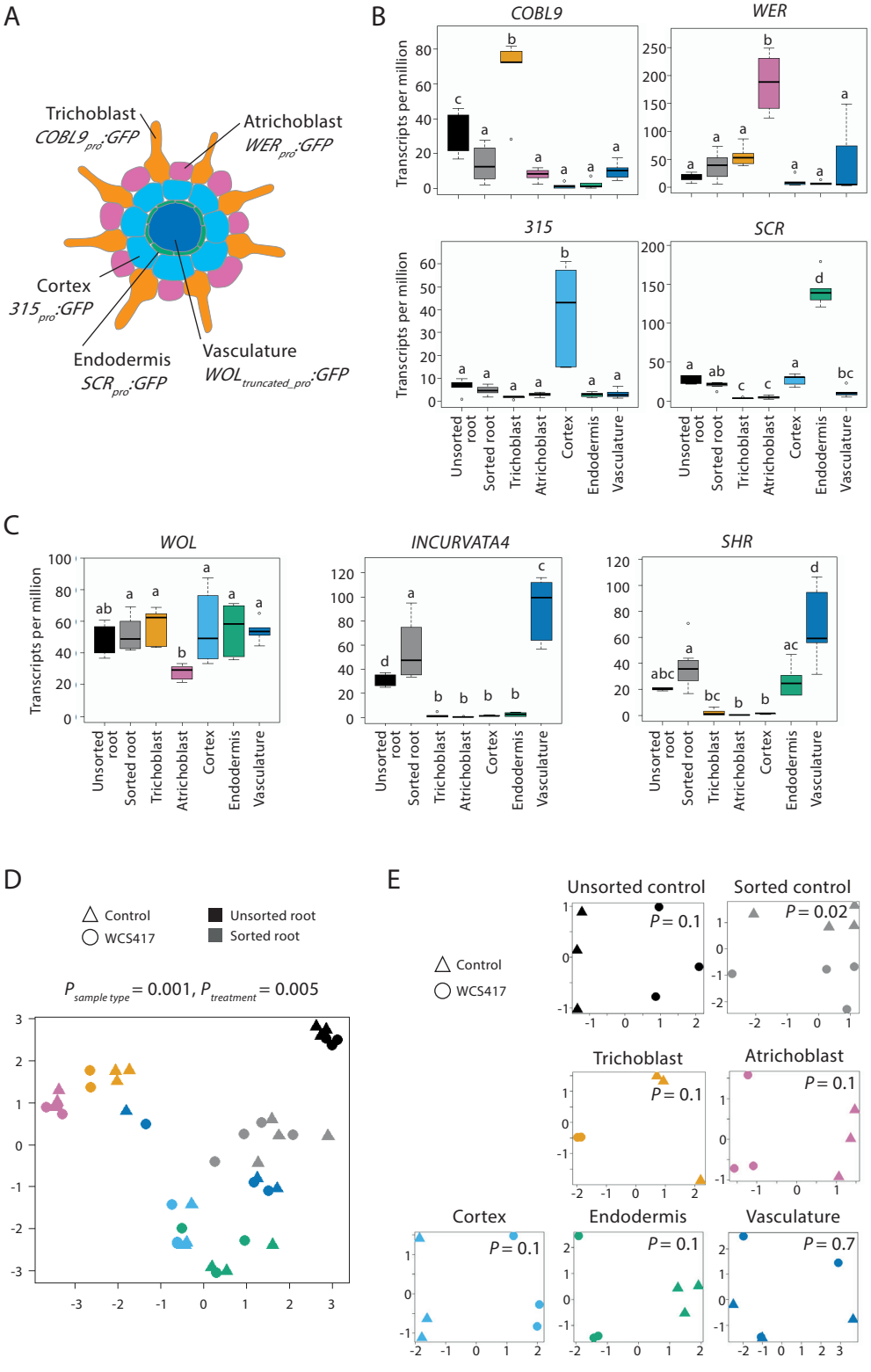
A
Trichoblast
COBL9pro:GFP
Atrichoblast
WERpro:GFP
Cortex
315pro:GFP
Endodermis
SCRpro:GFP
Vasculature
WOLtruncated_pro:GFP
B
COBL9
WER
315
SCR
Transcripts per million
Unsorted root
Sorted root
Trichoblast
Atrichoblast
Cortex
Endodermis
Vasculature
C
WOL
INCURVATA4
SHR
D
Control
WCS417
Unsorted root
Sorted root
P sample type = 0.001, P treatment = 0.005
E
Unsorted control
Sorted control
Trichoblast
Atrichoblast
Cortex
Endodermis
Vasculature
P = 0.1
P = 0.02
P = 0.7

Table 1 Genes up-regulated in single cell types are lost in whole root analyses

	Number of up-regulated genes	% shared with sorted control	% shared with unsorted control
Up in all cell types	6	100	67
Up in four out of five cell types	19	68	37
Up in trichoblast only	42	10	7
Up in atrichoblast only	9	0	0
Up in cortex only	337	3	2
Up in endodermis only	224	6	0
Up in vasculature only	1	100	0

identified as differentially expressed in one or more cell types (Table S4). In conclusion, genes affected in single cell types are often not identified as differentially expressed in the whole root. This explains the higher number of identified differentially expressed genes in the cell type-specific data set compared to the sorted whole root (1,862 genes versus 270 genes; Figure 4A) and suggests that cell type-specific profiling revealed details of the transcriptional response to bacteria that would have been missed with whole root profiling.

Distinct specializations of the trichoblasts and atrichoblasts

To obtain a broad overview of the biological processes affected by WCS417 colonization, we conducted biological process gene ontology (GO) term enrichment analyses on the DEGs (Table S5-S14). Most significant among the up-regulated DEGs in the trichoblasts, cortex, endodermis and vasculature are processes related to defense and immunity (Table 2). Interestingly, atrichoblasts do not respond to WCS417 with defense activation, but with activation of ion transport (Table 2). This suggests that the two cell types in contact with WCS417 activate distinct biological processes, as could be expected from the limited overlap in DEGs between these cell types (Figure 4B and 5A). To further analyze these differences, we examined the expression of all genes within the GO terms defense response (GO:0006952) and ion transport (GO:0009267) that are differentially expressed in one or both epidermal cell types. Based on their expression levels, the genes involved in the defense response form five clusters (Figure 5B, left). The two gene clusters containing the greatest number of genes (cluster 2 and 4) consist of genes

Figure 3 Gene expression differences among the samples reflect Arabidopsis root development patterns. A) Schematic cross section of the Arabidopsis root, with each cell type labeled with the *pro-motor::GREEN FLUORESCENT PROTEIN (GFP)* fusion used to enrich samples for that specific cell type using fluorescence-activated cell sorting (FACS). B) qRT-PCR analysis of the expression of *COBRA-LIKE 9 (COBL9)*, *WEREWOLF (WER)*, *315*, and *SCARECROW (SCR)*. C) qRT-PCR analysis of the expression of the marker gene *WOODENLEG (WOL),* and of the vasculature-specific *INCURVATA4* and *SHORTROOT (SHR)*. Different letter indicate statistically significant differences between treatments (PERMANOVA test followed by Tukey's test, $P < 0.05$). Multidimensional scaling (MDS) plots of the logged counts per million of all samples (D) and per cell type (E). WCS417-exposed samples are represented by circles, control samples by triangles. '*P*' represents the p-value of the WCS417-treatment effect obtained by performing a PERMANOVA. Colors in panel B-E correspond to the color scheme of the schematic in panel A.

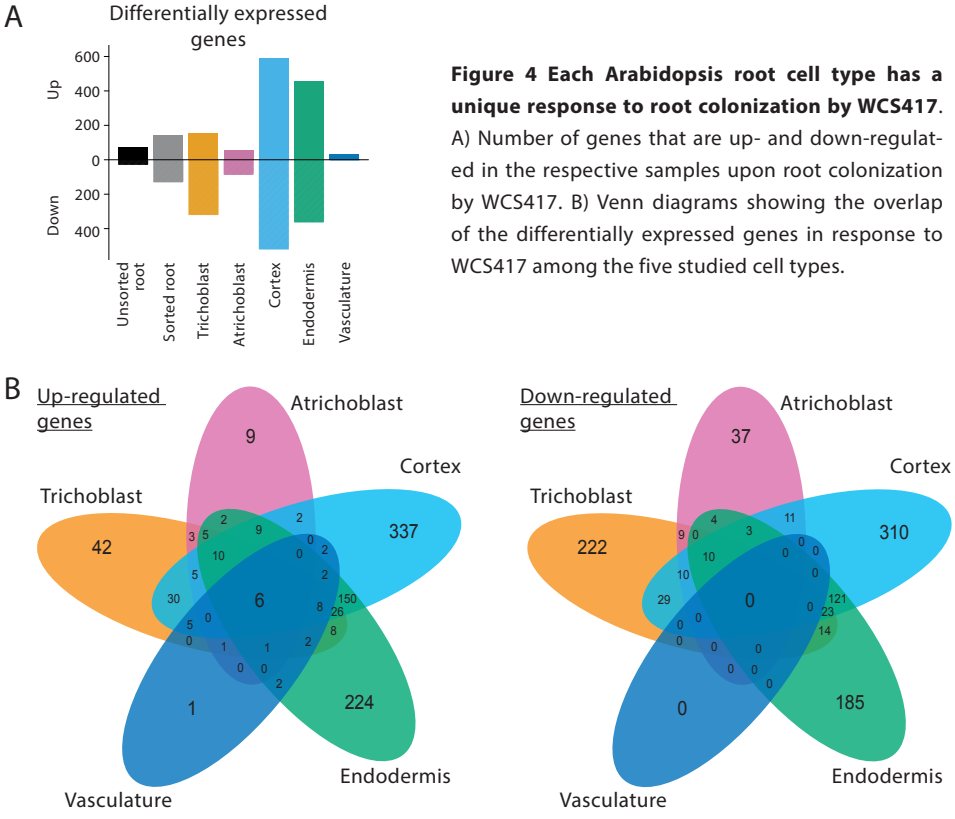

Figure 4 Each Arabidopsis root cell type has a unique response to root colonization by WCS417. A) Number of genes that are up- and down-regulated in the respective samples upon root colonization by WCS417. B) Venn diagrams showing the overlap of the differentially expressed genes in response to WCS417 among the five studied cell types.

that are induced by WCS417. Interestingly, the induction of these genes is observed in both WSC417-treated epidermal cell types. In contrast, the expression levels in sterile conditions are distinct, with lower gene expression in trichoblasts (Figure 5B, Table S15). When analyzing the expression patterns of ion transport-related genes, three out of six expression clusters (clusters 1,3 and 5) contain genes that are up-regulated in response to WCS417 in both cell types (Figure 5B, Table S16). However, the differences between trichoblasts and atrichoblasts are most clear in the other three clusters (clusters 2, 4 and 6), which are all composed of genes that are only expressed in trichoblasts in control conditions (Figure 5B, right).

Table 2 Top GO terms enriched in the list of genes up-regulated in response to WCS417

Cell type	GO term ID	p-value	Odds ratio	Expected count	Count	Size	Term
Trichoblast	GO:0050896	6.03E-09	3	42.3	73	5671	Response to stimulus
Atrichoblast	GO:0006811	3.56E-08	8	2.8	14	1005	Ion transport
Cortex	GO:0006952	1.90E-24	4	40.2	112	1397	Defense response
Endodermis	GO:0009605	6.21E-19	3	40.0	100	1833	Response to external stimulus
Vasculature	GO:0009620	2.11E-06	16	0.6	7	457	Response to fungus

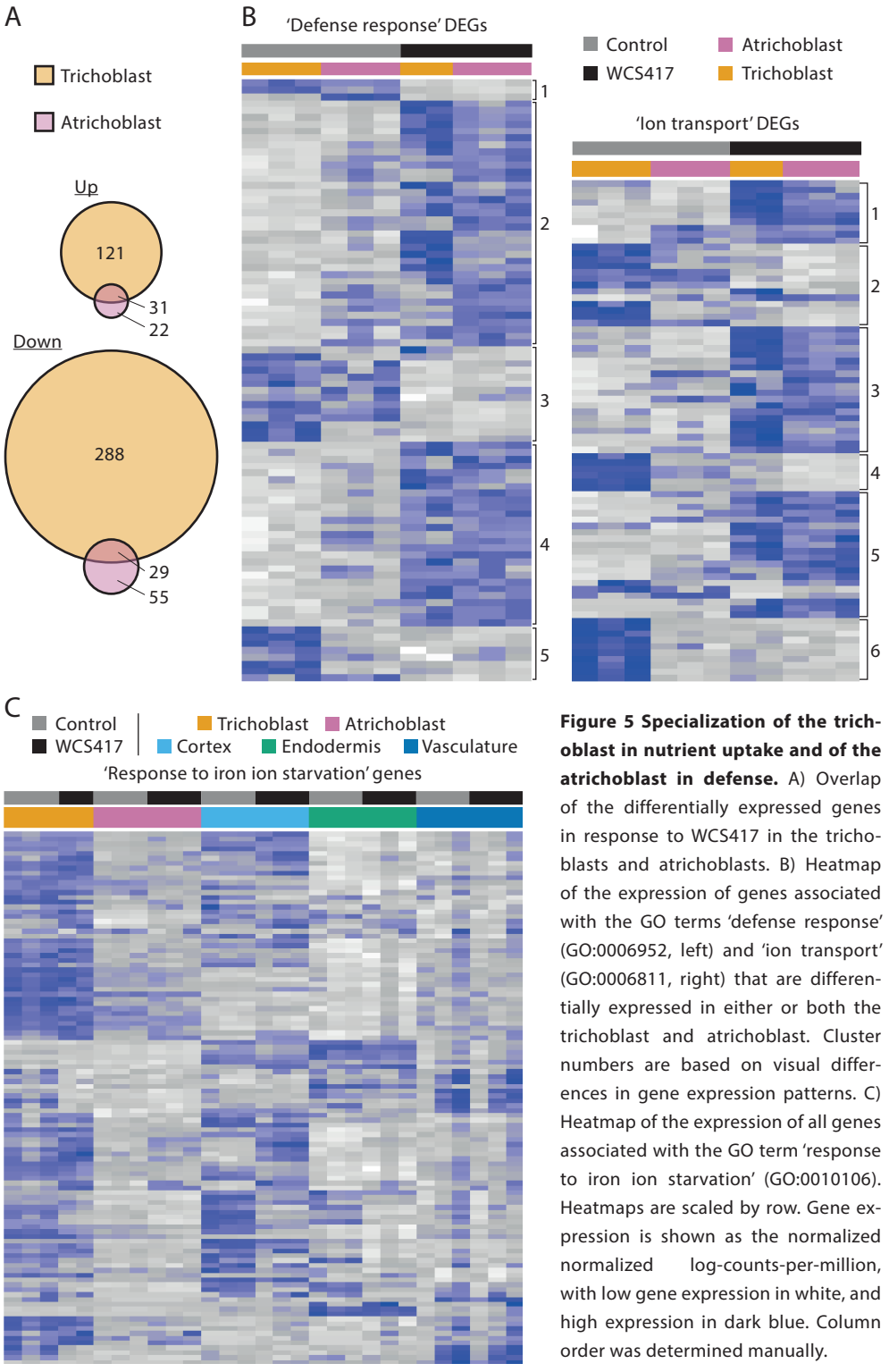

Figure 5 Specialization of the trichoblast in nutrient uptake and of the atrichoblast in defense. A) Overlap of the differentially expressed genes in response to WCS417 in the trichoblasts and atrichoblasts. B) Heatmap of the expression of genes associated with the GO terms 'defense response' (GO:0006952, left) and 'ion transport' (GO:0006811, right) that are differentially expressed in either or both the trichoblast and atrichoblast. Cluster numbers are based on visual differences in gene expression patterns. C) Heatmap of the expression of all genes associated with the GO term 'response to iron ion starvation' (GO:0010106). Heatmaps are scaled by row. Gene expression is shown as the normalized normalized log-counts-per-million, with low gene expression in white, and high expression in dark blue. Column order was determined manually.

These results suggest that the distinct responses of trichoblasts and atrichoblasts to WCS417 are in part due to differences in basal gene expression patterns. To find further support for this theory, we determined DEGs between the control trichoblasts and atrichoblasts (Table S17), and identified enriched GO terms. Genes that are expressed more in the atrichoblasts are enriched for genes involved in RNA modification or processing, defense responses, response to hypoxia, response to salicylic acid and glucosinolate biosynthesis (Table S18). Genes expressed more in trichoblasts are enriched for genes associated with the response to ion starvation, root hair differentiation, cell maturation, cell wall biosynthesis (Table S19). Among these latter processes, Fe ion starvation (GO:0010106) is enriched the most. Analysis of the expression of the genes involved in this process in all cell types shows that the expression of the majority of the genes involved in the response to Fe ion starvation is specific to the trichoblasts and, to a lesser extent, the cortex (Figure 5C, Table S20). This is in line with previous experiments showing cortex- and epidermis-specific expression of the genes *BGLU42* and *IRT1*, both known to be involved in the Fe deficiency response (Vert *et al.*, 2002; Zamioudis *et al.*, 2014), and the importance of trichoblasts for nutrient uptake (Tanaka *et al.*, 2014). Thus, defense gene activity and expression levels of genes involved in nutrient uptake and root hair elongation are indeed key differentiating factors between trichoblasts and atrichoblasts in control conditions in our experiment.

WCS417 might induce lateral root formation via auxin-mediated remodelling of the cell walls of the cell layers covering lateral root primordia

The most significant biological process among the down-regulated DEGs is the glucuronoxylan metabolic process (GO:0010413) in the cortex and endodermis (Table 3). Glucuronoxylan metabolic process is important for cell wall biosynthesis. In addition to this GO term, many other GO terms related to cell wall biosynthesis are enriched in down-regulated DEGs and, conversely, cell wall disassembly (GO:0044277) is enriched among the up-regulated DEGs in these cell types (Table S8-S11). Recently, it was shown that cell wall remodeling and cell volume loss in the cortex and endodermis are required to accommodate emerging lateral roots and are possibly even required for the initiation of lateral root primordia (Vermeer *et al.*, 2014; Stoeckle *et al.*, 2018). Among the genes upregulated in the cortex and endodermis that are involved in cell wall disassembly are *ARABIDOPSIS DEHISCENCE ZONE POLYGALACTURONASE2* (*ADPG2*) and *QUARTET2 (QRT2)*. Both these genes encode polygalacturonases (PGs) and have been shown to be expressed at the site of lateral root emergence. PGs have been implicated in cell separation, possibly to accommodate emerging lateral roots (Ogawa *et al.*, 2009). Up-regulation of these

Table 3 Top GO terms enriched in the list of genes down-regulated in response to WCS417

Cell type	GO term ID	p-value	Odds ratio	Expected count	Count	Size	Term
Trichoblast	GO:0009408	6.04E-06	4	4.2	16	281	Response to heat
Atrichoblast	GO:0008300	0.000391	90	0	2	8	Isoprenois catabolic process
Cortex	GO:0010413	1.87E-19	10	4.2	32	177	Glucuronoxylen metabolic process
Endodermis	GO:0010413	4.12E-07	6	3	15	177	Glucuronoxylen metabolic process

and other genes involved in cell wall disassembly and down-regulation of genes involved in cell wall biosynthesis in the cortex and endodermis might therefore be an integral part of the molecular and physiological changes that take place in response to WCS417 that lead to the observed increase in the number of lateral roots (Figure 1B and (Zamioudis *et al.*, 2013)).

Apart from genes involved in cell wall biosynthesis or disassembly, several other genes are known or suspected to be expressed in the endodermis and/or cortex and to be involved in lateral root emergence (Stoeckle *et al.*, 2018). Several of these genes are induced by WCS417, including *LATERAL ORGAN BOUNDARIES DOMAIN18 (LBD18)* and *LBD29* in the cortex. *LBD18* and *LBD29* are thought to promote lateral root emergence and are known to be induced in endodermal and cortical cells overlying lateral root primordia (Stoeckle *et al.*, 2018). In addition, we find increased expression of *PURIN PERMEASE PROTEIN10 (PUP10)*, *PUP12*, and *PUP21*. PUPs are cytokinin transport porteins and have been hypothesized to play a role in the overlying cell layers during lateral root emergence, although there was no evidence yet of their expression in the cortex and endodermis (Stoeckle *et al.*, 2018). In addition, we see up-regulation of *LATERAL ROOT PRIMORDIUM1* (*LRP1*) in the cortex. *LRP1* is typically expressed during the early stages of root primordium development (Smith and Fedoroff, 1995).

Cell wall remodeling in the cortex and endodermis to faciliate lateral root formation is thought to be mediated by the production of reactive oxygen species (ROS) downstream of auxin (Orman-Ligeza *et al.*, 2016). Auxin signaling is known to be induced in response to WCS417 (Zamioudis *et al.*, 2013; Stringlis *et al.*, 2018b). In our dataset, response to auxin (GO:0009733) is also enriched among upregulated DEGs, but only in the cortex. Reactive oxygen species metabolic process (GO:0072593), on the other hand, was enriched among up-regulated genes in trichoblasts, cortex, endodermis and vasculature (Table S5, S9, S11, S13).

Altogether these data suggest that the induction of lateral root formation in response to WCS417 involves cell wall remodeling in the cell layers overlying lateral root primordia. This remodeling might be mediated via interference with endogenous auxin signaling pathways.

WCS417 induces suberin biosynthesis in endodermal cells

Defense responses are in part the most significantly enriched GO terms in our cell type-specific gene expression analysis because many genes are known to be involved in these responses. To study biological processes in which fewer genes are known to be involved, we studied the enriched GO terms with the highest odds ratios, i.e. with the largest difference in expected versus actual count. In this analysis, the endodermis is the only cell type that has a GO term that is enriched based on the up-regulation of more than five genes: suberin biosynthesis (GO:0010345) (Table 4). Suberin is a hydrophobic polymer that is laid down between the primary cell wall and the plasma membrane of endodermal cells. There, it blocks free movement of water and nutrients into the endodermis and consequently the innermost cell layers of the Arabidopsis root (Geldner, 2013; Vishwanath *et al.*, 2015; Barberon, 2017). Like the formation of lateral roots and root hairs, the production of suberin lamellae is affected by nutrient availability (Barberon *et al.*, 2016). Enhanced or reduced suberin biosynthesis and deposition is also thought to play a role in the interaction of roots with micro-organisms by controlling the amounts of nutrient that are secreted into the soil and by presenting an inducible, protective barrier of the inner cell layers (Geldner, 2013; Vishwanath *et al.*, 2015).

We thus analyzed which genes involved in suberin biosynthesis are affected by WCS417. In

Table 4 Top GO terms based on oddsratio enriched in the up-regulated genes

Cell type	GO term ID	p-value	Odds ratio	Expected count	Count	Size	Term
Trichoblast	GO:0030418	0.000165	271	0	2	3	Nicotianamine biosynthetic process
Atrichoblast	GO:0009446	0.00553	369	0	1	2	Putrescine biosynthetic process
Cortex	GO:0070542	9.26E-05	102	0.1	3	4	Response to fatty acid
Endodermis	GO:0010345	1.11E-06	45	0.2	5	10	Suberin biosynthetic process
Vasculature	GO:0006809	1.91E-05	517	0	2	5	Nitric oxide biosynthetic process

this analysis, we included MYB transcription factors suggested to activate suberin biosynthesis (Kosma *et al.*, 2014; Lashbrooke *et al.*, 2016), and enzymes involved in suberin biosynthesis, including β-KETOACYL-CoA-SYNTHASEs (KCSs), fatty acid cytochrome P450 oxidases (CYP86A1 and CYP86B1), FATTY ACUL-CoA REDUCTASEs (FARs), GLYCEROL-3-PHOSPHATE SN2-ACYLTRANSFERASEs (GPATs) as well as transporters such as the ATP-binding cassette (ABC) transporter proteins (Panikashvili *et al.*, 2010; Yadav *et al.*, 2014; Vishwanath *et al.*, 2015; Barberon, 2017). As expected based on the available literature and our GO term analysis, spatial gene expression patterns show that suberin biosynthesis is primarily restricted to the endodermis and is significantly induced by WCS417 (Figure 6A-B). To validate the induction of suberin biosynthesis we studied fluorescence in the transgenic plant line *GPAT5*$_{pro}$*:mCITRINE-SYP122* (Barberon *et al.*, 2016), as *GPAT5* activity has been shown to match suberin deposition patterns (Naseer *et al.*, 2012). Consistent with our transcriptomic data, the activity of the *GPAT5* promotor is specific to the endodermis and is stimulated by WCS417 (Figure 6C).

Discussion

Creating a spatial map of gene expression changes in response to WCS417

Over the years, it has become clear that the 'hidden half' of plants, the root system, is of crucial importance when trying to breed for plants that are drought tolerant or better able to grow in nutrient-limiting conditions (Rogers and Benfey, 2015; Koevoets *et al.*, 2016). The importance of the roots becomes even clearer when considering that the root surface is the place of interaction between plants and the beneficial soil micro-organisms that increase plant growth and health (Lugtenberg and Kamilova, 2009; Pieterse *et al.*, 2014; Bakker *et al.*, 2018). In this chapter, we aimed to increase our understanding of the effect of the beneficial rhizobacterium WCS417 on the regulation of root system architecture by studying WCS417-induced gene expression changes in five Arabidopsis root cell types, the trichoblast, atrichoblast, cortex, endodermis and vasculature (Figure 2-3).

The number of DEGs in our spatial map uncovered two interesting patterns: 1) the cortex and endodermis respond most strongly to WCS417 in terms of the number of DEGs, and 2) the number of DEGs in the two epidermal cell types is different (Figure 4). The strong response of the cortex and endodermis is surprising, as these cell types are likely not in direct contact with WCS417. This observation might be a timing effect, as cell type-specific transcriptional profiling of the Arabidopsis root response to flagellin showed that the epidermis responded as strongly

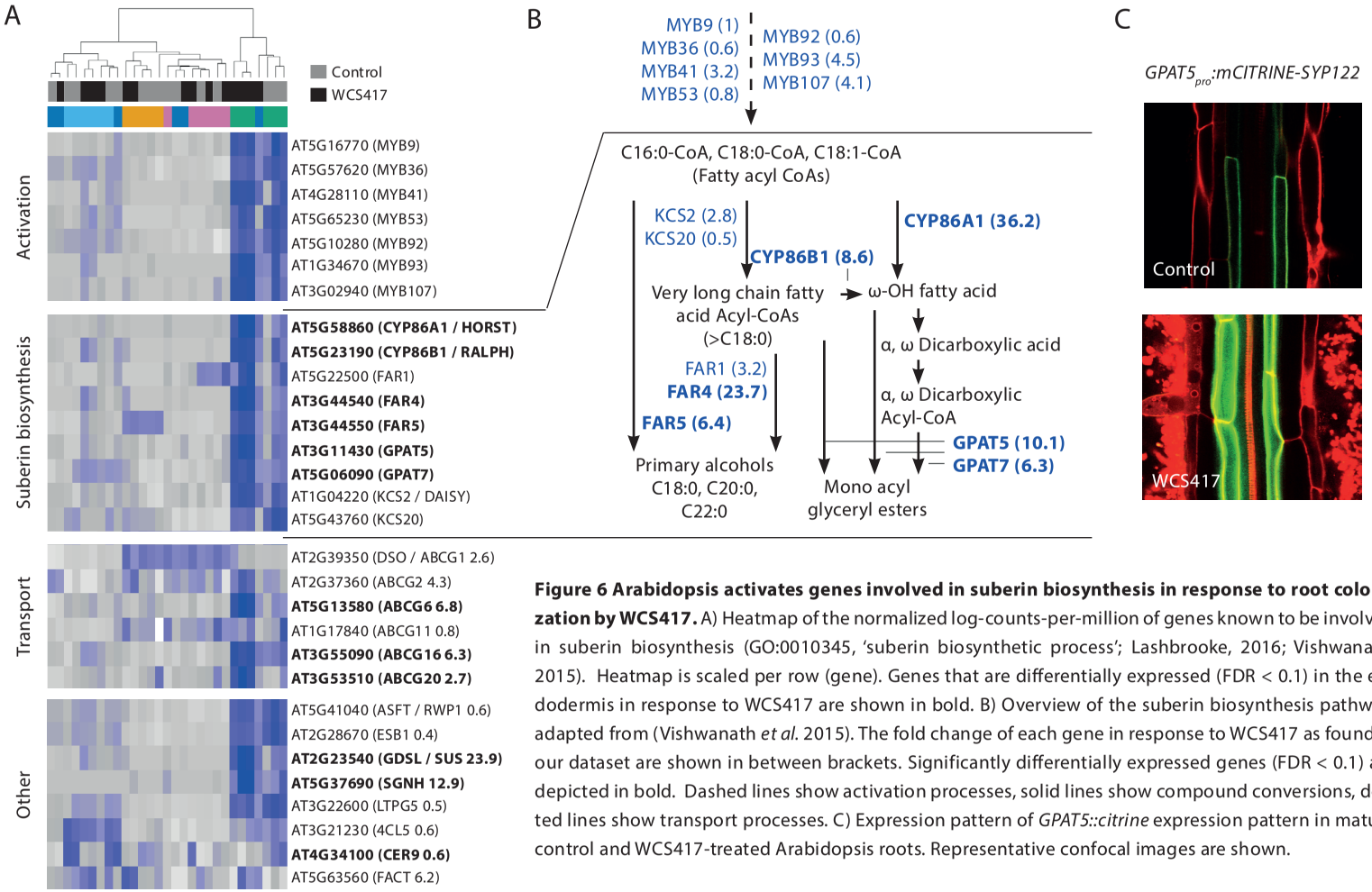

Figure 6 Arabidopsis activates genes involved in suberin biosynthesis in response to root colonization by WCS417. A) Heatmap of the normalized log-counts-per-million of genes known to be involved in suberin biosynthesis (GO:0010345, 'suberin biosynthetic process'; Lashbrooke, 2016; Vishwanath, 2015). Heatmap is scaled per row (gene). Genes that are differentially expressed (FDR < 0.1) in the endodermis in response to WCS417 are shown in bold. B) Overview of the suberin biosynthesis pathway, adapted from (Vishwanath *et al.* 2015). The fold change of each gene in response to WCS417 as found in our dataset are shown in between brackets. Significantly differentially expressed genes (FDR < 0.1) are depicted in bold. Dashed lines show activation processes, solid lines show compound conversions, dotted lines show transport processes. C) Expression pattern of *GPAT5::citrine* expression pattern in mature control and WCS417-treated Arabidopsis roots. Representative confocal images are shown.

as the cortex at two hours post inoculation (Rich *et al.*, 2018). Possibly, the epidermis responds strongly at first and down-regulates its response by two days after inoculation. Such an outside to inside directionality has been shown for the response to nitrogen (Walker *et al.*, 2017).

Analysis of the quantitative difference in the response of the trichoblasts versus the atrichoblasts showed that this difference was also qualitative: different biological responses are activated in the two cell types in response to WCS417. These differences are at least in part due to functional specialization of trichoblasts in nutrient uptake and atrichoblasts in basal defense gene activation (Figure 5). Expression of genes involved in nutrient uptake in specifically the trichoblasts is in line with previous findings showing increased expression of growth-related genes in progressively more differentiated trichoblasts (Denyer *et al.*, 2019) and specialization of trichoblasts in nutrient uptake (Vert *et al.*, 2002; Tanaka *et al.*, 2014; Zamioudis *et al.*, 2014). Possibly, the prioritization of growth in trichoblasts ensures ample exploration of soil, and thus sufficient nutrient uptake, while atrichoblasts function as a first line of defense against soil-borne micro-organisms. This would suggest that the differentiation of the outer root cell layer into two cells types allows the root to physically separate nutrient uptake and defense. The spatial separation of these processes might ensure that they can both be active at the same time.

The increased detection power of cell type-specific transcriptomic analyses

The total number of DEGs identified across the five cell types is approximately tenfold greater than the number of DEGs identified in the sorted whole root control. A similar increase in detection power of cell type-specific versus whole-root transcriptomic analyses was obtained previously when examining the Arabidopsis root response to salt, Fe deficiency and nitrogen (Dinneny *et al.*, 2008; Gifford *et al.*, 2008).

We show that the increased detection power can be traced to the cell type-specific nature of the root response to WCS417. The five cell types studied differ in their response to WCS417 both quantitatively, with large differences in the number of DEGs, and qualitatively, with little overlap in DEGs between cell types (Figure 4). This is in line with previous studies on cell type-specific gene transcription changes in response to both abiotic and biotic stresses (Dinneny *et al.*, 2008; Gifford *et al.*, 2008; Walker *et al.*, 2017; Rich *et al.*, 2018). The majority of the genes that are up- or down-regulated in only a single cell type is not identified as differentially expressed in our whole root controls (Table 1, S3-4). Thus, cell type-specific transcriptional profiling is more powerful than whole tissue transcriptional profiling because it detects cell type-specific DEGs that are otherwise lost to noise.

Arabidopsis might change root structure to optimally benefit from the interaction with WCS417

In this study, we uncovered several biological processes affected by WCS417. First, we show decreased cell wall biosynthesis in the endodermis and the cortex. This might allow the cells in these cell layers to lose volume. As cell volume loss is required for lateral root initiation and outgrowth (Vermeer *et al.*, 2014; Stoeckle *et al.*, 2018), this might explain the observed increase in lateral root formation in WCS417-exposed roots. In addition, we show increased expression of genes involved in suberin biosynthesis in the endodermis.

Both the amount of lateral roots and suberization are known to be influenced by nutrient availability (Barberon *et al.*, 2016; Shahzad and Amtmann, 2017). Previous research has shown that Arabidopsis activates the Fe deficiency response upon root colonization by WCS417 (Verhagen *et al.*, 2004; Zamioudis *et al.*, 2014, 2015). This response is normally activated upon Fe limitation, suggesting that WCS417 changes either nutrient availability or nutrient use within the plant. Thus, changing nutrient requirements in response to WCS417 might orchestrate the observed root architectural changes. Previously, WCS417-induced root architecture changes and WCS417-mediated activation of the Fe deficiency response were shown to be dependent on functional auxin signaling in the plant (Zamioudis *et al.*, 2013; Stringlis *et al.*, 2018b). Auxin signaling is also important for the regulation of lateral root development in general (Du and Scheres, 2018) and in response to Fe (Giehl *et al.*, 2012). Therefore, auxin might mediate the possible nutrient-dependent root architecture changes.

Alternatively, the cell type-specific changes underlying the changes in root system architecture might be induced by plants as part of the defense response, as our dataset uncovers strong induction of defense-related genes in response to WCS417 (Table 2). Defense responses in roots have been described to be cell type-specific (Wyrsch *et al.*, 2015), and could therefore theoretically result in cell type-specific biological effects, such as the endodermis-specific suberization that we identified. Initiation of suberization has been hypothesized before to be a defense response, as it could restrict microbial access into the root on the one hand and the secretion of compounds that can be used as nutrients by the surrounding micro-organisms on the other hand (Geldner, 2013; Vishwanath *et al.*, 2015). An increase in lateral root number, in turn, might be initiated to prevent future nutrient shortages due to nutrient capture by the perceived micro-organisms. The activation of a defense response might seem surprising in response to a beneficial rhizobacterium. However, the induction of defense responses upon colonization by WCS417 in the Arabidopsis root has been shown repeatedly (Verhagen *et al.*, 2004; Stringlis *et al.*, 2018b). The activation of the plant defense response upon root colonization by WCS417 is likely mediated via recognition of common microbe-associated molecular patterns (MAMPs) such as flagellin. While MAMP-triggered defense responses are activated in response to live beneficial rhizobacteria, their induction is lower than in response to MAMPs alone (Verhagen *et al.*, 2004; Millet *et al.*, 2010; Stringlis *et al.*, 2018b). Thus, if these root architectural changes are indeed induced as part of the defense response, one would expect greater changes in response to pathogenic micro-organisms.

Concluding remarks

In the study presented here, we created a spatial map of gene expression changes induced in the Arabidopsis root in response to colonization by the beneficial rhizobacterium WCS417. Our dataset uncovers gene expression patterns that might explain observed root architectural changes. Further study of the processes involved will shed new light on bacteria-plant interactions. In addition, we hope that further mining of our dataset will enable other researchers to determine the spatial pattern of other microbe-induced genes. Together with the data presented here, this will contribute to our understanding of plant immunity, plant growth and plant-microbe interactions.

Chapter 3

Rhizobacteria-mediated activation of the iron deficiency response in Arabidopsis roots: impact on iron status and signaling

Eline H. Verbon[1*], Pauline L. Trapet[1*], Sophie Kruijs[1], Coline Temple-Boyer-Dury[1], T. Gerrit Rouwenhorst[2], Corné M.J. Pieterse[1]

[*]These authors contributed equally to this work

[1]Plant-Microbe Interactions, Utrecht University, Department of Biology, The Netherlands
[2]Ecology and Biodiversity, Utrecht University, Department of Biology, The Netherlands

A modified version of this chapter has been published as:
Verbon, E.H., Trapet, P.L., Kruijs S., Temple-Boyer-Dury, C., Rouwenhorst, T.G., C.M.J. Pieterse, C.M.J. (2019) Rhizobacteria-mediated activation of the Fe deficiency response in Arabidopsis roots: impact on Fe status and signaling. Frontiers in Plant Science, 10: 909.

Abstract

The beneficial root-colonizing rhizobacterium *Pseudomonas simiae* WCS417 stimulates plant growth and induces systemic resistance against a broad spectrum of plant diseases. In *Arabidopsis thaliana* (Arabidopsis), the root transcriptional response to WCS417 shows significant overlap with the root response to iron (Fe) starvation, including activation of the marker genes *MYB72* and *IRT1*. Here, we investigated how colonization of Arabidopsis roots by WCS417 impacts Fe homeostasis in roots and shoots. Under Fe-sufficient conditions, root colonization by WCS417 induced a transient Fe deficiency response in the root and elevated both the total amount of Fe in the shoot and the shoot fresh weight. When WCS417-colonized plants were grown under Fe-starvation conditions, WCS417 still promoted plant growth. As Arabidopsis could not increase iron uptake, this resulted in chlorosis Thus, increased Fe uptake in response to WCS417 is essential for Fe homeostasis in the more rapidly growing plant. As the WCS417-induced Fe deficiency response is known to require a shoot-derived signal, we tested whether the Fe deficiency response is activated in response to an increased Fe demand in the more rapidly growing shoot. Exogenous application of Fe to the leaves to reduce a potential shoot Fe shortage did not prevent WCS417-mediated induction of the Fe deficiency response in the roots. Moreover, the leaf Fe status-dependent shoot-to-root signaling mutant *opt3-2*, which is impaired in the phloem-specific Fe transporter OPT3, still up-regulated the Fe deficiency response genes *MYB72* and *IRT1* in response to WCS417. Collectively, our results suggest that the WCS417-induced Fe deficency response in the root is controlled by a signalling system that is independent of both leaf Fe status and OPT3.

Introduction

The composition of the microbial community in the soil surrounding plant roots is different from the community in soil further away from the roots. This phenomenon, known as the rhizosphere effect, is associated with the secretion of carbon sources by plant roots. These carbon sources can serve as nutrients for soil microbes (Berendsen *et al.*, 2012; Lundberg *et al.*, 2012) or as selective agents that shape the composition of the root microbiome (Bakker *et al.*, 2018; Stringlis *et al.*, 2018a). In return, plant growth-promoting rhizobacteria (PGPR) within the root microbiome can improve plant growth and health (Lugtenberg and Kamilova, 2009; Berendsen *et al.*, 2012; Pieterse *et al.*, 2014). The PGPR *Pseudomonas simiae* WCS417 is among the best-studied PGPR. When WCS417 colonizes the root of the model plant *Arabidopsis thaliana* (Arabidopsis), it stimulates plant growth and induces systemic resistance (ISR) against a broad variety of pathogens (Zamioudis *et al.*, 2013; Pieterse *et al.*, 2014). WCS417-mediated ISR is not associated with immediate upregulation of defense responses in the leaves. Instead, the increased resistance is associated with a more rapid and stronger activation of defense responses upon pathogen attack, a cost-effective form of induced resistance known as defense priming (Martinez-Medina *et al.*, 2016). In the roots, WCS417 actively suppresses local defense responses triggered by its microbe-associated molecular patterns (MAMP) (Stringlis *et al.*, 2018b), possibly to facilitate colonization. Apart from downregulating defense responses, WCS417 mediates activation of the root-specific transcription factor gene *MYB72* and its downstream target *β-GLUCOSIDASE42* (*BGLU42*). These genes are essential for the onset of WCS417-mediated ISR in Arabidopsis, as the mutants *myb72* and *bglu42* do not mount systemic immunity upon colonization of the roots by WCS417 (Van der Ent *et al.*, 2008; Zamioudis *et al.*, 2014). *MYB72* is also required for ISR triggered by other beneficial microbes, including the beneficial fungus *Trichoderma asperellum* T-34 (Segarra *et al.*, 2009; Martínez-Medina *et al.*, 2017).

MYB72 and *BGLU42* are not only involved in WCS417-mediated ISR, they are also part of the iron (Fe) deficiency response that is initiated in plant roots under conditions of Fe starvation (Palmer *et al.*, 2013; Zamioudis *et al.*, 2014; Verbon *et al.*, 2017). Interestingly, 20% of all genes induced by WCS417 in Arabidopsis roots are also induced under Fe-limited conditions (Zamioudis *et al.*, 2015), providing evidence for a mechanistic link between the Fe deficiency response and ISR (Zamioudis *et al.*, 2014; Verbon *et al.*, 2017). Like WCS417, the beneficial ISR-inducing fungi *T. asperellum* T-34 and *Trichoderma harzianum* T-78 induce the Fe deficiency response in Arabidopsis and tomato (Martínez-Medina *et al.*, 2017), suggesting that activation of the Fe deficiency response by beneficial microbes is a wide-spread phenomenon (Romera *et al.*, 2019).

Plant Fe deficiency responses are elaborate molecular mechanisms that increase Fe uptake when plants experience Fe shortage (Römheld, 1987; Walker and Connolly, 2008; Ivanov *et al.*, 2012; Kobayashi and Nishizawa, 2012). This is essential for plant growth and health as Fe is required as an enzyme cofactor in many essential processes, such as respiration, DNA synthesis and photosynthesis (Briat *et al.*, 1995). Even though Fe is abundantly present in the Earth's crust, its bioavailability is limited because Fe is mainly present as ferric oxide, which is poorly soluble at neutral and high pH. Arabidopsis, like other non-grass plants, utilizes the root-specific Strategy I Fe deficiency response to safeguard sufficient Fe uptake under Fe starvation conditions (Römheld, 1987). The basic helix-loop-helix (bHLH) transcription factor FIT (FER-LIKE IRON DEFICIENCY TRANSCRIPTION FACTOR) is a central regulator of this response. FIT regulates

the expression of a number of critical Fe uptake genes including *FRO2,* which encodes the enzyme FERRIC REDUCTION OXIDASE2 that reduces soluble ferric Fe (Fe^{3+}) to ferrous Fe (Fe^{2+}); and *IRT1,* which encodes the high-affinity IRON-REGULATED TRANSPORTER1 that transports Fe^{2+} into the plant root (Colangelo and Guerinot, 2004).

In addition to the core Strategy I genes, FIT regulates *MYB72* gene expression (Colangelo and Guerinot, 2004; Zamioudis *et al.*, 2015). This root-specific transcription factor and its paralogue MYB10 are required for plant survival when Fe availability is limited (Palmer *et al.*, 2013). MYB72 regulates the biosynthesis and secretion of a subclass of Fe-mobilizing phenolic compounds called coumarins (Zamioudis *et al.*, 2014; Stringlis *et al.*, 2018a). Downstream of MYB72, the glucoside hydrolase BGLU42 converts glycosylated coumarins into their aglycone counterparts to enable their secretion into the rhizosphere (Zamioudis *et al.*, 2014; Stringlis *et al.*, 2018a). The most abundant metabolite whose biosynthesis and secretion is dependent on MYB72 and BGLU42 is the coumarin scopoletin (Stringlis *et al.*, 2018a). In addition to *MYB72* and *BGLU42*, several other genes with roles in the biosynthesis and secretion of Fe-mobilizing coumarins are induced in Arabidopsis roots upon colonization by WCS417, even when plants are grown under Fe-sufficient conditions (Zamioudis *et al.*, 2014). These include *FERULOYL-COA 6′-HYDROXYLASE1* (*F6′H1)*, *MYB10*, *SCOPOLETIN 8-HYDROXYLASE* (*S8H*) (Rajniak *et al.*, 2018; Tsai *et al.*, 2018), *CYP82C4* (Rajniak *et al.*, 2018), and *PLEIOTROPIC DRUG RESISTANCE9 PDR9*. F6′H1 is involved in the synthesis of coumarins in the phenylpropanoid pathway (Rodriguez-Celma *et al.*, 2013; Schmid *et al.*, 2014), whereas the ABC transporter PDR9 secretes the coumarins into the rhizosphere (Rodriguez-Celma *et al.*, 2013; Fourcroy *et al.*, 2014). Upon release in the rhizosphere, coumarins can chelate and mobilize Fe^{3+} and make it available for reduction and uptake by the roots, thus improving Fe nutrition of the plant (Schmid *et al.*, 2014; Fourcroy *et al.*, 2016; Tsai and Schmidt, 2017). Interestingly, some coumarins, including scopoletin, possess a selective antimicrobial activity that can help the plant to shape its microbiome in the rhizosphere in favor of PGPR that activate coumarin biosynthesis, such as WCS417 (Stringlis *et al.*, 2018a, 2019). Thus, WCS417 possibly hijacks the Fe deficiency response to trigger secretion of the antimicrobial coumarins to improve its own niche establishment in the rhizosphere.

In Arabidopsis roots, the WCS417-induced Fe deficiency response is under the control of a shoot-to-root signaling system (Zamioudis *et al.*, 2015). This is also the case for the activation of the Fe deficiency response upon Fe limitation (Grusak and Pezeshgi, 1996). After Fe is taken up from the soil, it is transported to the shoot (Hindt and Guerinot, 2012). The plasma membrane transporter OPT3, which loads Fe from the xylem into the phloem, regulates signaling of the leaf Fe status to the root to maintain Fe homeostasis and prevent Fe overload (Zhai *et al.*, 2014; Khan *et al.*, 2018). Misregulation of Fe status shoot-to-root signaling in mutant *opt3-2* plants results in a constitutively active Fe deficiency response in the roots, even under Fe-sufficient conditions (Stacey *et al.*, 2008). Fe overload results in oxidative stress (Aznar *et al.*, 2015a; Verbon *et al.*, 2017). To prevent oxidative stress, Fe storage in the plant is tightly controlled. Ferritins (FERs) are important players in this process (Ravet *et al.*, 2009). The expression of *FER* genes is typically upregulated when Fe content in the plant increases (Briat *et al.*, 1999). FERs can subsequently store up to 4500 Fe atoms in their cavity, thereby preventing free Fe from inducing oxidative stress (Briat *et al.*, 1999; Ravet *et al.*, 2009).

In recent years, several studies demonstrated that beneficial soil-borne microbes can improve Fe nutrition of plants, and that this is linked to their ability to trigger ISR (Romera *et al.*, 2019).

However, the biological mechanisms driving this microbial effect on Fe nutrition are not fully understood. In this study, we investigated how WCS417 affects Fe homeostasis in Arabidopsis. Moreover, we investigated the role of leaf Fe status in the activation of the Fe deficiency response by WCS417. Our results show that increased Fe uptake in response to colonization of the roots by WCS417 is essential to support WCS417-induced plant growth promotion. In addition, we show that the WCS417-induced activation of the Fe deficiency response is independent of Fe status-regulated shoot-to-root signaling.

Materials and methods

Plant material and growth conditions. Seedlings of *Arabidopsis thaliana* accession Col-0 and mutant *opt3-2* (Stacey *et al.*, 2008) were grown on a piece of nylon mesh (Nitex Cat 03-100/44, Sefar, Heiden, Switzerland) on standard Fe-sufficient growth medium consisting of modified Hoagland medium (Hoagland and Arnon, 1938) containing 5 mM KNO_3, 2 mM $MgSO_4$, 2 mM $Ca(NO_3)_2$, 2.5 mM KH_2PO_4, 70 µM H_3BO_3, 14 µM $MnCl_2$, 1 mM $ZnSO_4$, 0.5 mM $CuSO_4$, 10 µM NaCl, 0.2 µM Na_2MoO_4, 0.05% 2-ethanesulfonic acid (MES; Duchefa Biochemie, Haarlem, the Netherlands), 50 µM FeNaEDTA, 1% sucrose, and 1% plant agar (Duchefa Biochemie). The pH of the medium was set to 5.7. Fe-deficient medium was prepared by leaving out FeNaEDTA from the standard medium. Experiments that included treatments with the PGPR *Pseudomonas defensor* WCS358 (hereafter: WCS358) and *Pseudomonas capeferrum* WCS374 (hereafter: WCS374), were performed on standard medium without sucrose to prevent excessive growth of the bacteria.

Typically, Arabidopsis seeds were sown at low density on standard Fe-sufficient growth medium (a single row of twenty seeds per square Petri dish of 120 x 120 mm). For Fe measurement purposes, seeds were sown at high density (a dense 10-cm row of three seeds thick on a square Petri dish of 120 x 120 mm). Seeds sown at low density were sterilized by a 3-h exposure to the gas formed upon mixing 100 ml bleach with 3.2 ml hydrochloric acid fuming (37%) (Van Wees *et al.*, 2013). Seeds sown at high density were liquid sterilized in 60% bleach (v : v) for 10 min, followed by eight washes with MilliQ water (Dinneny *et al.*, 2008). After sowing, plates were sealed with a double layer of Parafilm and stratified in the dark at 4°C for 48 h. Plates were then placed vertically in the growth chamber under short-day conditions (14-h night, 10-h day; 21^{0}C; 100 µmol m^{-2} s^{-1}).

Bacterial and Fe-deficiency treatment. On the day of PGPR inoculation, after either 5 or 12 days of growth on standard Fe-sufficient medium, the pieces of nylon mesh with the plants op top were transferred to new standard or to Fe-deficient plates. One day before transfer, the PGPR strains *Pseudomonas simiae* WCS417, *Pseudomonas capeferrum* WCS358, and *Pseudomonas defensor* WCS374 (Berendsen *et al.*, 2015) were streaked from a frozen glycerol stock onto King's B medium agar plates (King *et al.*, 1954) and incubated overnight in the dark at 28°C. A bacterial suspension was prepared as described previously (Zamioudis *et al.*, 2015). In brief, bacteria were collected from the overnight plates, washed twice in 10 mM $MgSO_4$, and then suspended in 10 mM $MgSO_4$ to a final density of OD_{600} = 0.01, or 0.001 when specified, for experiments performed on sucrose-containing medium, and 0.1 for experiments performed on sucrose-lacking medium. Plants grown at low density were inoculated by applying 10 µl of the bacterial suspension halfway down each root. The remaining plants were similarly treated with 10 µl

of 10 mM $MgSO_4$ (mock) or remained untreated (Control). Plants grown at high density were inoculated by dividing 125 µl of a bacterial suspension at OD_{600} = 0.01 over the root systems of each row of plants. After treatment, plates were closed with a double layer of Parafilm and returned to the short-day growth chamber. Plant material was harvested 1 to 7 days later, as specified.

Fe supplementation to the shoot. Twelve-day-old Col-0 plants were transferred to new standard Fe-sufficient plates. Subsequently, 0.2 µl of MilliQ (mock) or 0.2 µl of a 5 µM, 50 µM, 500 µM, or 5 mM FeNaEDTA solution was added to two leaves of each plant, immediately after inoculation of the roots with WCS417. After 2 and 7 days, roots and shoots were harvested for gene expression analysis and shoot fresh weight (FW) measurement. Material for gene expression analysis was snap frozen in liquid nitrogen and stored at -80°C until RNA isolation.

Segmented plate assays. Segmented plates (square Petri dishes 120 x 120 mm) were prepared by removing a 5-mm strip of medium from an Fe-deficient plate, rendering two physically separated pieces of medium, as described previously (Giehl *et al.*, 2012). The strip was removed at 20 mm from the edge of the Petri dish. Fe concentrations in the small top part of the medium were amended to a final concentration of 40 µM or 200 µM FeNaEDTA by adding 42 or 205 µl, respectively, of 8 mM FeNaEDTA. The Fe concentration in the large bottom part was amended to a final concentration of 40 µM FeNaEDTA by adding 208 µl of 8 mM FeNaEDTA. Plates were left horizontally at room temperature (RT) overnight to allow the Fe to diffuse into the medium. Five-day-old seedlings were transferred on their nylon mesh to the segmented plates with the shoot part touching the small top part of the medium and the root part touching the large bottom part of the plate. Bacterial treatments in this system were performed by applying 10 µl of a bacterial suspension halfway down each root system, immediately after transfer of the plants to the segmented plates. Plants were decapitated just prior to treatment with WCS417 through removal of the shoot by cutting directly below the hypocotyl as described previously (Zamioudis *et al.*, 2015). Roots were harvested 2 days after transfer of the plants to the segmented plate system. Plant material was stored at -80°C until RNA isolation.

Quantitative reverse transcription-polymerase chain reaction (qRT-PCR). RNA was isolated from frozen roots and shoots (Oñate-Sánchez and Vicente-Carbajosa, 2008) and prepared for qRT-PCR as described previously (Caarls *et al.*, 2017). In short, cDNA was synthesized from DNase-treated total RNA samples using an oligo-dT primer. PCR reactions were performed using SYBR® green to monitor the synthesis of double-stranded DNA. Gene expression was analyzed using the comparative Ct method (Schmittgen and Livak, 2008). First, gene expression was normalized to the expression level of the reference gene *PP2AA3* (At1g13320) by subtracting the cycle threshold (Ct) of *PP2AA3* from the Ct of the gene of interest in the same sample, generating ΔCt values. ΔΔCt values were calculated by taking the average Ct of the control samples and subtracting this value from all ΔCt values. Statistical analyses were performed on the ΔΔCt values. Relative gene expression (fold change in gene expression relative to control), calculated as $2^{-\Delta\Delta Ct}$, was plotted. The gene-specific primers used are listed in Table S1 and available as part of the Online Supplementary Material here: https://cp.sync.com/dl/60fe897a0#fqt4xv25-em3ineic-y792dq3h-qrydpq97.

Plant growth and chlorophyll measurements. For growth measurements, shoots were cut from the roots just below the hypocotyl. Shoots from all the plants grown on a single plate were counted and pooled to obtain one biological replicate. The shoots were gently dried with tissue paper to remove any adhering moisture and weighed. Average shoot fresh weight (FW) was calculated by dividing the total shoot FW by the number of plants on the plate. Chlorophyll was measured as described previously (Hiscox and Israelstam, 1979) from the same samples. In brief, leaf tissue from the Arabidopsis seedlings from a single plate were placed in a vial containing 3 ml dimethylsulfoxide (DMSO) per 100 mg of shoot FW and incubated for 45 min at 65°C. After cooling to RT, chlorophyll (*a* + *b*) extracts were transferred to a cuvette, and spectrophotometer readings were performed using a DU-64 spectrophotometer (Beckman Coulter, Brea, USA) at a wavelength of 652 nm. Chlorophyll concentrations were calculated as described by Hiscox and Israelstam (1979).

Fe measurement. For Fe measurements, the collective shoot tissue from at least three high-density sown Arabidopsis plates were pooled to obtain one biological replicate. Plants were prepared for Fe content analyses as described previously (Trapet *et al.*, 2016). In brief, shoot material was gently dried with tissue paper and placed in 50-ml conical tubes containing 30 ml of MilliQ water. After 10 min of shaking at RT, plant tissue was washed twice in rinsing solution (5 mM EDTA, 1 mM KCl, 5 mM $Na_2S_2O_4$, 0.5 mM $CaSO_4.2H_2O$, pH = 6) at RT for 10 min on a shaker. After a final 10-min wash with MilliQ, the samples were gently dried with tissue paper and transferred into Pyrex tubes. Fe residues had been removed from these tubes by a 3-h rinse in 0.1 M hydrochloric acid, followed by a 1-h rinse in 5 mM EDTA and a final wash in MilliQ. The samples were dried completely by placing them in a 65°C incubator for 2 days. Subsequently, tissues were ground with a glass stick, after which the dry weight was measured. For mineralization, up to 10 mg of dry weight per sample was solubilized in 300 µl 65% nitric acid (Merck, Kenilworth, USA) and incubated at 120°C until all liquid was evaporated. The remaining material was mineralized a second time with 100 µl nitric acid and 200 µl hydrogen peroxide. This second mineralization step was repeated until all the material was mineralized. The mineralized material was dissolved in 200 µl nitric acid and 100 µl hydrogen peroxide. The final volume was subsequently adjusted to 10 ml by adding 9.7 ml of MilliQ. The Fe concentration of the samples was analyzed with an inductively coupled plasma atomic emission spectrometer (Thermo Scientific, Waltham, USA). The following settings were used: radio frequency power 1150 W, auxiliary gas flow 0.5 l min^{-1}, pump rate 50 rpm, nebulizer gas flow 0.5 l min^{-1}, coolant gas flow 12 l min^{-1}, optics temperature 38°C, camera temperature 45°C.

Results

Characteristics of the PGPR-induced Fe deficiency response

The *Pseudomonas* spp. PGPR WCS417, WCS374, and WCS358 have been demonstrated to trigger ISR and promote plant growth in different plant species (Berendsen *et al.*, 2015). In our standard *in vitro* plate system on Fe-sufficient medium, colonization of Arabidopsis Col-0 roots by these PGPR increased shoot fresh weight by approximately threefold (Figure 1A and 1B). Even though the plants grew on Fe-sufficient medium, colonization of the roots was associated with a transient increase in the expression of the Fe deficiency response marker genes *MYB72* and

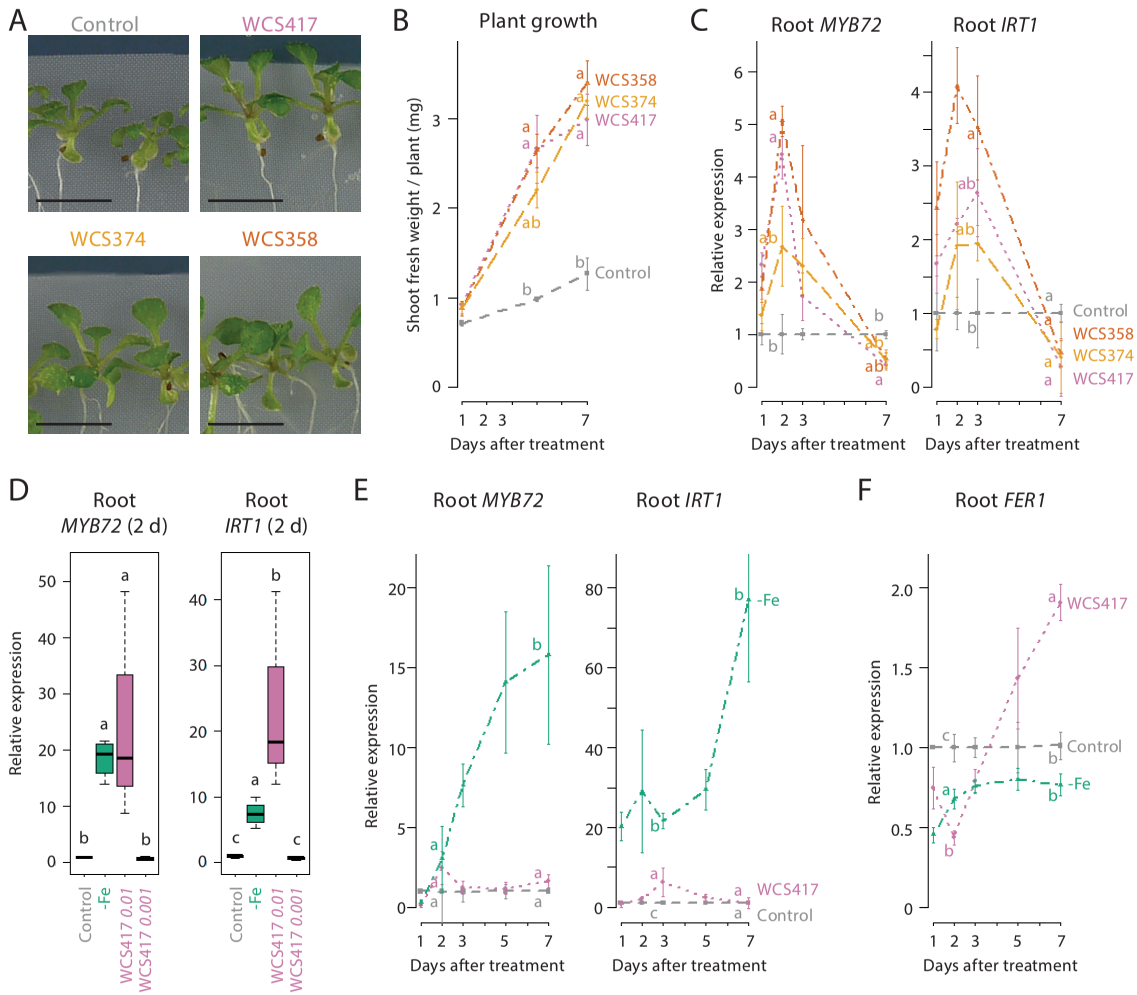

Figure 1 Plant growth promotion and activation of Fe deficiency marker genes in response to the PGPR WCS417, WCS374, and WCS358. A) Representative pictures of 19-day-old Arabidopsis Col-0 seedlings grown on standard Fe-sufficient medium, 7 days after inoculation of the roots with PGPR WCS417, WCS374, or WCS358 at OD_{600} = 0.1. Plant growth (B) and qRT-PCR analysis of *MYB72* and *IRT1* gene expression in the roots (C) of Col-0 plants at 2, 5 and 7 days after inoculation of the roots of 12-day-old plants with the indicated PGPR. D-F) qRT-PCR analysis of *MYB72*, *IRT1* and *FER1* gene expression in roots of Col-0 plants at different time points after inoculation of 12-day-old roots with WCS417 at OD_{600} = 0.01 or 0.001, or transfer to Fe-deficient medium (-Fe). Gene expression levels were normalized to that of the constitutively expressed reference gene *PP2AA3* (At1g13320). Plotted are fold-changes in PGPR- or Fe deficiency-induced gene expression levels relative to that of the average of the control treatment. Error bars represent standard errors of the mean. Per timepoint, different letters indicate statistically significant differences between treatments (One-way ANOVA followed by Tukey's test; $P < 0.05$; n=4-5). Scale bars represent 0.5 cm.

IRT1 (Figure 1C), which peaked at 2-3 days after application of the bacteria to the root system, confirming earlier findings (Zamioudis *et al.*, 2015). Previously, it was shown that a threshold of ISR-stimulating PGPR is required on the roots for the activation of ISR (Raaijmakers *et al.*, 1995). To test if the same holds true for the activation of the marker genes *MYB72* and *IRT1,* we tested the effect of two bacterial densities of WCS417. Application of WCS417 to the root system at the standard density of OD_{600} 0.01 significantly increased the expression of both *MYB72* and *IRT1* at day 2 after colonization (Figure 1D). A 10-fold lower bacterial density failed to induce expression of the Fe-deficiency marker genes, suggesting that the activation of these genes requires a threshold level of bacteria on the root system. Interestingly, two days after treatment, the increased *MYB72* and *IRT1* mRNA levels in WCS417 OD_{600} 0.01-treated roots growing on Fe-sufficient medium were in the same range (*MYB72*) or even higher (*IRT1*) than in roots growing on Fe-deficient medium (Figure 1D). When monitored over an extended period of 7 days, the expression profiles of *MYB72* and *IRT1* in WCS417-treated roots displayed a transient 2-5 fold increase, which peaked at day 2 or 3 after inoculation (Figure 1E, pink versus grey lines). In contrast, *MYB72* and *IRT1* mRNA levels in roots of Fe-starved plants continued to increase up to at least 7 days after treatment (Figure 1E, green versus grey lines). Together, these results indicate that PGPR induce the Fe deficiency response genes *MYB72* and *IRT1* even when sufficient Fe is available in the growth medium, but only when they are present at sufficient numbers on the root system. In addition, the PGPR-mediated Fe deficiency response on Fe-sufficient medium is mild and transient compared to the response induced by Fe limitation.

To investigate whether the WCS417-induced Fe deficiency response affects Fe status in the roots, we tested the expression of the Fe storage protein gene *FER1*. *FER1* expression reflects metabolic Fe needs and serves as a robust marker for the cellular Fe status (Gaymard *et al.*, 1996), with *FER1* expression typically high under conditions of Fe excess and low under Fe-deficient conditions (Petit *et al.*, 2001; Arnaud *et al.*, 2006). In Fe-starved plants, *FER1* mRNA levels remained low during the course of the experiment (Figure 1F, green versus grey line). In contrast, in WCS417-treated roots of plants growing on Fe-sufficient medium, *FER1* mRNA levels dropped during the first 2 days, but then increased to levels that were significantly higher than those in control plants growing on Fe-sufficient medium (Figure 1F, pink versus grey line), suggesting that Fe uptake increased in the roots in response to WCS417 colonization.

Shoot Fe status in PGPR-colonized plants

Next, we monitored the effect of WCS417 on chlorophyll and Fe content in the leaves of Col-0 plants growing on Fe-sufficient or Fe-deficient medium. Figure 2A shows that WCS417 significantly increased shoot FW on both Fe-sufficient and Fe-deficient medium, although the increase in shoot FW was more pronounced on Fe-sufficient medium. Interestingly, total chlorophyll content, which is an indicator for Fe nutrition in the leaves (Briat *et al.*, 2015), followed the WCS417-mediated increase in shoot FW when plants were grown on Fe-sufficient medium (Figure 2B, pink versus grey line). However, on Fe-deficient medium, total chlorophyll amount per WCS417-treated plant remained constant over time, even though plant FW increased (Figure 2A-B, blue versus green line). As a result, the relative chlorophyll content per gram of shoot FW was significantly lower in WCS417-treated plants growing in Fe deficient medium (Figure 2C), as was reflected by a more chlorotic appearance of the shoots (Figure 2A). As expected, measurement of the Fe content per gram of dry weight shows the same trend as

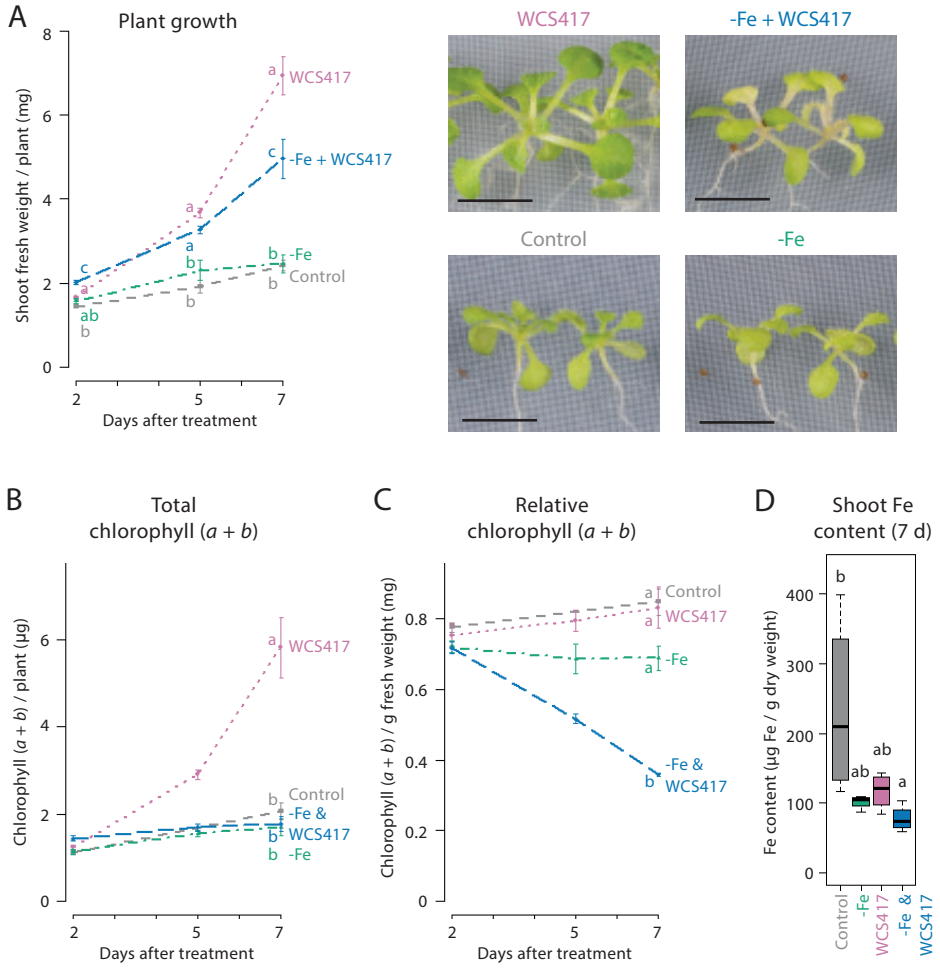

Figure 2 Effect of WCS417 on plant growth and Fe status under Fe-sufficient and Fe-deficient conditions. Plant growth (A) and total and relative chlorophyll (a + b) content (B and C) at 2, 5, and 7 days after 12-day-old Col-0 plants were transferred to control medium (grey and purple) or medium not supplemented with Fe (-Fe; green and blue) and half of each condition was inoculated with a WCS417 suspension with an OD_{600} of 0.01. Photographs are representative pictures from the experiment at 7 days post treatment. D) Leaf Fe content of 19-day-old plants7 days post treatment. These plants were grown at high density and inoculated with a WCS417 suspension with an OD_{600} of 0.1. Error bars represent standard errors of the mean. Per timepoint, different letters indicate statistically significant differences between treatments (One-way ANOVA followed by Tukey's test; $P < 0.05$; n=3-6). Scale bars represent 0.5 cm.

the chlorophyll content. While Fe content in the shoots did not significantly differ between WCS417-treated plants and their respective controls, the Fe content of Fe-starved plants tended to be lower (Figure 2D). Together, these data suggest that under conditions of sufficient Fe availability, enhanced Fe uptake ensures the maintenance of Fe homeostasis in the more rapidly growing WCS417-colonized plant.

Shoot-to-root Fe signaling in PGPR-treated plants

The Fe deficiency response in the root is activated in Fe deficient conditions by shoot-derived signals communicating leaf Fe status to the root (Grusak and Pezeshgi, 1996; Grillet *et al.*, 2018). The induction of the Fe deficiency response upon root colonization by WCS417 (Figure 1) was previously shown to also require a shoot-derived signal (Zamioudis *et al.*, 2015). Therefore, we hypothesized that this response is activated due to an enhanced Fe demand in the faster-growing shoots. To test this hypothesis, we studied whether exogenous Fe supply to the leaves prevents WCS417-mediated induction of the Fe deficiency response in the roots. A concentration range of 5 µM – 5 mM of exogenously supplied FeNaEDTA gradually increased *FER1* mRNA levels in the shoots of sterile-grown plants at 7 days after treatment, suggesting that Fe content increased in the Fe-supplemented shoots (Figure 3A). The concentration of 500 µM was chosen for further experiments as this was the highest concentration that could be supplied to leaves without causing visible symptoms of phytotoxicity (Figure 3B). Colonization of the roots by WCS417 promoted growth in Col-0 plants irrespective of whether the leaves were supplemented with 500 µM FeNaEDTA (Figure 3C). Application of the Fe supplement to the leaves had no effect on the WCS417-induced levels of *MYB72* and *IRT1* in the roots (Figure 3D), suggesting that leaf Fe shoot-to-root signaling does not affect WCS417-mediated induction of the Fe deficiency response in the roots. The WCS417-mediated growth promotion was associated with a decrease in *FER1* mRNA levels in the control shoots at 2 days after inoculation of the roots with WCS417 (Figure 3E), suggesting that WCS417-treated plants were in demand for Fe (Figure 3D). A similar drop in *FER1* mRNA levels was observed in WCS417-treated plants of which the shoots were supplemented with Fe. Hence, a single application of 500 µM FeNaEDTA to the leaves at the onset of root colonization by WCS417 was not sufficient to compensate for a possible increased Fe demand in the leaves during the early stages of WCS417-mediated plant growth promotion.

In order to supply a more continuous source of exogenous Fe to the leaves we made use of a segmented plate setup in which roots and shoots could be exposed to different Fe concentrations (Figure 4A). When both roots and shoots of sterile-grown plants were cultivated for 2 days on Fe-deficient medium, *MYB72* and *IRT1* were induced in the roots, as expected (Figure 4B). When the shoots were placed on Fe-sufficient medium and the roots on Fe-deficient medium, the levels of *MYB72* and *IRT1* gene expression were significantly reduced compared to plants grown on fully Fe-deficient plates (Figure 4B). Hence, in this experimental setup, leaf Fe status is an important determinant of the Fe deficiency response activity. Vice versa, when roots were placed on Fe-sufficient medium and shoots on Fe-deficient medium, *MYB72* and *IRT1* were not activated, likely because the roots had ample Fe to take up from the medium to supply the shoots with sufficient Fe (Figure 4B). Next, we tested the effect of WCS417 in this experimental set up. Again, plants of which both shoots and roots were grown on Fe-deficient segments showed increased expression of the Fe deficiency response genes *MYB72* and *IRT1* (Figure 4C). In response to WCS417 root colonization, plants of which both shoots and roots were grown on Fe-sufficient segments showed a similarly induced expression level of *MYB72* and *IRT1* (Figure 4C). Decapitation of the shoot from the root just prior to root inoculation with WCS417 completely prevented activation of *MYB72* and *IRT1* (Figure 4C, red X), confirming previous findings that a shoot-derived signal is required for the onset of the Fe deficiency response in the roots in response to WCS417 (Zamioudis *et al.*, 2015). To test whether the induction of the Fe deficiency response in roots in response to WCS417 is caused by an increased Fe demand in the

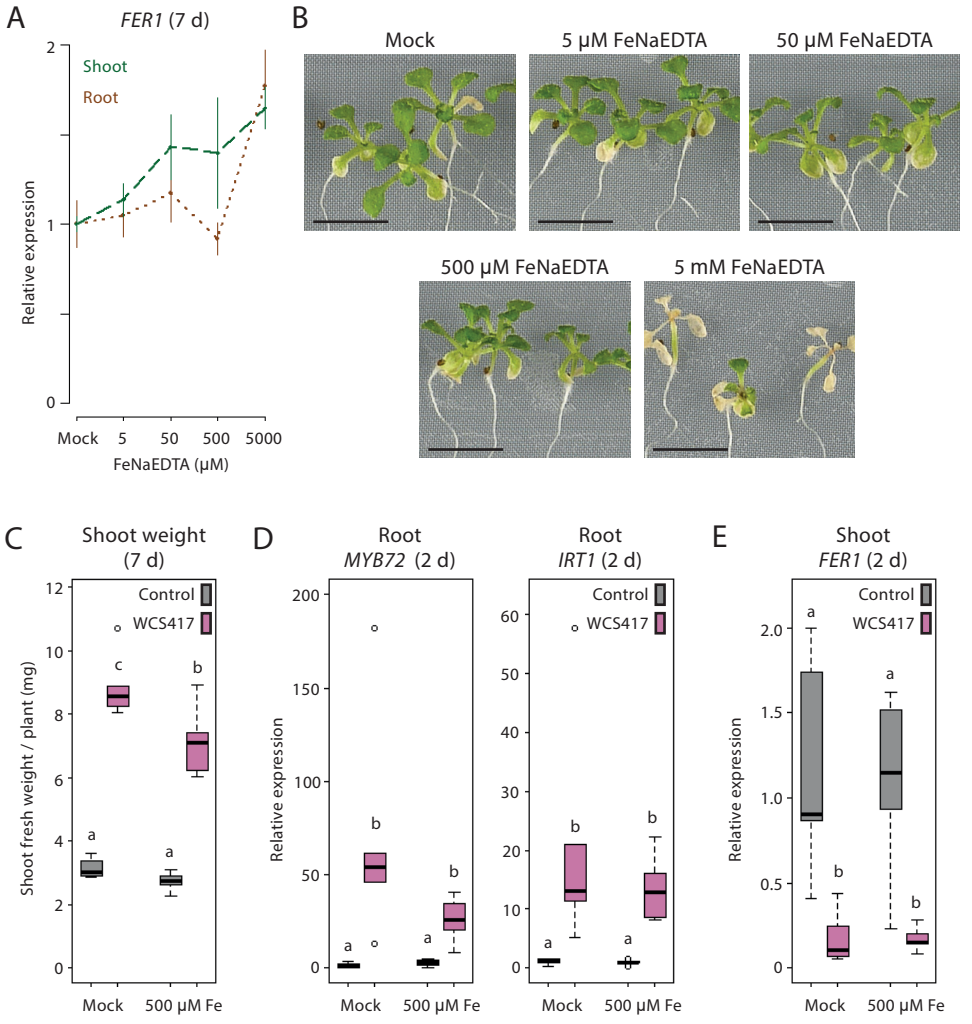

Figure 3 Effect of exogenous shoot Fe supply on the WCS417-mediated induction of the Fe deficiency response in roots. A) RT-qPCR analysis of *FER1* gene expression in roots and shoots of 19-day-old Col-0 plants (B), 7 days after 0.2 µl of a solution with indicated concentrations of FeNaEDTA was added on two leaves per plant. C) Shoot weight of 19-day-old plants, 7 days after WCS417 (OD_{600}=0.01) was added to the root and 500 µM FeNaEDTA was added to the shoot. qRT-PCR analysis of *MYB72* and *IRT1* in roots (D), and *FER1* gene expression in shoots (E) at 2 days after shoot Fe supply and inoculation with WCS417. Gene expression levels were normalized to that of the constitutively expressed reference gene *PP2AA3* (At1g13320). Plotted are fold-changes in gene expression levels relative to the average of non-inoculated, mock-treated plants. Error bars represent standard errors of the mean. Per timepoint, different letters indicate statistically significant differences between treatments (One-way ANOVA followed by Tukey's test; $P < 0.05$; n=5-6). Scale bars represent 0.5 cm.

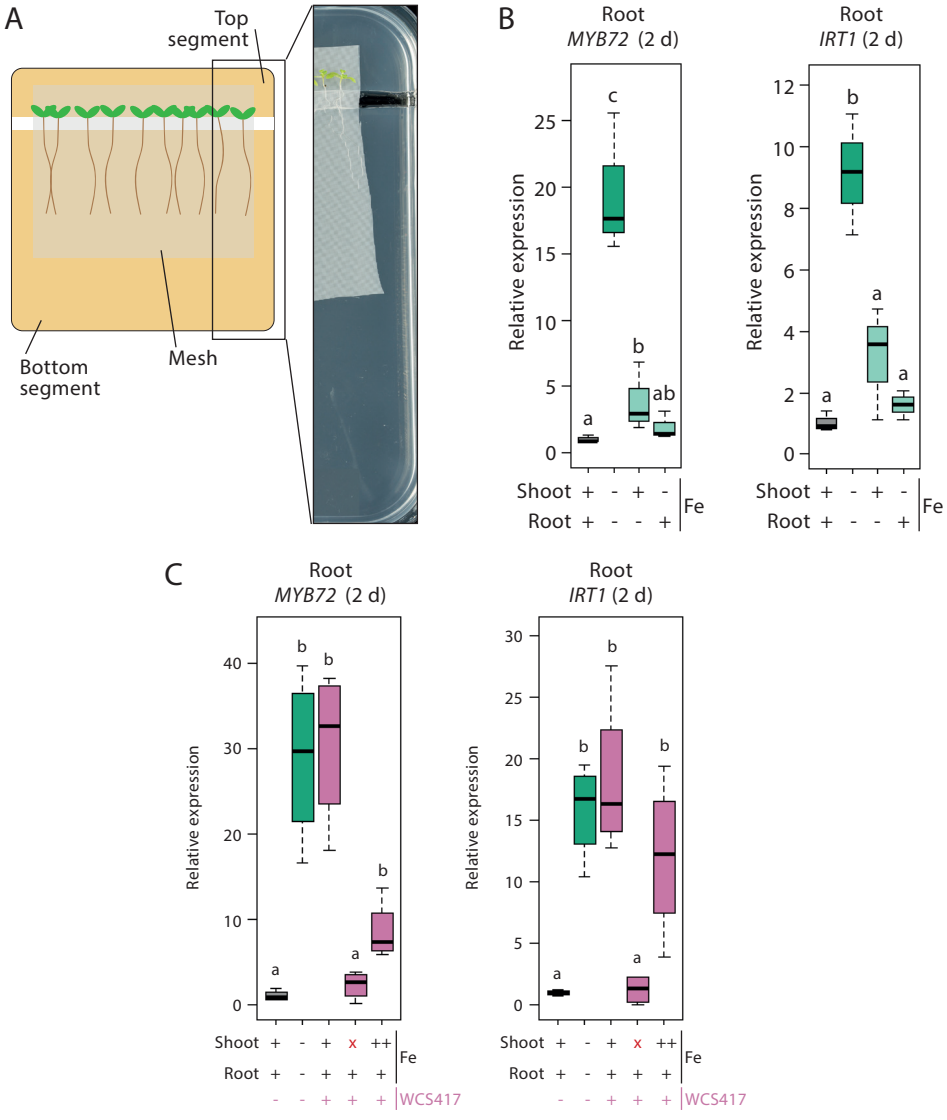

Figure 4 Effect of differential Fe supply to shoots and roots on the WCS417-mediated induction of the Fe deficiency response in roots. A) Schematic representation and picture of the segmented plate assay in which Col-0 plants on nylon mesh are positioned with their shoots on the top segment and with their root systems on the bottom segment of the plate. B-C) qRT-PCR analysis of *MYB72* or *IRT1* gene expression in roots, 2 days after transfer of 5-day-old Col-0 plants onto segmented plates in which the top and bottom segments contained either 0 µM (-), 40 µM (+) or 200 µM (++) FeNaEDTA. Root inoculations with WCS417 (OD_{600}=0.01) were performed immediately after transfer of the plants to the segmented plates. Decapitation of the shoot (indicated by a red "x") was performed by cutting at the shoot-root junction just prior to application of WCS417 to the roots. Gene expression levels were normalized to that of the constitutively expressed reference gene *PP2AA3* (At1g13320). Plotted are fold-changes in gene expression levels relative to that of non-inoculated plants growing with both shoots and roots on Fe-sufficient medium. Error bars represent standard errors of the mean. Different letters indicate statistically significant differences between treatments (One-way ANOVA followed by Tukey's test; $P < 0.05$; n=3-4).

shoot, we placed the shoots on medium with a five times higher concentration of Fe (200 µM Fe (++) instead of 40 µM Fe (+)). We reasoned that this high Fe concentration in the top segment would compensate for the potentially enhanced Fe demand in the shoots of WCS417-treated plants. In this setup, the roots were placed on standard Fe-sufficient medium. Figure 4C shows that when the shoots were exposed to a higher concentration of Fe in the medium, WCS417-induced expression of *MYB72* in the roots was reduced, but not statistically significantly. For *IRT1* gene expression, the effect of the enhanced Fe supply via the leaves was even weaker and also not statistically significant. Together, these results point to a scenario in which it is unlikely that an increased Fe demand in the shoots because of WCS417-mediated growth promotion is responsible for the shoot-to-root signaling that leads to the activation of the Fe deficiency response in WCS417-colonized roots.

PGPR-mediated shoot-to-root Fe signaling is independent of OPT3

The above-described results suggest that the WCS417-induced Fe deficiency response in the roots does not rely on the canonical Fe status-mediated shoot-to-root signaling system that communicates whether activation of the Fe uptake response is required. To find further proof for this conclusion, we made use of the knockdown mutant *opt3-2*, which is impaired in leaf Fe status signaling to the root (Mendoza-Cózatl *et al.*, 2014; Zhai *et al.*, 2014). Misregulation of shoot-to-root Fe status signaling in *opt3-2* plants results in a constitutively active Fe deficiency response in the roots under Fe-sufficient conditions. This leads to high Fe levels in the shoot (Stacey *et al.*, 2008) that are sensed, but not communicated to the root to suppress the Fe uptake response (Khan *et al.*, 2018). We reasoned that if the Fe deficiency response is activated in response to WCS417 because of an Fe shortage in the shoot, activation of *MYB72* should not take place in the *opt3-2* mutant because of its shoot Fe overload. To test this, we inoculated the roots of Col-0 and *opt3-2* plants growing on Fe-sufficient medium with WCS417 or a mock solution. Two days later, the expression level of the Fe storage gene *FER1* was significantly higher in the control shoots of *opt3-2* plants than in those of Col-0 (Figure 5A), which is indicative of the previously reported enhanced Fe levels in *opt3-2* leaves (Stacey *et al.*, 2008). In addition, basal *MYB72* mRNA levels were 19-fold higher in control *opt3-2* roots than in control Col-0 roots (Figure 5B), confirming that *opt3-2* roots constitutively express the Fe deficiency response (Khan *et al.*, 2018). WCS417 promoted growth in both Col-0 and *opt3-2,* resulting in a typical 2-3-fold increase in shoot FW (Figure 5C) and an increase in the total amount of chlorophyll per plant (Figure 5D). Inoculation of Col-0 roots with WCS417 resulted in a typical 3-fold increase in *MYB72* expression. In *opt3-2* mutants, *MYB72* transcript levels were also increased by 3-fold in response to WCS417, from 19- to 53-fold relative to mock-treated Col-0 roots. These results confirm that the WCS417-induced Fe uptake response in roots is not controlled by the canonical Fe status-mediated shoot-to-root signaling pathway but by a shoot-dependent signaling system that functions independently of the Fe status and OPT3.

Discussion

PGPR in the root microbiome enhance plant nutrient uptake, improve root system architecture, and stimulate the plant immune system (Berendsen *et al.*, 2012). Over the past few years, evidence has accumulated that plants evolved strategies to attract beneficial root-associated

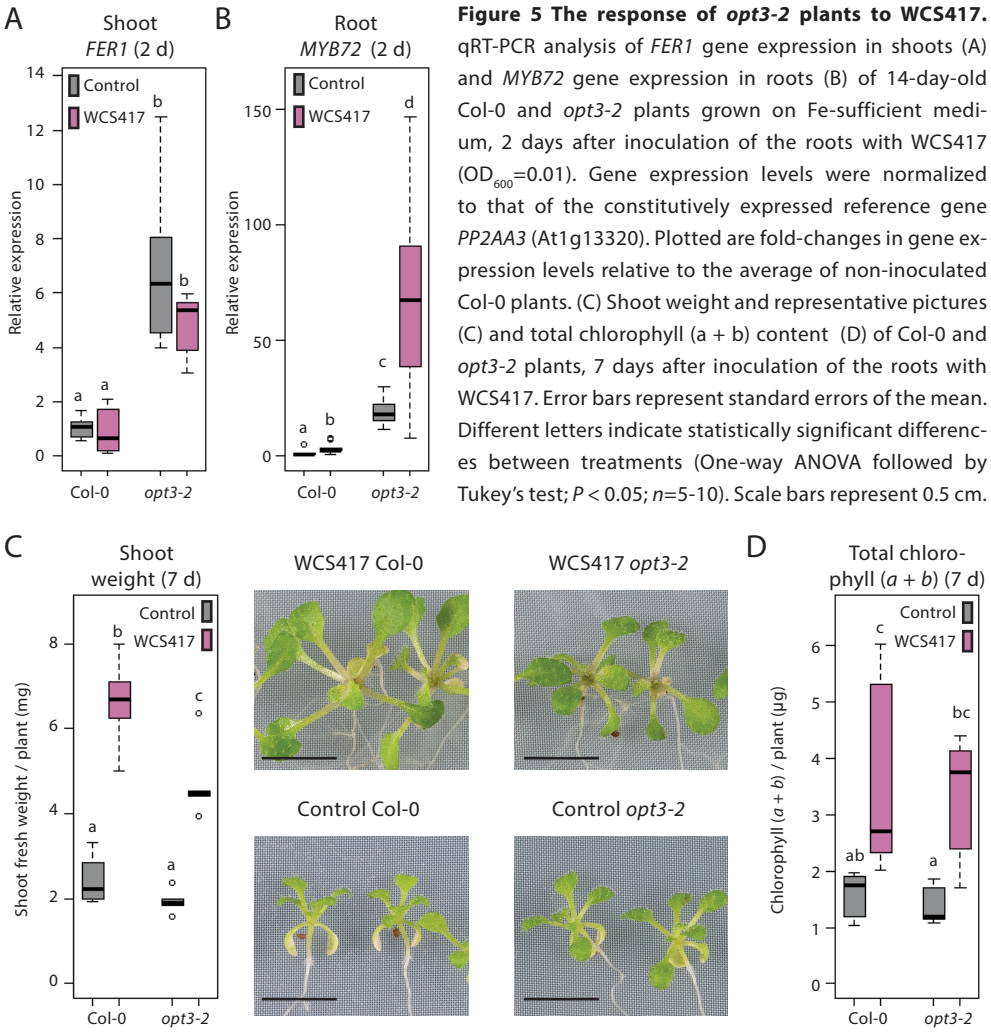

Figure 5 The response of *opt3-2* plants to WCS417. qRT-PCR analysis of *FER1* gene expression in shoots (A) and *MYB72* gene expression in roots (B) of 14-day-old Col-0 and *opt3-2* plants grown on Fe-sufficient medium, 2 days after inoculation of the roots with WCS417 (OD_{600}=0.01). Gene expression levels were normalized to that of the constitutively expressed reference gene *PP2AA3* (At1g13320). Plotted are fold-changes in gene expression levels relative to the average of non-inoculated Col-0 plants. (C) Shoot weight and representative pictures (C) and total chlorophyll (a + b) content (D) of Col-0 and *opt3-2* plants, 7 days after inoculation of the roots with WCS417. Error bars represent standard errors of the mean. Different letters indicate statistically significant differences between treatments (One-way ANOVA followed by Tukey's test; $P < 0.05$; n=5-10). Scale bars represent 0.5 cm.

microbiota to optimize both nutrient acquisition and immunity (Hiruma *et al.*, 2016; Castrillo *et al.*, 2017; Verbon *et al.*, 2017; Bakker *et al.*, 2018; Stringlis *et al.*, 2018a). One of the nutrients whose uptake is affected by PGPR is Fe. Fe is among the essential mineral nutrients required by plants, but its bioavailability in the soil is often limited (Palmer *et al.*, 2013; Tsai and Schmidt, 2017). Plants evolved elaborate Fe deficiency responses to increase Fe uptake in Fe limiting conditions (Römheld, 1987). Arabidopsis roots also activate the Fe deficiency response upon interaction with the model PGPR WCS417, even when the interaction takes place in Fe-sufficient conditions (Zamioudis *et al.*, 2014). Activation of the response results in increased production and excretion of MYB72-dependent Fe-mobilizing coumarins (Stringlis *et al.*, 2018a). As some coumarins have selective antimicrobial activity, the PGPR-induced secretion of these coumarins is thought to help the PGPR to establish in their niche on the root. In addition to activating the Fe deficiency response, PGPR can promote plant growth and trigger ISR. Activation of both the Fe deficiency response and ISR is a common phenomenon in interactions between

dicot plants and beneficial microbes (Romera *et al.*, 2019). However, little is known about the mechanism underlying the induction of the Fe deficiency response by PGPR, or about its effect on Fe homeostasis and signaling in the plant. In this study, we show that WCS417 activates the Fe deficiency response only when present in sufficient numbers on the roots. In comparison to conditions of Fe starvation, the WCS417-elicited Fe deficiency response is mild and transient (Figure 1). We further show that the induced Fe uptake response is not the cause of WCS417-mediated plant growth promotion, as WCS417 still promoted plant growth under Fe-limiting conditions. Nevertheless, WCS417-induced Fe uptake is essential for the plant to maintain Fe homeostasis during the WCS417-enhanced plant growth (Figure 1 and 2). Finally, we demonstrate that the WCS417-induced Fe deficiency response in the roots is regulated by a so far unidentified shoot-to-root signaling system that is independent of leaf Fe status and OPT3.

WCS417 does not cause Fe depletion in the soil environment

Colonization of the plant root by growth-promoting microbes induces molecular and morphological changes in the roots that resemble those induced under Fe starvation (Zamioudis *et al.*, 2013, 2014; Verbon and Liberman, 2016; Martínez-Medina *et al.*, 2017; Verbon *et al.*, 2017; Romera *et al.*, 2019). Many root microbiota, including the *Pseudomonas* spp. PGPR used in this study (Duijff *et al.*, 1993; Berendsen *et al.*, 2015), have the capacity to produce Fe-chelating siderophores that ensure microbial uptake of Fe when Fe is scarce. Interestingly, siderophores have also been shown to play a role in the onset of ISR (Duijff *et al.*, 1993; Meziane *et al.*, 2005; De Vleesschauwer *et al.*, 2008). This raises the question whether PGPR-mediated activation of the Fe deficiency response and ISR are caused by a microbially-inflicted Fe depletion in the root surroundings. Our results suggest that this is not the case, as WCS417 elicited a mild, transient activation of the Fe deficiency response, whereas Fe starvation triggered an Fe deficiency response that was stronger and increased gradually over time (Figure 1). The rejection of the Fe-depletion hypothesis is supported by the fact that Arabidopsis also activates the Fe deficiency response upon root colonization by WCS417 siderophore mutants and upon perception of volatile organic compounds (Zamioudis *et al.*, 2015; Martínez-Medina *et al.*, 2017).

The WCS417-induced Fe deficiency response in the root is independent of leaf Fe status

Previously, we showed that a shoot-derived signal is required for the activation of the Fe deficiency response by PGPR in Arabidopsis roots (Zamioudis *et al.*, 2015). As WCS417-mediated activation of the Fe deficiency response supports Fe nutrition in the faster growing plant (Fig. 2), we reasoned that the Fe deficiency response might be activated in response to an increased Fe demand in the faster growing shoots. This resembles the previously described leaf Fe status-dependent shoot-to-root signaling system that maintains Fe homeostasis via the regulatory activity of the leaf Fe transporter OPT3 (Zhai *et al.*, 2014; Khan *et al.*, 2018). However, while exogenous Fe supply to the leaves suppressed Fe starvation-mediated activation of the Fe uptake response in the roots, it did not prevent WCS417-mediated activation of the response (Figs. 3 and 4). Moreover, the leaf Fe status shoot-to-root signaling mutant *opt3-2*, which has an Fe overload in its shoots (Zhai *et al.*, 2014; Khan *et al.*, 2018), was still responsive to WCS417-mediated activation of the Fe deficiency response in the roots (Fig. 5). We therefore conclude that the Fe acquisition response triggered by WCS417 is under the control of a shoot-to-root signaling system that functions independently from OPT3 and leaf Fe status. Recently,

the IRON MAN (IMA) peptide family was discovered as a novel phloem-mobile shoot-to-root signal that controls Fe uptake in the roots under conditions of Fe starvation (Grillet *et al.*, 2018). Interestingly, *IMA1* is also induced upon colonization of the roots by WCS417 (Zamioudis *et al.*, 2014) and could therefore play a role in the shoot-to-root signaling required for the activation of the Fe deficiency response.

Auxin is required for the morphological and molecular root responses that are typically observed in roots in response to WCS417 and Fe starvation (Chen *et al.*, 2010; Zamioudis *et al.*, 2013; Stringlis *et al.*, 2018b). While WCS417 does not produce auxin itself, it stimulates an auxin response in Arabidopsis roots (Zamioudis *et al.*, 2013, Stringlis *et al.*, 2018b). As the auxin response in the root is also under the control of a shoot-to-root signaling system (Ljung *et al.*, 2005), auxin signaling might be involved in the shoot-to-root signaling pathway that activates the Fe deficiency response upon root colonization by WCS417. To test this hypothesis, further investigation into the interaction between the signaling pathways induced in response to PGPR, Fe starvation and auxin is required.

The fine balance between harmful and beneficial

WCS417 and many other biological control agents, promote plant growth, improve plant nutrition, and or prime the plant immune system in controlled experimental settings (Lugtenberg and Kamilova, 2009; Pieterse *et al.*, 2014; Liu *et al.*, 2017; Ab Rahman *et al.*, 2018). However, biological control agents often show inconsistent performance in the field. In this study, it becomes clear that a switch from beneficial to harmful effects of PGPR can be induced by environmental conditions. Colonization of the roots by WCS417 promoted plant growth irrespective of whether plants were grown on Fe-sufficient or Fe-deficient medium (Fig. 2). On Fe-sufficient medium, the WCS417-induced Fe deficiency response allowed plants to maintain Fe homeostasis while growing more rapidly. However, under Fe limiting conditions, the faster growing WCS417-stimulated plants had a significantly lower chlorophyll content and became chlorotic. Hence, under specific environmental conditions, when not all prerequisites for the potentially beneficial microbial functions are met, biological control agents can become detrimental for plant performance. This highlights the importance of basic research on understanding the biological mechanisms by which beneficial microbes promote plant growth and control diseases, as it will provide important information that may facilitate the successful application of novel biofertilizers and biopesticides in the field.

Chapter 4

Decreased susceptibility of iron-deficient plants requires a functional plant immune system

Pauline L. Trapet[1*], Eline H. Verbon[1*], Renda R. Bosma[1], Kirsten Voordendag[1], Johannes A. van Pelt[1], Corné M.J. Pieterse[1]

[*]These authors contributed equally to this work

[1]Plant-Microbe Interactions, Utrecht University, Department of Biology, The Netherlands

Abstract

Iron (Fe) is an essential element for most organisms on Earth because it functions as an enzyme cofactor in many fundamental cellular processes. Consequently, Fe availability affects the outcome of many cross-kingdom interactions. In *Arabidopsis thaliana* (Arabidopsis), limited Fe availability to the plant has been shown to decrease disease symptoms caused by necrotrophic pathogens. Here, we report that Fe deficiency not only decreases the symptoms caused by the necrotrophic fungus *Botrytis cinerea*, but also by the hemi-biotrophic bacterium *Pseudomonas syringae* pv. *tomato* DC3000 and the obligate biotrophic oomycete *Hyaloperonospora arabidopsidis*. We show that Fe deficiency-reduced disease severity is dependent on functional hormone signaling, as Fe deficiency does not decrease disease symptoms caused by *B. cinerea* and *H. arabidopsidis* in the ethylene response mutant *ein2-1* and the salicylic acid-biosynthesis mutant *sid2-1*, respectively. Thus, Fe deficiency seems to induce an active form of plant resistance. This Fe deficiency-induced resistance resembles the broad-spectrum induced systemic resistance (ISR) that is triggered upon colonization of roots by beneficial *Pseudomonas simiae* WCS417 bacteria. However, we show that Fe deficiency-induced resistance does not depend on the ISR regulators MYB72 and BGLU42, indicating that both types of induced resistance are regulated, at least partly, in a different manner. Interestingly, a mutant with an excess of Fe in its shoot and a mutant constitutively suffering from Fe starvation show resistance levels comparable to those in Fe-starved Col-0 plants. Therefore, we propose that a misregulation of Fe homeostasis might be sufficient for the onset of resistance. Collectively, our results suggest a complex interplay between the regulation of plant Fe homeostasis and plant immunity in which a disturbance in Fe homeostasis primes the immune system for enhanced defense against pathogen attack.

Introduction

Iron (Fe) functions as an enzyme cofactor in several important cellular processes, such as respiration, DNA synthesis, hormone production, and chlorophyll biosynthesis. Fe is therefore an essential nutrient for nearly all living organisms (Darbani *et al.*, 2013; Balk and Schaedler, 2014). As the bioavailability of Fe in soil is generally low (Guerinot and Ying, 1994), plants have developed sophisticated mechanisms to ensure sufficient Fe uptake. Two Fe uptake strategies have been described in plants: Strategy I, which is used by non-graminaceous plant species such as *Arabidopsis thaliana* (Arabidopsis), and Strategy II, which is used by grass plant species (Römheld, 1987). Strategy II is based on the production and secretion of phytosiderophores, which have a high affinity for Fe. Secreted phytosiderophores chelate Fe from the soil and can subsequently be taken up by the plant through a ferric Fe (Fe^{3+})-phytosiderophore-specific uptake system (Guerinot and Ying, 1994). This strategy is similar to Fe uptake mechanisms employed by bacteria and fungi, as these organisms also secrete Fe-chelating siderophores to enable Fe uptake from the environment (Miethke and Marahiel, 2007). Strategy I, in contrast, is based on the reduction of Fe. A major regulator of Strategy I in Arabidopsis is the transcription factor FER-LIKE IRON DEFICIENCY TRANSCRIPTION FACTOR (FIT). Among other genes, FIT activates *FERRIC REDUCTASE OXIDASE2* (*FRO2*), *IRON REGULATED TRANSPORTER1* (*IRT1*) and *MYB72* (Colangelo and Guerinot, 2004). FRO2 reduces soil-borne Fe^{3+} to ferrous Fe (Fe^{2+}) (Robinson *et al.*, 1999). Fe^{2+} is subsequently taken up in the root interior through IRT1 (Vert *et al.*, 2002). In Fe-deprived soils, the root-specific transcription factor MYB72 acts together with its paralogue MYB10 in the mobilization and uptake of Fe (Palmer *et al.*, 2013). MYB72 regulates the biosynthesis and secretion of Fe-mobilizing coumarins (Zamioudis *et al.*, 2014; Stringlis *et al.*, 2018a). Downstream of MYB72, activity of the glycoside hydrolase BGLU42 converts glycosylated coumarins into their aglycone counterparts, which is required for the secretion of the coumarins into the rhizosphere (Zamioudis *et al.*, 2014; Stringlis *et al.*, 2018a). The secretion of these Fe-chelating phenolic compounds into the soil results in Fe solubilization and increased effectivity of FRO2 (Santi and Schmidt, 2009; Fourcroy *et al.*, 2014). In addition to *MYB72* and *BGLU42*, *FERULOYL-COA 6'-HYDROXYLASE1* (*F6'H1*) is required for the production of these compounds (Schmid *et al.*, 2014; Tsai and Schmidt, 2017).

Upon uptake of Fe by the roots, different transporters, such as YELLOW STRIPE-LIKE (YSL) family members and NRAMPs, take care of proper distribution of Fe throughout the plant (Kobayashi *et al.*, 2019). As an excess of Fe can cause major damage to cells through the production of hydroxyl radicals (Fenton, 1894), various organic molecules, such as citrate, phenolics, and nicotianamine, act as chaperones of Fe during transport to prevent Fe toxicity. Ferritins (FERs), nicotianamine, and phytates are involved in buffering Fe once it is stored in the vacuole, mitochondria and chloroplasts (Darbani *et al.*, 2013; Kobayashi *et al.*, 2019). Once sufficient Fe has been transported to the shoot, the Fe deficiency response in the roots is down-regulated. The gene *OLIGO PEPTIDE TRANSPORTER 3* (*OPT3*), encoding a phloem-specific Fe transporter, is involved in leaf Fe status shoot-to-root signaling (Zhai *et al.*, 2014; García *et al.*, 2018; Khan *et al.*, 2018), as is the IRON MAN family of peptides (Grillet *et al.*, 2018).

Fe availability does not only affect plant nutrient status, but also plant susceptibility to disease (Aznar *et al.*, 2015b; Verbon *et al.*, 2017). For example, the Arabidopsis response to the pathogenic bacterium *Dickeya dadantii* is dependent on sufficient Fe content in the plant, as it involves the release of Fe from the vacuole to develop an oxidative burst to limit pathogen

growth (Segond *et al.*, 2009). Concomitantly, the plant increases the expression of the ferritin-encoding gene *FER1*, probably to protect the yet uninfected plant tissues from the oxidative stress (Aznar *et al.*, 2015a). Similarly, maize plants use the oxidative burst to protect themselves from *Colletotrichum graminicola*. Fe-deficient maize plants are therefore less resistant to *C. graminicola* because they cannot mount as strong an oxidative burst as plants grown in Fe-sufficient conditions (Ye *et al.*, 2014). The opposite strategy is also employed, in which plants do not expose pathogens to an excess of Fe, but rather withhold Fe from the pathogen. For example, enhanced sequestration of Fe in the apoplast by Arabidopsis in response to infection by *Pectobacterium carotovorum* subsp. *carotovorum* withholds Fe from the pathogen, thereby decreasing pathogen virulence (Hsiao *et al.*, 2017). Pathogen dependency on sufficient Fe availability for full virulence has also been documented for *Cochliobolus heterostrophus, Cochliobolus miyabeanus*, *Fusarium graminearum*, *Alternaria brassicicola* (Oide *et al.*, 2006), and *Fusarium oxysporum* (López-Berges *et al.*, 2012). In addition to Fe withholding, decreased susceptibility of Fe-deficient plants is in some cases due to the Fe deficiency-induced secretion of antimicrobial molecules. A well-described example is the Fe deficiency-induced secretion of coumarins that have antimicrobial properties (Stringlis *et al.*, 2019). Finally, Fe deficiency has been suggested to enhance Arabidopsis resistance to disease by enhancing the immune response, although data so far are inconclusive and the mechanisms involved are unknown (Kieu *et al.*, 2012).

Interestingly, the root-specific response to Fe deficiency is also activated in Arabidopsis in response to colonization by the beneficial rhizobacterium *Pseudomonas simiae* WCS417. Amongst the Fe deficiency response genes that are activated in response to WCS417 are *MYB72* and *BGLU42* (Van der Ent *et al.*, 2008; Zamioudis *et al.*, 2014). As described above, MYB72 and BGLU42 are involved in the secretion of Fe-chelating coumarins that increase Fe^{3+} availability in the soil (Schmid *et al.*, 2014; Fourcroy *et al.*, 2016; Tsai and Schmidt, 2017; Stringlis *et al.*, 2019). Upon root colonization by WCS417, both MYB72 and BGLU42 are required for the induction of systemic resistance (ISR) observed in WCS417-colonized plants. In fact, overexpression of BGLU42 in oxBGLU42 plants results in constitutive resistance (Zamioudis *et al.*, 2014). WCS417-mediated ISR does not involve constitutively active defense responses. Instead, WCS417 colonization primes the Arabidopsis immune system, resulting in a stronger and faster response to pathogen attack (Pieterse *et al.*, 2014). This increased resistance requires functional signaling of the plant defense hormones jasmonic acid (JA) and ethylene (ET). These and other defense hormones act as cellular signaling molecules in the regulation of immune processes in response to microbial pathogens, insect herbivores, and beneficial microbes. The hormones' signaling pathways are interconnected in a complex network to allow plants to rapidly adapt to their biotic and abiotic environment and to utilize limited resources in a cost-efficient manner (Pieterse et al., 2012). In Arabidopsis, salicylic acid (SA) is required for an adequate defense response to (hemi)biotrophic pathogens, while JA and ET are involved in the defense response against necrotrophic pathogens. Additionally, JA functions with abscisic acid (ABA) in the defense response that is activated upon insect herbivory (Bodenhausen and Reymond, 2007; Howe and Jander, 2008; Pieterse *et al.*, 2012; Broekgaarden *et al.*, 2015). Besides activating local defense responses, plant hormones play a role in systemic immune responses, such as the above-mentioned ISR, but also SA-dependent systemic acquired resistance (SAR), which is typically activated upon local pathogen infection (Durrant and Dong, 2004), and herbivory-

induced resistance, which is activated in response to wounding and herbivory attack and is dependent on JA signaling (Howe and Jander, 2008; Wu and Baldwin, 2010). Interestingly, plant defense hormones are also involved in the activation and repression of the Fe deficiency response: SA and ET are positive regulators of the Fe uptake response, whereas ABA and JA are negative regulators (Hindt and Guerinot, 2012; Brumbarova *et al.*, 2015; Shen *et al.*, 2016; Romera *et al.*, 2019). The dual role of these hormones and the induction of systemic resistance by WCS417 via the activation of the Fe deficiency response suggest an interplay between the maintenance of Fe homeostasis and plant immunity. This suggests that there might be an active role of the plant immune system in Fe deficiency-reduced disease susceptibility.

In this chapter, we show that the spectrum of pathogens that cause fewer disease symptoms on Fe-deficient plants than on Fe-sufficient plants is greater than known so far. Subsequently, we show that decreased susceptibility in Fe-deficient conditions requires functional plant hormone signaling. In these conditions, plants seem to develop a Fe deficiency-induced resistance that is based on priming of the immune response. WCS417-mediated ISR requires activation of Fe deficiency response genes and is also based on priming of the immune response (Zamioudis *et al.*, 2015). Therefore, we subsequently investigated whether the activation of these two resistances is based on the same root-specific molecular mechanism. This turned out not to be the case. Instead, any disruption of Fe homeostasis appears to result in increased plant resistance.

Materials and methods

Plant material and growth conditions. Wild-type *Arabidopsis thaliana* accession Columbia-0 (Col-0), mutants *myb72-2* (Van der Ent *et al.,* 2008), *bglu42* (Van der Ent *et al.*, 2008; Zamioudis *et al.*, 2014), *frd1-1* (Robinson *et al.*, 1999), *opt3-2* (Zhai *et al.*, 2014), *ein2-1* (Guzman and Ecker, 1990), and *sid2-1* (Wildermuth *et al.*, 2001), and the *BGLU42* overexpressing line ox*BGLU42* (Zamioudis *et al.*, 2014) were grown in hydroponic culture as described in Trapet et al. (2016), with minor modifications. Briefly, vapor-phase sterilized seeds were stratified at 4°C in half-strength modified Hoagland medium supplemented with 0.2% agar, with full-strength standard Hoagland medium (referred to as +Fe medium) containing 0.2 mM $Ca(NO_3)_2$, 0.5 mM KNO_3, 0.25 mM KH_2PO_4, 0.2 mM $MgSO_4$, 70 µM H_3BO_3, 14 µM $MnCl_2$, 1.0 µM $ZnSO_4$, 0.5 µM $CuSO_4$, 10 µM NaCl, 0.2 µM Na_2MoO_4, and 50 µM FeNaEDTA. After 4 days, seeds were sown on seed holders filled with 10-fold diluted +Fe medium supplemented with 0.65 % agar, and placed on top of hydroponic bins (Araponics, Liège, Belgium). The bins were filled with +Fe medium and placed in short-day growth conditions (21-22°C, 14-h night, 10-h day). A transparent lid was put on the bins for the first 10 days to maintain the high humidity necessary for proper seed germination. The hydroponic growth medium was renewed weekly from 2 weeks onwards. After 3 weeks, the plants were rearranged from a high-density set-up (35 plants per bin) to a low-density set-up (18 plants per bin) in which the liquid medium was aerated. The Fe-deficiency response mutant *frd1-1*, which carries a mutation in the *FRO2* gene (Robinson et al., 1999), was cultivated in +Fe medium supplemented to a final concentration of 300 µM FeNaEDTA, as it is not viable in +Fe medium containing 50 µM FeNaEDTA. The Fe-deficiency treatment was performed after 25-32 days of growth on Fe-sufficient medium, dependent on the experiment and as specified below. To this end, the liquid medium in the hydroponic bins was replaced with either +Fe medium (50 µM Fe, or 300 µM for *frd1-1*) or medium without added FeNaEDTA (referred to as -Fe medium).

In order to limit transfer of adhering Fe from the +Fe medium to the -Fe medium, roots were rinsed in -Fe medium before transfer to either fresh -Fe or + Fe medium.

Bioassays. Cultivation of the pathogens, preparation of the pathogen inocula, inoculation of the plants, and measurements of disease severity were carried out as described by Van Wees et al. (2013), with some minor modifications. Pathogen inoculation was performed 3 days after the final transfer of the plants to +Fe or -Fe medium.

Botrytis cinerea strain B05.10 (Van Kan *et al.*, 2017) was cultivated on half-strength potato-dextrose agar (PDA) plates for 10 days at 22°C (16-h night, 8-h day). Spores were harvested in half-strength potato dextrose broth (PBD), filtered through gauze and resuspended to an inoculum containing $5*10^5$ spores/ml. Hydroponically-grown plants were inoculated when they were 5 weeks old by applying a 5-µl droplet of the *B. cinerea* inoculum onto five mature leaves per plant. The bins containing the inoculated plants were kept in closed trays to ensure high humidity for optimal pathogen development. Inoculated leaves were harvested, and pictures were taken at 3 days post inoculation (dpi). Lesion area was measured using the publicly available image analysis program ImageJ (version 1.51n).

Pseudomonas syringae pv. *tomato* DC3000 (Kunkel *et al.*, 1993) was cultivated overnight on KB agar plates at 28°C. Subsequently, bacteria were collected in 10 mM $MgSO_4$ and washed twice by 5 min centrifugation at 5000 *g*. The bacteria were then resuspended to a density of $2.5*10^7$ colony forming units (cfu)/ml (OD_{660} = 0.025) in 10 mM $MgSO_4$ amended with 0.02% (v/v) Silwet L-77. Five-week-old plants were inoculated by dipping their rosette into the bacterial suspension for 3 s. The bins containing the inoculated plants were kept in closed trays to ensure high humidity. After 3 days, bacterial growth was determined in two leaf discs harvested from two different leaves per infected plant. The two leaf discs per plant were pooled and lysed using beads in 500 µl of 10 mM $MgSO_4$. Serial dilutions were plated on KB agar containing 25 mg/ml rifampicin to determine *in planta* bacterial growth.

Hyaloperonospora arabidopsidis isolate Noco2 (Lapin *et al.*, 2012) was maintained on susceptible Arabidopsis mutant *eds1* plants as described (van Damme *et al.*, 2009). Spores were obtained from these plants by washing infected seedlings in demi-water. The spore suspension was filtered through Miracloth and the final concentration was adjusted to $1*10^5$ spores/ml. Four-week-old plants were sprayed with the *H. arabidopsidis* inoculum and kept in closed trays to ensure high humidity. To facilitate development of the *H. arabidopsidis* infection, the trays were placed in growth conditions optimal for *H. arabidopsidis* development (16°C, short day: 15-h night, 9-h day). Two weeks after inoculation, plants were weighed and collected in a 50-ml conical tube containing 3 ml demi water. After vigorous shaking, the number of *H. arabidopsidis* spores in the suspension was estimated using a Bürker counting chamber. In addition to spore counting, *H. arabidopsidis* disease severity was assessed by visualizing hyphal growth using trypan blue staining. Fourteen days after inoculation six leaves were harvested from three plants per treatment . The leaves were boiled for 2 – 10 min in 1 ml trypan blue solution (1:1:1:1 lactic acid : glycerol : phenol : water and 25 % (m:v) trypan blue). After incubating for 1 h at room temperature, the solution was replaced by chloral hydrate for destaining overnight. Hyphal growth in the leaves, visible as strong blue coloration, was inspected using light microscopy.

Hormone treatment. Hormonal treatments were performed as described previously by Van

Wees *et al.* (2013) on 4-week-old plants, 3 days after the transfer to either +Fe or -Fe medium. In brief, 4-week-old plants were treated with methyl JA (MeJA) or SA by dipping the leaves for 4 s into a solution containing 0.015% (v/v) Silwet L-77 (Van Meeuwen Chemicals, Weesp, Netherlands), 0.1% EtOH and either 1 mM SA (Mallinckrodt Baker, Dublin, Ireland) or 100 µM MeJA (Serva, Brunschwig Chemie, Basel, Switzerland). Mock treatments were dipped into a solution containing 0.0015% (v/v) Silwet L-77 and 0.1% EtOH. Plants were then placed back in the hydroponic bins. Shoots were harvested and immediately frozen in liquid nitrogen at 6, 12 and 24 h after hormonal treatment. Tissues were stored at -80°C until RNA isolation.

RNA isolation and gene expression measurement by RT-qPCR. RNA was isolated from tissue samples using the protocol described by Oñate-Sánchez and Vicente-Carbajosa (2008). DNase I (Thermo Fisher Scientific, Waltham, USA) treatment was applied to RNA samples according to the manufacturer's instruction. RNA samples were reverse transcribed to cDNA using RevertAid H Minus Reverse Transcriptase (Thermo Fisher Scientific), again according to the manufacturer's instruction. Quantitative reverse transcription polymerase chain reaction was performed in technical duplicates on the cDNA using Power SYBR green PCR master mix (Applied Biosystems, Waltham, USA) to visualize double-stranded DNA and primers against the genes of interest (Table S1). The cycle threshold (Ct) was determined using the ViiA 7 Real-Time PCR system (Applied Biosystems). Gene expression data were normalized to the gene *PP2AA3* (*At1g13320*) (Czechowski *et al.*, 2005), the ΔΔCt values were used for statistical analyses, the relative gene expression ($2^{-\Delta Ct}$) was plotted. The gene-specific primers used are listed in Table S1, which is part of the Online Supplementary Material and can be found here: https://cp.sync.com/dl/60fe897a0#fqt4xv25-em3ineic-y792dq3h-qrydpq97.

Fe content measurement. Four-week-old Col-0 and *opt3-2* plants were transferred to +Fe or -Fe medium. Shoots were harvested for Fe content measurement at 3 and 7 days after transfer. The samples were dried and mineralized as described by Trapet et al. (2016). Fe content was subsequently measured by inductively coupled plasma-atomic emission spectroscopy (iCAP 6000 Series, Thermo Fisher Scientific).

Results

Fe deficiency confers enhanced resistance against pathogens with different life styles

Fe deficiency has been shown to decrease Arabidopsis susceptibility to necrotrophic leaf pathogens (Kieu *et al.*, 2012; Trapet *et al.*, 2016). To study this phenomenon, we obtained Fe-deficient and Fe-sufficient plants by growing 4-week-old wild-type Arabiopdis Col-0 plants with their roots in Fe-sufficient or Fe-deficient liquid Hoagland medium for up to 7 days (Figure 1A). Plants grown in Fe-deficient medium developed typical signs of Fe deficiency: reduction of plant growth (Figure 1B), chlorosis (Figure 1C), reduction in chlorophyll content (Figure 1D), and activation of the Fe deficiency response master regulatory gene *FIT* (Figure 1E).

To test the effect of Fe deficiency on disease susceptibility, leaves of Fe-sufficient and Fe-deficient Col-0 plants were inoculated with the necrotrophic fungus *B. cinerea*, the obligate biotrophic oomycete *H. arabidopsidis,* or the hemibiotrophic bacterium *P. syringae* pv. *tomato* DC3000 according to the inoculation scheme depicted in Figure 2A. Figure 2B-D show that

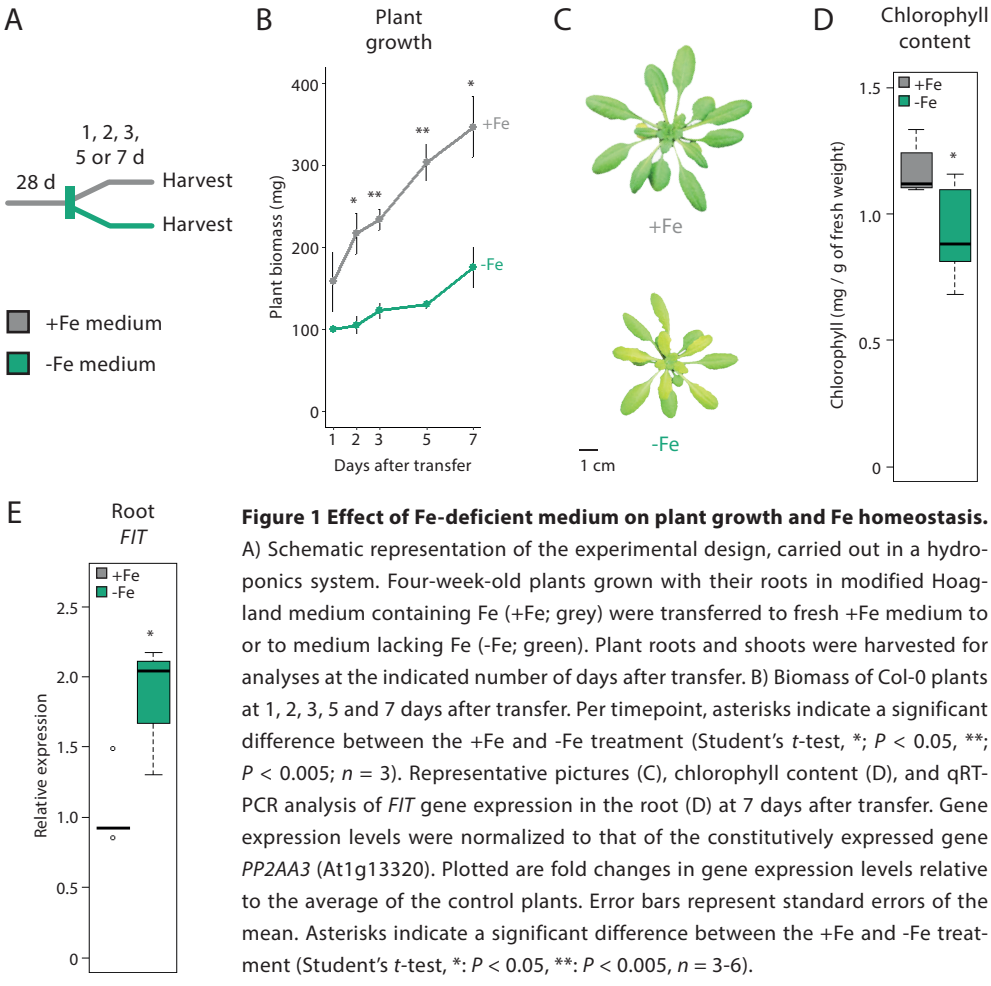

Figure 1 Effect of Fe-deficient medium on plant growth and Fe homeostasis. A) Schematic representation of the experimental design, carried out in a hydroponics system. Four-week-old plants grown with their roots in modified Hoagland medium containing Fe (+Fe; grey) were transferred to fresh +Fe medium to or to medium lacking Fe (-Fe; green). Plant roots and shoots were harvested for analyses at the indicated number of days after transfer. B) Biomass of Col-0 plants at 1, 2, 3, 5 and 7 days after transfer. Per timepoint, asterisks indicate a significant difference between the +Fe and -Fe treatment (Student's *t*-test, *; $P < 0.05$, **; $P < 0.005$; $n = 3$). Representative pictures (C), chlorophyll content (D), and qRT-PCR analysis of *FIT* gene expression in the root (D) at 7 days after transfer. Gene expression levels were normalized to that of the constitutively expressed gene *PP2AA3* (At1g13320). Plotted are fold changes in gene expression levels relative to the average of the control plants. Error bars represent standard errors of the mean. Asterisks indicate a significant difference between the +Fe and -Fe treatment (Student's *t*-test, *: $P < 0.05$, **: $P < 0.005$, $n = 3$-6).

Fe-starved Col-0 plants showed significantly fewer disease symptoms than Fe-sufficient Col-0 plants. Thus, Fe deficiency decreases plant susceptibility to pathogens with diverse life styles.

Previously, we demonstrated that overexpression of the Fe deficiency-responsive gene *BGLU42* in ox*BGLU42* plants is associated with enhanced resistance against *B. cinerea, P. syringae* pv. *tomato* DC3000, and *H. arabidopsidis* (Zamioudis *et al.*, 2014). For all three pathogens, the level of disease symptoms in Fe-sufficient ox*BGLU42* plants was the same as in Fe-starved Col-0 plants and was not further increased under Fe starvation (Figure 2B-D).

Fe deficiency-induced resistance requires a functional plant immune system

Plant hormones influence the activation of both the Fe deficiency response and plant immune responses. For example, ET activates both the Fe deficiency response (Lucena *et al.*, 2015; García *et al.*, 2018) and plant defenses against necrotrophic pathogens (Broekgaarden *et al.*, 2015). Likewise, SA is required for plant immunity against (hemi)biotrophic pathogens and functions upstream of ET to activate the Fe deficiency response (Broekgaarden *et al.*, 2015; Shen *et al.*,

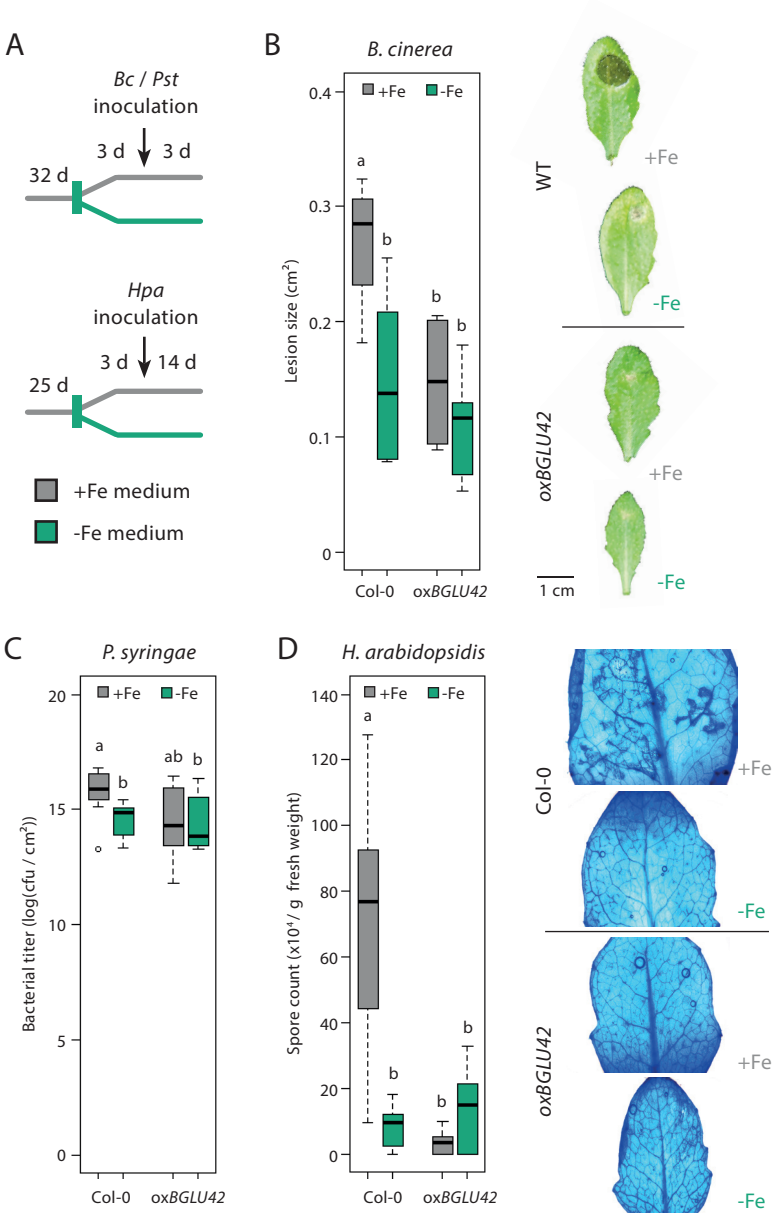

Figure 2 Effect of Fe deficient medium on plant susceptibility. A) Schematic representation of the experimental design, carried out in a hydroponics system. Plants initially grown with their roots in liquid medium containing Fe (+Fe) were transferred to a fresh +Fe medium or a medium without Fe (-Fe) 3 d before pathogen inoculations. Inoculations with *Botrytis cinerea* and *Pseudomonas syringae* pv *tomato* DC3000 were performed on 35-day-old plants, inoculation with *Hyaloperonospora arabidopsidis* on 28-day-old plants. Disease severity was evaluated 3 or 14 days later, as indicated. Levels of disease severity of +Fe and -Fe Col-0 and *oxBGLU42* plants after inoculation with *B. cinerea,* represented as the mean lesion area per leaf calculated from five inoculated leaves per plant (B), *P. syringae* pv *tomato* DC3000, represented as the number of colony forming units (cfu) per cm^2 leaf (C). and *H. arabidopsidis*, as the number of spores per gram of fresh weight (D). *H. arabidopsidis* disease severity was additionally visualized by trypan blue staining. Different letters indicate statistically significant differences (two-way ANOVA/Tukey HSD test, $P < 0.05$, $n = 4 - 8$).

2016; Zhang and Li, 2019). To test whether plant hormones are also involved in Fe deficiency-reduced susceptibility, we evaluated Fe deficiency-reduced susceptibility in the hormone signaling mutants *ein2-1* and *sid2-1*. The *ein2-1* mutant is affected in ET signaling, which is required for the resistance against necrotrophs (Broekgaarden *et al.*, 2015). We therefore tested the resistance of this mutant against the necrotrophic *B. cinerea*. We found that Fe starvation significantly decreased disease symptoms in Col-0, but not in the *ein2-1* mutant (Figure 3A). The *sid2-1* mutant is affected in SA signaling, which is required for the plant defense against (hemi) biotrophs (Pieterse *et al.*, 2012). Fe deficiency-reduced susceptibility against the biotroph *H. arabidopsidis* is absent in this mutant (Figure 3B). These results show that functional ET and SA response pathways are required for Fe deficiency-reduced susceptibility against *B. cinerea* and *H. arabidopsidis*, respectively. Therefore, the reduced disease symptoms seem to be based on increased plant resistance.

Hormone-regulated induced resistances are often based on defense priming, a state in which plants do not show constitutive activation of the immune response, but are conditioned to react faster and stronger to attack by pathogens or insects (Martinez-Medina *et al.*, 2016). Defense priming may therefore explain the broad-spectrum characteristic of Fe deficiency-induced resistance. To test this, we mimicked biotrophic or necrotrophic infections by spraying the leaves with SA or MeJA, respectively, and subsequently monitored the expression of the SA-responsive marker gene *PR-1* and the JA-responsive marker gene *VSP2* the over time. The mock-treated plants in both Fe-sufficient and Fe-deficient conditions did not increase the expression of either marker gene, indicating that Fe deficiency does not directly activate these plant defense responses. Exogenous application of SA induced the expression of *PR-1* in both Fe-sufficient and Fe-deficient Col-0 plants (Figure 3C). Although the level of SA-induced *PR-1* gene expression was higher in Fe-starved plants at 6 h after SA application, at later timepoints SA-induced *PR-1* mRNA levels were lower than in Fe-sufficient plants. Possibly, the SA-dependent defense response is activated faster in Fe-starved plants, resulting in the observed enhanced level of *Hpa* resistance in Fe-starved plants. MeJA induced the expression of *VSP2* in both Fe-sufficient and Fe-deficient Col-0 plants. There was a reproducible trend for a higher induction of this gene in Fe-deficient plants at all time points tested (Figure 3D). This suggests that Fe-deficient plants are primed for enhanced JA-dependent defenses.

Fe deficiency-induced resistance does not require the ISR regulators MYB72 and BGLU42

Fe deficiency-induced resistance and WCS417-mediated ISR are effective against the same three pathogens and both seem to be based on priming of the immune response. Therefore, we hypothesized that these two resistances are regulated by the same signaling pathway. To test this, we studied Fe deficiency-induced resistance against *B. cinerea* in the ISR mutants *myb72-2* and *bglu42*. Figure 4 shows that *myb72-2* and *bglu42* grown on Fe-sufficient medium displayed a similar level of disease resistance as wild-type Col-0, confirming previous findings (Van der Ent *et al.*, 2008; Zamioudis *et al.*, 2014). When grown on Fe-deficient medium, both ISR mutants mounted an Fe deficiency-induced resistance that was as strong as the Fe deficiency-induced resistance observed in Col-0. These results indicate that, in contrast to rhizobacteria-ISR, Fe deficiency-induced resistance does not require MYB72 and BGLU42.

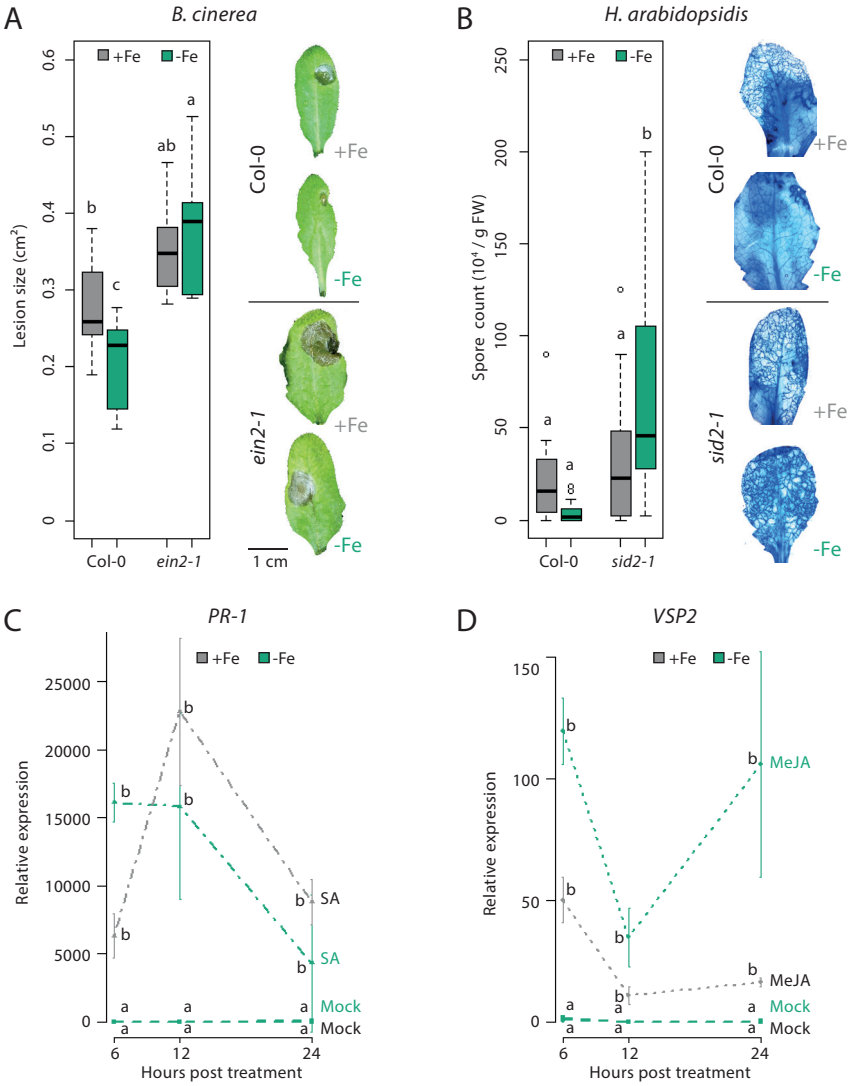

Figure 3 Fe deficiency-reduced susceptibility in hormone mutants. A) Disease severity in Col-0 and *ein2-1* plants grown with their roots in medium containing Fe (+Fe) or medium without Fe (-Fe), at 3 days after inoculation with *Botrytis cinerea*. The disease ratings are expressed as the mean lesion area from five inoculated leaves per plant (n = 5-13). Representative pictures of the inoculated leaves are shown. B) Disease severity in +Fe and -Fe Col-0 and *sid2-1* plants at 14 days after inoculation with *Hyaloperonospora arabidopsidis*. Disease severity is expressed as the number of spores per gram of fresh weight. Representative pictures of hyphal growth, visualized by trypan blue staining, are shown (all taken with the same magnification). Different letters indicate statistically significant differences (two-way ANOVA/Tukey HSD method, P < 0.05, n = 5-20). RT-qPCR analysis of *PR-1* (C) and *VSP2* (D) gene expression in the shoots of four-week-old +Fe and -Fe Col-0 plants treated with salicylic acid (SA), methyl jasmonate (MeJA) or a mock treatment (Mock). Gene expression levels were normalized to that of the constitutively expressed gene *PP2AA3* (At1g13320). Fold changes in gene expression levels relative to the average of the control plants are plotted. Error bars represent standard errors of the mean. Per timepoint, different letters indicate statistically significant differences between treatments per timepoint (one-way ANOVA/Tukey HSD method, P < 0.05; n = 4).

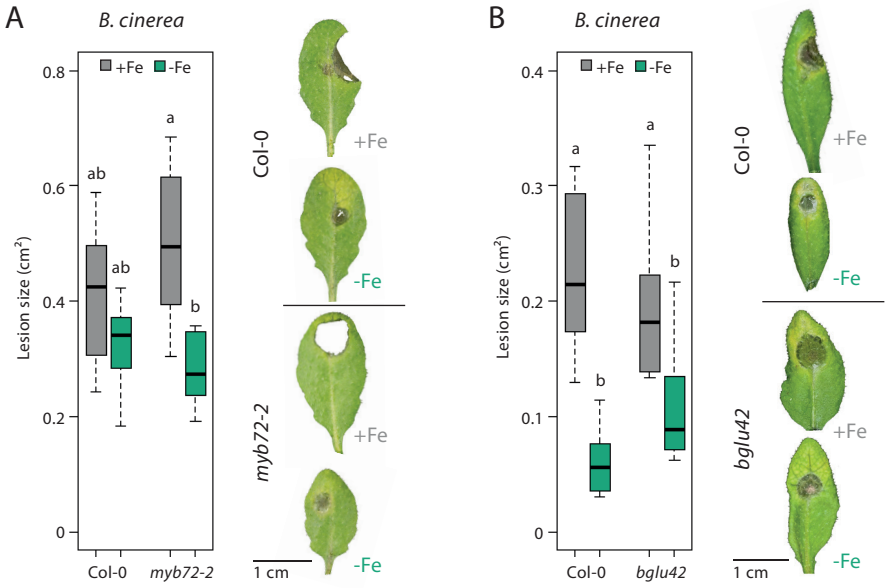

Figure 4 Fe deficiency-induced resistance in mutants unable to mount ISR. Disease severity on Col-0 and *myb72-2* (A) or *bglu42* (B) plants grown with their roots in liquid medium containing Fe (+Fe) or not containing Fe (-Fe) at 3 days after inoculation with *Botrytis cinerea*. Boxplots show the distribution of the mean lesion area per plant, calculated from the lesion area of five inoculated leaves. Pictures show representative disease phenotypes. Different letters indicate statistically significant differences (two-way ANOVA/Tukey HSD method, $P < 0.05$, $n = 5$-12).

Enhanced disease resistance is associated with misregulation of Fe homeostasis

As Fe deficiency results in increased plant resistance (Figure 3), we wondered what the effect would be of other changes in Fe homeostasis on plant immunity. To test this, we studied resistance against *B. cinerea* in two mutants with a disturbed Fe uptake response: the leaf Fe status shoot-to-root signaling mutant *opt3-2,* and the FRO2-deficient mutant *frd1-1*. The *opt3-2* mutant displays a constitutively active Fe deficiency response in the root, while over-accumulating Fe in the shoot (Zhai *et al.*, 2014; García *et al.*, 2018). The *frd1-1* mutant, in contrast, is deficient in taking up Fe from the root environment via Strategy I and typically has a low Fe content throughout the plant (Yi and Guerinot, 1996; Robinson *et al.*, 1999). Indeed, in our set-up, *opt3-2* has higher Fe levels in the shoot compared to wild-type plants (Figure 5A), while the *frd1-1* mutant required Fe supplementation in the growth medium to prevent severe chlorosis. Both the *opt3-2* and the *frd1-1* mutant displayed a constitutively enhanced resistance against *B. cinerea* on both Fe-sufficient and Fe-deficient medium (Figure 5B-C). As both the mutants and Fe-starved Col-0 plants have a disturbed regulation of Fe homeostasis, we hypothesize that a misregulation of Fe homeostasis results in plant hormone changes that induce resistance.

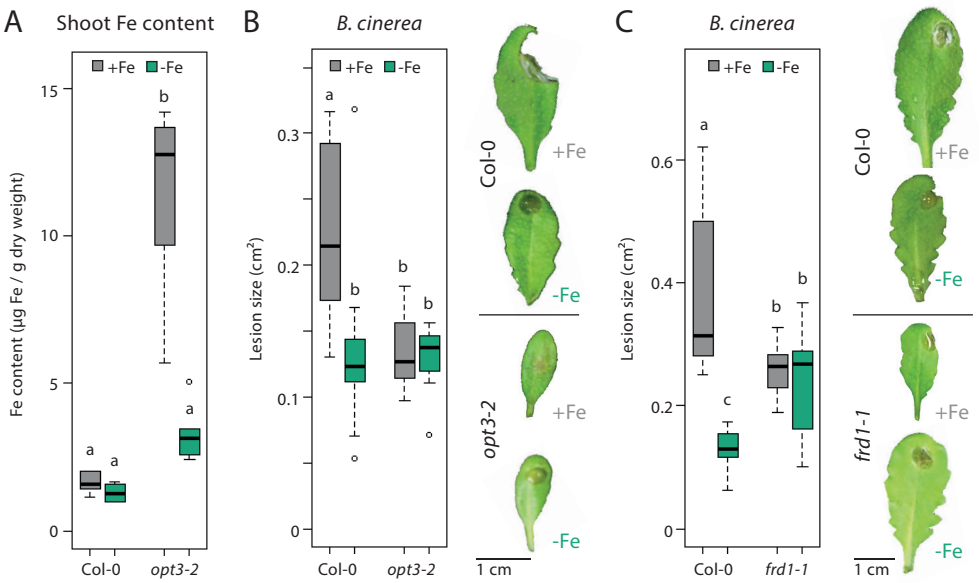

Figure 5 Fe deficiency-induced resistance in plants mutated in genes involved in Fe homeostasis. A) Fe content in the shoot of five-week-old Col-0 and *opt3-2* plants grown for 7 days with their roots in medium containing Fe (+Fe) or medium not containing Fe (-Fe). Levels of disease severity after inoculation with *Botrytis cinerea* in +Fe and -Fe Col-0 plants and *opt3-2* (B) or *frd1-1* mutants (C) at 3 days after inoculation. The disease ratings are expressed as the mean lesion area per leaf calculated from five inoculated leaves per plant. Different letters indicate statistically significant differences (two-way ANOVA/Tukey HSD method, $P < 0.05$, $n = 4$-5 for the Fe content, 6 - 17 for the disease tests).

Discussion

Fe starvation is harmful to plants as Fe functions as an enzyme co-factor in many cellular processes. Fe excess also has negative consequences, as it leads to oxidative stress (Briat *et al.*, 2010; Wu *et al.*, 2017; Kobayashi *et al.*, 2019). Maintaining stable Fe content is therefore a major determinant of plant performance and plant health (Guerinot and Ying, 1994; Balk and Schaedler, 2014; Connorton *et al.*, 2017). However, evidence is emerging that the effects of Fe availability on plant health are not only due to the necessity for plants to maintain a stable Fe content. First, Fe status of the plant can affect plant defense mechanisms that are based on exposure of the pathogen to an excess of Fe or, conversely, on withholding Fe from the pathogen (Segond *et al.*, 2009; Hsiao *et al.*, 2017). Second, molecular mechanisms controlling Fe homeostasis can, possibly inadvertently, affect pathogens. For example, Fe starvation results in the secretion of Fe-chelating coumarins that have antimicrobial properties (Lee *et al.*, 2014; Gutiérrez-Barranquero *et al.*, 2015; Stringlis *et al.*, 2018a). Finally, Fe starvation is associated with decreased disease severity upon necrotrophic pathogen attack (Kieu *et al.*, 2012), but it is unclear how this reduced susceptibility is established.

In this chapter, we show that Fe deficiency also reduces susceptibility to the hemibiotrophic bacterial pathogen *P. syringae* pv. *tomato* DC3000 and the biotrophic oomycete *H. arabidopsidis* (Figure 2). Next, we show that the Fe deficiency-induced resistance is dependent on SA- and JA-dependent defense signaling and is probably associated with priming of the plant immune

system (Figure 3). As both a mutant with an excess of Fe in its shoot and a mutant suffering from Fe starvation show resistance levels comparable to those in Fe-starved Col-0 plants (Figure 5), we propose that a mis-regulation of Fe homeostasis might be sufficient for the onset of resistance.

BGLU42 and MYB72 do not confer induced resistance via misregulation of Fe homeostasis

Our results show that the level of Fe deficiency-induced resistance is similar to the level of resistance displayed by *oxBGLU42* (Figure 2) (Zamioudis *et al.*, 2014). *BGLU42* is required for rhizobacteria-mediated ISR and is involved in the production and secretion of Fe-chelating coumarins in response to Fe starvation (Van der Ent *et al.*, 2008; Zamioudis *et al.*, 2014; Stringlis *et al.*, 2018a). Moreover, we show that Fe deficiency-induced resistance against *B. cinerea* and *H. arabidopsidis* is absent in the ET response mutant *ein2-1* and the SA-biosynthesis mutant *sid2-1*, respectively (Figure 3). (Pieterse *et al.*, 2014). WCS417-mediated ISR also requires functional signaling of plant defense hormones (Pieterse *et al.*, 2014). These results suggest similar mechanisms for ISR and Fe deficiency-induced resistance. However, subsequent experiments indicated that the resistances induced by beneficial rhizobacteria and by Fe starvation differ at least in the activation pathways, as the ISR-defective *myb72* and *bglu42* mutants still display Fe deficiency-induced resistance (Figure 4).

Finally, we show that *opt3-2* and *frd1-1* mutants are constitutively as resistant as Fe-starved Col-0 plants (Figure 5). This suggests that misregulation of Fe homeostasis *per se* results in increased resistance. This constitutive resistance to *B. cinerea* is not observed in *myb72* and the *bglu42* mutants. Thus, the hypothesis that mis-regulation of Fe homeostasis induces resistance only holds up if, in contrast to the *frd1-1* and the *opt3-2* mutants, *myb72* and *bglu42* do not suffer from Fe mis-regulation under Fe-sufficient conditions. Indeed, *myb72* shows no Fe-starved phenotype on Fe-sufficient soil (Palmer *et al.*, 2013) and Stringlis *et al.*, (2018a) have shown that the exudation patterns of *myb72* and *bglu42* in Fe-sufficient conditions does not vary strongly from that of Fe-sufficient Col-0 plants. Hence, this information points to a scenario in which MYB72 and BGLU42 do not confer disease resistance upon root colonization to WCS417 by changing Fe homeostasis, corroborating our finding that Fe deficiency-induced resistance and ISR are regulated via different mechanisms.

Plants might have evolved to perceive misregulation of Fe homeostasis as a stress signal to prime the immune system

Plants have elaborate mechanisms to cope with abiotic and biotic stress and have developed mechanisms to induce systemic resistance upon the perception of a stress signal (Pieterse *et al.*, 2012; Conrath *et al.*, 2015). Interestingly, Fe is involved in several of these forms of systemic resistance. Beneficial rhizobacteria-mediated ISR is dependent on the activation of genes involved in the Fe deficiency response (Van der Ent *et al.*, 2008; Zamioudis *et al.*, 2014) and BABA is known to activate a transient Fe deficiency response when priming the plant for enhanced defense against a broad spectrum of stresses (Koen *et al.*, 2014; Conrath *et al.*, 2015). In this chapter, we have shown that Fe deficiency also leads to systemic resistance against pathogens with various lifestyles.

We propose that, due the ubiquitous need of Fe for plants and pathogens, plants might

have evolved to prime the plant immune system upon perception of any disturbance of Fe homeostasis. This is in line with experiments that showed that microbe-produced siderophores activate plant immunity, possibly through a disruption of the Fe homeostasis (van Loon *et al.*, 2008; Aznar *et al.*, 2014). Future research will be directed towards increasing our understanding of how Fe deficiency interacts with the plant immune system and how this contributes to plant performance and survival in both natural and agricultural settings.

Chapter 5

Towards a translatomic understanding of the Arabidopsis root response to iron deficiency and beneficial rhizobacteria

Eline H. Verbon[1], Eline Eggermont[1], Corné M.J. Pieterse[1], Kaisa Kajala[2], Ronnie de Jonge[1]

[1]Plant-Microbe Interactions, Utrecht University, Department of Biology, The Netherlands
[2]Plant Ecophysiology, Utrecht University, Department of Biology, The Netherlands

Abstract

Plants are sessile organisms and can thus not move away from harmful environmental changes. Instead, they evolved complex molecular signaling pathways to deal with environmental stress. Examples include the iron (Fe) deficiency response, which is activated upon Fe limitation and enhances Fe uptake, and the complex signaling networks that result in defense responses upon pathogen attack. So far, these signaling pathways have mostly been studied by identifying changes in messenger RNA (mRNA) levels to identify biological processes that are activated or repressed in response to a stress. However, there is increasing scientific evidence that mRNA levels are not necessarily correlated with protein levels, in part because post-transcriptional regulation reduces or enhances recruitment of specific mRNA molecules to ribosomes. Ribosome-bound mRNA molecule levels are therefore postulated to correlate better with protein levels. In this chapter, we describe the isolation of the translatome, i.e. the fraction of the mRNA pool which is bound to ribosomes, from control and Fe-deficient *Arabidopsis thaliana* plant roots using a method known as translating ribosome affinity purification (TRAP). Preliminary analyses comparing the translatome to the transcriptome at 6, 12, 24 and 48 h after Fe deficiency suggest that translational control results in selective ribosomal recruitment of only part of the mRNA molecules that are up-regulated in the transcriptome in response to Fe deficiency. In addition, we pave the way for translatome studies on the Arabidopsis response to soil micro-organisms by conducting a successful trial TRAP experiment with Arabidopsis roots exposed to the beneficial rhizobacterium *Pseudomonas simiae* WCS417 and by generating novel TRAP plant lines.

Introduction

Iron (Fe) is an essential micronutrient for plants. Unfortunately, it is predominantly present in soil in its insoluble form, which plants cannot take up (Guerinot and Ying, 1994; Balk and Schaedler, 2014). Because of this low bioavailability, Fe is a limiting factor for biomass and seed yield in several crops (Briat *et al.*, 2015). To increase Fe uptake in Fe-deficient conditions, plants have evolved sophisticated Fe-uptake strategies. The model plant *Arabidopsis thaliana* (Arabidopsis) uses the so-called Strategy I Fe uptake response that consists of the reduction of ferric Fe (Fe^{3+}) to ferrous Fe (Fe^{2+}) by FERRIC REDUCTASE OXIDASE2 (FRO2) and subsequent Fe uptake through the IRON-REGULATED TRANSPORTER1 (IRT1) (Römheld, 1987; Robinson *et al.*, 1999; Vert *et al.*, 2002). One of the master regulators of this strategy is FER-LIKE IRON DEFICIENCY INDUCED TRANSCRIPTION FACTOR (FIT) (Colangelo and Guerinot, 2004). Apart from the genes known to be involved in Strategy I, many other genes are differentially regulated upon Fe deficiency in Arabidopsis. In sterile conditions on plant nutritive medium, more than 1,000 genes are differentially expressed in the Arabidopsis roots 24 hours after transfer to Fe-deficient medium (Dinneny *et al.*, 2008). After five weeks of Fe deficiency in a hydroponics system, close to 5,000 genes are differentially regulated (Forieri *et al.*, 2017).

While the analysis of the transcriptome changes provides insight into molecular mechanisms governing the Arabidopsis response to stress, there is increasing scientific evidence for and awareness of the fact that transcriptional changes do not necessarily lead to changes at the protein level, because messenger RNA (mRNA) molecules are not always translated. Instead, they can end up stored or degraded, depending on the RNA-binding proteins that bind the mRNA molecule (Bailey-Serres *et al.*, 2009). Indeed, a study performing both proteomic and transcriptomic analyses of the Arabidopsis response to Fe deficiency showed that only 13% of the protein abundance changes in the root after three days of Fe deficiency was accompanied by a similar change in transcript abundance of the encoding mRNA (Pan *et al.*, 2015). A thorough understanding of the Arabidopsis response to Fe deficiency therefore requires studying post-transcriptional processes (Pan *et al.*, 2015).

One way to study such processes is by comparing the transcriptome, i.e. all mRNA molecules present in the cell, to the translatome, i.e. the subset of mRNA molecules bound to ribosomes. Ribosome-bound mRNA can be specifically extracted by ribosome pull-downs using translating ribosome affinity purification (TRAP) (Zanetti *et al.*, 2005). TRAP on oxygen deprived plants showed that these plants reduce the amount of ribosome-bound mRNA molecules for about 70% of all cellular mRNAs, while less than a quarter of the cellular mRNAs is affected in total RNA levels. This repression of the ribosome-bound mRNA levels is quickly reversed upon reoxygenation and is thought to function as a mechanism to save energy and facilitate the transition to anaerobic metabolism (Branco-Price *et al.*, 2008). Like hypoxia, exposing plants to darkness in the middle of the day, a procedure commonly referred to as unanticipated darkness, reduces the amount of ribosome-bound mRNA more than the total mRNA population, with a striking 10-fold difference. Most of these mRNAs return to their original ribosome-bound levels by ten minutes of re-illumination. mRNAs that are translationally but not transcriptionally repressed in the dark are enriched for proteins involved in translation and photosynthesis (Juntawong and Bailey-Serres, 2012). These examples show that translational control allows plants to rapidly finetune their biological processes in response to environmental stimuli.

Translational regulation is also crucial for plant responses to biotic stimuli. Upon interaction of

the legume *Medicago truncatula* with the symbiotic rhizobacterium *Sinorhizobium meliloti*, the mRNA levels of several genes required for the symbiosis between both species are upregulated in plant ribosomes, but not or only slightly in the transcriptome (Reynoso *et al.*, 2013). Likewise, Arabidopsis increases ribosome-bound mRNA levels, but not total mRNA levels of several genes in response to the *Pseudomonas syringae* effector AvrRpm1. These genes are required for plant defense, indicating that effector-triggered immunity induces and depends on a strong translational response (Meteignier *et al.*, 2017). Selective recruitment of mRNA to the ribosomes upon interaction with a pathogen can also be disadvantageous to a plant. Genes encoding peptidase inhibitors have lower ribosome-bound versus total mRNA ratios in leaves inoculated with the *Turnip mosaic virus* than in control leaves. Possibly, the virus interferes with translation of the plant peptidase inhibitors to prevent interference with the peptidases it needs for the generation of its proteins (Moeller *et al.*, 2012). Together, these results show that studying the translational response of plants can uncover novel components determining the outcome of cross-kingdom interactions.

In this chapter, we describe a timecourse analysis using TRAP to study changes in the ribosome-bound mRNA pool versus changes in the total mRNA pool upon Fe deficiency. Preliminary data analysis shows that while the translatome and the transcriptome are different, the effect of Fe deficiency on both mRNA pools is similar. The major differences observed are due to genes being differentially expressed in the transcriptome, but not in the translatome. These results suggest that translational regulation forms an extra layer of control that selectively recruits the mRNA molecules of a specific subset of the Fe deficiency-responsive genes to the ribosomes.

Besides our study on the Arabidopsis root response to Fe deficiency, we paved the way for TRAP studies studying the Arabidopsis response to colonization by pathogenic and beneficial microbes. To this end, we conducted a trial experiment in which we isolated the transcriptome and the translatome from plants exposed to the beneficial rhizobacterium *Pseudomonas simiae* WCS417. We show that it is possible to measure bacteria-induced translational changes in whole roots and in cortical cells specifically. Finally, we expanded the currently available TRAP line repertoire with TRAP lines for the root epidermis. These plant lines will be instrumental for future experiments studying the cell type-specific response to microbes and might uncover novel processes that are affected in the translatome specifically.

Materials and methods

TRAP to study the Arabidopsis response to Fe deficiency

Plant material and growth conditions. Col-0 seeds transformed with the Cauliflower mosaic virus *35S* promotor (*p35S*) driving the expression of *FLAG-GFP-RPL18* (*35S:His$_6$FLAG-GFP-RPL18*) were sterilized by a 3-h exposure to the gas emitted by 100 ml bleach combined with 3.2 ml 37% hydrochloric acid (Van Wees *et al.*, 2013). The sterilized seeds were sown on modified Hoagland medium (Hoagland and Arnon, 1938) (5 mM KNO_3, 2 mM $MgSO_4$, 2 mM $Ca(NO_3)_2$, 2.5 mM KH_2PO_4, 70 µM H_3BO_3, 14 µM $MnCl_2$, 1 mM $ZnSO_4$, 0.5 mM $CuSO_4$, 10 µM NaCl, 0.2 µM Na_2MoO_4, 50 µM Fe-EDTA, 1% sucrose, 0.05% 2-ethanesulfonic acid (MES), 1% plant agar, pH 5.7), hereafter referred to as +Fe medium. Twenty seeds were sown on each plate on top of a nylon mesh (Nitex Cat 03-100/44, Sefar) (Dinneny *et al.*, 2008). Plates were sealed with a double layer of Parafilm and the seeds stratified in the dark at 4°C for a minimum of 2 nights. They were

then placed vertically in short-day conditions (14-h night, 10-h day; 21^{o}C) for nine days. On the ninth day, the plates were placed in long-day conditions (8-h night, 16-h day, 21^{o}C). On the twelfth day after putting the seeds into the short-day conditions, the plants were transferred on their nylon mesh onto either new control Hoagland plates or onto Hoagland plates without Fe-EDTA. Plates were wrapped in Parafilm before being returned to the growth chamber. Shoots and roots were separated by cutting with a carbon steel surgical blade at 6, 12, 24 or 48 hours after transfer. Roots from four plates (approximately 80 plants in total) were combined into one Eppendorf tube and frozen in liquid nitrogen. They were then stored at -80°C until further use.

Confocal microscopy. *35S:His$_6$FLAG-GFP-RPL18* plants were grown as described above on control Hoagland medium. After seven days of growth, half of the plants was transferred to new control Hoagland medium, while the other half was transferred to Hoagland medium without Fe-EDTA. Three days after transfer, GFP expression was visualized in the roots using an LSM700 confocal microscope (Zeiss) with a 488-nm argon laser and ZEN imaging software. GFP-fluorescence was detected at a wavelength of 500-550 nm and propidium iodide, a cell wall marker, at 570-620 nm.

Translating Ribosome Affinity Purification (TRAP). TRAP was performed as described previously, with minor modifications (Mustroph *et al.*, 2009). In short, washed Dynabeads Protein G (ThermoFisher Scientific) were coupled to monoclonal ANTI-FLAG® M2 antibody produced in mouse (Sigma) by incubating in a binding buffer (0.2 M Tris pH 9.0, 0.2 M KCl, 0.025 M EGTA, 0.035 M $MgCl_2$, 0.02% polyoxyethylene sorbitan monolaurate 20 (Tween-20)) for 1 h.

In the meantime, frozen root samples from two Eppendorf tubes were combined and lysed in liquid nitrogen with a mortar and pestle. The lysed samples were suspended in a polysome extraction buffer (0.2 M Tris pH 9.0, 0.2 M KCl, 0.025 M EGTA, 0.035 M $MgCl_2$, 1 % polyoxyethylene(23)lauryl ether (Brij-35), 1 % triton X-100, 1 % octylphenyl-polyethylene glycol (Igepal CA 630), 1 % Tween 20, 1 % polyoxyethylene 10 tridecyl ether (PTE), 5 mM dithiothreitol (DTT), 1 mM phenylmethylsulfonyl fluoride (PMSF), 100 µg/ml cycloheximide, 50 µg/ml chloramphenicol). Subsequently, they were homogenized on ice. The homogenized samples were centrifuged at 16.000 *g*, at 4°C for 15 min. The supernatant was filtered through autoclaved Miracloth to give the clarified extract. A volume of 0.25 ml of the non-filtered sample was collected separately and kept on ice.

The clarified extract was incubated with the antibody-bound beads for 2 h at 4°C. The beads were washed six times at 4°C by putting the tubes next to a magnet, removing the supernatant, adding washing buffer (0.2 M Tris pH 9.0, 0.2 M KCl, 0.025 M EGTA, 0.035 M $MgCl_2$, 5 mM DTT, 1 mM PMSF, 100 µg / ml cycloheximide, 50 µg/ml chloramphenicol) and leaving for gentle agitation for 5 min. After the final wash, all the supernatant was removed. Subsequently, warm lysis/binding buffer (LBB; 100 mM Tris-HCl, 1 M lithium chloride, 10 mM EDTA, 1% SDS, 5 mM dithiothreitol and antifoam A) was added to both the beads (the TRAP samples) and the non-filtered samples that were kept on ice (the total samples). The tubes were vortexed at room temperature for 5 minutes and then left at room temperature for a further 10 minutes. Afterwards, the samples were spun down for 10 min and the supernatants transferred to fresh tubes. Samples were stored at -80°C until further processing.

RNA library generation. RNA was isolated and libraries generated with an adapted version of a

previously described protocol (Townsley *et al.*, 2015). Briefly, first the polyadenylated mRNA was isolated. Biotin-linked oligo-dT primers were added to the samples while streptavidin beads were washed with LBB. Subsequently, 10 µl of the beads were added to each of the samples and left to bind under gentle agitation for 10 min at room temperature. The beads were washed using a 96-well magnetic separator and 200 µl of three subsequent washing buffers (WBA: 10 mM Tris-HCl, 150 mM lithium-chloride, 1 mM EDTA, 0.1% SDS; WBB: 10 mM Tris-HCl, 150 mM lithium-chloride, 1 mM EDTA; LSB: 20 mM Tris-HCl, 150 mM NaCl, 2 mM EDTA). RNA was eluted and separated from the beads in 10 µl 10 mM Tris-HCl pH 9 containing 1 mM β-mercaptoethanol and heating to 80°C. These steps were performed twice.

Subsequently, RNA was fragmented and primed for cDNA synthesis by adding 1.5 µl 5x RT buffer and 0.5 µl random primers to 8 µl of the sample and heating to 94°C for 1.5 min before cooling down to 4°C for 5 min. The first strand of the cDNA was synthesized as described using RevertAid H minus Reverse Transcriptase (Thermo Scientific, #EP0451) (Townsley *et al.*, 2015). The second strand was synthesized by adding 1.5 µl H_2O, 0.4 µl 25 mM dNTPs, 1 µl Polymerase I (Thermo Scientific, #EP0042), 0.1 µl RNase H (New England Biolabs, #M02975), 0.4 µl End Repair Enzyme Mix (New England Biolabs Inc, #E6051AA), 0.2 µl Taq polymerase (New England Biolabs Inc, #M0273L), 1.4 µl End Repair Buffer and placing it in a thermocycler with the following program: 16°C 20 min, 20°C 20 min, 72°C 20 min, 4°C forever.

Fragments of 350 bp were selected by mixing in 30 µl AMPure XP beads (Beckman Coulter, #A63881) and leaving the mix to stand for five minutes. Beads were then washed twice with 300 µl 80% ethanol on a 96-well magnetic tray. After the second wash all ethanol was removed and the beads were left to air-dry. Once the beads were dry, 3 µl of annealed 1 µM universal adapters was added. Universal adapters were synthesized as follows: a solution of 1 µM PE1-lig CAC TCT TTC CCT ACA CGA CGC TCT TCC GAT CT and 1 µM IL-lig P-GAT CGG AAG AGC ACA CGT CTG AAC TCC AGT CAC were annealed by running the following program: 94°C 1 min, 94°C 10 sec, followed by 60x 10 sec in which the temperature drops by 1°C in each step, 20°C 1 min, 4°C forever. The adapters were ligated to the DNA by adding 1.75 µl H_2O, 5 µl 2x Rapid Ligation Buffer and 0.25 µl T4 DNA ligase (Rapid) (Enzymatics, #L6030-HC-L) to each sample. After 15 minutes at room temperature, 10 µl 50 mM EDTA and 25 µl AMPure XP Beads Resuspension Buffer (15% PEG 8000, 2.5 M NaCl) were added. After 5 min incubation the beads were washed twice with 200 µl 80% ethanol as described above. Once dry, beads were resuspended in 21 µl Tris-HCl, mixed well, left to stand 1 min and then placed in the magnetic tray. Subsequently, 20 µl of the supernatant, containing the adapterized cDNA, was transferred to new tubes.

PCR enrichment was performed as described (Townsley *et al.*, 2015): 2 µl 5X Phusion HF Buffer, 1.3 µl H_2O, 0.5 µl 2 µM PE1 primer (PE1 5'-AAT GAT ACG GCG ACC ACC GAG ATC TAC ACT CTT TCC CTA CAC GAC GCT CTT CCG ATC T-3'), 0.5 µl 8 µM each S1 + S2 primers (S1 5'-AAT GATACGGCGACCACCGA-3', S2 5'-CAAGCAGAAGACGGCATACGA-3'), 0.1 µl 25 mM dNTPs, and 0.1 µl Phusion Polymerase (Thermo scientific, #F-530L) were combined with 0.5 µl of a 2 µM uniquely-indexed barcode (Table S1: barcode sequence per sample). Of the sample, 4.5 µl was added to the mix and placed in a thermocycle with the following program: 98°C 30 sec, (98°C 10 sec, 65°C 30 sec, 72°C 30 sec) 15 cycles, 72°C 5 min, 10°C forever. Of each library, 2 µl was run on a 1% agarose gel at 100 volts for 20 min to check fragment size. Library samples were cleaned and size-selected with 110% AMPure beads (8.8 µl beads for 8 µl sample) and washed with 80% ethanol twice before eluting in 10 µl 10 mM Tris-HCl.

Libraries were quantified using SYBR green and a plate reader. Briefly, 198 µl (samples), 199 µl (standard) or 200 µl (blanks) 10 mM Tris HCl with 1x SYBR green was added to the wells of a white, flat bottom 96-well plate. Nothing further was added to the blank wells. One µl of the standards was added to the standard wells, in triplicate. Two µl of the library samples was added to the sample wells. Fluorescence was measured in a spectrophotometer with excitation 485/20, emission 528/20 and gain 35. The average of the blank values was subtracted from all values. The slope of the concentration versus the measured value was calculated using the standards. This slope was used to calculate the DNA concentrations in the library samples. Finally, the amount of each sample needed to get a final 100-µl suspension with a concentration of 12 nM, equally divided over the libraries, was calculated and mixed. The pooled libraries were cleaned and selected twice more with 80% AMPure XP beads. The libraries were suspended in MQ and sent for sequencing on two lanes of the Illumina NextSeq500 (Utrecht Sequencing Facility, Utrecht, The Netherlands) with 1 x 75-bp single-end and high-output configuration, yielding between 4.4 and 16.3 million (M) reads per sample in total (mean 10.8 M reads).

Data analysis. The reads generated by Illumina sequencing were pseudoaligned to the AtRTD2v2 database (Zhang *et al.*, 2017) using Kallisto (v0.45.0) with 100 bootstraps and default settings (Bray *et al.*, 2016). Between 3.1 M and 13.6 M reads, with an average of 76% of the reads, were aligned to the reference transcriptome per sample. The resulting transcript counts were subsequently summarized to the gene level with tximport (v1.2.0) (Soneson *et al.*, 2015). Only genes with more than two counts per million (cpm) in at least three samples were kept for the remaining analysis. The counts per gene of the remaining samples and genes were used to generate a digital gene expression list (DGE list) in EdgeR (v3.16.5) (Robinson *et al.*, 2010). A generalized linear model (glm) was fit using a negative binomial model and quasi-likelihood (QL) dispersion estimated from the deviance with the glmQLFit function in EdgeR. Differentially expressed genes were then determined by comparing the Fe-starved and control samples per time point with the glmQLFTest (FDR < 0.1; $-2 < \log_2 FC > 2$). GO term analysis was performed in R based on the genome wide annotation for Arabidopsis within org.At.tair.db (Carlson M, 2018) with the program GOstats (Falcon and Gentleman, 2007).

TRAP to study the Arabidopsis response to *P. simiae* WCS417

Plant material and growth conditions. Col-0 transformed with the Cauliflower mosaic virus *35S* promotor (*p35S*) or the root cortex-specific promotor of an endopeptidase (*pPEP*) driving the expression of *FLAG-GFP-RPL18* were sterilized and sown on plates as described above. Stratified seeds were placed vertically in short-day conditions (14-h night, 10-h day; 21^{0}C). *Pseudomonas simiae* WCS417 was added after five days of plant growth as described before (Zamioudis *et al.*, 2015). Briefly, WCS417 was streaked from a frozen glycerol stock onto solid King's B (KB; (King *et al.*, 1954)) medium and grown at 28°C overnight. On the following day, the fifth day after putting the plants in short day conditions, WCS417 was resuspended and washed in 10 mM $MgSO_4$ twice. Ten µl of a final bacterial suspension with an OD_{600} of 0.01 (containing 8 * 10^4 bacteria) was added to each root of half of the plants. Plates were wrapped in Parafilm before being returned to the growth chamber. After 48 hours of bacterial exposure, roots were cut with a carbon steel surgical blade. Roots from five to ten plates (200 to 400 plants) were combined into one Eppendorf tube and frozen in liquid nitrogen. Roots were stored at -80°C until use.

Generating two TRAP epidermis-specific vectors and transforming them into *Agrobacterium tumefaciens*. TRAP lines with the FLAG-epitope tagged ribosomal protein 18 (RPL18) (His_6FLAG-GFP-RPL18) behind epidermis-specific promotors were generated as described previously for TRAP lines with other promotors (Mustroph *et al.*, 2009). Briefly, the 2,400-bp *COBL9* (AT5G49270) promotor was amplified from Arabidopsis accession Col-0 gDNA using the primers COBL9F 5'-CAC CAA TAA TGT GGC CAG ATC CGT AGA TCT-3' and COBL9R 5'-TGT GTC TTT CTC CAG AGA AAA GTT AAG-3' (Brady *et al.*, 2007b). The amplified promotor was inserted into a pENTR™/D-TOPO vector with the pENTR™/D-TOPO cloning kit (Life Technologies) and transformed into chemically competent One Shot TOP10 *Escherichia coli* cells (Thermo Scientific) by heat shock for vector amplification. After amplification the entry vector was isolated and the promotor transferred by LR reaction from the entry vector into the destination vector: the TRAP vector containing GFP, the FLAG-epitope tagged RPL18 and kanamycin resistance (Mustroph *et al.*, 2009). The *COBL9*-containing destination vector was subsequently amplified in One Shot TOP10 *E. coli* cells. In addition to the *COBL9*-containing destination vector, a TRAP vector in which the His_6FLAG-GFP-RPL18 is driven by *pWER* (*WEREWOLF*, AT5G14750) was amplified in One Shot TOP10 *E. coli* cells. The promotor sequences in the isolated vectors were verified by sequencing (Macrogen). Verified vectors were electroporated into *Agrobacterium tumefaciens* (Agrobacterium), strain AGL1. Glycerol stocks were made and stored at -80°C until use.

Transformation of Arabidopsis with the TRAP vector-containing Agrobacterium. Arabidopsis was transformed using a transformation protocol based on published work (Clough and Bent, 1998). Briefly, the first bolts of seven-week old wild-type Col-0 plants were clipped to induce the formation of many secondary bolts. On the same day, the Agrobacteria containing the TRAP vectors were streaked on Lysogeny broth (LB) selective plates containing carbenicillin, rifampicin and spectinomycin and put at 28°C. Two days later, the transformed bacterial transformants were replated onto new plates. Five days after clipping the plants, an Agrobacterium transformant suspension was prepared in 120 ml 5% sucrose, 0.05% Silwet L-77 and 30 ml LB medium. The plants' flowers were dipped into this bacterial suspension for 10 s, left to dry and put into the suspension again for another 10 s. Plants were then placed back in a long-day growth room (8-h night, 16-h day, 21^{o}C). The plants were fully covered with plastics for one night to increase humidity. Three, seven and ten days later the dipping procedure was repeated. Three weeks after the final dip the seeds were harvested.

Selection of T1 and T2 seeds transformed with a TRAP vector and fluorescence validation in control, Fe-deficient and bacteria-treated plants. Gas-sterilized seeds were sown on Hoagland plates containing 50 µg kanamycin/ml. The seeds were stratified in the dark at 4°C for two nights and placed in the growth room. Green and healthy plants were selected from among the non-resistant small yellow plants after ten to eleven days. About 1% of the obtained T1 seeds was resistant to kanamycin, the antibiotic against which a resistance gene was present in the introduced construct. The resistant T1 plants were transferred to plates without antibiotics to recuperate and then put on soil to generate seeds. Seeds harvested from the T1 plants, the T2 seeds, were again sown on plates containing kanamycin. All T2 *pWER:His6FLAG-GFP-RPL18* plants were resistant to the antibiotic, as expected for heterozygous seeds. About 10% of the

T2 *pCOBL9:His6FLAG-GFP-RPL18* were not resistant, with non-resistant plants among the seed batches obtained from each of the three T1 plants. Resistant seven-day-old T2 plants were transferred to control or Fe-deficient Hoagland plates without antibiotics. Half of the plants on control plates were treated with 10 µl of a WCS417 suspension in 10 mM $MgSO_4$ with an OD_{600} value of 0.01. Ten-day-old plants were imaged with a confocal microscope (Zeiss) and ZEN software. Root cell walls were visualized by mounting plants in 10 µM propidium iodide (PI). Gain (master) was set to 650 for PI, digital offset to 0 and digital gain to 1.5. Gain (master) was set to 800 for GFP, digital offset to 0 and digital gain to 1.1.

Data accessibility Analysis scripts and the supplementary tables are part of the Online Supplementary Material and can be found here: https://cp.sync.com/dl/60fe897a0#fqt4xv25-em3ineic-y792dq3h-qrydpq97.

Results

TRAP to study the Arabidopsis response to Fe deficiency

Expression patterns are affected by RNA type, time of the day and Fe deficiency

Changes in the Arabidopsis root proteome in response to Fe deficiency can only partly be explained by transcriptome changes (Pan *et al.*, 2015). This suggests that there are post-transcriptional processes that influence protein production and activity. These processes can be studied more closely by comparing the transcriptome, i.e. all the mRNA present in the cell, to the translatome, i.e. all the ribosome-bound mRNA. We isolated the transcriptome and the translatome from plant lines expressing the ribosomal protein L18 (RPL18) with a FLAG-tag behind the constitutively active *35S* promotor (*p35S:FLAG-GFP-RPL18*) (Figure 1A). Ribosomes, and with them the ribosome-bound mRNA, were isolated from the roots of these plants using ANTI-FLAG-coated magnetic beads after 6, 12, 24 and 48 h of Fe deficiency (Figure 1B) (Zanetti *et al.*, 2005; Mustroph *et al.*, 2009). Total mRNA was isolated from the same samples before ribosome extraction. The time points were chosen based on previous studies that observed the first Fe deficiency-related changes after 6 h of Fe deficiency and the major transcriptional changes in Arabidopsis roots after 24 h (Dinneny *et al.*, 2008; Buckhout *et al.*, 2009).

After processing the RNA-seq data, we performed multidimensional scaling on the normalized gene expression levels to study the global similarities and dissimilarities among the samples (Figure 2A-B). The samples cluster first by transcriptome versus translatome (PERMANOVA; $P_{RNA\ type} = 0.001$). Analysis of the genes expressed more in all transcriptomes versus all translatomes shows enrichment of 36 biological process gene ontology (GO) terms (Table S2). The most significant ones are related to translation, RNA modification and DNA-templated transcription. Interestingly, all six genes in the GO term 'ribosome assembly' (GO:0042255) are enriched in this mRNA pool, as are all five genes in 'rRNA transport' (GO:0051029). In the translatome, close to 1,000 GO terms are enriched (Table S3). The most significant among these are related to carbohydrate -, oxoacid - and organic acid metabolic processes.

The samples subsequently cluster by the time point of harvest (PERMANOVA; $P_{time\ point} = 0.001$). The clustering pattern suggests an influence of the circadian clock, rather than the time after transfer, as the Fe deficiency treatment does not seem to affect the clustering pattern and the 6 h time point, harvested in the afternoon, clusters closer to the 24 h and 48 h timepoints,

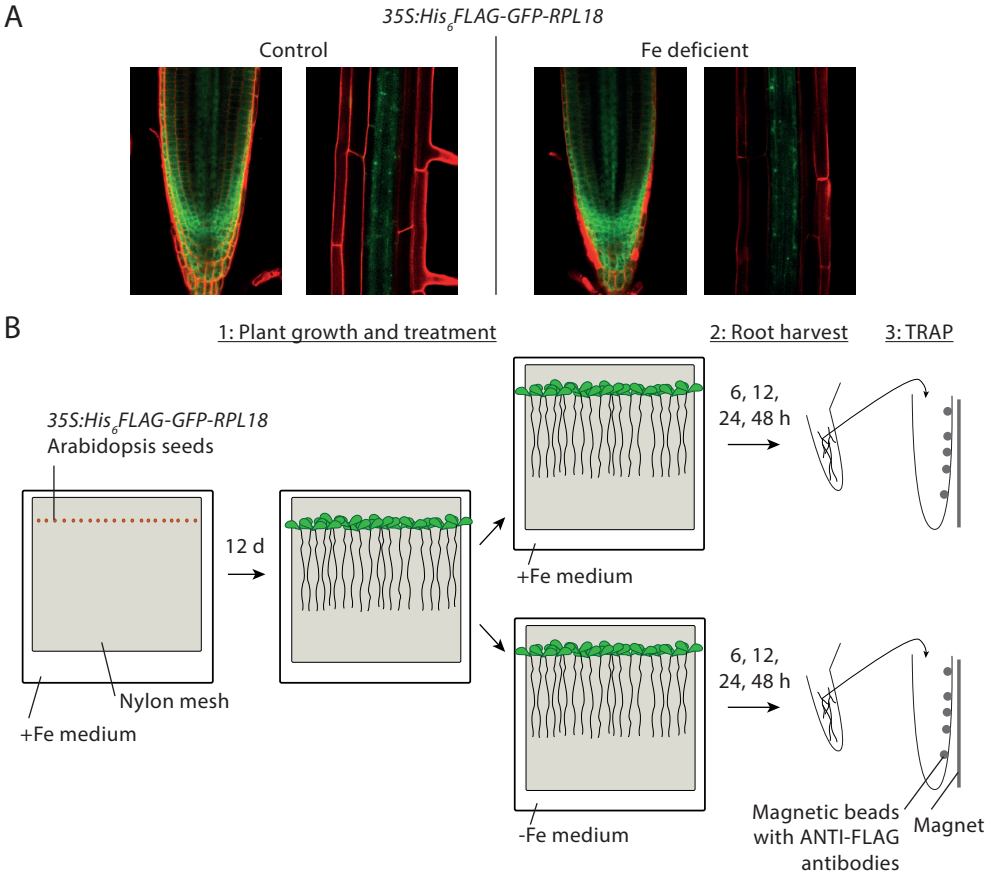

Figure 1 Experimental set-up to isolate total and ribosome-bound mRNA from control and Fe-deficient *35S:His$_6$FLAG-GFP-RPL18* plants. A) Roots of 10-day-old seedlings transformed with *35S:His$_6$FLAG-GFP-RPL18,* grown on sterile Hoagland medium with Fe (+Fe medium), or without added Fe (-Fe medium) for the last 3 days. Red shows cell walls as stained by Propidium Iodide (PI). Green shows green fluorescent protein (GFP). B) Schematic of the experimental design. Sterilized *35S:His$_6$FLAG-GFP-RPL18* Arabidopsis seeds were sown on Hoagland medium on a nylon mesh. Plants were grown on +Fe medium for 12 days, of which 9 in short-day conditions and the final 3 in long-day conditions. On the twelfth day, all plants were transferred on their mesh to either +Fe or -Fe medium. After 6, 12, 24 or 48 h, roots were cut from the shoot and frozen in liquid nitrogen. Frozen root tissue from 140-160 plants was used per replicate to isolate RNA bound to ribosomes with Translating Ribosome Affinity Purification (TRAP). Total RNA samples were collected from the same samples.

harvested at noon, than the 12 h timepoint, which was harvested at night. We studied the circadian clock marker genes *CIRCADIAN CLOCK ASSOCIATED 1 (CCA1)* and *CHLOROPHYLL A/B-BINDING PROTEIN (CAB)*, known to be induced in the morning, and *EARLY FLOWERING 4 (ELF4)*, known to be expressed most strongly 12 h after dawn (Doyle *et al.*, 2002). In line with the known expression patterns, *CCA1* and *CAB* are expressed highly in samples harvested at noon, whereas *EARLY FLOWERING 4 (ELF4)* is expressed highest in the 6 h sample, which was harvested approximately 12 h after the start of the day (Figure 2C).

Finally, we observe non-significant clustering of our samples based on the transfer to Fe-

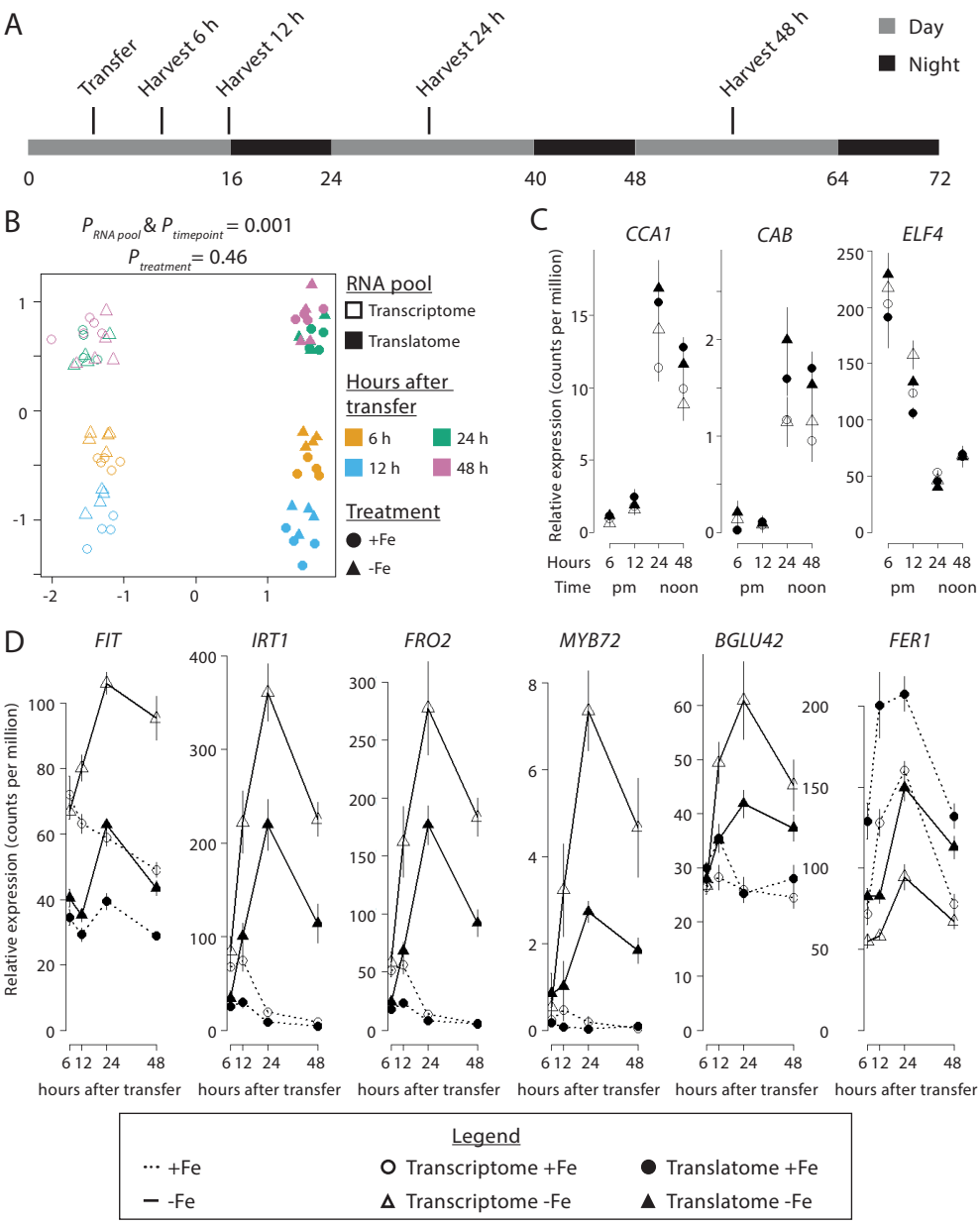

Figure 2 A timecourse analysis of the transcriptome and translatome of control and Fe-deficient plants. A) Schematic of the experimental design. 12-day-old plants grown on Hoagland medium (+Fe medium) were transferred to new +Fe medium or to Hoagland medium without Fe (-Fe medium). Roots were harvested 6, 12, 24 or 48 h later. B) MDS plot of the normalized and filtered gene counts of all samples. C) Normalized expression of *CCA1*, *CAB*, and *ELF4* in the transcriptome (open circles for +Fe and open triangles for -Fe) and translatome (filled circles for +Fe and filled triangles for -Fe) at 6, 12, 24 and 48 hours after transfer. The 6 h and 12 h samples were harvested in the afternoon and evening ('pm'), the 24 h and 48 h samples were harvested at noon. D) Normalized expression of *FIT*, *IRT1*, *FRO2*, *MYB72*, *BGLU42*, and *FER1* in the transcriptome (open shapes) and translatome (filled shapes) at 6, 12, 24 and 48 hours after transfer to +Fe (dotted line) or -Fe (solid line) medium.

deficient or control medium ($P_{treatment}$ = 0.46). To verify whether the Fe deficiency treatment was successful, we checked the expression of several genes known to be up-regulated as part the Arabidopsis Fe deficiency response, namely *FIT*, *IRT1*, *FRO2*, *MYB72* and *β-GLUCOSIDASE 42 (BGLU42)* (Robinson *et al.*, 1999; Vert *et al.*, 2002; Colangelo and Guerinot, 2004; Zamioudis *et al.*, 2014), in addition to the expression of *FERRITIN1 (FER1)*, which is known to be inversely correlated with Fe content (Briat *et al.*, 1999). As expected, *FIT*, *IRT1*, *FRO2*, *MYB72* and *BGLU42* are activated by Fe deficiency, whereas *FER1* is repressed (Figure 2D; Table S2). The genes are similarly affected in both mRNA pools. This is in line with a previous study in which all these genes except *MYB72* were among the genes affected similarly in the transcriptome and the proteome of Fe-deficient plants (Pan *et al.*, 2015).

Translational regulation restricts translational changes to a subset of the induced genes

Subsequently, we determined the differentially expressed genes (DEGs; FDR < 0.1) in response to Fe starvation per time point in the transcriptome and the translatome separately. More than twice as many genes are affected in the transcriptome compared to the translatome. In both mRNA pools, the number of DEGs increases with the time after harvest (Figure 3A; Table S4-5).

Subsequently, we checked the overlap between the DEGs in the transcriptome and the translatome, again per time point. As expected from the greater number of DEGs in the transcriptome, we find many genes that are differentially expressed in the transcriptome only (Figure 3B, orange). The majority of the translatome changes are shared with the transcriptome (Figure 3B, black), with only a few genes affected in the translatome only (Figure 3B, blue). The number of genes affected in only the translatome seems to be greater in the first two time points. This might mean that changes in the translatome occur before changes in the transcriptome. Alternatively, changes that occur early might be more likely to be smaller and less stable and therefore have a higher chance to be lost to noise in the total mRNA pool.

Translational control has been proposed to allow for a faster response of a plant to an environmental stress. To analyze whether gene-specific translational changes precede changes in the transcription, we subsequently analyzed the overlap between DEGs over the mRNA pools over the different time points. We find only four up- and three down-regulated genes that are induced at an earlier time point in the translatome than in the transcriptome (Figure 3B, pink). Thus, our data suggest that rather than a quicker or stronger response of the translatome, translational control selectively recruits genes among the genes that are up-regulated in the transcriptome.

Figure 3 Comparison of the transcriptome and translatome changes in response to Fe deficiency. A) The number of differentially expressed genes (DEGs) in response to Fe deficiency in the transcriptome and translatome. B) Scatterplot of the translatome versus the transcriptome $\log_2$fold change ($\log_2$FC) in response to Fe deficiency of the genes that were DE at 6, 12, 24 and 48 h after transfer. Genes DE in both mRNA pools are depicted in black, genes DE in only the transcriptome are colored orange, genes DE only in the translatome are blue. B) UpSet plots showing the overlap of the up-regulated (left) and down-regulated (right) DEGs (FDR < 0.1) across the translatome and the transcription and across time points. Black bars represent genes that are DE in both mRNA pools at at least one time point. Pink bars represent genes that are DE in both mRNA pools, at an earlier time point in the translatome than in the transcriptome. Orange bars represent genes that are only DE in the transcriptome, blue bars represent genes that are only DE in the translatome.

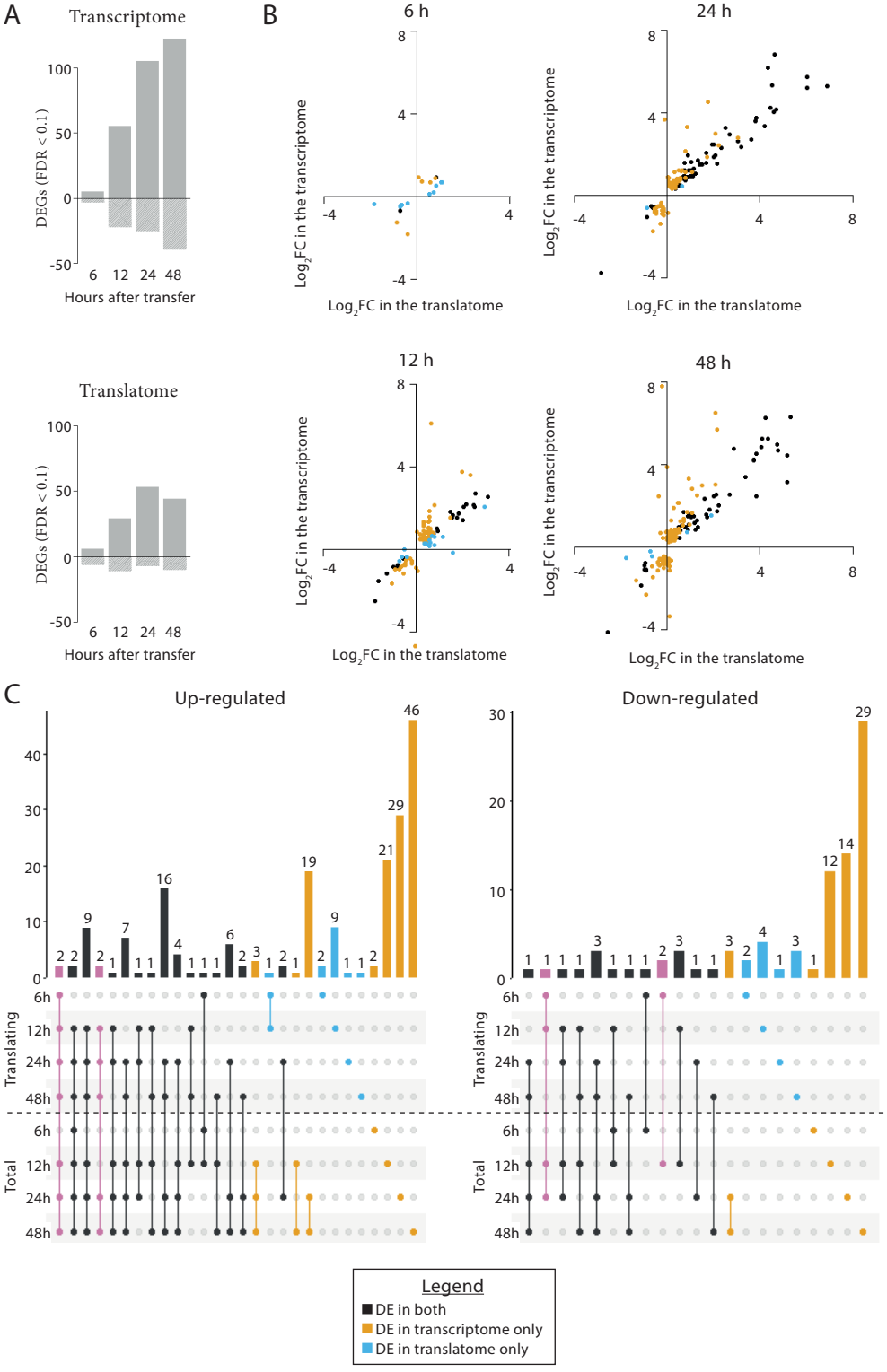
A
Transcriptome
DEGs (FDR < 0.1)
Hours after transfer
Translatome
B
6 h
12 h
24 h
48 h
Log2FC in the transcriptome
Log2FC in the translatome
C
Up-regulated
Down-regulated
Translating
Total
6h
12h
24h
48h
Legend
DE in both
DE in transcriptome only
DE in translatome only

Fe-related processes are affected in both mRNA pools

To gain insight into the biological processes affected by Fe deficiency in both mRNA pools, we performed gene ontology (GO) term enrichment analysis on the lists of DEGs. Only gene lists with > 20 DEGs were analyzed. Thus, none of the gene lists obtained at 6 h were analyzed, nor were the down-regulated gene lists from the translatome. In both mRNA pools, responses to Fe starvation and cellular responses to Fe ion, nitric oxide and oxidative stress are enriched in the up-regulated genes (Table S6-S11). Ion transport and responses to Fe ion starvation and reactive oxygen species are enriched among the down-regulated genes in the transcriptome (Table S12-S14).

By comparing the DEGs in the two mRNA pools, we showed that there are more changes in the transcriptome than in the translatome (Figure 3). To determine the biological significance of this difference, we determined which biological processes are enriched in the genes that are affected in the transcriptome only. At 12 h after treatment, responses to nitric oxide and Fe ion transport are enriched among the genes up-regulated in the transcriptome only (Table S15), at 24 h coumarin biosynthetic process is the most enriched biological process (Table S16) and at 48 h the responses to reactive oxygen species and to Fe ions (Table S17). Only at 48 h more than 20 genes were down-regulated in the transcriptome only. These genes are related to the cellular response to Fe ion starvation and ion transport (Table S18). Further research will need to determine which genes underlie the enrichment of these processes and how the transcription versus translation changes affect the plant-bacterium interaction.

Studying the Arabidopsis root translatome response to a beneficial rhizobacterium

Cell type-specific TRAP on WCS417-exposed samples

Biologically significant changes in the translatome that could not be traced back to changes in the transcriptome have been identified in Arabidopsis in response to several biotic stresses (Moeller *et al.*, 2012; Reynoso *et al.*, 2013; Meteignier *et al.*, 2017). To investigate whether such changes also occur in response to pathogenic and mutualistic soil bacteria, we set up TRAP with plants exposed to the beneficial rhizobacterium WCS417.

We isolated total and ribosome-bound mRNA from control and WCS417-treated plant roots transformed with *35S:GFP-FLAG-RPL18*, thus expressing FLAG-tagged ribosomes in all cells, and from plants expressing similarly tagged ribosomes in cortical cells only using the cortex-specific *pPEP* promotor with *pPEP:GFP-FLAG-RPL18* (Mustroph *et al.*, 2009). Quantitative RT-PCR (qRT-PCR) confirmed highest expression of *PEP* in the ribosome-bound mRNA pool obtained from *pPEP:GFP-FLAG-RPL18* lines, whereas the trichoblast-specific GPI-anchored protein-encoding *COBL9* (Brady *et al.*, 2007a; b) was not enriched in this pool (Figure 4A). Thus, the cell type-specific isolation of the mRNA of bacteria-exposed plants was successful.

Subsequently, we checked induction of the known WCS417-inducible genes *MYB72* and *BGLU42* (Van der Ent *et al.*, 2008; Zamioudis *et al.*, 2014, 2015). Of these two, *BGLU42* is known to be induced in response to WCS417 in the cortex and trichoblasts specifically (Zamioudis *et al.*, 2014). *MYB72* is strongly upregulated in response to WCS417 in both ribosome-bound mRNA pools. A less clear, but similar trend is seen for *BGLU42*. Up-regulation of both genes is less clear in the total mRNA pools (Figure 4B). While no definite conclusions can be drawn from this experiment because of the low sample number, these results suggest that translational control adds an extra, yet uninvestigated layer to the Arabidopsis response to WCS417.

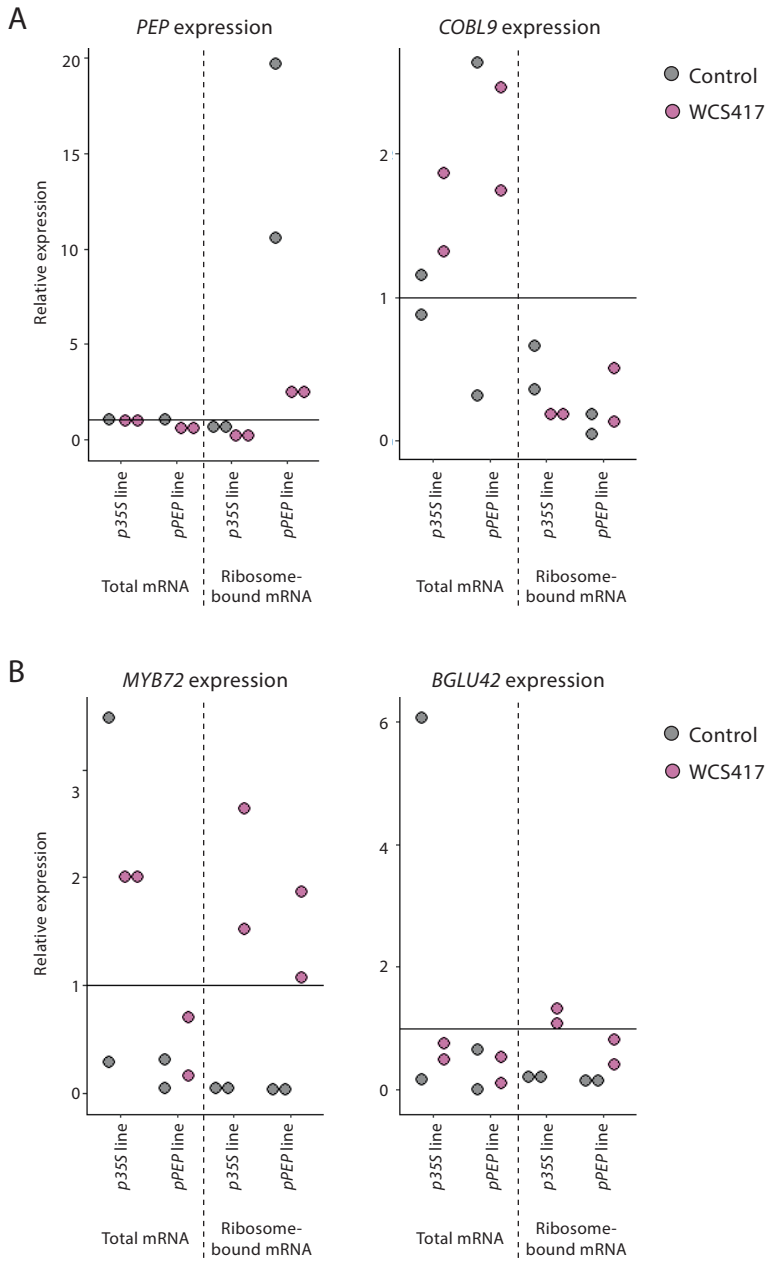

Figure 4 TRAP on roots colonized by WCS417 shows WCS417-induced activation of *MYB72* and *BGLU42*. qRT-PCR analysis of the expression of the cell-type specific genes *PEP* (cortex) and *COBL9* (root hair epidermis) (A) and of the WCS-inducible genes *MYB72* and *BGLU42* (B) in the total mRNA and the ribosome-bound mRNA pool obtained from 7-day-old plants transformed with either *p35S:GFP-FLAG-RPL18* or *pPEP:GFP-FLAG-RPL18* after 2 days of exposure to WCS417 (pink) or no bacteria (grey). Gene expression levels were normalized to that of the constitutively expressed gene *PP2AA3* (At1g13320). Plotted are fold changes in gene expression levels relative to the *p35S* line without bacteria (n = 1-2).

Generation of two novel epidermis-specific TRAP lines

One of the interesting observations in the cell type-specific gene expression data obtained in Chapter 2 is the specialization of the trichoblasts and atrichoblasts and, consequently, their differential response to WCS417. To study this difference in more detail, we generated TRAP lines in which FLAG-RPL18 expression is driven by the promotor of *WEREWOLF* (*WER*), specific for atrichoblasts, or *COBL9*, specific for trichoblasts (Chapter 2). Confocal microscopy of transformed plants showed no fluorescence in the *pCOBL9:His$_6$FLAG-GFP-RPL18* T2 plants. Additional transformants should be studied microscopically to identify plants with correct GFP expression patterns. Fluorescence patterns in the *pWER:His$_6$FLAG-GFP-RPL18* plants were as expected and were not visibly affected by Fe deficiency or WCS417 treatment (Figure 5).

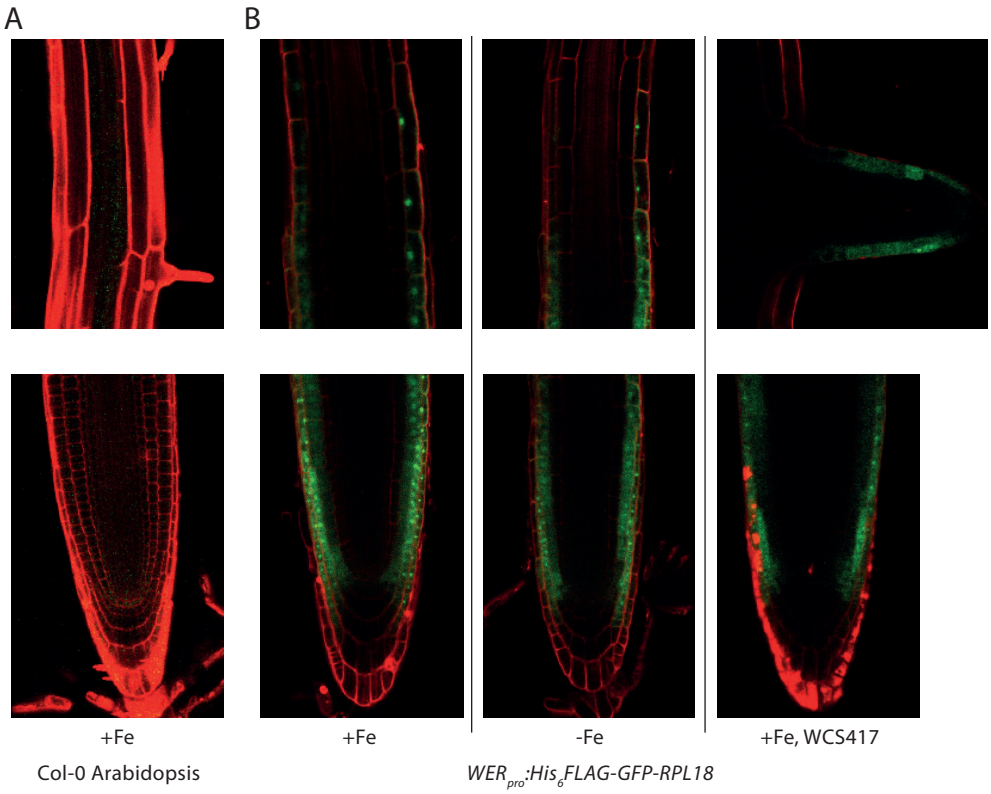

Figure 5 Arabidopsis Col-0 transformed with *WER$_{pro}$:His$_6$FLAG-GFP-RPL18B* expresses green fluorescent protein in atrichoblasts independent of the presence of Fe or WCS417. A) Root of a wild-type 10-day-old Col-0 seedling grown on sterile Hoagland with Fe (+Fe). B) Roots of 10-day-old seedlings transformed with *WER$_{pro}$:His$_6$FLAG-GFP-RPL18B* that were grown on sterile Hoagland with Fe (+Fe), sterile Hoagland without Fe (-Fe) or on +Fe with WCS417 for the last 3 days. Red shows cell walls as stained by propidium iodide (PI). Green shows green fluorescent protein (GFP). Representative images are shown.

Discussion

Transcriptome sequencing is currently the status quo when studying biological systems. However, there is increasing scientific evidence that changes in mRNA levels do not always correlate with changes in protein levels. This is in part due to post-transcriptional modifications of the mRNA molecules, which can result in reduced recruitment to ribosomes, mRNA degradation or storage of the mRNA molecules (Bailey-Serres *et al.*, 2009; Liu *et al.*, 2016). A better idea of proteome changes can therefore be obtained by sequencing only the mRNA molecules that are bound to ribosomes. The isolation of specifically these mRNA molecules from Arabidopsis roots is possible using translating ribosome affinity purification (TRAP) (Zanetti *et al.*, 2005). Studies using TRAP have shown that Arabidopsis responds to hypoxia and unanticipated darkness by reducing the number of ribosome-bound copies of certain mRNA molecules, without concurrent changes in the total number of copies present (Branco-Price *et al.*, 2008; Juntawong and Bailey-Serres, 2012). The authors speculate that this translational control might be a means of plants to rapidly adapt to the changed environmental conditions.

Arabidopsis has been suggested to also exert translational control over its response to Fe deficiency, as the transcriptome changes upon Fe deficiency do not to correlate with the protein changes (Pan *et al.*, 2015). Fe is an essential element for plants as it is required for many fundamental cellular processes, such as DNA replication and photosynthesis (Balk and Schaedler, 2014). To deal with Fe limitation, Arabidopsis makes use of the Strategy I Fe deficiency response, which revolves around the reduction of ferrous Fe (Fe^{3+}) to ferric Fe (Fe^{2+}) that can more readily be taken up by the plant (Walker and Connolly, 2008; Palmer and Guerinot, 2009; Darbani *et al.*, 2013). In this chapter, we studied the changes in both the transcriptome and the translatome Arabidopsis roots exposed to Fe deficiency (Figure 1).

Translational control results in selective recruitment of Fe deficiency-responsive mRNA molecules to the ribosomes

The previous study uncovering the difference in transcriptome versus proteome changes in response to Fe deficiency showed that 22 genes are similarly regulated in both the transcriptome and proteome of Fe-deficient plants (Pan *et al.*, 2015). We confirm this finding for several of these genes, demonstrating that the expression of the Fe storage gene *FER1* is reduced and the expression of multiple key genes involved in the Fe deficiency response is induced in both the transcriptome and the translatome of the Arabidopsis root in response to Fe deficiency (Figure 2). Also in line with previous studies (Dinneny *et al.*, 2008), we find a strong increase in the number of DEGs from 6 h up to 24 h after Fe deficiency (Figure 3A). This time-dependency is observed in both the transcriptome and the translatome. The number of DEGs in the translatome is considerably lower than in the transcriptome and few genes are differentially expressed in the translatome only (Figure 3B-C). These data indicate that translational control in response to Fe deficiency results in the selective ribosomal recruitment of a subset of the mRNA molecules encoded by Fe deficiency-responsive genes. Possibly, this allows plants to finetune their response to the exact environmental conditions at hand.

An analysis of the biological processes enriched in the up-regulated gene lists shows a strong signature for the response to Fe starvation. In addition, we show strong enrichment of the cellular response to nitric oxide. This is in line with previous studies showing activation of

the Arabidopsis Fe deficiency response upon nitric oxide accumulation downstream of auxin (Meiser *et al.*, 2011; Romera *et al.*, 2011). We observe up-regulation of *MYB72* and *BGLU42,* both of which are involved in coumarin biosynthesis, in both the transcriptome and the translatome at 24 h (Zamioudis *et al.*, 2014; Stringlis *et al.*, 2018a). However, coumarin biosynthesis is enriched in the list of genes up-regulated in the transcriptome only. Many coumarins exist, with different properties (Tsai and Schmidt, 2017; Stringlis *et al.*, 2019). Possibly, translational control allows the plant to select the biosynthesis of those coumarins best suited for the current environmental conditions.

Analyzing translational control of the Arabidopsis response to rhizobacteria

In addition to whole root translatome profiling, TRAP can be used to study cell type-specific translatome changes (Mustroph *et al.*, 2009). We show successful isolation of cortical cell-specific ribosome-bound mRNA from roots exposed to the beneficial rhizobacterium WCS417 (Figure 4). Cell type-specific sequencing of the translatome of WCS417-treated roots would be interesting as a follow-up on the experiment described in Chapter 2 for two reasons. First, studying the translatome instead of the transcriptome might uncover biological processes that are regulated at the translational instead of, or in addition to, the transcriptional level in a cell-type specific manner. Translational control has been shown to be potentially significant for the outcome of the Arabidopsis response to the *Pseudomonas syringae* effector AvrRpm1 and the *Turnip mosaic virus* (Moeller *et al.*, 2012; Meteignier *et al.*, 2017). Second, the fluorescence-activated cell sorting (FACS) procedure described in Chapter 2 involved a protoplasting step. This step has several drawbacks, including the risk of continued exposure to bacteria and bacteria-derived cell fragments. In the case of TRAP, cryopreserved tissue is used to extract ribosomes and ribosome-bound mRNA, and protoplasting is not required. Thus, there is no risk for direct contact between bacteria and plant cells during the protoplasting and sorting phases, as is the case with FACS.

TRAP lines are available with which ribosome-bound mRNA can be isolated from cortical, endodermal and vasculature cells (Mustroph *et al.*, 2009). However, no lines had yet been described for the isolation of ribosome-bound mRNA from trichoblasts and atrichoblasts. The newly generated TRAP lines in which FLAG-RPL18 is expressed in the trichoblasts and atrichoblasts specifically (Figure 5) will be essential for our own experimental plans to study the response of Arabidopsis to WCS417, and for other groups interested in epidermis-specific biological processes.

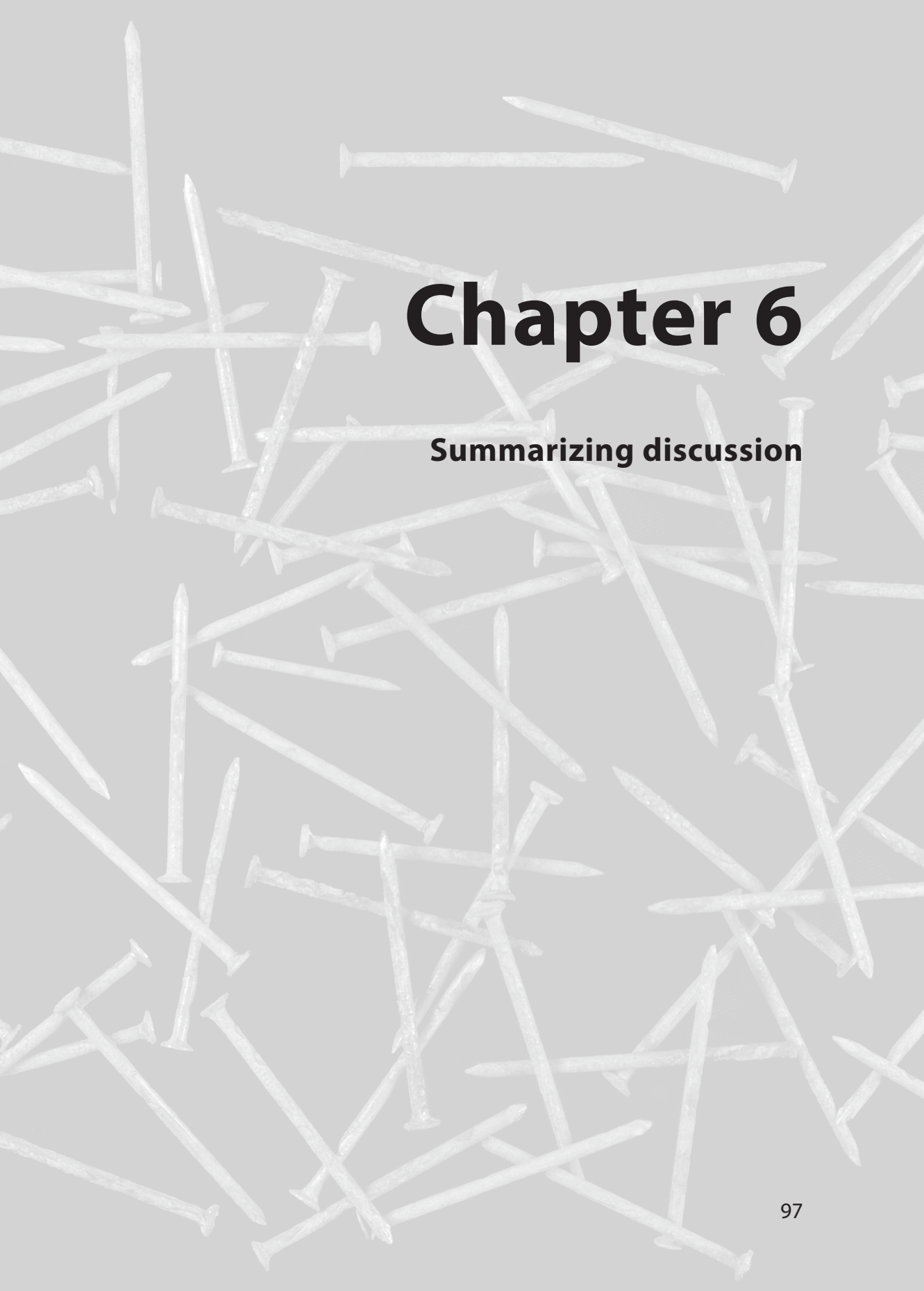

Chapter 6

Summarizing discussion

The importance of the plant's hidden half

The world's population is growing, and with it the demand for food is increasing as well. High-yielding crop varieties that require little to no synthetic pesticides or fertilizers are fundamental to sustainably producing sufficient food to meet this growing demand. For many decades, efforts to produce such crops focused solely on improving aboveground plant properties. However, it has become clear that the hidden, underground, half of plants is at least as important for plant health and productivity (Rogers and Benfey, 2015; Koevoets *et al.*, 2016; Li *et al.*, 2016; Shahzad and Amtmann, 2017). Plant roots are responsible for taking up nutrients and water from soil and respond to limited availability of these resources by changing their spatial arrangement to ensure optimal resource uptake (Gilroy and Jones, 2000; Müller and Schmidt, 2004; Vishwanath *et al.*, 2015; Barberon *et al.*, 2016; Salazar-Henao *et al.*, 2016; Barberon, 2017). Studying root system architecture and responses of roots to environmental changes might therefore uncover mechanisms that can be exploited to produce crops that have the optimal root system architecture given the nutrient and water availability in their surroundings (Rogers and Benfey, 2015; Koevoets *et al.*, 2016; Li *et al.*, 2016; Shahzad and Amtmann, 2017).

In addition to taking up nutrients and water, plant roots interact with billions diverse soil micro-organisms. Rape, sorghum, red clover and the model plant *Arabidopsis thaliana* (Arabidopsis) have all been shown to grow less when grown on sterile soil compared to when they are grown on soil containing micro-organisms (Rroço *et al.*, 2003; Jin *et al.*, 2006; Carvalhais *et al.*, 2013). Thus, plants depend on the micro-organisms in and around their roots, the root microbiome, for optimal growth. Among the micro-organisms in the root microbiome are plant growth-promoting rhizobacteria (PGPR). In addition to increasing plant growth, some PGPR increase plant resistance to disease (Lugtenberg and Kamilova, 2009). A well-studied example of a PGPR is *Pseudomonas simiae* WCS417 (WCS417). Root colonization by WCS417 stimulates Arabidopsis shoot growth (Pieterse and van Loon, 1999), and induces resistance against a broad range of pathogens in both Arabidopsis (Pieterse *et al.*, 1996) and several crop species (Bakker *et al.*, 2007; Pieterse *et al.*, 2014).

Arabidopsis changes the spatial arrangement of its roots in response to rhizobacteria

In response to root colonization by WCS417 and several other beneficial rhizobacteria, Arabidopsis increases the formation of lateral roots and root hairs (Vacheron *et al.*, 2013; Zamioudis *et al.*, 2013; Verbon and Liberman, 2016). The formation of these protrusions from the root is initiated by different Arabidopsis root cell types. Root hairs are formed by epidermal cells overlying two cortical cells, the so-called trichoblasts (Gilroy and Jones, 2000; Schiefelbein, 2000; Ryan *et al.*, 2001). Lateral roots originate in the pericycle, the cell layer in the vasculature neigboring the endodermis. These roots need to pass through the endodermis, cortex and epidermis to emerge from the primary root (Figure 1A) (Malamy and Benfey, 1997; Möller *et al.*, 2017; Ötvös and Benková, 2017; Du and Scheres, 2018).

The increased formation of lateral roots and root hairs in response to colonization by WCS417 suggests that the root responds to WCS417 by inducing cell type-specific transcriptional changes. We studied such changes in Chapter 2 by performing fluorescence-activated cell sorting (FACS) of control and WCS417-colonized Arabidopsis roots followed by RNA sequencing. We identified the highest numbers of differentially expressed genes in the cortex and endodermis. Previous

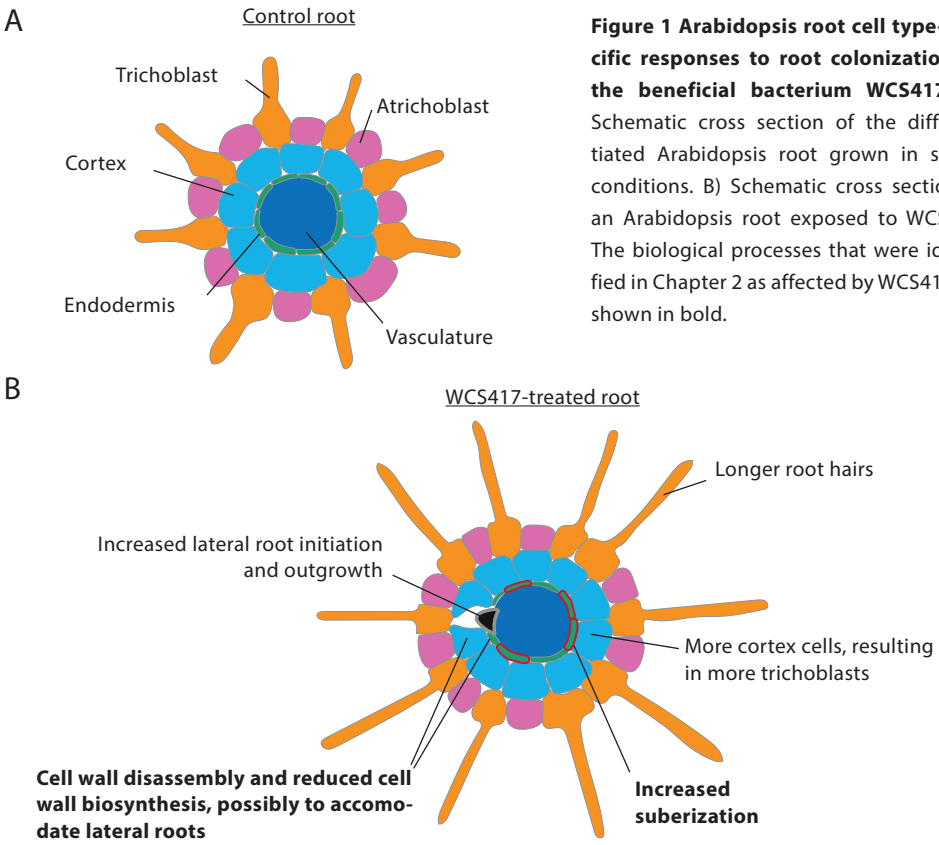

Figure 1 Arabidopsis root cell type-specific responses to root colonization by the beneficial bacterium WCS417. A) Schematic cross section of the differentiated Arabidopsis root grown in sterile conditions. B) Schematic cross section of an Arabidopsis root exposed to WCS417. The biological processes that were identified in Chapter 2 as affected by WCS417 are shown in bold.

research has shown that the increased number of root hairs observed in WCS417-colonized roots is due to an increased number of cortical cells (Zamioudis *et al.*, 2013). Regarding the increase in lateral root number, we show that the cortex and endodermis reduce the expression of genes involved in cell wall biosynthesis and induce the expression of genes involved in cell wall disassembly in response to WCS417 (Figure 1B). Recently, it was shown that cell volume loss in the cortex and endodermis is essential for lateral root emergence and lateral root initiation (Stoeckle et al., 2018; Vermeer et al., 2014). The reduced activation of genes involved in cell wall biosynthesis that we observe in our data might contribute to this morphological change. Thus, transcriptional changes in the cortex and endodermis might orchestrate the increase in both root hairs and lateral roots in response to WCS417. In addition to reduced cell wall biosynthesis, we show that the endodermis increases the expression of genes involved in suberin biosynthesis (Figure 1B). Suberin is a hydrophobic polymer that is deposited between the cell wall and plasma membrane of differentiated endodermal cells. This extra layer prevents free movement of nutrients and water into and out of the central cylinder of the root (Geldner, 2013; Barberon, 2017).

Hypothetically speaking, the observed changes in response to WCS417 could be a response to the successful establishment of a mutually beneficial association. Plants are known to affect the root microbiome composition via their root exudates, resulting in different microbiomes on the roots of different plant species (Berg and Smalla, 2009; Bulgarelli *et al.*, 2013; Philippot *et*

al., 2013). In addition, plants can selectively modify the microbiome composition in response to environmental changes. In the case of downy mildew-infected Arabidopsis plants, the composition of the root microbiome is changed in favor of micro-organisms that decrease plant disease symptoms caused by the pathogen, while simultaneously promoting plant growth (Berendsen *et al.*, 2018). Likewise, plants grown in iron (Fe)-deficient conditions attract micro-organisms that mediate increased Fe uptake by the plant (Jin *et al.*, 2006; Stringlis *et al.*, 2018a). Possibly, plants also respond to beneficial rhizobacteria by changing features that attract or repel other micro-organisms. As suberin prevents free movement of nutrients and water into and out of the endodermis (Geldner, 2013; Barberon, 2017), increased suberin deposition might allow a plant to restrict the amount of nutrients leaving the root. As attraction of beneficial micro-organisms would be less of a priority after establishment of a beneficial interaction, this would save energy that can be directed to growth or disease resistance instead. An increase in lateral root number might also be an evolutionarily advantageous response to root colonization by a beneficial rhizobacterium, as it increases the area that can be colonized by said rhizobacterium. However, the opposite hypothesis could also be true: as we show that defense responses are induced by WCS417, suberization and lateral root formation might be induced as part of these defense responses. Indeed, suberin deposition has been hypothesized to be involved in restricting microbial access to the central cylinder (Geldner, 2013; Vishwanath *et al.*, 2015). The increase in lateral roots, in the meantime, might be initiated to prevent possible nutrient shortages due to competition for nutrient with the colonizing micro-organisms.

Finally, the root architectural changes observed upon root colonization by WCS417 might be induced by changes in nutrient availability or plant nutrient usage, as both suberization and lateral root number are affected by nutrient availability (Barberon *et al.*, 2016; Shahzad and Amtmann, 2017). Indeed, WCS417 induces the Fe deficiency response in Arabidopsis (Verhagen *et al.*, 2004; Van der Ent *et al.*, 2008; Zamioudis *et al.*, 2014), suggesting that it affects either Fe availability or Fe usage in the plant. Further research with beneficial and pathogenic soil micro-organisms will have to show whether suberin deposition is indeed increased by WCS417 and other micro-organisms, and how the increased suberin deposition and lateral root formation affect plant nutrient status and plant immunity, and vice versa.

Nutrient uptake is specific to trichoblasts

The Fe deficiency response is a set of molecular changes that allow for increased Fe uptake by the plant (Römheld, 1987; Verbon *et al.*, 2017). This response is fundamental to plant health, as Fe is an essential nutrient (Balk and Schaedler, 2014) and the bioavailability of Fe in the soil is often limited (Palmer et al., 2013; Tsai and Schmidt, 2017). In Arabidopsis, the Fe deficiency response includes upregulation of *FERRIC REDUCTASE OXIDASE 2* (*FRO2*) and *IRON REGULATED TRANSPORTER 1* (*IRT1*) downstream of the major Fe deficiency response regulator FER-LIKE IRON DEFICIENCY TRANSCRIPTION FACTOR (FIT) (Colangelo and Guerinot, 2004). FRO2 reduces Fe in the soil to its ferrous form (Fe^{2+}) (Robinson *et al.*, 1999), which can be taken up into the root through IRT1 (Vert *et al.*, 2002). The amount of Fe available for reduction by FRO2 is increased via the root-mediated secretion of protons and of phenolic compounds such as coumarins, which results in Fe solubilization (Santi and Schmidt, 2009; Fourcroy *et al.*, 2016; Tsai and Schmidt, 2017; Stringlis *et al.*, 2018a). The β-glucosidase-encoding gene *BGLU42* is among the genes responsible for the modification of coumarins before their secretion into the rhizosphere

(Zamioudis *et al.*, 2014; Stringlis *et al.*, 2018a).

Interestingly, both *BGLU42* and *IRT1* are induced in specifically the trichoblasts, and to a lesser extent the cortex, upon activation of the Fe deficiency response (Vert *et al.*, 2002; Zamioudis *et al.*, 2014). The trichoblast-specific expression pattern of genes involved in nutrient uptake could explain why trichoblasts are essential for nutrient uptake (Tanaka *et al.*, 2014). In Chapter 2, we show that not only *BGLU42* and *IRT1*, but the majority of genes involved in the response to Fe starvation is activated specifically in the trichoblasts.

These data raise the question as to why not all epidermal cells form root hairs. In line with previous research (Lan *et al.*, 2013), we show that RNA modification and processing are performed preferentially in atrichoblasts. In addition, we find higher defense gene expression in these cells in control conditions. As the epidermis is the outermost layer of the Arabidopsis root, it forms the first line of defense. We therefore speculate that the differentiation into trichoblasts and atrichoblasts in the epidermis allows plants to physically separate nutrient uptake and defense processes to ensure that both processes can take place simultaneously.

Increased Fe uptake is required for a beneficial interaction of WCS417 with Arabidopsis

The Fe deficiency response is activated in response to root colonization by WCS417. In Chapter 3 we show that increased Fe uptake is essential for the maintenance of plant health upon exposure to WCS417, as WCS417-mediated growth induction in Fe-limited conditions results in severe plant chlorosis. As we have shown in Chapter 2 that the majority of the genes involved in Fe uptake are active in root hairs specifically, the increased Fe uptake in response to WCS417 might be achieved by a combined effect of the activation of the Fe deficiency response and the increase in root hair number (Zamioudis *et al.*, 2013).

These results do not yet explain in response to what signal the Fe deficiency response is activated. To identify such a signal, we first confirmed previous findings that the shoot is required for the activation of the Fe deficiency response upon root colonization by WCS417 (Zamioudis *et al.*, 2013). Subsequently, we checked what is known about the activation of the Fe deficiency response in Fe-limiting conditions. In such conditions, the activation of the Fe deficiency response is dependent on leaf Fe status signaling to the root (Zhai *et al.*, 2014; Grillet *et al.*, 2018; Khan *et al.*, 2018). Possibly, WCS417-mediated growth induction results in a shoot Fe shortage that leads to the induction of the Fe deficiency response. We tested this hypothesis by supplying the shoots of WCS417-treated plants with Fe. Our results show that shoot Fe supplementation does not prevent the activation of the Fe deficiency response, suggesting that the Fe deficiency response is not activated in response to a shoot Fe shortage. Instead, we hypothesize that the Fe deficiency response is induced in response to a growth promotion signal in the shoot. As Fe is required for many fundamental cellular processes, this would be evolutionarily advantageous compared to a mechanism where the response is activated only after an Fe shortage. Our data on the stable Fe content in the more rapidly growing shoots of WCS417-treated plants are in line with this hypothesis.

WCS417-mediated resistance is different from Fe deficiency-induced resistance

In Chapter 3 we have shown that activation of the Fe deficiency response upon root colonization by WCS417 is probably essential to prevent chlorosis in the more rapidly growing

plant. Previously, the activation of the Fe deficiency response was already shown to be essential for another beneficial effect of WCS417: the induction of systemic resistance (ISR). ISR was discovered in 1991, when two groups showed that root colonization by PGPR can increase shoot resistance to pathogen attack (Van Peer *et al.*, 1991; Wei *et al.*, 1991). WCS417 was among the first PGPR for which beneficial rhizobacteria-mediated ISR was demonstrated that year (Van Peer *et al.*, 1991). Ever since, it has served as a model PGPR for studies on ISR (Berendsen *et al.*, 2015) and was shown to induce resistance in Arabidopsis and several crop species (Van Peer *et al.*, 1991; Leeman *et al.*, 1995; Duijff *et al.*, 1998). The WCS417-mediated induced resistance is characterized by a stronger and faster immune response upon pathogen attack, a phenomenon known as priming (Pieterse *et al.*, 1996, 2014). Several years ago, WCS417-mediated ISR was shown to be dependent on the activation of at least two genes that are induced as part of the Fe deficiency response: *MYB72* and *BGLU42* (Van der Ent *et al.*, 2008; Zamioudis *et al.*, 2014, 2015). In fact, over-expression of *BGLU42* is sufficient to induce resistance in Arabidopsis (Zamioudis *et al.*, 2014).

Interestingly, Fe deficiency by itself is known to decrease plant susceptibility to several pathogens (Kieu *et al.*, 2012; Hsiao *et al.*, 2017; Verbon *et al.*, 2017). We studied the molecular mechanisms of Fe deficiency-reduced susceptibility and its similarities to WCS417-induced resistance in Chapter 4. First, we show that Fe-deficient Arabidopsis plants become less diseased upon attack by the necrotroph *Botrytis cinerea*, the biotroph *Hyaloperonospora arabidopsidis* and the hemibiotrophic bacterium *P. syringae* pv. *tomato* DC3000 than Fe-sufficient plants. The Arabidopsis immune response to (hemi)biotrophic pathogen attack involves the defense hormone salicylic acid (SA), whereas the response again necrotrophic pathogen attack requires the defense hormones jasmonic acid (JA) and ethylene (ET) (Berendsen *et al.*, 2012; Broekgaarden *et al.*, 2015). We show Fe deficiency does not induce resistance against *B. cinerea* and *H. arabidopsidis* in an ET response mutant and an SA biosynthesis mutant, respectively. Thus, Fe deficiency seemt to induce a plant-mediated increase in resistance. Subsequently, we studied the activation of defense genes downstream of these hormones in Fe-sufficient versus Fe-deficient plants. Our data show that the defense genes are not induced by Fe deficiency when there are no pathogens present. However, upon attack, there are trends for stronger or faster expression of these genes in Fe-deficient plants. These results suggest that Fe deficiency-induced resistance is based on priming of the immune response.

As both WCS417-mediated ISR and Fe deficiency-induced resistance seem to be based on priming of the immune system and WCS417-mediated resistance requires the Fe-deficiency genes *MYB72* and *BGLU42*, we wondered whether Fe deficiency-induced resistance and WCS417-mediated ISR are activated by the same root-specific signaling pathways. We tested this using the ISR-defective *myb72* and *bglu42* mutants. We show that while these mutants cannot mount increased resistance in response to WCS417, they do mount resistance in response to Fe deficiency. Thus, ISR and Fe deficiency-induced resistance must, at least partly, be regulated in a different manner. Finally, we show increased resistance in mutants with either a higher or a lower Fe content compared to wild-type plants. This suggests that any disturbance in Fe homeostasis results in increased plant resistance. This further corroborates that Fe deficiency-induced resistance is different from WCS417-mediated ISR, as we show in Chapter 3 that the Fe content of Arabidopsis is not affected by WCS417. In addition, it confirms that the pathways regulating iron homeostasis and plant immunity are tightly linked.

Studying the Arabidopsis response at a different level

In chapter 2, we studied the effect of WCS417 on gene transcription in specific cell types. In chapters 3 and 4 we studied the link between WCS417 and Fe deficiency, a link that was uncovered previously by studying gene transcription changes in the whole root. While transcriptome changes give insight into the molecular processes affected in plant roots, they do not always correlate with changes in protein production. For example, only 13% of the protein abundance changes in Fe-deficient Arabidopsis roots is accompanied by a similar change in transcript abundance of the encoding messenger RNA (mRNA) (Pan et al., 2015). Part of this discrepancy is due to post-transcriptional modifications of mRNA molecules that lead to differential mRNA translation (Bailey-Serres *et al.*, 2009).

Splicing is a post-transcriptional modification in which introns are removed from the mRNA strand and the adjacent exons are joined together. Alternative splicing is defined as the splicing of one gene in different ways. In Arabidopsis, alternative splicing has been shown for 42 – 61% of the genes (Filichkin *et al.*, 2010; Marquez *et al.*, 2012). Alternative splicing can result in stable versus unstable mRNA products, or in mRNA products with different localization patterns or function. Patterns of alternative splicing are affected by environmental changes, such as high temperature, high salinity, elevated zinc levels and treatment with ABA, indicating that alternative splicing is an additional means on top of gene transcription changes to adapt to the environment (Shang *et al.*, 2017; Laloum *et al.*, 2018). An example of the biological significance of environment-dependent alternative splicing is the splicing of FLOWERING LOCUS M (FLM) into either FLM-β or FLM-δ. The ratio of FLM-β versus FLM-δ decreases with increasing temperature. As FLM-β binds DNA, whereas FLM-δ does not, the changed ratio might release the repression of the transcription of floral activator genes by FLM-β, resulting in flowering (Shang *et al.*, 2017).

In addition to alternative splicing upon environmental stress, differential alternative splicing is also observed between Arabidopsis cell types (Lan *et al.*, 2013). Conceivably, alternative splicing adds another tuning layer to the genetic and molecular mechanisms driving Arabidopsis root cell differentiation. It will therefore be of interest to study cell type-specific alternative splicing patterns and the effect of WCS on these patterns using the gene expression dataset generated in Chapter 2. Preliminary analyses in this direction indicate that Arabidopsis indeed responds to WCS417 root colonization with differential alternative splicing in the different cell layers.

In chapter 5 we took a different approach to study the effect of post-transcriptional modifications. In this chapter, we set up translating ribosome affinity purification (TRAP), a procedure that allows for the isolation and sequencing of ribosome-bound mRNA molecules. Although the translation of these molecules could still be stalled inside the ribosomes, ribosome-bound mRNA profiles are believed to be better correlated with protein levels than total mRNA profiles (Zanetti *et al.*, 2005; Mustroph *et al.*, 2009). Previous studies using TRAP have shown that translational regulation is important for effective Arabidopsis responses to sudden darkness, hypoxia and pathogenic bacteria (Branco-Price *et al.*, 2008; Juntawong and Bailey-Serres, 2012; Meteignier *et al.*, 2017). We used TRAP to compare the transcriptome, i.e. all mRNA molecules in a cell, and the translatome, i.e. all mRNA molecules bound to ribosomes, of Fe-deficient and Fe-sufficient plants. Preliminary data analysis indicates that more genes are differentially expressed in the transcriptome than in the translatome in response to Fe deficiency. This suggests that translational regulation recruits only a subset of the mRNA molecules that are up-regulated at the transcriptional level to the ribosomes, thereby adding

an additional level of regulation to the plant's response to the environment. In addition, we add to the currently available TRAP line repertoire (Mustroph *et al.*, 2009) by constructing TRAP lines specific to the epidermal Arabidopsis root cell types.

Concluding remarks

Plants have the amazing ability to use sunlight, carbon dioxide and soil-borne macro- and micronutrients to produce almost all the nutrients that we humans require. While at first glance this seems to be a solitary endeavor, a more detailed analysis reveals that this is not the case; plants interact with billions of micro-organisms on and in their root to increase plant growth and health. While there is evidence that plants can "eat" micro-organisms, in a process termed microbivory (Paungfoo-Lonhienne *et al.*, 2010, 2013, White *et al.*, 2018, 2019), the majority of plant-microbe interactions is believed to depend on symbiotic or mutualistic relationships. In this thesis, we show that a mutualistic interaction between plant roots and beneficial rhizobacteria impacts plant nutrition in several, possibly connected, ways (Figure 2). In Chapter 2, we identify transcriptional changes that underlie changes in the Arabidopsis root system architecture in response to WCS417. The changes in the spatial arrangement of the roots increase the capacity of the roots to explore the soil and could consequently result in increased nutrient uptake. In addition, we find increased activity of the suberin biosynthesis pathway in the root. Increased suberin biosynthesis might prevent excessive leaching of nutrients into the rhizosphere or restrict entry of micro-organisms into the central cylinder. In Chapter 3, we show that increased Fe uptake in response to WCS417 is required for the establishment of an interaction that is beneficial to the plant. The increased Fe uptake is probably partly mediated by the activation of the Fe deficiency response and partly by the changes in root system architecture as found in Chapter 2. How the Fe deficiency response is activated remains uncertain, but we hypothesize that it is activated in response to a growth signal originating from the aboveground parts of the plant. In Chapter 4 we show that the decreased susceptibility of Fe-starved plants to several pathogens is dependent on a functional immune system. Like WCS417-mediated ISR This Fe deficiency-induced resistance is similar to WCS417-mediated ISR as it is possibly based on priming of the immune response. Moreover, WCS417-mediated ISR is known to require the activation of several genes involved in the Fe deficiency response. However, we show in Chapter 4 that Fe deficiency-induced resistance is not activated by the same root-specific signaling pathways as WCS417-mediated resistance.

For hundreds of years, plant root traits were not considered when selecting the 'best' crops for crop advancement. By now, the importance of the hidden half of plants has become clear: root traits are crucial for both optimal nutrient and water uptake and the establishment of beneficial interactions with soil-borne micro-organisms. In this thesis, we present results on transcriptional processes regulating root architectural changes, and on the effects of Fe availability in and around plants on their interaction with both beneficial rhizobacteria and pathogens. **Nailing down the Arabidopsis root response to beneficial rhizobacteria** through continued research will contribute to harnessing root traits to optimize the uptake of resources by crop plants and to successfully applying beneficial rhizobacteria in the field to increase crop growth and resistance against disease. Together, these advancements will enhance crop yield while limiting the use of synthetic pesticides and fertilizers, thereby ensuring sufficient food production for the growing world population.

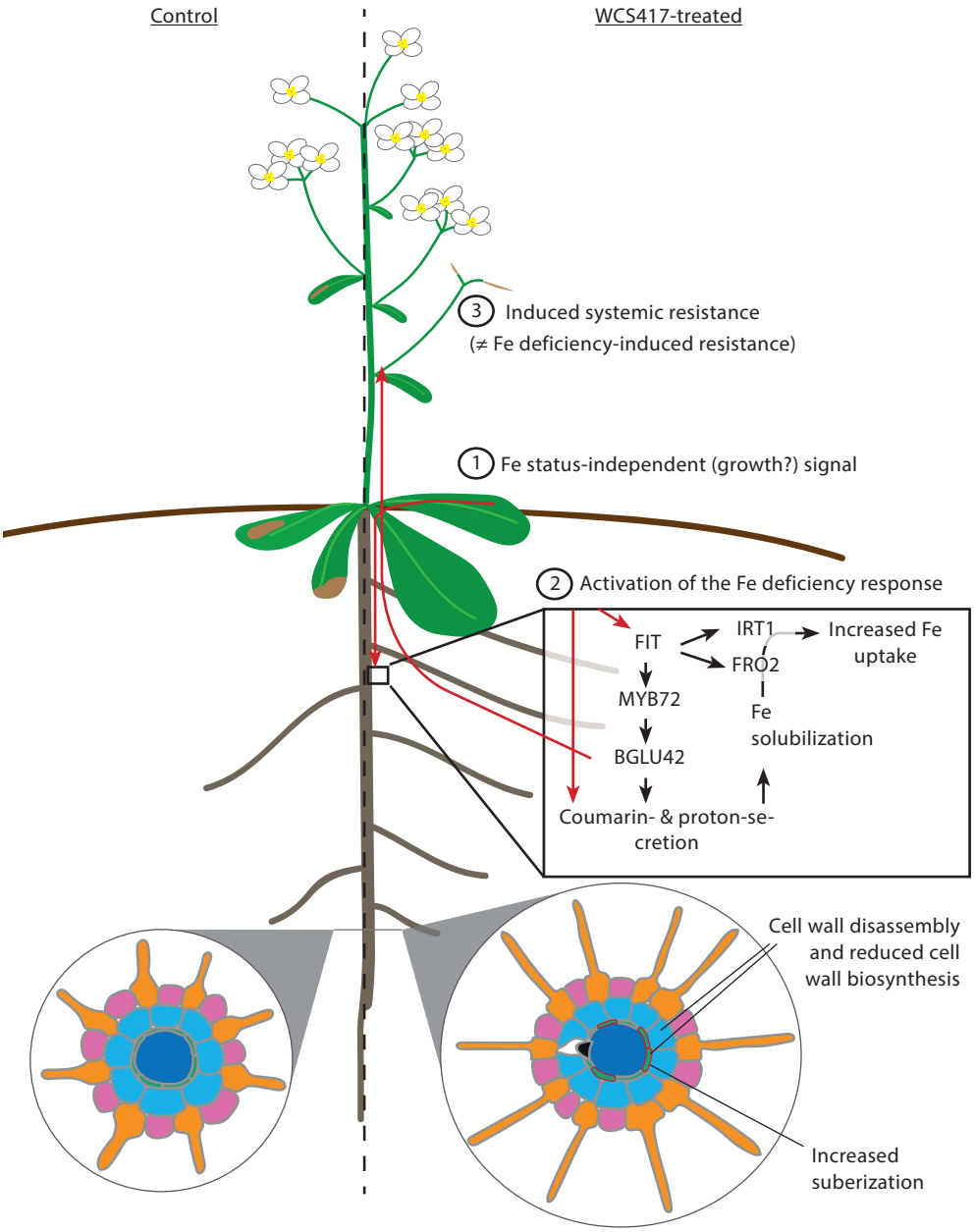

Figure 2 Induction of the iron deficiency response and root architecture changes in response to WCS417 allows for increased plant growth and resistance without a decrease in plant Fe content. Based on the results presented in this thesis we hypothesize that the root activates the Fe deficiency response upon perception of a shoot-derived growth promotion signal to prevent an Fe shortage accompanying the WCS417-mediated increase in plant growth. Activation of *MYB72* and *BGLU42* is required for the WCS417-mediated induction of systemic resistance. This is not the case for Fe deficiency-induced resistance, even though it also seems to be based on priming of the plant immune response. In addition, Arabidopsis changes its root system architecture in response to WCS417. These changes might be induced in response to the beneficial association, as part of a defense response or in response to nutrient changes.

Appendix

References

Ab Rahman, S.F.S., Singh, E., Pieterse, C.M.J., and Schenk, P.M. (2018) Emerging microbial biocontrol strategies forplant pathogens. *Plant Science*, **267**, 102–111.

Aida, M., Beis, D., Heidstra, R., Willemsen, V., Blilou, I., Galinha, C., Nussaume, L., Noh, Y.-S., Amasino, R., and Scheres, B. (2004) The *PLETHORA* genes mediate patterning of the *Arabidopsis* root stem cell niche. *Cell*, **119**, 109–120.

Arnaud, N., Murgia, I., Boucherez, J., Briat, J.-F., Cellier, F., and Ric Gaymard, F. (2006) An iron-induced nitric oxide burst precedes ubiquitin-dependent protein degradation for *Arabidopsis AtFer1* ferritin gene expression. *Journal of Biological Chemistry*, **281**, 23579–23588.

Asari, S., Tarkowská, D., Rolčík, J., Novák, O., Palmero, D.V., Bejai, S., and Meijer, J. (2017) Analysis of plant growth-promoting properties of *Bacillus amyloliquefaciens* UCMB5113 using *Arabidopsis thaliana* as host plant. *Planta*, **245**, 15–30.

Asghar, H., Zahir, Z., Arshad, M., and Khaliq, A. (2002) Relationship between in vitro production of auxins by rhizobacteria and their growth-promoting activities in *Brassica juncea* L. *Biology and Fertility of Soils*, **35**, 231–237.

Aznar, A., Chen, N.W.G., Rigault, M., Riache, N., Joseph, D., Desmaële, D., Mouille, G., Boutet, S., Soubigou-Taconnat, L., Renou, J.-P., Thomine, S., Expert, D., and Dellagi, A. (2014) Scavenging iron: a novel mechanism of plant immunity activation by microbial siderophores. *Plant Physiology*, **164**, 2167–2183.

Aznar, A., Patrit, O., Berger, A., and Dellagi, A. (2015a) Alterations of iron distribution in Arabidopsis tissues infected by *Dickeya dadantii*. *Molecular Plant Pathology*, **16**, 521–528.

Aznar, A., Chen, N.W.G., Thomine, S., and Dellagi, A. (2015b) Immunity to plant pathogens and iron homeostasis. *Plant Science*, **240**, 90–97.

Badri, D. V, Quintana, N., El Kassis, E.G., Kim, H.K., Choi, Y.H., Sugiyama, A., Verpoorte, R., Martinoia, E., Manter, D.K., and Vivanco, J.M. (2009) An ABC transporter mutation alters root exudation of phytochemicals that provoke an overhaul of natural soil microbiota. *Plant Physiology*, **151**, 2006–2017.

Bailey-Serres, J., Sorenson, R., and Juntawong, P. (2009) Getting the message across: cytoplasmic ribonucleoprotein complexes. *Trends in Microbiology*, **14**, 443–453.

Bailly, A., Groenhagen, U., Schulz, S., Geisler, M., Eberl, L., and Weisskopf, L. (2014) The inter-kingdom volatile signal indole promotes root development by interfering with auxin signalling. *The Plant Journal*, **80**, 758–771.

Bakker, P.A.H.M., Pieterse, C.M.J., and Van Loon, L.C. (2007) Induced systemic resistance by fluorescent *Pseudomonas* spp. *Phytopathology*, **97**, 239–243.

Bakker, P.A.H.M., Pieterse, C.M.J., De Jonge, R., and Berendsen, R.L. (2018) The soil-borne legacy. *Cell*, **172**, 1178–1180.

Balk, J. and Schaedler, T.A. (2014) Iron cofactor assembly in plants. *Annual Review of Plant Biology*, **65**, 125–153.

Barash, I., Zion, R., Krikun, J., and Nachmias, A. (1988) Effect of iron status on verticillium wilt disease and on *in vitro* production of siderophores by *verticillium dahliae*. *Journal of Plant Nutrition*, **11**, 893–905. Taylor & Francis Group.

Barberon, M. (2017) The endodermis as a checkpoint for nutrients. *New Phytologist*, **213**, 1604–1610.

Barberon, M., Vermeer, J.E.M., De Bellis, D., Wang, P., Naseer, S., Andersen, T.G., Humbel, B.M., Nawrath, C., Takano, J., Salt, D.E., and Geldner, N. (2016) Adaptation of root function by nutrient-induced plasticity of endodermal differentiation. *Cell*, **164**, 447–459.

Bashir, K. and Nishizawa, N.K. (2006) Deoxymugineic acid synthase. *Plant Signaling and Behavior*, **1**, 290–292.

Benfey, P.N., Linstead, P.J., Roberts, K., Schiefelbein, J.W., Hauser, M.T., and Aeschbacher, R.A. (1993) Root development in *Arabidopsis*: four mutants with dramatically altered root morphogenesis. *Development*, **119**, 57–70.

Benková, E. and Bielach, A. (2010) Lateral root organogenesis - from cell to organ. *Current Opinion in Plant Biology*, **13**, 677–683.

Benková, E., Michniewicz, M., Sauer, M., Teichmann, T., Seifertová, D., Jürgens, G., and Friml, J. (2003) Local, efflux-dependent auxin gradients as a common module for plant organ formation. *Cell*, **115**, 591–602.

Berendsen, R.L., Pieterse, C.M.J., and Bakker, P.A.H.M. (2012) The rhizosphere microbiome and plant health. *Trends in Plant Science*, **17**, 478–486.

Berendsen, R.L., Van Verk, M.C., Stringlis, I.A., Zamioudis, C., Tommassen, J., Pieterse, C.M.J., and Bakker, P.A.H.M. (2015) Unearthing the genomes of plant-beneficial *Pseudomonas* model strains WCS358, WCS374 and WCS417. *BMC Genomics*, **16**, 539.

Berendsen, R.L., Vismans, G., Yu, K., Song, Y., de Jonge, R., Burgman, W.P., Burmølle, M., Herschend, J., H

M Bakker, P.A., and J Pieterse, C.M. (2018) Disease-induced assemblage of a plant-beneficial bacterial consortium. *The ISME Journal*, **12**, 1496–1507.

van den Berg, C., Willemsen, V., Hendriks, G., Weisbeek, P., and Scheres, B. (1997) Short-range control of cell differentiation in the *Arabidopsis* root meristem. *Nature*, **390**, 287–289.

Van den Berg, C., Willemsen, V., Hage, W., Weisbeek, P., and Scheres, B. (1995) Cell fate in the *Arabidopsis* root meristem determined by directional signalling. *Nature*, **378**, 62–65.

Berg, G. and Smalla, K. (2009) Plant species and soil type cooperatively shape the structure and function of microbial communities in the rhizosphere. *FEMS Microbiology Ecology*, **68**, 1–13.

Bielach, A., Podlesáková, K., Marhavy, P., Duclercq, J., Cuesta, C., Müller, B., Grunewald, W., Tarkowski, P., and Benková, E. (2012) Spatiotemporal regulation of lateral root organogenesis in *Arabidopsis* by cytokinin. *Plant Cell*, **24**, 3967–3981.

Birnbaum, K., Shasha, D.E., Wang, J.Y., Jung, J.W., Lambert, G.M., Galbraith, D.W., and Benfey, P.N. (2003) A gene expression map of the *Arabidopsis* root. *Science*, **302**, 1956–1960.

Birnbaum, K., Jung, J.W., Wang, J.Y., Lambert, G.M., Hirst, J.A., Galbraith, D.W., and Benfey, P.N. (2005) Cell type–specific expression profiling in plants via cell sorting of protoplasts from fluorescent reporter lines. *Nature Methods*, **2**, 615–619.

Bodenhausen, N. and Reymond, P. (2007) Signaling pathways controlling induced resistance to insect herbivores in *Arabidopsis*. *Molecular Plant-Microbe Interactions*, **20**, 1406–1420.

Brady, S.M., Orlando, D.A., Lee, J.-Y., Wang, J.Y., Koch, J., Dinneny, J.R., Mace, D., Ohler, U., and Benfey, P.N. (2007a) A high-resolution root spatiotemporal map reveals dominant expression patterns. *Science*, **318**, 801–806.

Brady, S.M., Song, S., Dhugga, K.S., Rafalski, J.A., and Benfey, P.N. (2007b) Combining expression and comparative evolutionary analysis. The *COBRA* gene family. *Plant Physiology*, **143**, 172–187.

Branco-Price, C., Kaiser, K.A., Jang, C.J.H., Larive, C.K., and Bailey-Serres, J. (2008) Selective mRNA translation coordinates energetic and metabolic adjustments to cellular oxygen deprivation and reoxygenation in *Arabidopsis thaliana*. *The Plant Journal*, **56**, 743–755.

Bray, N.L., Pimentel, H., Melsted, P., and Pachter, L. (2016) Near-optimal probabilistic RNA-seq quantification. *Nature Biotechnology*, **34**, 525–527.

Briat, J.-F., Fobis-Loisy, I., Grignon, N., Lobréaux, S., Pascal, N., Savino, G., Thoiron, S., Von Wirén, N., and Van Wuytswinkel, O. (1995) Cellular and molecular aspects of iron metabolism in plants. *Biology of the Cell*, **84**, 69–81.

Briat, J.-F., Lobréaux, S., Grignon, N., and Vansuyt, G. (1999) Regulation of plant ferritin synthesis: how and why. *Cellular and Molecular Life Sciences*, **56**, 155–166.

Briat, J.-F., Dubos, C., Dé, F., and Gaymard, R. (2015) Iron nutrition, biomass production, and plant product quality. *Trends in Plant Science*, **20**, 33–40.

Briat, J.F., Ravet, K., Arnaud, N., Duc, C., Boucherez, J., Touraine, B., Cellier, F., and Gaymard, F. (2010) New insights into ferritin synthesis and function highlight a link between iron homeostasis and oxidative stress in plants. *Annals of Botany*, **105**, 811–822.

Vande Broek, A., Lambrecht, M., and Vanderleyden, J. (1998) Bacterial chemotactic motility is important for the initiation of wheat root colonization by *Azospirillum brasilense*. *Microbiology*, **144**, 2599–2606.

Broekgaarden, C., Caarls, L., Vos, I.A., Pieterse, C.M.J., and Van Wees, S.C.M. (2015) Ethylene: traffic controller on hormonal crossroads to defense. *Plant Physiology*, **169**, 2371–2379.

Brumbarova, T., Bauer, P., and Ivanov, R. (2015) Molecular mechanisms governing *Arabidopsis* iron uptake. *Trends in Plant Science*, **20**, 124–133.

Buckhout, T.J., Yang, T.J., and Schmidt, W. (2009) Early iron-deficiency-induced transcriptional changes in *Arabidopsis* roots as revealed by microarray analyses. *BMC Genomics*, **10**, 147.

Bulgarelli, D., Rott, M., Schlaeppi, K., Ver Loren van Themaat, E., Ahmadinejad, N., Assenza, F., Rauf, P., Huettel, B., Reinhardt, R., Schmelzer, E., Peplies, J., Gloeckner, F.O., Amann, R., Eickhorst, T., and Schulze-Lefert, P. (2012) Revealing structure and assembly cues for *Arabidopsis* root-inhabiting bacterial microbiota. *Nature*, **488**, 91–95.

Bulgarelli, D., Schlaeppi, K., Spaepen, S., van Themaat, E.V.L., and Schulze-Lefert, P. (2013) Structure and functions of the bacterial microbiota of plants. *Annual Review of Plant Biology*, **64**, 807–838.

Caarls, L., Elberse, J., Awwanah, M., Ludwig, N.R., De Vries, M., Zeilmaker, T., Van Wees, S.C.M., Schuurink, R.C., and Van den Ackerveken, G. (2017) *Arabidopsis* JASMONATE-INDUCED OXYGENASES down-regulate plant immunity by hydroxylation and inactivation of the hormone jasmonic acid. *Proceedings of the National Academy of Sciences of the United States of America*, **114**, 6388–6393.

Carlson M. (2018) org.At.tair.db: Genome wide annotation for Arabidopsis. R package version 3.7.0.

Carvalhais, L.C., Muzzi, F., Tan, C.-H.H., Hsien-Choo, J., and Schenk, P.M. (2013) Plant growth in *Arabidopsis* is

assisted by compost soil-derived microbial communities. *Frontiers in Plant Science*, **4**, 235.

Caspary, R. (1865) Bemerkungen über die Schutzscheide und die Bildung des Stammes und der Wurzel. *Jahrbücher für Wissenschaftliche Botanik*, **4**, 101–124.

Castrillo, G., Teixeira, P.J.P.L., Paredes, S.H., Law, T.F., de Lorenzo, L., Feltcher, M.E., Finkel, O.M., Breakfield, N.W., Mieczkowski, P., Jones, C.D., Paz-Ares, J., and Dangl, J.L. (2017) Root microbiota drive direct integration of phosphate stress and immunity. *Nature*, **543**, 513–518.

Chaparro, J.M., Badri, D. V, Bakker, M.G., Sugiyama, A., Manter, D.K., and Vivanco, J.M. (2013) Root exudation of phytochemicals in Arabidopsis follows specific patterns that are developmentally programmed and correlate with soil microbial functions. *PLoS ONE*, **8**, e55731.

Chen, L.M., Dick, W.A., Streeter, J.G., and Hoitink, H.A.J. (1998) Fe chelates from compost microorganisms improve Fe nutrition of soybean and oat. *Plant and Soil*, **200**, 139–147.

Chen, W.W., Yang, J.L., Qin, C., Jin, C.W., Mo, J.H., Ye, T., and Zheng, S.J. (2010) Nitric oxide acts downstream of auxin to trigger root ferric-chelate reductase activity in response to iron deficiency in Arabidopsis. *Plant Physiology*, **154**, 810–819.

Clough, S.J. and Bent, A.F. (1998) Floral dip: a simplified method for *Agrobacterium*-mediated transformation of *Arabidopsis thaliana*. *The Plant Journal*, **16**, 735–743.

Colangelo, E.P. and Guerinot, M.L. (2004) The essential basic helix-loop-helix protein FIT1 is required for the iron deficiency response. *Plant Cell*, **16**, 3400–3412.

Connorton, J.M., Balk, J., and Rodríguez-Celma, J. (2017) Iron homeostasis in plants - a brief overview. *Metallomics*, **9**, 813–823.

Conrath, U., Beckers, G.J.M., Langenbach, C.J.G., and Jaskiewicz, M.R. (2015) Priming for enhanced defense. *Annual Review of Phytopathology*, **53**, 97–119.

Contreras-Cornejo, H.A., Macías-Rodríguez, L., Cortés-Penagos, C., and López-Bucio, J. (2009) *Trichoderma virens*, a plant beneficial fungus, enhances biomass production and promotes lateral root growth through an auxin-dependent mechanism in Arabidopsis. *Plant Physiology*, **149**, 1579–1592.

Curie, C., Alonso, J., Le Jean, M., Ecker, J., and Briat, J. (2000) Involvement of NRAMP1 from *Arabidopsis thaliana* in iron transport. *Biochemical Journal*, **347**, 749–755.

Curie, C., Panaviene, Z., Loulergue, C., Dellaporta, S.L., Briat, J.-F., and Walker, E.L. (2001) Maize *yellow stripe1* encodes a membrane protein directly involved in Fe(III) uptake. *Nature*, **409**, 346–349.

Czechowski, T., Stitt, M., Altmann, T., Udvardi, M.K., and Scheible, W.-R. (2005) Genome-wide identification and testing of superior reference genes for transcript normalization in Arabidopsis. *Plant Physiology*, **139**, 5–17.

van Damme, M., Zeilmaker, T., Elberse, J., Andel, A., de Sain-van der Velden, M., and van den Ackerveken, G. (2009) Downy mildew resistance in *Arabidopsis* by mutation of *HOMOSERINE KINASE*. *Plant Cell*, **21**, 2179–2189.

Darbani, B., Briat, J.-F., Holm, P.B., Husted, S., Noeparvar, S., and Borg, S. (2013) Dissecting plant iron homeostasis under short and long-term iron fluctuations. *Biotechnology Advances*, **31**, 1292–1307.

Dardanelli, M.S., Manyani, H., González-Barroso, S., Rodríguez-Carvajal, M.A., Gil-Serrano, A.M., Espuny, M.R., López-Baena, F.J., Bellogín, R.A., Megías, M., and Ollero, F.J. (2010) Effect of the presence of the plant growth promoting rhizobacterium (PGPR) *Chryseobacterium balustinum* Aur9 and salt stress in the pattern of flavonoids exuded by soybean roots. *Plant and Soil*, **328**, 483–493.

Deák, M., Horváth, G. V, Davletova, S., Török, K., Sass, L., Vass, I., Barna, B., Király, Z., and Dudits, D. (1999) Plants ectopically expressing the ironbinding protein, ferritin, are tolerant to oxidative damage and pathogens. *Nature Biotechnology*, **17**, 192–196.

Dellagi, A., Rigault, M., Segond, D., Roux, C., Kraepiel, Y., Cellier, F., Briat, J.-F., Gaymard, F., and Expert, D. (2005) Siderophore-mediated upregulation of Arabidopsis ferritin expression in response to *Erwinia chrysanthemi* infection. *The Plant Journal*, **43**, 262–272.

Dellagi, A., Segond, D., Rigault, M., Fagard, M., Simon, C., Saindrenan, P., and Expert, D. (2009) Microbial siderophores exert a subtle role in Arabidopsis during infection by manipulating the immune response and the iron status. *Plant Physiology*, **150**, 1687–1696.

Dennis, P.G., Miller, A.J., and Hirsch, P.R. (2010) Are root exudates more important than other sources of rhizodeposits in structuring rhizosphere bacterial communities? *FEMS Microbiology Ecology*, **72**, 313–327.

Denyer, T., Ma, X., Klesen, S., Scacchi, E., Nieselt, K., and Timmermans, M.C.P. (2019) Spatiotemporal developmental trajectories in the *Arabidopsis* root revealed using high-throughput single-cell RNA sequencing. *Developmental Cell*, **48**, 840–852.

DiDonato, R.J., Roberts, L.A., Sanderson, T., Eisley, R.B., and Walker, E.L. (2004) *Arabidopsis Yellow Stripe-Like2 (YSL2)*: a metal-regulated gene encoding a plasma membrane transporter of nicotianamine-metal complexes. *The Plant Journal*, **39**, 403–414.

Dinneny, J.R., Long, T.A., Wang, J.Y., Jung, J.W., Mace, D., Pointer, S., Barron, C., Brady, S.M., Schiefelbein, J., and Benfey, P.N. (2008) Cell identity mediates the response of *Arabidopsis* roots to abiotic stress. *Science*, **320**, 942–945.

Dixon, R.A. (2001) Natural products and plant disease resistance. *Nature*, **411**, 843–847.

Dolan, L., Janmaat, K., Willemsen, V., Linstead, P., Poethig, S., Roberts, K., and Scheres, B. (1993) Cellular organisation of the *Arabidopsis thaliana* root. *Development*, **119**, 71–84.

Dolan, L., Duckett, C.M., Grierson, C., Linstead, P., Schneider, K., Lawson, E., Dean, C., Poethig, S., and Roberts, K. (1994) Clonal relationships and cell patterning in the root epidermis of *Arabidopsis*. *Development*, **120**, 2465–2474.

Doyle, M.R., Davis, S.J., Bastow, R.M., McWatters, H.G., Kozma-Bognár, L., Nagy, F., Millar, A.J., and Amasino, R.M. (2002) The *ELF4* gene controls circadian rhythms and flowering time in *Arabidopsis thaliana*. *Nature*, **419**, 74–77.

Du, Y. and Scheres, B. (2018) Lateral root formation and the multiple roles of auxin. *Journal of Experimental Botany*, **69**, 155–167.

Dubos, C., Stracke, R., Grotewold, E., Weisshaar, B., Martin, C., and Lepiniec, L. (2010) MYB transcription factors in *Arabidopsis*. *Trends in Plant Science*, **15**, 573–581.

Dubrovsky, J.G., Gambetta, G.A., Hernández-Barrera, A., Shishkova, S., and González, I. (2006) Lateral root initiation in *Arabidopsis*: developmental window, spatial patterning, density and predictability. *Annals of Botany*, **97**, 903–915.

Duijff, B.J., Meijer, J.W., Bakker, P.A.H.M., and Schippers, B. (1993) Siderophore-mediated competition for iron and induced resistance in the suppression of fusarium wilt of carnation by fluorescent *Pseudomonas* spp. *Netherlands Journal of Plant Pathology*, **99**, 277–289.

Duijff, B.J., De Kogel, W.J., Bakker, P., and Schippers, B. (1994) Influence of pseudobactin 358 on the iron nutrition of barley. *Soil Biology and Biochemistry*, **26**, 1681–1688.

Duijff, B.J., Pouhair, D., Olivain, C., Alabouvette, C., and Lemanceau, P. (1998) Implication of systemic induced resistance in the suppression of fusarium wilt of tomato by *Pseudomonas fluorescens* WCS417r and by nonpathogenic *Fusarium oxysporum* Fo47*. *European Journal of Plant Pathology*, **104**, 903–910.

Durrant, W.E. and Dong, X. (2004) Systemic acquired resistance. *Annual Review of Phytopathology*, **42**, 185–209.

Eichhorn, H., Lessing, F., Winterberg, B., Schirawski, J., Kämper, J., Müller, P., and Kahmann, R. (2006) A ferroxidation/permeation iron uptake system is required for virulence in *Ustilago maydis*. *Plant Cell*, **18**, 3332–3345.

Eide, D., Broderius, M., Fett, J., and Guerinot, M.L. (1996) A novel iron-regulated metal transporter from plants identified by functional expression in yeast. *Proceedings of the National Academy of Sciences*, **93**, 5624–5628.

Van der Ent, S., Verhagen, B.W.M., Van Doorn, R., Bakker, D., Verlaan, M.G., Pel, M.J.C., Joosten, R.G., Proveniers, M.C.G., Van Loon, L.C., Ton, J., and Pieterse, C.M.J. (2008) *MYB72* is required in early signaling steps of rhizobacteria-induced systemic resistance in Arabidopsis. *Plant Physiology*, **146**, 1293–1304.

Falcon, S. and Gentleman, R. (2007) Using GOstats to test gene lists for GO term association. *Bioinformatics*, **23**, 257–258.

Farag, M.A., Zhang, H., and Ryu, C.-M. (2013) Dynamic chemical communication between plants and bacteria through airborne signals: induced resistance by bacterial volatiles. *Journal of Chemical Ecology*, **39**, 1007–1018.

Felten, J., Kohler, A., Morin, E., Bhalerao, R.P., Palme, K., Martin, F., Ditengou, F.A., and Legue, V. (2009) The ectomycorrhizal fungus *Laccaria bicolor* stimulates lateral root formation in Poplar and Arabidopsis through auxin transport and signaling. *Plant Physiology*, **151**, 1991–2005.

Fenton, H.J.H. (1894) Oxidation of tartaric acid in presence of iron. *Journal of the Chemical Society, Transactions*, **65**, 899–910.

Ferguson, B.J. and Mathesius, U. (2014) Phytohormone regulation of legume-rhizobia interactions. *Journal of Chemical Ecology*, **40**, 770–790.

Fierer, N. and Jackson, R.B. (2006) The diversity and biogeography of soil bacterial communities. *Proceedings of the National Academy of Sciences of the United States of America*, **103**, 626–631.

Filichkin, S.A., Priest, H.D., Givan, S.A., Shen, R., Bryant, D.W., Fox, S.E., Wong, W.-K., and Mockler, T.C. (2010) Genome-wide mapping of alternative splicing in *Arabidopsis thaliana*. *Genome Research*, **20**, 45–58.

Forieri, I., Sticht, C., Reichelt, M., Gretz, N., Hawkesford, M.J., Malagoli, M., Wirtz, M., and Hell, R. (2017) System analysis of metabolism and the transcriptome in *Arabidopsis thaliana* roots reveals differential co-regulation upon iron, sulfur and potassium deficiency. *Plant, Cell and Environment*, **40**, 95–107.

Fourcroy, P., Sisó-Terraza, P., Sudre, D., Savirón, M., Reyt, G., Gaymard, F., Abadía, A., Abadia, J., Álvarez-Fernández, A., and Briat, J.-F. (2014) Involvement of the ABCG37 transporter in secretion of scopoletin and derivatives by *Arabidopsis* roots in response to iron deficiency. *New Phytologist*, **201**, 155–167.

Fourcroy, P., Tissot, N., Gaymard, F., Briat, J.-F., and Dubos, C. (2016) Facilitated Fe nutrition by phenolic compounds excreted by the *Arabidopsis* ABCG37/PDR9 transporter requires the IRT1/FRO2 high-affinity root Fe^{2+} transport system. *Molecular Plant*, **9**, 485–488.

Franza, T., Mahé, B., and Expert, D. (2005) *Erwinia chrysanthemi* requires a second iron transport route dependent of the siderophore achromobactin for extracellular growth and plant infection. *Molecular Microbiology*, **55**, 261–75.

Galinha, C., Hofhuis, H., Luijten, M., Willemsen, V., Blilou, I., Heidstra, R., and Scheres, B. (2007) PLETHORA proteins as dose-dependent master regulators of Arabidopsis root development. *Nature*, **449**, 1053–7.

Galway, M.E., Masucci, J.D., Lloyd, A.M., Walbot, V., Davis, R.W., and Schiefelbein, J.W. (1994) The TTG gene is required to specify epidermal cell fate and cell patterning in the Arabidopsis root. *Developmental Biology*, **166**, 740–754.

García, M.J., Lucena, C., Romera, F.J., Alcántara, E., and Pérez-Vicente, R. (2010) Ethylene and nitric oxide involvement in the up-regulation of key genes related to iron acquisition and homeostasis in Arabidopsis. *Journal of Experimental Botany*, **61**, 3885–3899.

García, M.J., Corpas, F.J., Lucena, C., Alcántara, E., Pérez-Vicente, R., Zamarreño, Á.M., Bacaicoa, E., García-Mina, J.M., Bauer, P., and Romera, F.J. (2018) A shoot Fe signaling pathway requiring the OPT3 transporter controls GSNO reductase and ethylene in *Arabidopsis thaliana* roots. *Frontiers in Plant Science*, **9**, 1325.

Gaymard, F., Boucherez, J., and Briat, J.-F. (1996) Characterization of a ferritin mRNA from *Arabidopsis thaliana* accumulated in response to iron through an oxidative pathway independent of abscisic acid. *Biochemical Journal*, **318**, 67–73.

Geldner, N. (2013) The endodermis. *Annual Review of Plant Biology*, **64**, 531–558.

Giehl, F.H., Lima, J.E., and Von Wirén, N. (2012) Localized iron supply triggers lateral root elongation in *Arabidopsis* by altering the AUX1-mediated auxin distribution. *Plant Cell*, **24**, 33–49.

Gifford, M.L., Dean, A., Gutierrez, R.A., Coruzzi, G.M., and Birnbaum, K.D. (2008) Cell-specific nitrogen responses mediate developmental plasticity. *Proceedings of the National Academy of Sciences*, **105**, 803–808.

Gilroy, S. and Jones, D.L. (2000) Through form to function: root hair development and nutrient uptake. *Trends in Plant Science*, **5**, 56–60.

Grieneisen, V.A., Xu, J., Marée, A.F.M., Hogeweg, P., and Scheres, B. (2007) Auxin transport is sufficient to generate a maximum and gradient guiding root growth. *Nature*, **449**, 1008–1013.

Grillet, L., Lan, P., Li, W., Mokkapati, G., and Schmidt, W. (2018) IRON MAN is a ubiquitous family of peptides that control iron transport in plants. *Nature Plants*, **4**, 953–963.

Grusak, M.A. and Pezeshgi, S. (1996) Shoot-to-root signal transmission regulates root Fe(III) reductase activity in the *dgl* mutant of pea. *Plant Physiology*, **110**, 329–334.

Guerinot, M.L. and Ying, Y. (1994) Iron: nutritious, noxious, and not readily available. *Plant Physiology*, **104**, 815–820.

Gutiérrez-Barranquero, J.A., Reen, F.J., McCarthy, R.R., Dobson, A.D.W., and O'Gara, F. (2015) Deciphering the role of coumarin as a novel quorum sensing inhibitor suppressing virulence phenotypes in bacterial pathogens. *Applied Microbiology and Biotechnology*, **99**, 2923–2923.

Guzman, P. and Ecker, J.R. (1990) Exploiting the triple response of *Arabidopsis* to identify ethylene-related mutants. *Plant Cell*, **2**, 513–523.

Haas, H., Eisendle, M., and Turgeon, B.G. (2008) Siderophores in fungal physiology and virulence. *Annual Review of Phytopathology*, **46**, 149–187.

Haber, F. and Weiss, J. (1934) The catalytic decomposition of hydrogen peroxide by iron salts. *Proceedings of the Royal Society of London A: Mathematical, Physical and Engineering Sciences*, **147**.

Haichar, F. el Z., Marol, C., Berge, O., Rangel-Castro, J.I., Prosser, J.I., Balesdent, J., Heulin, T., and Achouak, W. (2008) Plant host habitat and root exudates shape soil bacterial community structure. *The ISME Journal*, **2**, 1221–1230.

Heulin, T., Guckert, A., and Balandreau, J. (1987) Stimulation of root exudation of rice seedlings by *Azospirillum* strains: carbon budget under gnotobiotic conditions. *Biology and Fertility of Soils*, **4**, 9–14.

Hiltner, L. (1904) Uber neure Erfahrungen und probleme auf dem gebeit der bodenbackteriologie und unter besonderer berucksichtigung der grundungung und brache. *Arb. Deut. Landwirsch Ges.*, **98**, 59–78.

Hindt, M.N. and Guerinot, M.L. (2012) Getting a sense for signals: regulation of the plant iron deficiency response. *Biochimica et Biophysica Acta*, **1823**, 1521–1530.

Hiruma, K., Gerlach, N., Sacristán, S., Nakano, R.T., Hacquard, S., Kracher, B., Neumann, U., Ramírez, D., Bucher, M., O'Connell, R.J., and Schulze-Lefert, P. (2016) Root endophyte *Colletotrichum tofieldiae* confers plant fitness benefits that are phosphate status dependent. *Cell*, **165**, 464–474.

Hiscox, J.D. and Israelstam, G.F. (1979) A method for the extraction of chlorophyll from leaf tissue without maceration. *Canadian Journal of Botany*, **57**, 1332–1334.

Hoagland, D.R. and Arnon, D.I. (1938) The water-culture method for growing plants without soil. *California Agricultural Experiment Station Bulletin*, **347**, 36–39.

Hofhuis, H., Laskowski, M., Du, Y., Prasad, K., Grigg, S., Pinon, V., and Scheres, B. (2013) Phyllotaxis and rhizotaxis in *Arabidopsis* are modified by three PLETHORA transcription factors. *Current Biology*, **23**, 956–962.

Howe, G.A. and Jander, G. (2008) Plant immunity to insect herbivores. *Annual Review of Plant Biology*, **59**, 41–66.

Hsiao, P.-Y., Cheng, C.-P., Koh, K.W., and Chan, M.-T. (2017) The *Arabidopsis* defensin gene, *AtPDF1.1*, mediates defence against *Pectobacterium carotovorum* subsp. *carotovorum* via an iron-withholding defence system. *Scientific Reports*, **7**, 9175.

Huang, X.-F., Zhou, D., Lapsansky, E.R., Reardon, K.F., Guo, J., Andales, M.J., Vivanco, J.M., and Manter, D.K. (2017) *Mitsuaria* sp. and *Burkholderia* sp. from *Arabidopsis* rhizosphere enhance drought tolerance in *Arabidopsis thaliana* and maize (*Zea mays* L.). *Plant and Soil*, **419**, 523–539.

Inoue, H., Kobayashi, T., Nozoye, T., Takahashi, M., Kakei, Y., Suzuki, K., Nakazono, M., Nakanishi, H., Mori, S., and Nishizawa, N.K. (2009) Rice OsYSL15 is an iron-regulated iron(III)-deoxymugineic acid transporter expressed in the roots and is essential for iron uptake in early growth of the seedlings. *Journal of Biological Chemistry*, **284**, 3470–3479.

Dello Ioio, R., Nakamura, K., Moubayidin, L., Perilli, S., Taniguchi, M., Morita, M.T., Aoyama, T., Costantino, P., and Sabatini, S. (2008) A genetic framework for the control of cell division and differentiation in the root meristem. *Science*, **322**, 1380–1384.

Ivanov, R., Brumbarova, T., and Bauer, P. (2012) Fitting into the harsh reality: regulation of iron-deficiency responses in dicotyledonous plants. *Molecular Plant*, **5**, 27–42.

Jakoby, M., Wang, H.Y., Reidt, W., Weisshaar, B., and Bauer, P. (2004) *FRU (BHLH029)* is required for induction of iron mobilization genes in *Arabidopsis thaliana*. *FEBS Letters*, **577**, 528–534.

Jin, C.W., He, Y.F., Tang, C.X., Wu, P., and Zheng, S.J. (2006) Mechanisms of microbially enhanced Fe acquisition in red clover (*Trifolium pratense* L.). *Plant, Cell and Environment*, **29**, 888–897.

Jin, C.W., Chen, W.W., Meng, Z., and Zheng, S.J. (2008) Iron deficiency-induced increase of root branching contributes to the enhanced root ferric chelate reductase activity. *Journal of Integrative Plant Biology*, **50**, 1557–1562.

Jin, C.W., Li, G.X., Yu, X.H., and Zheng, S.J. (2010) Plant Fe status affects the composition of siderophore-secreting microbes in the rhizosphere. *Annals of Botany*, **105**, 835–841.

Jones, D.L., Hodge, A., and Kuzyakov, Y. (2004) Plant and mycorrhizal regulation of rhizodeposition. *New Phytologist*, **163**, 459–480.

Jones, J.D.G. and Dangl, J.L. (2006) The plant immune system. *Nature*, **444**, 323–329.

Juntawong, P. and Bailey-Serres, J. (2012) Dynamic light regulation of translation status in *Arabidopsis thaliana*. *Frontiers in Plant Science*, **3**, 66.

Kai, K., Shimizu, B., Mizutani, M., Watanabe, K., and Sakata, K. (2006) Accumulation of coumarins in *Arabidopsis thaliana*. *Phytochemistry*, **67**, 379–386.

Van Kan, J.A.L., Stassen, J.H.M., Mosbach, A., Van Der Lee, T.A.J., Faino, L., Farmer, A.D., Papasotiriou, D.G., Zhou, S., Seidl, M.F., Cottam, E., Edel, D., Hahn, M., Schwartz, D.C., Dietrich, R.A., Widdison, S., and Scalliet, G. (2017) A gapless genome sequence of the fungus *Botrytis cinerea*. *Molecular Plant Pathology*, **18**, 75–89.

Khalid, A., Arshad, M., and Zahir, Z.A. (2004) Screening plant growth-promoting rhizobacteria for improving growth and yield of wheat. *Journal of Applied Microbiology*, **96**, 473–480.

Khan, A., Hossain, M.T., Park, H.C., Yun, D.-J., Shim, S.H., and Chung, Y.R. (2016) Development of root system architecture of *Arabidopsis thaliana* in response to colonization by *Martelella endophytica* YC6887 depends on auxin signaling. *Plant and Soil*, **405**, 81–96.

Khan, M.A., Castro-Guerrero, N.A., McInturf, S.A., Nguyen, N.T., Dame, A.N., Wang, J., Bindbeutel, R.K., Joshi, T., Jurisson, S.S., Nusinow, D.A., and Mendoza-Cozatl, D.G. (2018) Changes in iron availability in Arabidopsis are rapidly sensed in the leaf vasculature and impaired sensing leads to opposite transcriptional programs in leaves and roots. *Plant, Cell & Environment*, **41**, 2263–2276.

Kieu, N.P., Aznar, A., Segond, D., Rigault, M., Simond-Côte, E., Kunz, C., Soulie, M.-C., Expert, D., and Dellagi, A. (2012) Iron deficiency affects plant defence responses and confers resistance to *Dickeya dadantii* and *Botrytis cinerea*. *Molecular Plant Pathology*, **13**, 816–827.

King, E.O., Ward, M.K., and Raney, D.E. (1954) Two simple media for the demonstration of pyocyanin and fluorescin. *Journal of Laboratory and Clinical Medicine*, **44**, 301–307.

Kloepper, J.W., Leong, J., Teintze, M., and Schroth, M.N. (1980) *Pseudomonas* siderophores: A mechanism explaining disease-suppressive soils. *Current Microbiology*, **4**, 317–320.

Kobayashi, T. and Nishizawa, N.K. (2012) Iron uptake, translocation, and regulation in higher plants. *Annual*

Review of Plant Biology, **63**, 131–152.

Kobayashi, T., Nozoye, T., and Nishizawa, N.K. (2019) Iron transport and its regulation in plants. *Free Radical Biology and Medicine*, **133**, 11–20.

Koen, E., Besson-Bard, A., Duc, C., Astier, J., Gravot, A., Richaud, P., Lamotte, O., Boucherez, J., Gaymard, F., and Wendehenne, D. (2013) *Arabidopsis thaliana* nicotianamine synthase 4 is required for proper response to iron deficiency and to cadmium exposure. *Plant science*, **209**, 1–11.

Koen, E., Trapet, P., Brulé, D., Kulik, A., Klinguer, A., Atauri-Miranda, L., Meunier-Prest, R., Boni, G., Glauser, G., Mauch-Mani, B., Wendehenne, D., and Besson-Bard, A. (2014) β-aminobutyric acid (BABA)-induced resistance in *Arabidopsis thaliana*: link with iron homeostasis. *Molecular Plant-Microbe Interactions*, **27**, 1226–1240.

Koevoets, I.T., Venema, J.H., Elzenga, J.T.M., and Testerink, C. (2016) Roots withstanding their environment: exploiting root system architecture responses to abiotic stress to improve crop tolerance. *Frontiers in Plant Science*, **07**, 1335.

Kosma, D.K., Murmu, J., Razeq, F.M., Santos, P., Bourgault, R., Molina, I., and Rowland, O. (2014) AtMYB41 activates ectopic suberin synthesis and assembly in multiple plant species and cell types. *The Plant Journal*, **80**, 216–229.

Krikun, J. and Frank, Z.R. (1975) Effect of sequestrene on the reaction to *Verticillium dahliae* of peanuts growing in calcareous loess soil. *Phytoparasitica*, **3**, 77–78.

Kumpf, R.P. and Nowack, M.K. (2015) The root cap: a short story of life and death. *Journal of Experimental Botany*, **66**, 5651–5662.

Kunkel, B.N., Bent, A.F., Dahlbeck, D., Innes, R.W., and Staskawicz, B.J. (1993) *RPS2*, an Arabidopsis disease resistance locus specifying recognition of *Pseudomonas syringae* strains expressing the avirulence gene *avrRpt2*. *Plant Cell*, **5**, 865–75.

Laloum, T., Martín, G., and Duque, P. (2018) Alternative splicing control of abiotic stress responses. *Trends in Plant Science*, **23**, 140–150.

Lamesch, P., Berardini, T.Z., Li, D., Swarbreck, D., Wilks, C., Sasidharan, R., Muller, R., Dreher, K., Alexander, D.L., Garcia-Hernandez, M., Karthikeyan, A.S., Lee, C.H., Nelson, W.D., Ploetz, L., Singh, S., Wensel, A., and Huala, E. (2012) The Arabidopsis Information Resource (TAIR): improved gene annotation and new tools. *Nucleic Acids Research*, **40**, D1202–D1210.

Lamont, I.L., Beare, P.A., Ochsner, U., Vasil, A.I., and Vasil, M.L. (2002) Siderophore-mediated signaling regulates virulence factor production in *Pseudomonas aeruginosa*. *Proceedings of the National Academy of Sciences of the United States of America*, **99**, 7072–7077.

Lan, P., Li, W., Lin, W.-D., Santi, S., and Schmidt, W. (2013) Mapping gene activity of *Arabidopsis* root hairs. *Genome Biology*, **14**, R67.

Lanquar, V., Lelièvre, F., Bolte, S., Hamès, C., Alcon, C., Neumann, D., Vansuyt, G., Curie, C., Schröder, A., Krämer, U., Barbier-Brygoo, H., and Thomine, S. (2005) Mobilization of vacuolar iron by AtNRAMP3 and AtNRAMP4 is essential for seed germination on low iron. *The EMBO Journal*, **24**, 4041–4051.

Lapin, D., Meyer, R.C., Takahashi, H., Bechtold, U., and Van den Ackerveken, G. (2012) Broad-spectrum resistance of Arabidopsis C24 to downy mildew is mediated by different combinations of isolate-specific loci. *New Phytologist*, **196**, 1171–1181.

Laplaze, L., Benkova, E., Casimiro, I., Maes, L., Vanneste, S., Swarup, R., Weijers, D., Calvo, V., Parizot, B., Herrera-Rodriguez, M.B., Offringa, R., Graham, N., Doumas, P., Friml, J., Bogusz, D., Beeckman, T., and Bennett, M. (2007) Cytokinins act directly on lateral root founder cells to inhibit root initiation. *Plant Cell*, **19**, 3889–3900.

Lashbrooke, J., Cohen, H., Levy-Samocha, D., Tzfadia, O., Panizel, I., Zeisler, V., Massalha, H., Stern, A., Trainotti, L., Schreiber, L., Costa, F., and Aharoni, A. (2016) MYB107 and MYB9 homologs regulate suberin deposition in angiosperms. *Plant Cell*, **28**, 2097–2116.

Laskowski, M., Biller, S., Stanley, K., Kajstura, T., and Prusty, R. (2006) Expression profiling of auxin-treated *Arabidopsis* roots: toward a molecular analysis of lateral root emergence. *Plant and Cell Physiology*, **47**, 788–792.

Laulhere, J.P. and Briat, J.F. (1993) Iron release and uptake by plant ferritin: effects of pH, reduction and chelation. *Biochemical Journal*, **290**, 693–699.

Lebeis, S.L., Paredes, S.H., Lundberg, D.S., Breakfield, N., Gehring, J., McDonald, M., Malfatti, S., Glavina del Rio, T., Jones, C.D., Tringe, S.G., and Dangl, J.L. (2015) Salicylic acid modulates colonization of the root microbiome by specific bacterial taxa. *Science*, **349**, 860–864.

Lee, J.-H., Kim, Y.-G., Cho, H.S., Ryu, S.Y., Cho, M.H., and Lee, J. (2014) Coumarins reduce biofilm formation and the virulence of *Escherichia coli* O157:H7. *Phytomedicine*, **21**, 1037–1042.

Lee, J.-Y., Colinas, J., Wang, J.Y., Mace, D., Ohler, U., and Benfey, P.N. (2006) Transcriptional and posttranscriptional

regulation of transcription factor expression in *Arabidopsis* roots. *Proceedings of the National Academy of Sciences of the United States of America*, **103**, 6055–6060.

Lee, M.M. and Schiefelbein, J. (1999) WEREWOLF, a MYB-related protein in *Arabidopsis*, is a position-dependent regulator of epidermal cell patterning. *Cell*, **99**, 473–483.

Leeman, M., Van Pelt, J.A., Den Ouden, F.M., Heinsbroek, M., Bakker, P.A.H.M., and Schippers, B. (1995) Induction of systemic resistance against fusarium wilt of radish by lipopolysaccharides of *Pseudomonas fluorescens*. *The American Phytopathological Society*, **85**, 1021–1027.

Lemanceau, P., Alabouvette, C., and Couteaudier, Y. (1988) Studies on the disease suppressiveness of soils. XIV. Modification of the receptivity level of a suppressive and a conducive soil to fusarium wilt in response to the supply of iron or of glucose. *Agronomie*, **8**, 155–162.

Lemanceau, P., Expert, D., Gaymard, F., Bakker, P., and Briat, J.-F. (2009) Role of iron in plant–microbe interactions. *Advances in Botanical Research*, **51**, 491–549.

Li, X., Mo, X., Shou, H., and Wu, P. (2006) Cytokinin-mediated cell cycling arrest of pericycle founder cells in lateral root initiation of *Arabidopsis*. *Plant and Cell Physiology*, **47**, 1112–1123.

Li, X., Zeng, R., and Liao, H. (2016) Improving crop nutrient efficiency through root architecture modifications. *Journal of Integrative Plant Biology*, **58**, 193–202.

Liberman, L.M., Sparks, E.E., Moreno-Risueno, M.A., Petricka, J.J., and Benfey, P.N. (2015) MYB36 regulates the transition from proliferation to differentiation in the *Arabidopsis* root. *Proceedings of the National Academy of Sciences*, **112**, 12099–12104.

Lim, J.-H. and Kim, S.-D. (2009) Synergistic plant growth promotion by the indigenous auxins-producing PGPR *Bacillus subtilis* AH18 and *Bacillus licheniforims* K11. *Journal of the Korean Society for Applied Biological Chemistry*, **52**, 531–538.

Liu, F., Bian, Z., Jia, Z., Zhao, Q., and Song, S. (2012) The GCR1 and GPA1 participate in promotion of *Arabidopsis* primary root elongation induced by N -acyl-homoserine lactones, the bacterial quorum-sensing signals. *Molecular Plant-Microbe Interactions*, **25**, 677–683.

Liu, G., Greenshields, D.L., Sammynaiken, R., Hirji, R.N., Selvaraj, G., and Wei, Y. (2007) Targeted alterations in iron homeostasis underlie plant defense responses. *Journal of Cell Science*, **120**, 596–605.

Liu, H., Carvalhais, L.C., Crawford, M., Singh, E., Dennis, P.G., Pieterse, C.M.J., and Schenk, P.M. (2017) Inner plant values: diversity, colonization and benefits from endophytic bacteria. *Frontiers in Microbiology*, **8**, 2552.

Liu, J., Osbourn, A., and Ma, P. (2015) MYB transcription factors as regulators of phenylpropanoid metabolism in plants. *Molecular Plant*, **8**, 689–708.

Liu, Y., Beyer, A., and Aebersold, R. (2016) On the dependency of cellular protein levels on mRNA abundance. *Cell*, **165**, 535–550. Cell Press.

Ljung, K., Hull, A.K., Celenza, J., Yamada, M., Estelle, M., Normanly, J., and Sandberg, G. (2005) Sites and regulation of auxin biosynthesis in Arabidopsis roots. *Plant Cell*, **17**, 1090–1104.

Long, T.A., Tsukagoshi, H., Busch, W., Lahner, B., Salt, D.E., and Benfey, P.N. (2010) The bHLH transcription factor POPEYE regulates response to iron deficiency in *Arabidopsis* roots. *Plant Cell*, **22**, 2219–2236.

van Loon, L.C., Bakker, P.A.H.M., van der Heijdt, W.H.W., Wendehenne, D., and Pugin, A. (2008) Early responses of tobacco suspension cells to rhizobacterial elicitors of induced systemic resistance. *Molecular Plant-Microbe Interactions*, **21**, 1609–1621.

Loper, J.E. and Buyer, J.S. (1991) Siderophores in microbial interactions on plant surfaces. *Molecular plant-microbe interactions*, **4**, 5–13.

López-Berges, M.S., Capilla, J., Turrà, D., Schafferer, L., Matthijs, S., Jöchl, C., Cornelis, P., Guarro, J., Haas, H., and Di Pietro, A. (2012) HapX-mediated iron homeostasis is essential for rhizosphere competence and virulence of the soilborne pathogen *Fusarium oxysporum*. *Plant Cell*, **24**, 3805–3822.

López-Bucio, J., Campos-Cuevas, J.C., Hernández-Calderón, E., Velásquez-Becerra, C., Farías-Rodríguez, R., Macías-Rodríguez, L.I., and Valencia-Cantero, E. (2007) *Bacillus megaterium* rhizobacteria promote growth and alter root-system architecture through an auxin- and ethylene-independent signaling mechanism in *Arabidopsis thaliana*. *Molecular Plant-Microbe Interactions*, **20**, 207–217.

Lucena, C., Romera, F.J., García, M.J., Alcántara, E., and Pérez-Vicente, R. (2015) Ethylene participates in the regulation of Fe deficiency responses in Strategy I plants and in rice. *Frontiers in Plant Science*, **6**, 1056.

Lugtenberg, B. and Kamilova, F. (2009) Plant-growth-promoting rhizobacteria. *Annual Review of Microbiology*, **63**, 541–556.

Lundberg, D.S., Lebeis, S.L., Paredes, S.H., Yourstone, S., Gehring, J., Malfatti, S., Tremblay, J., Engelbrektson, A., Kunin, V., del Rio, T.G., Edgar, R.C., Eickhorst, T., Ley, R.E., Hugenholtz, P., Tringe, S.G., and Dangl, J.L. (2012) Defining the core *Arabidopsis thaliana* root microbiome. *Nature*, **488**, 86–90.

Luo, Y., Han, Z., Chin, S.M., and Linn, S. (1994) Three chemically distinct types of oxidants formed by iron-

mediated Fenton reactions in the presence of DNA. *Proceedings of the National Academy of Sciences*, **91**, 12438–12442.

Macur, R.E., Mathre, D.E., and Olsen, R.A. (1991) Interactions between iron nutrition and Verticillium wilt resistance in tomato. *Plant and Soil*, **134**, 281–286.

Mähönen, A.P., Bonke, M., Kauppinen, L., Riikonen, M., Benfey, P.N., and Helariutta, Y. (2000) A novel two-component hybrid molecule regulates vascular morphogenesis of the *Arabidopsis* root. *Genes and Development*, **14**, 2938–2943.

Malamy, J.E. and Benfey, P.N. (1997) Organization and cell differentiation in lateral roots of *Arabidopsis thaliana*. *Development*, **124**, 33–44.

Marquez, Y., Brown, J.W.S., Simpson, C., Barta, A., and Kalyna, M. (2012) Transcriptome survey reveals increased complexity of the alternative splicing landscape in *Arabidopsis*. *Genome Research*, **22**, 1184–1195.

Martinez-Medina, A., Flors, V., Heil, M., Mauch-Mani, B., Pieterse, C.M.J., Pozo, M.J., Ton, J., Van Dam, N.M., and Conrath, U. (2016) Recognizing plant defense priming. *Trends in Plant Science*, **21**, 818–822.

Martínez-Medina, A., Van Wees, S.C.M., and Pieterse, C.M.J. (2017) Airborne signals from *Trichoderma* fungi stimulate iron uptake responses in roots resulting in priming of jasmonic acid-dependent defences in shoots of *Arabidopsis thaliana* and *Solanum lycopersicum*. *Plant, Cell and Environment*, **40**, 2691–2705.

Matilla, M.A., Ramos, J.L., Bakker, P.A.H.M., Doornbos, R., Badri, D. V., Vivanco, J.M., and Ramos-González, M.I. (2009) *Pseudomonas putida* KT2440 causes induced systemic resistance and changes in Arabidopsis root exudation. *Environmental Microbiology Reports*, **2**, 381–388.

Maurer, F., Müller, S., and Bauer, P. (2011) Suppression of Fe deficiency gene expression by jasmonate. *Plant Physiology and Biochemistry*, **49**, 530–536.

Mei, B., Buddet, A.D., and Leong, S.A. (1993) *sid1*, a gene initiating siderophore biosynthesis in *Ustilago maydis*: molecular characterization, regulation by iron, and role in phytopathogenicity. *Proceedings of the National Academy of Sciences of the United States of America*, **90**, 903–907.

Meiser, J., Lingam, S., and Bauer, P. (2011) Posttranslational regulation of the iron deficiency basic helix-loop-helix transcription factor FIT is affected by iron and nitric oxide. *Plant Physiology*, **157**, 2154–2166.

Mendoza-Cózatl, D.G., Xie, Q., Akmakjian, G.Z., Jobe, T.O., Patel, A., Stacey, M.G., Song, L., Demoin, D.W., Jurisson, S.S., Stacey, G., and Schroeder, J.I. (2014) OPT3 is a component of the iron-signaling network between leaves and roots and misregulation of *OPT3* leads to an over-accumulation of cadmium in seeds. *Molecular Plant*, **7**, 1455–1469.

Meteignier, L.-V., El Oirdi, M., Cohen, M., Barff, T., Matteau, D., Lucier, J.-F., Rodrigue, S., Jacques, P.-E., Yoshioka, K., and Moffett, P. (2017) Translatome analysis of an NB-LRR immune response identifies important contributors to plant immunity in Arabidopsis. *Journal of Experimental Botany*, **68**, 2333–2344.

Meziane, H., Van der Sluis, I., Van Loon, L.C., Höfte, M., and Bakker, P.A.H.M. (2005) Determinants of *Pseudomonas putida* WCS358 involved in inducing systemic resistance in plants. *Molecular Plant Pathology*, **6**, 177–185.

Micallef, S.A., Shiaris, M.P., and Colon-Carmona, A. (2009a) Influence of *Arabidopsis thaliana* accessions on rhizobacterial communities and natural variation in root exudates. *Journal of Experimental Botany*, **60**, 1729–1742.

Micallef, S.A., Channer, S., Shiaris, M.P., and Colón-Carmona, A. (2009b) Plant age and genotype impact the progression of bacterial community succession in the Arabidopsis rhizosphere. *Plant Signaling and Behavior*, **4**, 777–780.

Miethke, M. and Marahiel, M.A. (2007) Siderophore-based iron acquisition and pathogen control. *Microbiology and Molecular Biology Reviews*, **71**, 413–451.

Millet, Y.A., Danna, C.H., Clay, N.K., Songnuan, W., Simon, M.D., Werck-Reichhart, D., and Ausubel, F.M. (2010) Innate immune responses activated in *Arabidopsis* roots by microbe-associated molecular patterns. *Plant Cell*, **22**, 973–990.

Moeller, J.R., Moscou, M.J., Bancroft, T., Skadsen, R.W., Wise, R.P., and Whitham, S.A. (2012) Differential accumulation of host mRNAs on polyribosomes during obligate pathogen-plant interactions. *Molecular BioSystems*, **8**, 2153.

Möller, B.K., Xuan, W., and Beeckman, T. (2017) Dynamic control of lateral root positioning. *Current Opinion in Plant Biology*, **35**, 1–7.

Morant, A. V, Jorgensen, K., Jorgensen, C., Paquette, S.M., Sanchez-Perez, R., Moller, B.L., and Bak, S. (2008) beta-Glucosidases as detonators of plant chemical defense. *Phytochemistry*, **69**, 1795–1813.

Moreno-Risueno, M.A., Van Norman, J.M., Moreno, A., Zhang, J., Ahnert, S.E., and Benfey, P.N. (2010) Oscillating gene expression determines competence for periodic *Arabidopsis* root branching. *Science*, **329**, 1306–1311.

van de Mortel, J.E., de Vos, R.C.H., Dekkers, E., Pineda, A., Guillod, L., Bouwmeester, K., van Loon, J.J.A.,

Dicke, M., and Raaijmakers, J.M. (2012) Metabolic and transcriptomic changes induced in Arabidopsis by the rhizobacterium *Pseudomonas fluorescens* SS101. *Plant Physiology*, **160**, 2173–2188.

Motte, H., Vanneste, S., and Beeckman, T. (2019) Molecular and environmental regulation of root development. *Annual Review of Plant Biology*, **70**, 465–488.

Moubayidin, L., Di Mambro, R., Sozzani, R., Pacifici, E., Salvi, E., Terpstra, I., Bao, D., van Dijken, A., Dello Ioio, R., Perilli, S., Ljung, K., Benfey, P.N., Heidstra, R., Costantino, P., and Sabatini, S. (2013) Spatial coordination between stem cell activity and cell differentiation in the root meristem. *Developmental Cell*, **26**, 405–415.

Müller, M. and Schmidt, W. (2004) Environmentally induced plasticity of root hair development in Arabidopsis. *Plant Physiology*, **134**, 409–419.

Murashige, T. and Skoog, F. (1962) A revised medium for rapid growth and bio assays with tobacco tissue cultures. *Physiologica Plantarum*, **15**, 473–497.

Mustroph, A., Zanetti, M.E., Jang, C.J.H., Holtan, H.E., Repetti, P.P., Galbraith, D.W., Girke, T., and Bailey-Serres, J. (2009) Profiling translatomes of discrete cell populations resolves altered cellular priorities during hypoxia in *Arabidopsis*. *Proceedings of the National Academy of Sciences of the United States of America*, **106**, 18843–18848.

Nakajima, K., Sena, G., Nawy, T., and Benfey, P.N. (2001) Intercellular movement of the putative transcription factor SHR in root patterning. *Nature*, **413**, 307–311.

Naseer, S., Lee, Y., Lapierre, C., Franke, R., Nawrath, C., and Geldner, N. (2012) Casparian strip diffusion barrier in *Arabidopsis* is made of a lignin polymer without suberin. *Proceedings of the National Academy of Sciences of the United States of America*, **109**, 10101–10106.

Van Norman, J.M., Xuan, W., Beeckman, T., and Benfey, P.N. (2013) To branch or not to branch: the role of pre-patterning in lateral root formation. *Development*, **140**, 4301–4310.

Nouet, C., Motte, P., and Hanikenne, M. (2011) Chloroplastic and mitochondrial metal homeostasis. *Trends in Plant Science*, **16**, 395–404.

Nozoye, T., Nagasaka, S., Kobayashi, T., Takahashi, M., Sato, Y., Sato, Y., Uozumi, N., Nakanishi, H., and Nishizawa, N.K. (2011) Phytosiderophore efflux transporters are crucial for iron acquisition in Graminaceous plants. *Journal of Biological Chemistry*, **286**, 5446–5454.

Ogawa, M., Kay, P., Wilson, S., and Swain, S.M. (2009) ARABIDOPSIS DEHISCENCE ZONE POLYGALACTURONASE1 (ADPG1), ADPG2, and QUARTET2 are polygalacturonases required for cell separation during reproductive development in *Arabidopsis*. *Plant Cell*, **21**, 216–233.

Ohata, T., Kanazawa, K., Mihashi, S., Kishi-Nishizawa, N., Fushiya, S., Nozoe, S., Chino, M., and Mori, S. (1993) Biosynthetic pathway of phytosiderophores in iron-deficient graminaceous plants. *Soil Science and Plant Nutrition*, **39**, 745–749.

Oide, S., Moeder, W., Krasnoff, S., Gibson, D., Haas, H., Yoshioka, K., and Turgeon, B.G. (2006) *NPS6*, encoding a nonribosomal peptide synthetase involved in siderophore-mediated iron metabolism, is a conserved virulence determinant of plant pathogenic ascomycetes. *Plant Cell*, **18**, 2836–2853.

El Oirdi, M., Trapani, A., and Bouarab, K. (2010) The nature of tobacco resistance against *Botrytis cinerea* depends on the infection structures of the pathogen. *Environmental Microbiology*, **12**, 239–253.

Oñate-Sánchez, L. and Vicente-Carbajosa, J. (2008) DNA-free RNA isolation protocols for *Arabidopsis thaliana*, including seeds and siliques. *BMC Research Notes*, **1**, 93.

Orman-Ligeza, B., Parizot, B., de Rycke, R., Fernandez, A., Himschoot, E., Van Breusegem, F., Bennett, M.J., Périlleux, C., Beeckman, T., and Draye, X. (2016) RBOH-mediated ROS production facilitates lateral root emergence in *Arabidopsis*. *Development*, **143**, 3328–3339.

Ortiz-Castro, R., Díaz-Pérez, C., Martínez-Trujillo, M., del Río, R.E., Campos-García, J., and López-Bucio, J. (2011) Transkingdom signaling based on bacterial cyclodipeptides with auxin activity in plants. *Proceedings of the National Academy of Sciences of the United States of America*, **108**, 7253–7258.

Ortiz-Castro, R., Pelagio-Flores, R., Méndez-Bravo, A., Ruiz-Herrera, L.F., Campos-García, J., and López-Bucio, J. (2014) Pyocyanin, a virulence factor produced by *Pseudomonas aeruginosa*, alters root development through reactive oxygen species and ethylene signaling in Arabidopsis. *Molecular Plant-Microbe Interactions*, **27**, 364–378.

Ortíz-Castro, R., Martínez-Trujillo, M., and López-Bucio, J. (2008) N-acyl-L-homoserine lactones: a class of bacterial quorum-sensing signals alter post-embryonic root development in *Arabidopsis thaliana*. *Plant, Cell and environment*, **31**, 1497–1509.

Ötvös, K. and Benková, E. (2017) Spatiotemporal mechanisms of root branching. *Current Opinion in Genetics and Development*, **45**, 82–89.

Palmer, C.M. and Guerinot, M.L. (2009) Facing the challenges of Cu, Fe and Zn homeostasis in plants. *Nature Chemical Biology*, **5**, 333–340.

Palmer, C.M., Hindt, M.N., Schmidt, H., Clemens, S., and Guerinot, M.L. (2013) *MYB10* and *MYB72* are required for growth under iron-limiting conditions. *PLoS Genetics*, **9**, e1003953.

Pan, I.-C., Tsai, H.-H., Cheng, Y.-T., Wen, T.-N., Buckhout, T.J., and Schmidt, W. (2015) Post-transcriptional coordination of the *Arabidopsis* iron deficiency response is partially dependent on the E3 ligases RING DOMAIN LIGASE1 (RGLG1) and RING DOMAIN LIGASE2 (RGLG2). *Molecular and Cellular Proteomics*, **14**, 2733–2752.

Panikashvili, D., Shi, J.X., Bocobza, S., Franke, R.B., Schreiber, L., and Aharoni, A. (2010) The *Arabidopsis* DSO/ABCG11 transporter affects cutin metabolism in reproductive organs and suberin in roots. *Molecular Plant*, **3**, 563–575.

Paungfoo-Lonhienne, C., Rentsch, D., Robatzek, S., Webb, R.I., Sagulenko, E., Näsholm, T., Schmidt, S., and Lonhienne, T.G.A. (2010) Turning the table: plants consume microbes as a source of nutrients. *PLoS ONE*, **5**, e11915.

Paungfoo-Lonhienne, C., Schmidt, S., Webb, R.I., and Lonhienne, T.G.A. (2013) Rhizophagy-a new dimension of plant-microbe interactions. Pp. 1199–1207 in: *Molecular Microbial Ecology of the Rhizosphere*. John Wiley & Sons, Inc., Hoboken, NJ, USA.

Van Peer, R., Niemann, G., and Schippers, B. (1991) Induced resistance and phytoalexin accumulation in biological control of fusarium wilt of carnation by *Pseudomonas* sp strain WCS417r. *Phytophathology*, **81**, 728–734.

Péret, B., De Rybel, B., Casimiro, I., Benková, E., Swarup, R., Laplaze, L., Beeckman, T., and Bennett, M.J. (2009) *Arabidopsis* lateral root development: an emerging story. *Trends in Plant Science*, **14**, 399–408.

Pérez-Montaño, F., Alías-Villegas, C., Bellogín, R.A., del Cerro, P., Espuny, M.R., Jiménez-Guerrero, I., López-Baena, F.J., Ollero, F.J., and Cubo, T. (2014) Plant growth promotion in cereal and leguminous agricultural important plants: from microorganism capacities to crop production. *Microbiological Research*, **169**, 325–336.

Persello-Cartieaux, F., David, P., Sarrobert, C., Thibaud, M.C., Achouak, W., Robaglia, C., and Nussaume, L. (2001) Utilization of mutants to analyze the interaction between *Arabidopsis thaliana* and its naturally root-associated *Pseudomonas*. *Planta*, **212**, 190–198.

Petit, J., Briat, J., and Lobréaux, S. (2001) Structure and differential expression of the four members of the *Arabidopsis thaliana* ferritin gene family. *Biochemical Journal*, **359**, 575–582.

Petricka, J.J., Winter, C.M., and Benfey, P.N. (2012) Control of *Arabidopsis* root development. *Annual Review of Plant Biology*, **63**, 563–590.

Philippot, L., Raaijmakers, J.M., Lemanceau, P., and van der Putten, W.H. (2013) Going back to the roots: the microbial ecology of the rhizosphere. *Nature Reviews Microbiology*, **11**, 789–799.

Phillips, D.A., Fox, T.C., King, M.D., Bhuvaneswari, T. V, and Teuber, L.R. (2004) Microbial products trigger amino acid exudation from plant roots. *Plant Physiology*, **136**, 2887–2894.

Pieterse, C., Van Wees, S.C.M., Hoffland, E., Van Pelt, J.A., and Van Loon, L.C. (1996) Systemic resistance in Arabidopsis induced by biocontrol bacteria is independent of salicylic acid accumulation and pathogenesis-related gene expression. *Plant Cell*, **8**, 1225–1237.

Pieterse, C.M. and van Loon, L.C. (1999) Salicylic acid-independent plant defence pathways. *Trends in Plant Science*, **4**, 52–58.

Pieterse, C.M.J., Van der Does, D., Zamioudis, C., Leon-Reyes, A., and Van Wees, S.C.M. (2012) Hormonal modulation of plant immunity. *Annual Review of Cell and Developmental Biology*, **28**, 489–521.

Pieterse, C.M.J., Zamioudis, C., Berendsen, R.L., Weller, D.M., Van Wees, S.C.M., and Bakker, P.A.H.M. (2014) Induced systemic resistance by beneficial microbes. *Annual Review of Phytopathology*, **52**, 347–375.

Prashar, P., Kapoor, N., and Sachdeva, S. (2013) Rhizosphere: its structure, bacterial diversity and significance. *Reviews in Environmental Science and Bio/Technology*, **13**, 63–77.

Raaijmakers, J.M., Leeman, M., Van Oorschot, M.M.P., Van der Sluis, I., Schippers, B., and Bakker, P.A.H.M. (1995) Dose-response relationships in biological control of fusarium wilt of radish by *Pseudomonas* spp. *Phytopathology*, **85**, 1075–1081.

Radzki, W., Gutierrez Manero, F.J., Algar, E., Lucas Garcia, J.A., Garcia-Villaraco, A., and Ramos Solano, B. (2013) Bacterial siderophores efficiently provide iron to iron-starved tomato plants in hydroponics culture. *Antonie Van Leeuwenhoek International Journal of General and Molecular Microbiology*, **104**, 321–330.

Rajniak, J., Giehl, R.F.H., Chang, E., Murgia, I., Von Wirén, N., and Sattely, E.S. (2018) Biosynthesis of redox-active metabolites in response to iron deficiency in plants. *Nature Chemical Biology*, **14**, 442–450.

Ravet, K., Touraine, B., Boucherez, J., Briat, J.-F., Gaymard, F., and Cellier, F. (2009) Ferritins control interaction between iron homeostasis and oxidative stress in Arabidopsis. *The Plant Journal*, **57**, 400–412.

Remans, R., Beebe, S., Blair, M., Manrique, G., Tovar, E., Rao, I., Croonenborghs, A., Torres-Gutierrez, R., El-Howeity, M., Michiels, J., and Vanderleyden, J. (2007) Physiological and genetic analysis of root

responsiveness to auxin-producing plant growth-promoting bacteria in common bean (*Phaseolus vulgaris* L.). *Plant and Soil*, **302**, 149–161.

Reynoso, M.A., Blanco, F.A., Bailey-Serres, J., Crespi, M., and Zanetti, M.E. (2013) Selective recruitment of mRNAs and miRNAs to polyribosomes in response to rhizobia infection in *Medicago truncatula*. *The Plant Journal*, **73**, 289–301.

Rich, C., Reitz, M., Eichmann, R., Hermann, S., Jenkins, D.J., Kogel, K.-H., Esteban, E., Ott, S., and Schafer, P. (2018) Cell type identity determines transcriptomic immune responses in *Arabidopsis thaliana* roots. *bioRxiv*, 302448.

Robinson, M.D., McCarthy, D.J., and Smyth, G.K. (2010) edgeR: a Bioconductor package for differential expression analysis of digital gene expression data. *Bioinformatics*, **26**, 139–140.

Robinson, N.J., Procter, C.M., Connolly, E.L., and Guerinot, M.L. (1999) A ferric-chelate reductase for iron uptake from soils. *Nature*, **397**, 694–697.

Rodriguez-Celma, J., Lin, W.D., Fu, G.M., Abadia, J., Lopez-Millan, A.F., and Schmidt, W. (2013) Mutually exclusive alterations in secondary metabolism are critical for the uptake of insoluble iron compounds by *Arabidopsis* and *Medicago truncatula*. *Plant Physiology*, **162**, 1473–1485.

Rogers, E.D. and Benfey, P.N. (2015) Regulation of plant root system architecture: implications for crop advancement. *Current Opinion in Biotechnology*, **32**, 93–98.

Romera, F.J., Alcantara, E., and De La Guardia, M.D. (1999) Ethylene production by Fe-deficient roots and its involvement in the regulation of Fe-deficiency stress responses by strategy I plants. *Annals of Botany*, **83**, 51–55.

Romera, F.J., García, M.J., Alcántara, E., and Pérez-Vicente, R. (2011) Latest findings about the interplay of auxin, ethylene and nitric oxide in the regulation of Fe deficiency responses by Strategy I plants. *Plant Signaling & Behavior*, **6**, 167–170.

Romera, F.J., García, M.J., Lucena, C., Martínez-Medina, A., Aparicio, M.A., Ramos, J., Alcántara, E., Angulo, M., and Pérez-Vicente, R. (2019) Induced systemic resistance (ISR) and Fe deficiency responses in dicot plants. *Frontiers in Plant Science*, **10**, 287.

Römheld, V. (1987) Different strategies for iron acquisition in higher plants. *Physiologica Plantarum*, **79**, 231–234.

Rroço, E., Kosegarten, H., Harizaj, F., Imani, J., and Mengel, K. (2003) The importance of soil microbial activity for the supply of iron to sorghum and rape. *European Journal of Agronomy*, **19**, 487–493.

Ryan, E., Steer, M., and Dolan, L. (2001) Cell biology and genetics of root hair formation in *Arabidopsis thaliana*. *Protoplasma*, **215**, 140–149.

Ryu, C.-M., Farag, M.A., Hu, C.-H., Reddy, M.S., Wei, H.-X., Paré, P.W., and Kloepper, J.W. (2003) Bacterial volatiles promote growth in *Arabidopsis*. *Proceedings of the National Academy of Sciences of the United States of America*, **100**, 4927–4932.

Ryu, C.-M., Farag, M.A., Hu, C.-H., Reddy, M.S., Kloepper, J.W., and Paré, P.W. (2004) Bacterial volatiles induce systemic resistance in Arabidopsis. *Plant Physiology*, **134**, 1017–1026.

Ryu, C.-M., Hu, C.-H., Locy, R.D., and Kloepper, J.W. (2005) Study of mechanisms for plant growth promotion elicited by rhizobacteria in *Arabidopsis thaliana*. *Plant and Soil*, **268**, 285–292.

Sabatini, S., Heidstra, R., Wildwater, M., and Scheres, B. (2003) SCARECROW is involved in positioning the stem cell niche in the *Arabidopsis* root meristem. *Genes and Development*, **17**, 354–358.

Salazar-Henao, J.E., Cristina Veíez-Bermúdezbermúdez, I., and Schmidt, W. (2016) The regulation and plasticity of root hair patterning and morphogenesis. *Development*, **143**, 1848–1858.

Santi, S. and Schmidt, W. (2009) Dissecting iron deficiency-induced proton extrusion in Arabidopsis roots. *New Phytologist*, **183**, 1072–1084.

Schenk, S.T., Stein, E., Kogel, K.-H., and Schikora, A. (2012) Arabidopsis growth and defense are modulated by bacterial quorum sensing molecules. *Plant Signaling & Behavior*, **7**, 178–181.

Scheres, B., Wolkenfelt, H., Willemsen, V., Terlouw, M., Lawson, E., Dean, C., and Weisbeek, P. (1994) Embryonic origin of the *Arabidopsis* primary root and root-meristem initials. *Development*, **120**, 2475–2487.

Scheres, B., Dilaurenzio, L., Willemsen, V., Hauser, M., Janmaat, K., Weisbeek, P., and Benfey, P. (1995) Mutations affecting the radial organization of the *Arabidopsis* root display specific defects throughout the embryonic axis. *Development*, **121**, 53–62.

Schiefelbein, J.W. (2000) Constructing a plant cell. The genetic control of root hair development. *Plant Physiology*, **124**, 1525–1531.

Schlaeppi, K., Dombrowski, N., Oter, R.G., Ver Loren van Themaat, E., and Schulze-Lefert, P. (2014) Quantitative divergence of the bacterial root microbiota in *Arabidopsis thaliana* relatives. *Proceedings of the National Academy of Sciences of the United States of America*, **111**, 585–592.

Schmid, N.B., Giehl, R.F.H., Döll, S., Mock, H.-P., Strehmel, N., Scheel, D., Kong, X., Hider, R.C., and Von Wirén, N. (2014) Feruloyl-CoA 6′ -hydroxylase1-dependent coumarins mediate iron acquisition from alkaline

substrates in Arabidopsis. *Plant Physiology*, **164**, 160–172.

Schmidt, H., Gunther, C., Weber, M., Sporlein, C., Loscher, S., Bottcher, C., Schobert, R., and Clemens, S. (2014) Metabolome analysis of *Arabidopsis thaliana* roots identifies a key metabolic pathway for iron acquisition. *PLoS ONE*, **9**, e102444.

Schmidt, R. and Schippers, J.H.M. (2015) ROS-mediated redox signaling during cell differentiation in plants. *Biochimica et Biophysica Acta*, **1850**, 1497–1508.

Schmidt, W. (1999) Mechanisms and regulation of reduction-based iron uptake in plants. *New Phytologist*, **141**, 1–26.

Schmittgen, T.D. and Livak, K.J. (2008) Analyzing real-time PCR data by the comparative CT method. *Nature Protocols*, **3**, 1101–1108.

Segarra, G., Van der Ent, S., Trillas, I., and Pieterse, C.M.J. (2009) MYB72, a node of convergence in induced systemic resistance triggered by a fungal and a bacterial beneficial microbe. *Plant Biology*, **11**, 90–96.

Segond, D., Dellagi, A., Lanquar, V., Rigault, M., Patrit, O., Thomine, S., and Expert, D. (2009) *NRAMP* genes function in *Arabidopsis thaliana* resistance to *Erwinia chrysanthemi* infection. *The Plant Journal*, **58**, 195–207.

Séguéla, M., Briat, J., Vert, G., and Curie, C. (2008) Cytokinins negatively regulate the root iron uptake machinery in Arabidopsis through a growth-dependent pathway. *The Plant Journal*, **55**, 289–300.

Selote, D., Samira, R., Matthiadis, A., Gillikin, J.W., and Long, T.A. (2015) Iron-binding E3 ligase mediates iron response in plants by targeting basic helix-loop-helix transcription factors. *Plant Physiology*, **167**, 273–286.

Shahzad, Z. and Amtmann, A. (2017) Food for thought: how nutrients regulate root system architecture. *Current Opinion in Plant Biology*, **39**, 80–87.

Shang, X., Cao, Y., and Ma, L. (2017) Alternative splicing in plant genes: a means of regulating the environmental fitness of plants. *International Journal of Molecules Sciences*, **18**, e432.

Shen, C., Yang, Y., Liu, K., Zhang, L., Guo, H., Sun, T., and Wang, H. (2016) Involvement of endogenous salicylic acid in iron-deficiency responses in Arabidopsis. *Journal of Experimental Botany*, **67**, 4179–4193.

Shimizu, B., Fujimori, A., Miyagawa, H., Ueno, T., Watanabe, K., and Ogawa, K. (2000) Resistance against Fusarium wilt induced by non-pathogenic *Fusarium* in *Ipomoea tricolor*. *Journal of Pesticide Science*, **25**, 365–372.

Singh, B.K., Millard, P., Whiteley, A.S., and Murrell, J.C. (2004) Unravelling rhizosphere-microbial interactions: opportunities and limitations. *Trends in Microbiology*, **12**, 386–393.

Sivitz, A.B., Hermand, V., Curie, C., and Vert, G. (2012) Arabidopsis bHLH100 and bHLH101 control iron homeostasis via a FIT-independent pathway. *PLoS ONE*, **7**, e44843.

Smith, D.L. and Fedoroff, N. V. (1995) *LRP1*, a gene expressed in lateral and adventitious root primordia of Arabidopsis. *Plant Cell*, **7**, 735–745.

Soneson, C., Love, M.I., and Robinson, M.D. (2015) Differential analyses for RNA-seq: transcript-level estimates improve gene-level inferences. *F1000 Research*, **4**, 1521.

Soyano, T., Hirakawa, H., Sato, S., Hayashi, M., and Kawaguchi, M. (2014) Nodule inception creates a long-distance negative feedback loop involved in homeostatic regulation of nodule organ production. *Proceedings of the National Academy of Sciences of the United States of America*, **111**, 14607–14612.

Spaepen, S., Bossuyt, S., Engelen, K., Marchal, K., and Vanderleyden, J. (2014) Phenotypical and molecular responses of *Arabidopsis thaliana* roots as a result of inoculation with the auxin-producing bacterium *Azospirillum brasilense*. *New Phytologist*, **201**, 850–861.

Splivallo, R., Fischer, U., Göbel, C., Feussner, I., and Karlovsky, P. (2009) Truffles regulate plant root morphogenesis via the production of auxin and ethylene. *Plant Physiology*, **150**, 2018–2029.

Stacey, M.G., Patel, A., McClain, W.E., Mathieu, M., Remley, M., Rogers, E.E., Gassmann, W., Blevins, D.G., and Stacey, G. (2008) The Arabidopsis AtOPT3 protein functions in metal homeostasis and movement of iron to developing seeds. *Plant Physiology*, **146**, 589–601.

Stoeckle, D., Thellmann, M., and Vermeer, J.E. (2018) Breakout — lateral root emergence in *Arabidopsis thaliana*. *Current Opinion in Plant Biology*, **41**, 67–72.

Stringlis, I.A., Yu, K., Feussner, K., de Jonge, R., Van Bentum, S., Van Verk, M.C., Berendsen, R.L., Bakker, P.A.H.M., Feussner, I., and Pieterse, C.M.J. (2018a) MYB72-dependent coumarin exudation shapes root microbiome assembly to promote plant health. *Proceedings of the National Academy of Sciences of the United States of America*, **115**, E5213–E5222.

Stringlis, I.A., Proietti, S., Hickman, R., Van Verk, M.C., Zamioudis, C., and Pieterse, C.M.J. (2018b) Root transcriptional dynamics induced by beneficial rhizobacteria and microbial immune elicitors reveal signatures of adaptation to mutualists. *The Plant Journal*, **93**, 166–180.

Stringlis, I.A., de Jonge, R., and Pieterse, C.M.J. (2019) The age of coumarins in plant-microbe interactions. *Plant and Cell Physiology*, pcz076.

Sukumar, P., Legué, V., Vayssières, A., Martin, F., Tuskan, G.A., and Kalluri, U.C. (2013) Involvement of auxin

pathways in modulating root architecture during beneficial plant-microorganism interactions. *Plant, Cell and Environment*, **36**, 909-019.

Sun, H., Wang, L., Zhang, B., Ma, J., Hettenhausen, C., Cao, G., Sun, G., Wu, J., and Wu, J. (2014) Scopoletin is a phytoalexin against *Alternaria alternata* in wild tobacco dependent on jasmonate signalling. *Journal of Experimental Botany*, **65**, 4305–4315.

Taguchi, F., Suzuki, T., Inagaki, Y., Toyoda, K., Shiraishi, T., and Ichinose, Y. (2010) The siderophore pyoverdine of *Pseudomonas syringae* pv. tabaci 6605 is an intrinsic virulence factor in host tobacco infection. *Journal of Bacteriology*, **192**, 117–126.

Tanaka, N., Kato, M., Tomioka, R., Kurata, R., Fukao, Y., Aoyama, T., and Maeshima, M. (2014) Characteristics of a root hair-less line of *Arabidopsis thaliana* under physiological stresses. *Journal of Experimental Botany*, **65**, 1497–1512.

Theil, E.C. (1987) Ferritin: structure, gene regulation, and cellular function in animals, plants, and microorganisms. *Annual Review of Biochemistry*, **56**, 289–315.

Torsvik, V., Øvreås, L., and Thingstad, T.F. (2002) Prokaryotic diversity-magnitude, dynamics, and controlling factors. *Science*, **296**, 1064–1066.

Townsley, B.T., Covington, M.F., Ichihashi, Y., Zumstein, K., and Sinha, N.R. (2015) BrAD-seq: Breath Adapter Directional sequencing: a streamlined, ultra-simple and fast library preparation protocol for strand specific mRNA library construction. *Frontiers in Plant Science*, **6**, 366.

Trapet, P., Avoscan, L., Klinguer, A., Pateyron, S., Citerne, S., Chervin, C., Mazurier, S., Lemanceau, P., Wendehenne,
D., and Besson-Bard, A. (2016) The *Pseudomonas fluorescens* siderophore pyoverdine weakens *Arabidopsis thaliana* defense in favor of growth in iron-deficient conditions. *Plant Physiology*, **171**, 675–693.

Tsai, H.H. and Schmidt, W. (2017) Mobilization of iron by plant-borne coumarins. *Trends in Plant Science*, **22**, 538–548.

Tsai, H.H., Rodríguez-Celma, J., Lan, P., Wu, Y.-C., Vélez-Bermúdez, I.C., and Schmidt, W. (2018) Scopoletin 8-hydroxylase-mediated fraxetin production is crucial for iron mobilization. *Plant Physiology*, **177**, 194–207.

Tsukagoshi, H., Busch, W., and Benfey, P.N. (2010) Transcriptional regulation of ROS controls transition from proliferation to differentiation in the root. *Cell*, **143**, 606–616.

Vacheron, J., Desbrosses, G., Bouffaud, M.-L., Touraine, B., Moënne-Loccoz, Y., Muller, D., Legendre, L., Wisniewski-Dyé, F., and Prigent-Combaret, C. (2013) Plant growth-promoting rhizobacteria and root system functioning. *Frontiers in Plant Science*, **4**, 356.

Vacheron, J., Desbrosses, G., Renoud, S., Padilla, R., Walker, V., Muller, D., and Prigent-Combaret, C. (2018) Differential contribution of plant-beneficial functions from *Pseudomonas kilonensis* F113 to root system architecture alterations in *Arabidopsis thaliana* and *Zea mays*. *Molecular Plant-Microbe Interactions*, **31**, 212–223.

Vansuyt, G., Robin, A., Briat, J.-F., Curie, C., and Lemanceau, P. (2007) Iron acquisition from Fe-pyoverdine by *Arabidopsis thaliana*. *Molecular Plant-Microbe Interactions*, **20**, 441–447.

Verbelen, J.-P., Cnodder, T. De, Le, J., Vissenberg, K., and Baluška, F. (2006) Root apex of *Arabidopsis thaliana* consists of four distinct zones of growth activities: meristematic zone, transition zone, fast elongation zone, and growth terminating zone. *Plant Signaling and Behavior*, **1**, 296–304.

Verbon, E.H. and Liberman, L.M. (2016) Beneficial microbes affect endogenous mechanisms controlling root development. *Trends in Plant Science*, **21**, 218–229.

Verbon, E.H., Trapet, P.L., Stringlis, I.A., Kruijs, S., Bakker, P.A.H.M., and Pieterse, C.M.J. (2017) Iron and immunity. *Annual Review of Phytopathology*, **55**, 355–375.

Verhagen, B.W.M., Glazebrook, J., Zhu, T., Chang, H.-S., Van Loon, L.C., and Pieterse, C.M.J. (2004) The transcriptome of rhizobacteria-induced systemic resistance in *Arabidopsis*. *Molecular Plant-Microbe Interactions*, **17**, 895–908.

Vermeer, J.E.M., von Wangenheim, D., Barberon, M., Lee, Y., Stelzer, E.H.K., Maizel, A., and Geldner, N. (2014) A spatial accommodation by neighboring cells is required for organ initiation in *Arabidopsis*. *Science*, **343**, 178–183.

Vert, G., Grotz, N., Dédaldéchamp, F., Guerinot, M.L., Briat, J.F., Curie, C., Gaymard, F., Guerinot, M. Lou, Briat, J.F., and Curie, C. (2002) IRT1, an Arabidopsis transporter essential for iron uptake from the soil and for plant growth. *Plant Cell*, **14**, 1223–1233.

Vert, G.A., Briat, J.F., and Curie, C. (2003) Dual regulation of the Arabidopsis high-affinity root iron uptake system by local and long-distance signals. *Plant Physiology*, **132**, 796–804.

Vishwanath, S.J., Delude, C., Domergue, F., and Rowland, O. (2015) Suberin: biosynthesis, regulation, and polymer assembly of a protective extracellular barrier. *Plant Cell Reports*, **34**, 573–586.

De Vleesschauwer, D., Djavaheri, M., Bakker, P.A.H.M., and Höfte, M. (2008) *Pseudomonas fluorescens* WCS374r-

induced systemic resistance in rice against </i>Magnaporthe oryzae</i> is based on pseudobactin-mediated priming for a salicylic acid-repressible multifaceted defense response. *Plant Physiology*, **148**, 1996–2012.

Vogt, T. (2010) Phenylpropanoid biosynthesis. *Molecular Plant*, **3**, 2–20.

Walker, E.L. and Connolly, E.L. (2008) Time to pump iron: iron-deficiency-signaling mechanisms of higher plants. *Current Opinion in Plant Biology*, **11**, 530–535.

Walker, L., Boddington, C., Jenkins, D., Wang, Y., Grønlund, J.T., Hulsmans, J., Kumar, S., Patel, D., Moore, J.D., Carter, A., Samavedam, S., Bomono, G., Hersh, D.S., Coruzzi, G.M., Burroughs, N.J., and Gifford, M.L. (2017) Root architecture shaping by the environment is orchestrated by dynamic gene expression in space and time. *Plant Cell*, **29**, 2393–2412.

Wang, N., Cui, Y., Liu, Y., Fan, H., Du, J., Huang, Z., Yuan, Y., Wu, H., and Ling, H.-Q. (2013) Requirement and functional redundancy of Ib subgroup bHLH proteins for iron deficiency responses and uptake in *Arabidopsis thaliana*. *Molecular Plant*, **6**, 503–513.

Weert, S. de, Vermeiren, H., Mulders, I.H.M., Kuiper, I., Hendrickx, N., Bloemberg, G. V., Vanderleyden, J., Mot, R. De, and Lugtenberg, B.J.J. (2002) Flagella-driven chemotaxis towards exudate components is an important trait for tomato root colonization by *Pseudomonas fluorescens*. *Molecular Plant-Microbe Interactions*, **15**, 1173–1180.

Van Wees, S.C.M., Van Pelt, J.A., Bakker, P.A.H.M., and Pieterse, C.M.J. (2013) Bioassays for assessing jasmonate-dependent defenses triggered by pathogens, herbivorous insects, or beneficial rhizobacteria. *Methods in Molecular Biology*, **1011**, 35–49.

Wei, G., Kloepper, J., and Tuzun, S. (1991) Induction of systemic resistance of cucumber to *Colletotrichum orbiculare* by select strains of plant growth-promoting rhizobacteria. *Phytophathology*, **81**, 1508–1512.

Wei, Z. and Li, J. (2018) Receptor-like protein kinases: Key regulators controlling root hair development in *Arabidopsis thaliana*. *Journal of Integrative Plant Biology*, **60**, 841–850.

White, J., Kingsley, K., Verma, S., Kowalski, K., White, J.F., Kingsley, K.L., Verma, S.K., and Kowalski, K.P. (2018) Rhizophagy cycle: an oxidative process in plants for nutrient extraction from symbiotic microbes. *Microorganisms*, **6**, 95.

White, J.F., Torres, M.S., Verma, S.K., Elmore, M.T., Kowalski, K.P., and Kingsley, K.L. (2019) Evidence for widespread microbivory of endophytic bacteria in roots of vascular plants through oxidative degradation in root cell periplasmic spaces. *PGPR Amelioration in Sustainable Agriculture*, 167–193.

Wild, M., Davière, J.-M., Regnault, T., Sakvarelidze-Achard, L., Carrera, E., Lopez Diaz, I., Cayrel, A., Dubeaux, G., Vert, G., and Achard, P. (2016) Tissue-specific regulation of gibberellin signaling fine-tunes *Arabidopsis* iron-deficiency responses. *Developmental Cell*, **37**, 190–200.

Wildermuth, M.C., Dewdney, J., Wu, G., and Ausubel, F.M. (2001) Isochorismate synthase is required to synthesize salicylic acid for plant defence. *Nature*, **414**, 562–565.

Wu, J. and Baldwin, I.T. (2010) New insights into plant responses to the attack from insect herbivores. *Annual Review of Genetics*, **44**, 1–24.

Wu, L., Ueda, Y., Lai, S., and Frei, M. (2017) Shoot tolerance mechanisms to iron toxicity in rice (Oryza sativa L.). *Plant, Cell and Environment*, **40**, 570–584.

Wyrsch, I., Domínguez-Ferreras, A., Geldner, N., and Boller, T. (2015) Tissue-specific FLAGELLIN-SENSING 2 (FLS2) expression in roots restores immune responses in Arabidopsis *fls2* mutants. *New Phytologist*, **206**, 774–784.

Wysocka-Diller, J.W., Helariutta, Y., Fukaki, H., Malamy, J.E., and Benfey, P.N. (2000) Molecular analysis of SCARECROW function reveals a radial patterning mechanism common to root and shoot. *Development*, **127**, 595–603.

Xuan, W., Audenaert, D., Parizot, B., Möller, B.K., Njo, M.F., De Rybel, B., De Rop, G., Van Isterdael, G., Mähönen, A.P., Vanneste, S., and Beeckman, T. (2015) Root cap-derived auxin pre-patterns the longitudinal axis of the *Arabidopsis* root. *Current bBology*, **25**, 1381–1388.

Xuan, W., Band, L.R., Kumpf, R.P., Van Damme, D., Parizot, B., De Rop, G., Opdenacker, D., Möller, B.K., Skorzinski, N., Njo, M.F., De Rybel, B., Audenaert, D., Nowack, M.K., Vanneste, S., and Beeckman, T. (2016) Cyclic programmed cell death stimulates hormone signaling and root development in Arabidopsis. *Science (New York, N.Y.)*, **351**, 384–7. American Association for the Advancement of Science.

Yadav, V., Molina, I., Ranathunge, K., Castillo, I.Q., Rothstein, S.J., and Reed, J.W. (2014) ABCG transporters are required for suberin and pollen wall extracellular barriers in *Arabidopsis*. *Plant Cell*, **26**, 3569–3588.

Ye, F., Albarouki, E., Lingam, B., Deising, H.B., and Von Wirén, N. (2014) An adequate Fe nutritional status of maize suppresses infection and biotrophic growth of *Colletotrichum graminicola*. *Physiologia Plantarum*, **151**, 280–292.

Yehuda, Z., Shenker, M., Hadar, Y., and Chen, Y.N. (2000) Remedy of chlorosis induced by iron deficiency in

plants with the fungal siderophore rhizoferrin. *Journal of Plant Nutrition*, **23**, 1991–2006.

Yi, Y. and Guerinot, M.L. (1996) Genetic evidence that induction of root Fe(III) chelate reductase activity is necessary for iron uptake under iron deficiency. *The Plant Journal*, **10**, 835–844.

Yuan, Y., Wu, H., Wang, N., Li, J., Zhao, W., Du, J., Wang, D., and Ling, H.-Q. (2008) FIT interacts with AtbHLH38 and AtbHLH39 in regulating iron uptake gene expression for iron homeostasis in *Arabidopsis*. *Cell Research*, **18**, 385–397.

Yuan, Y.X., Zhang, J., Wang, D.W., and Ling, H.Q. (2005) *AtbHLH29* of *Arabidopsis thaliana* is a functional ortholog of tomato *FER* involved in controlling iron acquisition in strategy I plants. *Cell Research*, **15**, 613–621.

Zamioudis, C., Mastranesti, P., Dhonukshe, P., Blilou, I., and Pieterse, C.M.J. (2013) Unraveling root developmental programs initiated by beneficial *Pseudomonas* spp. bacteria. *Plant Physiology*, **162**, 304–318.

Zamioudis, C., Hanson, J., and Pieterse, C.M.J. (2014) β-Glucosidase BGLU42 is a MYB72-dependent key regulator of rhizobacteria-induced systemic resistance and modulates iron deficiency responses in *Arabidopsis* roots. *New Phytologist*, **204**, 368–379.

Zamioudis, C., Korteland, J., Van Pelt, J.A., Van Hamersveld, M., Dombrowski, N., Bai, Y., Hanson, J., Van Verk, M.C., Ling, H.-Q., Schulze-Lefert, P., and Pieterse, C.M.J. (2015) Rhizobacterial volatiles and photosynthesis-related signals coordinate *MYB72* expression in Arabidopsis roots during onset of induced systemic resistance and iron-deficiency responses. *The Plant Journal*, **84**, 309–322.

Zanetti, M.E., Chang, I.-F., Gong, F., Galbraith, D.W., and Bailey-Serres, J. (2005) Immunopurification of polyribosomal complexes of Arabidopsis for global analysis of gene expression. *Plant Physiology*, **138**, 624–635.

Zhai, Z., Gayomba, S.R., Jung, H.-I., Vimalakumari, N.K., Pineros, M., Craft, E., Rutzke, M.A., Danku, J., Lahner, B., Punshon, T., Guerinot, M.L., Salt, D.E., Kochian, L. V., and Vatamaniuk, O.K. (2014) OPT3 is a phloem-specific iron transporter that is essential for systemic iron signaling and redistribution of iron and cadmium in *Arabidopsis*. *Plant Cell*, **26**, 2249–2264.

Zhang, H., Sun, Y., Xie, X., Kim, M.-S., Dowd, S.E., and Paré, P.W. (2009) A soil bacterium regulates plant acquisition of iron via deficiency-inducible mechanisms. *The Plant Journal*, **58**, 568–577.

Zhang, R., Calixto, C.P.G., Marquez, Y., Venhuizen, P., Tzioutziou, N.A., Guo, W., Spensley, M., Entizne, J.C., Lewandowska, D., ten Have, S., Frei dit Frey, N., Hirt, H., James, A.B., Nimmo, H.G., Barta, A., Kalyna, M., and Brown, J.W.S. (2017) A high quality Arabidopsis transcriptome for accurate transcript-level analysis of alternative splicing. *Nucleic Acids Research*, **45**, 5061–5073.

Zhang, Y. and Li, X. (2019) Salicylic acid: biosynthesis, perception, and contributions to plant immunity. *Current Opinion in Plant Biology*, **50**, 29–36.

Zhou, C., Guo, J., Zhu, L., Xiao, X., Xie, Y., Zhu, J., Ma, Z., and Wang, J. (2016) *Paenibacillus polymyxa* BFKC01 enhances plant iron absorption via improved root systems and activated iron acquisition mechanisms. *Plant Physiology and Biochemistry*, **105**, 162–173.

Nederlandse samenvatting

Goedaardige bacteriën op plantenwortels

Op, in en rondom plantenwortels leven miljarden micro-organismen. Sommige van deze bodembacteriën en -schimmels beïnvloeden de plant negatief; ze kapen belangrijke voedingsstoffen weg of maken de plant ziek. Andere micro-organismen beïnvloeden de plant juist positief. Zo kunnen ze extra voedingsstoffen beschikbaar maken, de plant weerbaarder maken tegen ziekteverwekkers of het aantal ziekteverwekkende micro-organismen rondom de wortels verminderen door met ze te concurreren voor voedingsstoffen en ruimte.

De bacterie *Pseudomonas simiae* WCS417 is een voorbeeld van zo'n goedaardig micro-organisme. Wanneer deze bacterie zich vestigt op de wortel van het zandraketje – in de plantenwetenschap beter bekend als *Arabidopsis thaliana* – wordt de plant groter en is de plant weerbaarder tegen ziekteverwekkers. In dit proefschrift onderzoek ik op welke wijze WCS417 deze positieve invloed op de plant uitoefent.

Veranderingen in de wortelstructuur

Naast de verhoogde weerbaarheid en de versterkte groei, reageert de plant op WCS417 met de vorming van extra zijwortels (Figuur 1A). Zijwortels vergroten het worteloppervlak, waardoor er meer oppervlak is waarover voedingsstoffen kunnen worden opgenomen én er meer ruimte is voor WCS417 om zich te vestigen. Zijwortels worden gevormd door cellen in het binnenste van de wortel, het vasculaire weefsel. Deze cellen zijn omgeven door drie andere cellagen: de endodermis, de cortex en tenslotte de epidermis (Figuur 1B). De zijwortels moeten deze cellagen passeren voordat zij uit de wortel tevoorschijn komen. Onderzoek van andere onderzoeksgroepen heeft aangetoond dat de cellen in de endodermis en de cortex moeten krimpen om zo ruimte te maken om de uitgroei van zijwortels mogelijk te maken. Hoe de cellen in staat zijn om te krimpen was nog niet duidelijk.

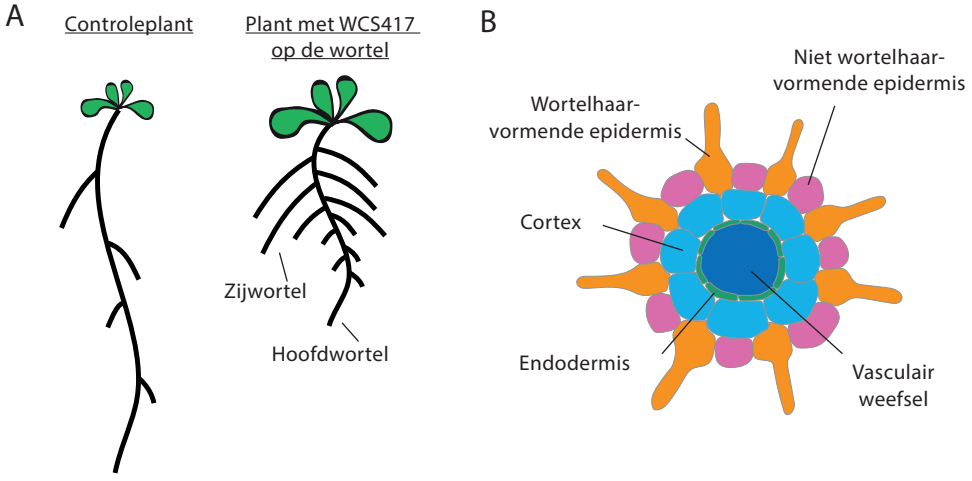

Figuur 1 De plant *Arabidopsis thaliana* vormt meer zijwortels als de bodembacterie WCS417 zich vestigt op de wortel. A) Schematische weergave van een plant zonder WCS417 op de wortel (links) en een plant met WCS417 op de wortel (rechts). B) Schematische dwarsdoorsnede van de plantenwortel, waarin de verschillende celtypen gelabeld zijn.

Om te begrijpen hoe de plant de wortelstructuur verandert, hebben we in hoofdstuk 2 gekeken hoe de verschillende wortelceltypen reageren op de vestiging van WCS417 op de wortel. We laten zien dat de endodermis en de cortex genen activeren die de celwanden rond deze cellen afbreken. Mogelijk zorgt deze afbraak ervoor dat de cellen kunnen krimpen om de zijwortels door te laten. Daarnaast laten we zien dat cellen in de endodermis in reactie op WCS417 genen activeren die betrokken zijn bij het produceren van een wasachtige laag om deze cellen heen. Deze laag is ondoordringbaar voor voedingsstoffen en water en voorkomt daardoor dat deze weglekken uit het binnenste deel van de wortel. Wellicht voorkomt deze laag ook dat microorganismen de wortel binnendringen.

Tenslotte identificeren we activiteit van genen die een al langer bekend fenomeen verklaren. De buitenste cellaag van de wortel, de epidermis, bestaat uit wortelhaar-vormende cellen en niet-wortelhaar-vormende cellen. Het was al bekend dat specifiek de wortelhaar-vormende cellen belangrijk zijn voor de opname van voedingsstoffen. Wij laten zien dat genen die betrokken zijn bij de opname van voedingsstoffen specifiek in die wortelhaar-vormende cellen en niet in de niet-wortelhaar-vormende cellen actief zijn.

De activatie van ijzeropname

Uit onderzoek van mijn voorgangers in het lab is gebleken dat de wortel op WCS417 reageert door processen die tot ijzeropname leiden te activeren. In hoofdstuk 3 onderzoeken we waarom de plant de ijzeropname activeert in reactie op WCS417. Eerst bevestigen we eerdere onderzoeksresultaten: namelijk dat de activatie van de ijzeropname in reactie op WCS417 niet meer plaatsvindt als de bovengrondse delen van de plant worden weggesneden. Dit geeft aan dat er een signaal uit de bovengrondse delen van de plant nodig is om de ijzeropname te activeren. Wellicht leidt de door WCS417 versterkte groei tot een ijzertekort in de bovengrondse delen van de plant. De hypothese die we daarom hebben getest is of een ijzertekort in de bovengrondse delen van de plant leidt tot de verhoogde ijzeropname in de wortel in reactie op WCS417. Uit onze experimenten blijkt dat toediening van ijzer op de bovengrondse delen van de plant tegelijkertijd met de toediening van WCS417 op de wortel de activatie van de ijzeropname niet voorkomt. Onze hypothese was dus niet juist.

Onze huidige hypothese is dat de plant de ijzeropname verhoogt in reactie op een bovengronds groeisignaal in plaats van een bovengronds ijzertekort om zo een eventueel ijzertekort vóór te zijn. Deze hypothese wordt ondersteund door onze data waaruit blijkt dat de ijzerconcentratie in de plant niet vermindert in reactie op WCS417. In plaats daarvan neemt de hoeveelheid ijzer gelijkmatig toe met de vorming van nieuw bladmateriaal. Vanuit evolutionair oogpunt is dit voordelig voor de plant: aangezien ijzer essentieel is voor veel processen in de plant, is het gunstig om ijzertekorten te voorkomen in plaats van te genezen.

Het induceren van verhoogde weerbaarheid

In hoofdstuk 4 gaan we verder waar we in hoofdstuk 3 gebleven waren: de activatie van ijzeropname in reactie op WCS417. We kijken naar het effect hiervan op de verhoogde weerbaarheid van planten met WCS417. Zoals in de introductie is vermeld, wordt een plant met WCS417 minder snel ziek na aanvallen van ziekteverwekkers. Eerder onderzoek heeft aangetoond dat enkele genen die worden geactiveerd in reactie op WCS417 en leiden tot verhoogde ijzeropname, name-

lijk de genen *MYB72* en *BGLU42*, essentieel zijn voor de verhoogde weerbaarheid van planten met WCS417. Daarnaast weten we dat hoewel een omgeving met weinig ijzer ervoor zorgt dat planten minder hard groeien, zo'n omgeving ook leidt tot verminderde ziekteverschijnselen. Het is echter nog niet duidelijk hoe ijzertekort leidt tot verlaagde vatbaarheid voor ziekten.

IJzer is niet alleen een essentiële voedingsstof voor planten, maar ook voor de meeste andere organismen. Wij hebben daarom getest of een plant met een ijzertekort minder ziek wordt omdat er weinig ijzer beschikbaar is voor de aanvallende ziekteverwekker. Dit blijkt niet het geval te zijn. In plaats daarvan tonen we aan dat de verhoogde weerbaarheid van een plant met ijzertekort afhankelijk is van de verdedigingshormonen van de plant.

Een omgeving met weinig ijzer leidt, net als blootstelling aan WCS417, tot activatie van ijzeropname en dus tot activatie van *MYB72* en *BGLU42*. We hebben daarom getest of deze genen ook essentieel zijn voor de verhoogde weerbaarheid na een ijzertekort. Als dat het geval is, zijn beide vormen van verhoogde weerbaarheid wellicht gebaseerd op hetzelfde mechanisme en is de activatie van de ijzeropname op zichzelf genoeg om resistentie te induceren. Om dit te testen, gebruikten we gemuteerde planten waarin de genen *MYB72* en *BGLU42* niet meer werkzaam zijn. We laten zien dat deze planten geen verhoogde resistentie vertonen nadat WCS417 zich vestigt op hun wortels, maar wel na ijzertekort. Hiermee tonen we aan dat de twee vormen van verhoogde weerbaarheid niet door dezelfde genen gereguleerd worden.

Het opzetten van een nieuwe techniek

In het laatste experimentele hoofdstuk, hoofdstuk 5, beschrijven we de opzet van een relatief nieuwe experimentele techniek die ons in staat stelt om op een ander niveau naar de effecten van WCS417 en ijzertekort op de plantenwortel te kijken. In hoofdstuk 2 tot en met 4 keken we naar de activiteit van genen. De activatie van een gen ligt aan de basis van de productie van een eiwit. Echter, instructies van actieve genen leiden niet altijd tot de vorming van eiwitten. In plaats daarvan worden de instructies soms afgebroken of tijdelijk opgeslagen. De activiteit van genen correleert daarom niet altijd met de productie van eiwitten en de activiteit van de biologische processen die door de eiwitten uitgevoerd worden. Met de nieuwe techniek kunnen we bestuderen welke instructies daadwerkelijk worden gebruikt om eiwitten te produceren. We laten zien dat deze methode werkt met zowel planten blootgesteld aan WCS417 als met planten blootgesteld aan een ijzertekort. Uit de eerste resultaten kunnen we opmaken dat in reactie op ijzertekort een verandering in de activiteit van een gen inderdaad niet altijd resulteert in een verandering van het gebruik van de instructie om een eiwit te maken. De plant reguleert zijn reactie dus niet alleen door de activiteit van genen te reguleren. Verder onderzoek zal moeten uitwijzen wat dit betekent voor de reactie van de plant op het ijzertekort.

Van kennis naar voedselzekerheid

De resultaten in dit proefschrift vergroten onze kennis over het effect van de goedaardige bacterie WCS417 op Arabidopsis. Zo identificeren we in hoofdstuk 2 veranderingen in genactiviteit in de endodermis en de cortex die wellicht aan de basis liggen van de verhoogde zijwortelvorming in planten met WCS417. Daarnaast vinden we aanwijzingen voor een tot zover onbekende reactie van de wortel op WCS417: de verhoogde productie van de wasach-

tige laag rondom endodermis cellen. Het was al bekend dat de plantenwortel in reactie op WCS417 de ijzeropname activeert. Naar aanleiding van de data gepresenteerd in hoofdstuk 3 hypothetiseren we dat de ijzeropname geactiveerd wordt in reactie op een groeisignaal in de bovengrondse delen van de plant. In hoofdstuk 4 laten we zien dat de verhoogde weerbaarheid van planten met WCS417 niet geactiveerd wordt door hetzelfde proces als de verhoogde weerbaarheid van planten met een ijzertekort. Tenslotte laten we in hoofdstuk 5 zien dat we succesvol een nieuwe techniek hebben opgezet waarmee we op een ander niveau de reactie van plantenwortels op veranderingen in hun omgeving kunnen bestuderen.

Behalve nieuwe inzichten, leveren deze data weer veel nieuwe vragen op: wat is het effect van de wasachtige laag op de interactie van planten met micro-organismen? Door wat voor signaal wordt groei gecommuniceerd tussen de wortels en de bovengrondse delen van de plant? Hoe leiden een ijzertekort en WCS417 tot verhoogde weerbaarheid van de plant? Verder onderzoek is nodig om deze en andere nieuwe vragen te beantwoorden.

De hier gepresenteerde data en data van mogelijk vervolgonderzoek kunnen bijdragen aan het vergroten van de voedselzekerheid. Kennis over de regulatie van de wortelstructuur stelt ons in staat om gewassen te selecteren met de meest optimale wortelstructuur voor een bepaalde regio. Kennis over de effecten van goedaardige bacteriën, op zijn beurt, kan bijdragen aan het gebruik van deze bacteriën in het veld als natuurlijke groei- en resistentie-bevorderaars. Op deze manier kan kennis uit het laboratorium bijdragen aan het realiseren van hogere voedselopbrengsten met een verminderde hoeveelheid synthetische meststoffen en pesticiden.

Acknowledgements

By the time you read these acknowledgements, the time has come: my thesis is finished! This would not have been possible without the many people that had my back along the way.

Ten eerste, Johannes Boonstra en Koen Verhoeven. ~~Meneer~~ Johannes Boonstra, jij leerde me denken, schrijven en presenteren als een wetenschapper. En nog veel belangrijker dan dat: jij leerde me hoe ontzettend leuk dat is. Koen, bij jou deed ik mijn eerste onderzoekservaring op. Wat had ik een mazzel met jou als mijn begeleider! Je deur stond altijd open voor discussies over het project en over het leven als wetenschapper. Jouw enthousiasme over onderzoek was en is een grote inspiratiebron. Ik ben trots dat ik mijn eerste review, respectievelijk onderzoekspaper met jullie heb kunnen schrijven.

Vervolgens Corné, mijn promotor. Samen met jou schrijven was voor mij altijd een feestje. Jij stond ook open voor míjn feedback en zo maakten we samen stukken alsmaar beter. Ronnie, mijn co-promotor, ik heb ongelooflijk geluk gehad dat jij na mij ook bij PMI kwam. Je enthousiasme, gedrevenheid en oprechte belangstelling maakten het werk voor mij heel veel leuker. Dankjewel voor je vele input en je constante interesse. Ik ben trots op wat we samen hebben bereikt en hoop dat jij er nog wat aan zult hebben.

A very big thank you to my students: the short-term students Marco and Theo, but most importantly Sophie, Coline, Ellen and Eline. Many thanks for your enthusiasm, team spirit, help and friendship along the way, they made all the difference. I am proud of you and hope you will all find a place where you will be happy and appreciated. Speciale dank voor Sophie. Jij kwam al toen ik zelf pas een paar weken bij PMI zat en bleek de beste eerste student te zijn die ik me had kunnen wensen. Ik ben blij dat jij als vriendin en paranimf naast mij zult staan bij mijn promotie.

Next, many thanks go to my long-term office mates: Hao, Erqin and Pauline. Pauline, apart from office mates, we were the two 'iron ladies'. We needed some time at the start to find a way to work together that suited both of us, and we managed to do so very well. I am proud of the work we did together and feel incredibly lucky that you came to join me in my iron research. Erqin, you started off as the silent Chinese girl next to me, but over the years we had more and more good conversations. Thank you for your wise insights and advice, I will miss them. And finally Hao, my second paranimph. I am still thankful that you joined our office and am grateful for having you as a friend. Thank you for your 'gezelligheid' and good conversations in the office, for your support when things did not go as I had planned, for inspiration to start playing piano, and for a great trip with Joep to your home country.

And then there are many more people in the lab that helped me somewhere along the way. Lotte, mijn buddy, jij leerde me RNA isoleren en, vele malen belangrijker nog, stond altijd klaar om mijn vragen te beantwoorden. Dat maakte mijn start veel makkelijker en plezieriger. Anja, ook zonder jou zou de start van mijn project moeilijker zijn geweest. Dank voor je hulp bij van alles, van het uitzoeken van Christos' data en het doen van sorting trials tot het genotyperen van mutanten. Dank ook aan Hans, voor de vele foto's die je voor mij en mijn studenten maakte, met als ~~kers op de taart~~ plant op de cover de fotoshoot voor mijn boekje. Ik vind het zo mooi geworden, duizendmaal dank daarvoor. Aster, veel dank voor de honderden (duizenden?) platen die je voor me goot. Manon, sorry dat ik ons, zonder het je te vragen, zomaar voorstelde als organisatoren van ons eerste PMI kerstdiner, maar hé, it was fun! Net als de escape room, BBQ, retreatactiviteit en latere twee kerstdiners die we organiseerden. Daarnaast

was het fijn om vanaf het begin met jou over de struggles en successen van onze PhDs te kunnen sparren. Merel, je was maar voor even een office roomie, maar wel in een voor ons beiden belangrijke, en stressvolle, tijd. Dank voor je steun in die periode. And of course a big thank you to all other PMI-ers, past and present, for good advice, welcome distraction in the lab, useful work discussions, thorough proofreading of my manuscripts and nice lunch breaks, conferences, retreats, Pheidippides runs and borrels.

There are also many people in science outside of PMI to thank. Dina, tijdens het schrijven van onze PhD voorstellen - en het wachten op de uitslag! - was het ontzettend fijn om jou en Lieke als maatjes te hebben. Dank ook aan jou en de andere Nijmegenaren voor het gezelschap in Lunteren en Soest, ik heb daar erg goede herinneringen aan. Many thanks also to Philip Benfey and Louisa Liberman. It was a great experience to be part of your ambitious and talented lab for eight, and later another two, months. Thank you for giving me that chance and other chances along the way, including writing an invited review, helping me with scholarship applications and introducing me to many people at my first international conference. Hideki Takahashi, thank you for inviting me to visit your lab last year. It was wonderful to meet you and the other plant researchers at Tohoku University and to experience Japanese culture. Finally, a huge thank you to Kaisa and Sarah. With my TRAP experiment I possibly bit off a bit more than I could chew. However, it all worked out in the end, which would not have been the case without your help and interest in the project. Many thanks.

En dan zijn er natuurlijk nog veel mensen buiten de wetenschap die me hebben bijgestaan de afgelopen jaren. Dankjulliewel Jet, Anna, Heleen en Saskia. We kennen elkaar nu tien jaar en ik vind het mooi om te zien hoe we er allemaal steeds meer achter komen wat we écht willen in het leven. Dat proces is enthousiasmerend en bevrijdend, maar soms ook heel lastig en confronterend. Ik prijs mezelf heel gelukkig dat ik deze emoties met jullie kan delen en we elkaar er bij kunnen steunen.

Dankjewel ook aan Marlou, Jolijn en Lisa, mijn oudste vriendinnen. We zien elkaar niet vaak, maar als we elkaar zien, is het altijd goed. Bij jullie kon ik mijn PhD altijd écht even loslaten.

Veel dank en liefde voor jou, Susanne. Ik voel me ontzettend gesteund en begrepen door jou. Wat ik ook denk of zeg, jij vindt niets gek of raar en dat is ongelooflijk fijn. Dankjewel voor de wijze inzichten de afgelopen jaren, het luisteren naar mijn twijfels en frustraties en de interesse die jij hebt voor alles wat mij bezig houdt.

Lieve Marja, Ep en Tom, jullie stonden altijd voor mij en Joep klaar. Een nacht bij jullie slapen of jullie auto lenen: we hoefden maar te bellen of jullie vonden het al oké. Dankjulliewel daarvoor en voor de liefde die daarbij komt kijken.

Lieve mama, papa, Annelie, Avi en Ilse, dankjulliewel voor jullie nooit aflatende interesse en steun. Jullie betrokkenheid bij mijn PhD was heel belangrijk voor me. Extra dank aan Avi, voor het proeflezen van een van mijn hoofdstukken, en aan mama en papa voor de uitgebreide hulp met het begrijpbaar maken van de Nederlandse samenvatting.

En tenslotte, Joep. Lieve Joep, jij was er altijd, om chocolade te halen of een knuffel te geven als het even niet liep, en om samen feest te vieren als iets juist wel gelukt was. Je hielp me als ik niet meer wist hoe ik verder moest met een experiment, analyse of email, stond een paar keer met mij in het lab en ontwierp de figuren voor één van mijn reviews. Dat je daar niet in de acknowledgements staat is bij deze hopelijk vergeven. Ik houd van jou en kijk uit naar het vervolg van ons gezamenlijke avontuur. Groenlo, here we come!

About the author

List of publications

List of presentations

Students supervised

Curriculum vitae

List of publications

Verbon EH, Post JA, Boonstra J (2012) The influence of reactive oxygen species on cell cycle progression in mammalian cells. Gene, 511: 1-6.

Verbon EH, Liberman LM (2016) Beneficial microbes affect endogenous mechanisms controlling root development. Trends in Plant Science, 21: 218-229.

Verbon EH, Trapet PL, Stringlis IA, Kruijs S, Bakker PAHM, Pieterse CMJ (2017) Iron and Immunity. Annual Review of Phytopathology, 55: 355-375.

Verhoeven K, **Verbon EH**, van Gurp TP, Oplaat C, Ferreira de Carvalho J, Morse AM, Stahl M, Macel M, McIntyre LM (2018) Intergenerational environmental effects: funtional signals in offspring transcriptomes and metabolomees after parental jasmonic acid treatment in apomictic dandelion. New Phytologist, 217: 871-882.

Verbon, E.H., Trapet, P.L., Kruijs S., Temple-Boyer-Dury, C., Rouwenhorst, T.G., C.M.J. Pieterse, C.M.J. (2019) Rhizobacteria-mediated activation of the Fe deficiency response in Arabidopsis roots: impact on Fe status and signaling. Frontiers in Plant Science,10: 909.

List of presentations

2015
Poster pitch at the international conference 'Rhizosphere4'
Presentation at the 'Utrecht PhD Summer School on Environmental Signaling in Plants'

2016
Presentation at the 'Science4life Symposium' in Utrecht

2017
Research seminar for the course 'Systems Biology' at Utrecht University
Presentation at the NWO symposium 'Co-Creation? Naturally!' in Amersfoort
Presentation at the 'Dutch Seed Symposium' in Wageningen
Pitch for reputation managers as part of the World 100 conference at Utrecht University

2018
Presentation at the PhD get2gether in Soest
Pitch at the TKI (Topconsortia voor Kennis en Innovatie) network event in Nieuwegein
Research seminar and course lecture at Tohoku University, Japan
Seminar at 'De Booghkring' for people with a higher eduction who have acquired brain injury
Lectures at the Leidsche Rijn College for high school students (5 and 6 VWO)
Presentation at the 3rd Max Planck Institute for Terrestrial Microbiology - ARBRE workshop on Molecular Plant Fungal Interactions

Students supervised

High school project
Theo Curran, junior high school student at Croton-Harmon High School, NY, USA

BSc theses
Sophie Kruijs, 'Biology' at Utrecht University
Marco Bentlage, 'Biology' at Utrecht University
Eline Eggermont, 'University College Utrecht' at Utrecht University

MSc theses
Sophie Kruijs, 'Environmental Biology' at Utrecht University
Coline Temple-Boyer-Dury, 'Biologie Fonctionelle des Plantes' at the University of Montpellier
Ellen Hensels, 'Environmental Biology' at Utrecht University

Curriculum vitae

Eline Hendrike Verbon was born on March 29th 1991 in Tilburg, the Netherlands. She obtained her Gymnasium diploma *cum laude* at the Mill-Hillcollege in Goirle and then moved to Utrecht to study at University College Utrecht. During her undergraduate degree Eline performed a research internship at the Netherlands Institute for Ecology (NIOO) under supervision of Dr. Koen Verhoeven. In addition, she wrote an honours thesis with Prof. Dr. Johannes Boonstra. Both projects were published in academic journals. Upon obtaining her undergraduate degree *summa cum laude*, Eline spent her summer at Syracuse Medical University for a Summer Undergraduate Research Fellowship (SURF), during which she studied B-cell signaling in mice. In September 2012 she started the Masters programme 'Biology' in Wageningen. During this programme, she performed two research projects in Wageningen. In the first she studied actin dynamics in mammalian cells in the department of Cell Biology and Immunology. In the second she studied lateral root development in plants in the department of Developmental Biology. Finally, she did a research intership at Beijing Agricultural University on chemical attraction of longhorn beetles. At the end of her Masters, which she completed *cum laude*, Eline took part in the 'Experimental Plant Sciences (EPS) MSc Talent Program', during which she wrote a PhD proposal with Prof. Dr. Corné Pieterse. This proposal was awarded with a personal grant from the NWO to carry out the proposed research project at the department of Plant-Microbe Interactions at Utrecht University. Before starting her PhD, Eline travelled to Duke University in the USA for an eight-month internship in the lab of Prof. Dr. Philip Benfey. During her PhD, Eline actively sought to share her knowledge via interaction with her students, presentations to peers and laymen and her Instagram account 'elinethescientist'. This thesis presents the results of Eline's PhD research.